

**A Method to Delineate Runoff Processes in a Catchment and its
Implications for Runoff Simulations**

A dissertation submitted to the
SWISS FEDERAL INSTITUTE OF TECHNOLOGY ZÜRICH

For the degree of
DOCTOR SCIENCES ETH

Presented by

Petra Schmocker-Fackel

Dipl.-Hydr., Albert-Ludwigs-Universität, Freiburg im Breisgau

Born on July 14, 1971
from Germany

Accepted on the recommendation of:

Prof. Dr. Wolfgang Kinzelbach,	ETH Zürich,	Referee
Prof. Dr. Jeffrey J. McDonnell,	Oregon State University,	Co-Referee
Dr. Felix Naef,	ETH Zürich,	Co-Referee

Tabel of content

ABSTRACT	V
ZUSAMMENFASSUNG	VII
1 INTRODUCTION	1
2 RUNOFF PROCESSES AND FLOOD FORMATION	3
2.1 Introduction.....	3
2.2 Runoff processes.....	3
2.3 Theories about flood formation	5
2.4 Methods to delineate runoff processes in a catchment	6
2.5 Runoff process research at ETH.....	8
2.6 Aim of this work.....	10
3 EXPERIMENTAL SETUP	11
3.1 Introduction.....	11
3.2 Experimental catchments.....	11
3.3 Mapping of dominant runoff processes	12
3.4 Hydrometric instrumentation.....	13
4 PROCESS IDENTIFICATION ON A SOIL PROFILE	17
4.1 Introduction.....	17
4.2 Runoff formation on the plot scale	17
4.3 Important parameters for the process evaluation and their determination in the field ..	19
4.3.1 Matrix permeability.....	19
4.3.2 Macroporosity	21
4.3.3 Processes reducing infiltration and vertical flow capacity	25
4.3.3.1 Soil Compaction.....	25
4.3.3.2 Soil surface sealing	27
4.3.3.3 Soil hydrophobicity	28
4.3.4 Hydromorphic features.....	29
4.3.5 Soil morphology	31
4.3.6 Sprinkling and infiltration experiments.....	31
4.3.7 Lateral flow capacity.....	32
4.4 Dominant runoff processes	34
4.5 Determination of the dominant runoff processes on a soil profile	35
4.6 Process decision scheme.....	39

5	AUTOMATED PROCESS IDENTIFICATION	43
5.1	Introduction.....	43
5.2	Hydrological interpretation of soil maps and other spatial data.....	43
5.2.1	General information	43
5.2.2	Soil type.....	43
5.2.3	Soil water regime and storage capacity.....	46
5.2.4	Soil sub-types	47
5.2.5	Other information contained in soil map.....	48
5.2.6	Geology, land-use and other information.....	49
5.3	Set of rules to estimate the DRP from soil map data.....	49
5.4	Evaluation of DRP set of rules	51
6	PROCESS DELINEATION IN CATCHMENTS	53
6.1	Introduction.....	53
6.2	Incorporating spatial data	54
6.3	Mapping of hydrological relevant features.....	56
6.4	Hillslope interactions between DRP - The process catena	57
6.5	Dominant runoff process maps.....	59
6.5.1	Dominant runoff process map of test area	59
6.5.2	Dominant runoff process map of Ror catchment	60
6.5.3	Dominant runoff process map for Isert catchment.....	62
6.6	Comparison of mapped and automatically delineated DRP map.....	64
7	HYDROLOGICAL CONSEQUENCES OF THE DIFFERENT RUNOFF PROCESSES	67
7.1	Introduction.....	67
7.2	Soil water levels.....	67
7.3	Catchment runoff.....	73
7.4	Electric conductivity.....	76
7.5	Conclusions.....	78
8	RAINFALL-RUNOFF MODELLING BASED ON PROCESS MAPS	79
8.1	Introduction.....	79
8.2	Model structure.....	80
8.3	Process modules.....	81
8.3.1	Hortonian overland flow	81
8.3.2	Saturated overland flow	82
8.3.3	Tile drain flow	84
8.3.4	Subsurface flow.....	85
8.3.5	Deep percolation	86

8.4	Model parameters	87
8.4.1	Determination of model parameters	87
8.4.2	Sensitivity analysis	89
8.4.3	Initial conditions	92
8.5	Performance of modules	94
8.5.1	SOF module	94
8.5.2	SSF module	96
8.5.3	Drainage module	98
8.5.4	Performance on the catchment scale	99
8.5.5	Evaluation of soil drainage concepts	100
8.6	Simulation of other floods	100
8.6.1	Catchment runoff	100
8.6.2	Event water	102
8.6.3	Extent of saturated areas	103
8.7	Model evaluation	104
9	TESTING MAPPING AND MODELLING RESULTS USING PESTICIDES AS TRACERS	105
9.1	Introduction	105
9.2	Pesticide study	105
9.3	Results	108
9.4	Conclusions	111
10	APPLICATIONS OF MAPPING AND MODELLING APPROACH	113
10.1	Introduction	113
10.2	Extrapolation to areas larger than calibration area	113
10.3	Extrapolation to events outside of calibration range	114
10.4	Prediction of floods in ungauged catchments	116
10.5	Summary and conclusions	117
11	CONCLUSIONS	119
	REFERENCES	121
	ACKNOWLEDGMENTS	131
	ABBREVIATIONS	133
	APPENDIX A: SOIL PROFILE DATA	135
	APPENDIX B: HYDROMETRIC MEASUREMENTS	184

APPENDIX C: KENDALL RANK CORRELATION COEFFICIENT	186
APPENDIX D: OBJECTIVE FUNCTION	186
CURRICULUM VITAE	187

Abstract

Runoff formation in catchments is governed by runoff processes like Hortonian overland flow HOF, saturated overland flow SOF, subsurface stormflow SSF and deep percolation to groundwater DP. Dominant runoff processes were determined on the plot scale and spatially delineated in a catchment. Information from soil, geological and land-use maps was hydrologically interpreted and a set of rules developed that allows an automated process determination on the plot and catchment scale. A rainfall-runoff model was developed that models each runoff process separately and considers the spatial distribution of dominant runoff processes in a catchment. The procedure of mapping and modelling was applied in two 2 km² experimental catchments and tested with hydrometric and pesticide tracer data.

The runoff process on a given site depends on soil characteristics like macroporosity, matrix permeability or layering of the soil, topography and vegetation. On over 40 soil profiles in the Ror and Isert catchments, the important dominant runoff processes were determined.

To spatially delineate the dominant runoff processes in the Ror and Isert experimental catchments, topography, interactions between neighbouring process areas and process observations during flood events were considered as well. This was done by drawing of a process catena. In the Ror catchment, areas with fast reacting saturated overland flow dominate while in Isert retarded reacting deep percolation and subsurface flow areas do.

With the data and experience gained, the detailed soil map 1: 5000 of the Kanton Zuerich was hydrologically interpreted and a set of rules was set up to automatically determine runoff processes from soil maps and maps of geology and land-use only. With this method the correct process could be determined for 52 % of the area in the Ror catchment and for 47 % of the area in Isert.

A rainfall-runoff model was developed where each process was conceptualized separately and with as few model parameters as possible. Each process module accounts for the storage capacity of the respective process area and the soil drainage. Runoff from each process module was then multiplied with the respective process area to yield total runoff. While the model parameters for the storage capacity could be determined from field data only, the soil drainage had to be calibrated. Gaps in process knowledge about soil drainage processes could be identified.

The model was calibrated with a smaller flood event in two sub-catchments of the Ror catchment. Without a change in calibration parameters, the model was then applied to the whole Ror and Isert catchment and to larger flood events with good results. The model was also used to calculate runoff from separate corn fields in the Ror catchment, on which different pesticides were applied

by Leu et al. (2004b). The pesticide concentrations were measured in catchment runoff during a flood event with a high temporal resolution. From fields where the mapping and modelling suggested large runoff contributions, large pesticide concentrations could be found in runoff, while from fields where no or little runoff was expected, little or no pesticides could be found.

With the described procedures, flood formation in the two experimental catchments could be well understood and successfully incorporated into a rainfall runoff model.

Zusammenfassung

Abflussprozesse wie Hortonischer Oberflächenabfluss (HOF), gesättigter Oberflächenabfluss (SOF), Schneller Unterirdischer Abfluss (SSF) und Langsamer Unterirdischer Abfluss (DP) bestimmen die Abflussbildung in einem Einzugsgebiet. In dieser Arbeit wurden die dominierenden Abflussprozesse für verschiedene Standorte bestimmt und im Einzugsgebiet kartiert. Informationen aus Boden-, geologischen und Landnutzungskarten wurden hydrologisch interpretiert. Zudem wurden Regeln aufgestellt, die eine automatische Prozessbestimmung am Standort und im Einzugsgebiet erlauben. Ein Niederschlagsabflussmodell wurde entwickelt, das jeden Abflussprozess einzeln modelliert und die räumliche Verteilung der Abflussprozesse in einem Einzugsgebiet berücksichtigt. Die Kartierung und Modellierung wurde in zwei Testgebieten angewendet und mit hydrometrischen und Pestizidtracerdaten überprüft.

Abflussprozesse an einem Standort werden durch Bodeneigenschaften wie Makroporosität, Matrixdurchlässigkeit oder Bodenschichtung sowie der Topographie und Vegetation bestimmt. Die dominierenden Abflussprozesse wurden an über 40 Bodenprofilen im Ror- und Iserteinzugsgebiet kartiert. Um die dominierenden Abflussprozesse in den beiden Einzugsgebieten zu kartieren, müssen auch die Topographie und die gegenseitige Beeinflussung benachbarter Prozessflächen berücksichtigt werden. Zu diesem Zwecke wurde eine Prozesskatena erstellt. Auch Prozessbeobachtungen während Hochwasserereignissen können für die Kartierung benutzt werden. Im Roreinzugsgebiet dominieren schnell reagierende Flächen mit gesättigtem Oberflächenabfluss, während im Iserteinzugsgebiet verzögert reagierende Flächen mit unterirdischem Abfluss vorherrschen.

Mit den erhobenen Daten und den gewonnenen Erkenntnissen aus der Kartierung wurde die sehr genaue Bodenkarte des Kanton Zürich im Massstab 1:5'000 hydrologisch interpretiert und ein Regelwerk aufgestellt, das es erlaubt, die Abflussprozesse automatisch mit Boden-, geologischen und Landnutzungskarten zu erstellen. Im Roreinzugsgebiet konnten für 52% und im Iserteinzugsgebiet für 47% der Fläche der richtige Abflussprozess bestimmt werden. Ein Niederschlagsabflussmodell wurde entwickelt, in dem jeder Prozess einzeln und mit der geringstmöglichen Anzahl Modellparameter konzeptionalisiert wurde. Jedes Prozessmodul berücksichtigt das Speichervermögen der jeweiligen Prozessfläche und die Entwässerung des Bodens. Während die Modellparameter für das Speichervermögen aus Felddaten bestimmt werden konnten, mussten die Parameter zur Berechnung der Bodenentwässerung kalibriert werden. Wissenslücken zu Prozessen der Bodenentwässerung konnten identifiziert werden.

Das Modell wurde in zwei Teileinzugsgebieten des Roreinzugsgebietes an einem kleinen Hochwasser kalibriert. Anschliessend wurde es ohne weitere Kalibrierung auf das gesamte Ror- und Iserteinzugsgebiet und für grössere Hochwasserereignisse angewendet. Gute Modellergebnisse konnten erzielt werden. Das Modell wurde auch dazu verwendet, den Abfluss von Maisfeldern, auf denen verschiedene Pestizide von Leu et al. (2004b) aufgebracht worden waren, im Roreinzugsgebiet zu berechnen. Pestizidkonzentrationen wurden mit hoher zeitlicher Auflösung während eines Hochwasserereignisses im Abfluss gemessen. Felder, von denen die Kartierung und Modellierung grosse Abflüsse erwarten liess, zeigten hohe Pestizidkonzentrationen im Abfluss. Demgegenüber wurden im Abfluss von Feldern, bei denen kein oder nur geringer Abfluss zu erwarten war, keine Pestizide vorgefunden.

Mit der vorgestellten Methode konnte die Hochwasserentstehung in den zwei Einzugsgebieten Ror und Isert verstanden werden. Dieses Wissen konnte in die Niederschlagsabflussmodellierung eingebracht werden, womit die Modellrechnungen zuverlässiger werden.

1 Introduction

Rainfall-runoff modelling is an important field in hydrological research and has many applications. A large number of different model conceptualization can be found in literature as well as work on model parameter determination and calibration. However, a rainfall-runoff model can only produce reliable results, if it represents adequately the main processes and if not all important model parameters have to be calibrated simultaneously using rainfall and runoff data.

The aim of this study is to improve flood discharge estimations in small catchments ($< 10 \text{ km}^2$) by introducing runoff process knowledge into rainfall-runoff modelling. To this effect, the processes governing flood formation were studied in literature and in the field and parameters were evaluated, which allow an identification of the different runoff processes in the field (Chapter 2 and 4).

In a next step, the runoff processes have to be delineated for whole catchments. To get a map of runoff processes, spatial data has to be incorporated and the interactions between neighbouring process areas and the topographic control on runoff have to be considered (Chapter 6). To reduce the amount of field work necessary for the delineation, available data can be hydrologically interpreted and used for an automated process determination (Chapter 5).

The real processes of runoff formation are complex and ways have to be found to simplify them for model conceptualization. The resulting model conceptualization should adequately represent each process and important model parameters should be related to field data (Chapter 7 and 8).

Due to the high spatial resolution of the process areas and the physical model, the mapping and modelling approach can be tested using measured data like soil water levels and discharge and spatial observations during flood events. Pesticide tracers applied to different fields with different process distributions are also an independent method for the testing (Chapter 9).

It is demonstrated that such a process based rainfall-runoff model allows a detailed insight into the processes during floods and can be used for extrapolation purposes with more confidence (Chapter 10).

2 Runoff processes and flood formation

2.1 Introduction

The amount of rainfall that can be stored in the soil or substrate and the amount that contributes to runoff determine the reaction of a catchment to intense precipitation. The water storage capacity and the dominant flow paths depend on the soil and underlying bedrock. On soils with low permeability, fast surface runoff develops due to limited infiltration, while on permeable soils much water can be stored and surface or subsurface runoff is formed retarded. In permeable soils and substrates vertical flow dominates, while impermeable layers restrict vertical drainage, leading to lateral flow. Therefore different runoff processes influence runoff formation (Beven, 1989a and Scherrer, 1997). In the following, the most important runoff processes and approaches to delineate runoff processes in a catchment are discussed.

2.2 Runoff processes

In literature many different runoff processes are discussed. Bonell (1993 and 1998) gives a good review of runoff generation processes. In the following, processes and terms as used in this study will be defined. The nomenclature corresponds to the one used by Scherrer (1997).

The main classification distinguishes between runoff flowing on the soil surface (overland flow) and runoff in the soil and underlying substrate (subsurface flow). These two processes can be further differentiated. The processes defined in the following are shown in Figure 2.1.

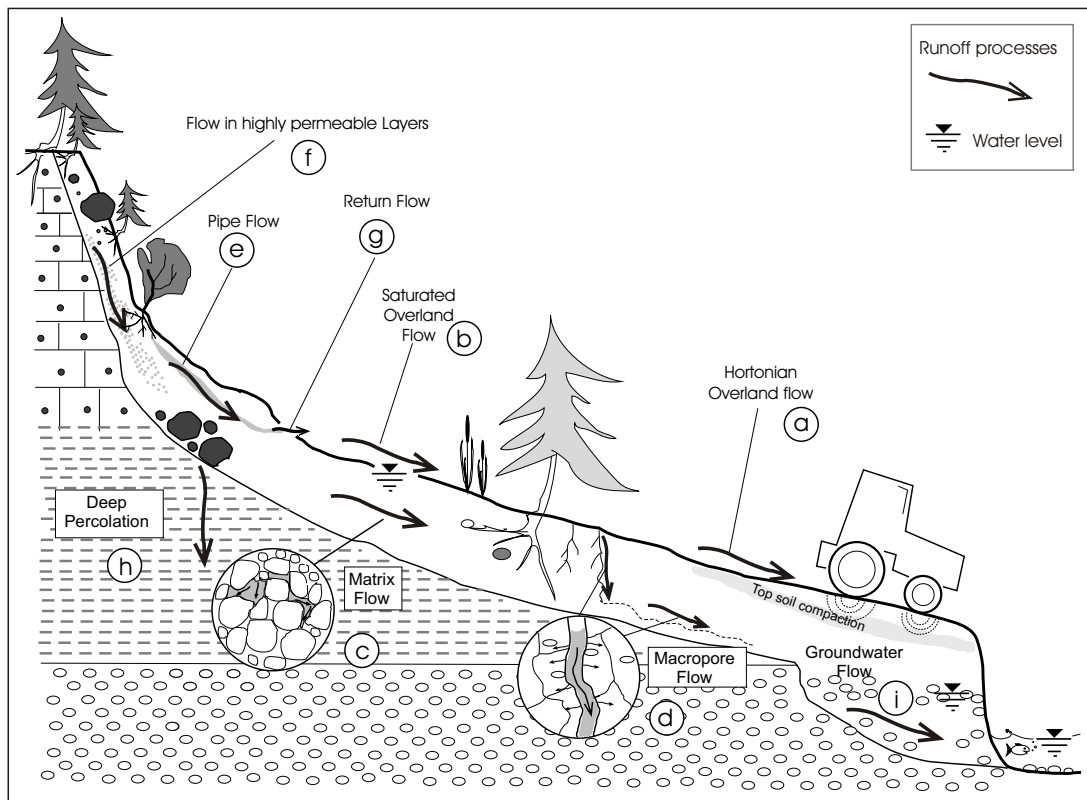


Fig. 2.1 Runoff processes on a hillslope (from Scherrer, 1997 slightly changed).

Surface runoff

(a) *Hortonian overland flow HOF*, also called infiltration excess overland flow, occurs if rainfall intensity exceeds infiltration capacity which is often the case on impermeable or low permeable soils (Horton, 1933).

(b) After the soil has been saturated no further infiltration is possible and all subsequent rainfall flows off as surface runoff. This is also called *saturation overland flow SOF* (Kirkby and Chorly, 1967).

Subsurface runoff

Water that infiltrates into the soil is either stored in the soil or flows vertically and laterally within the soil. Several flow processes can be distinguished:

(c) *Matrix Flow* is the flow of water through the micro- and meso pores of the soil, driven by capillary forces and differences in potential heads.

(d) *Macropore Flow* is vertical flow driven by gravitation in structural features in the soil like wormholes, root channels or cracks.

(e) *Pipes* are slope parallel channels that allow lateral flow in the soil. Animal burrows, large dead root channels or channels formed or enlarged by subsoil erosion fall into this category.

(f) *Highly permeable layers* in the soil or geological underground above layers with reduced permeability allow lateral flow. Through time the permeability of such layers can be increased through erosion of fine material.

(g) Subsurface flow that re-emerges to the soil surface after a short flow distance is called *return flow* (Dunne and Black, 1970b). Return flow can emerge preferentially through macropores or pipes or diffuse due to a change in slope and above low permeable layers.

Water percolation through the soil into the underlying geology is defined as *deep percolation DP*

(h) and contributes delayed to runoff as *groundwater flow* (i).

Fast and effective flow in pipes and highly permeable layers is called *subsurface stormflow SSF*.

2.3 Theories about flood formation

Horton (1933) proposed infiltration excess overland flow (HOF) as a process that leads to flood runoff. Based on this process understanding Betson (1964) developed the partial area concept. He states that storm runoff results from that part of a catchment where rainfall intensity exceeds infiltration capacity.

Work done in humid catchments (often forested or with thick and permeable soils) showed, that rainfall intensities often do not exceed infiltration capacity and storm runoff is produced mainly on saturated areas (e.g. Hursh, 1944; Dunne and Black, 1970a,b). Saturated areas are formed either on areas with low soil storage capacity (e.g. shallow soils) or at the base of hillslopes and in the valley bottoms where saturation is caused by water flowing from the hillslopes laterally downslope in the soil. Based on these observations, the variable source area concept was developed (Cappus, 1960; Hewlett, 1961; Hewlett and Hibbert, 1967). It assumes that the area which contributes to storm runoff varies seasonally and throughout a storm - it increases during the storm event and decreases again afterwards. Ambroise (2004) further distinguishes between the variable active and the contributing area. The variable active area is the area where a process occurs under given conditions (e.g. soil structure, topography, rainfall characteristics) while the contributing area is only that part of the active area which is connected to the channel and therefore contributes to runoff.

Subsurface flow can either directly contribute to storm runoff or influences the onset of surface runoff on saturated of areas by rapidly draining the soil (Anderson and Burt, 1990). The rapid flow

of water through preferential flowpaths in the soil was recognised in hillslope studies conducted in the 60s and 70s, in which subsurface flow from hillslopes was measured in ditches and artificial tracers were used to measure subsurface flow velocities (e.g. Mosely, 1982; Mosely, 1979; Pilgrim et al. 1978; Whipkey, 1965; Weyman, 1973). These workers found high flow velocities in the soil that could only be explained with preferential flow in macropores and pipes. Mosely (1979) observed and measured pipe flow directly. More recent experimental work done also points to the importance of macropores and preferential pathways in runoff generation on the catchment scale (Feyen, 1998; McDonnell, 1990; Peters et al., 1995; Tani, 1997) and on the hillslope or plot scale (Beven and Germann, 1982; Bronstert, 1999; Flury et al., 1994; Germann 1990; Mikovari et al., 1995, Scherrer, 1997, Weiler et al., 1998, Weiler 2001). However, McGlynn et al. (1999) state that “[...], *the mechanism or mechanisms responsible for rapid delivery of upland water to the riparian zone and stream remain in question*”. A good overview of hydrological research on hillslopes also called “Hillslope Hydrology” can be found in Kirkby (1978), Anderson and Burt (1990) and Anderson and Brooks (1996).

Zuidema (1985) developed the physically based, two-dimensional model Qsoil to simulate runoff formation on a hillslope. The model describes the different flow processes overland, matrix, macropore and pipe flow. An interaction module defining the water exchange between the matrix and macropore systems is an integral component of the model. Using this model to simulate and interpret results from sprinkling experiments conducted on several hillslopes, Kölla (1986), Faeh (1997) and Scherrer (1997) found that different runoff processes can occur on neighbouring plots and within a catchment. Pilgrim et al. (1978) also observed different runoff processes within a small area and Beven (1989a) suggests that all known runoff processes can occur on different areas in one catchment during the same rainfall event.

2.4 Methods to delineate runoff processes in a catchment

Different approaches to map spatial patterns of runoff formation in catchments have been described. They can be classified into three groups: approaches mapping either contributing areas and runoff coefficients, landscape units or runoff processes.

Contributing areas and runoff coefficients. Dunne et al. (1975) and Moore et al. (1976) mapped the spatial distribution of contributing areas and their temporal changes based on soil parameters, topography and vegetation. Methods were developed to predict the spatial patterns of saturated areas using topography (e.g. Beven and Kirkby, 1979; Sivapalan et al., 1987; Barling et al., 1994). Remote sensing techniques have been used to identify the spatial pattern of contributing

areas through observation of soil moisture content changes (Troch et al. 2000; Verhoest et al. 1998).

Bunza et al. (1996) and Löhmannsröben and Schauer (1996) mapped the hydrological characteristics of alpine catchments based on sprinkling experiments and soil and vegetation surveys. They distinguish between surface runoff dominated areas, areas where water is stored in the soil and areas producing interflow. Markart et al. (1996 and 2004) also carried out numerous sprinkling experiments and derived maps of surface runoff coefficients for alpine catchments, using vegetation and soil texture of the top soil as most important mapping parameters.

Pedotransfer functions. Soil hydraulic properties, mainly saturated and unsaturated hydraulic conductivity and water retention, can be derived from soil properties like soil texture and bulk density using pedotransfer functions. Pedotransfer functions are often used to parameterize catchment models using soil map information (Elsenbeer, 2001). Sobieraj et al. (2001) used several pedotransfer functions to calculate the saturated hydraulic conductivity and found that all calculated K_{sat} values were inadequate to model stormflow generation in a tropical rainforest catchment.

Landscape units. Another group of workers define landscape or geomorphological units that show a uniform hydrological behaviour (McGlynn and McDonnell (2003a), Merz and Mosely 1998, Sidle et al. 2000; Uhlenbrook and Leibundgut, 2002). Typical units are riparian zone, hillslope, zero-order basin, landslide, debris fan, hilly upland or permanently saturated areas. While these units are useful to describe the hydrology in an experimental catchment their transferability to other catchments with different geomorphology and hydrology is limited.

Runoff processes. The Institute of Hydrology (Wallingford) developed the HOST¹ classification scheme based on the soil map of Great Britain 1: 250'000. Three main concepts of water movement through the soil and substrate are distinguished (1) Aquifer or groundwater normally present and at > 2 m depth, (2) Aquifer or groundwater normally present and at < 2 m depth (3) No significant aquifer or groundwater. A further sub-division into 29 concepts is done according to the existence and depth of an impermeable or gleyed layer and the substrate hydrogeology (Boormann et al.,1995). The classification is dominantly based on soil and substrate characteristics (e.g. groundwater levels, gleyed layers) that indicate the long-term and mean process behaviour. Processes occurring during flood events are less well captured, since for example soil surface characteristics or preferential flowpaths are poorly considered in the classification. Additionally, the small mapping scale does not allow to assess the spatial distribution of soil properties and consequently runoff processes in small catchments.

1. HOST: Hydrology of Soil Types

Peschke et al., 1998; Peschke et al., 1999 developed the rule-based model called FLAB² to automatically delineate areas with the same dominant runoff process. Four main groups of runoff processes are distinguished: (1) surface runoff, (2) interflow, (3) storage, (4) percolation. These four groups are sub-divided into 18 groups according to soil hydraulic parameters (especially storage capacity and hydraulic conductivity of different soil layers), topography and distance to channel. Only the hydraulic conductivity is used to estimate infiltration and vertical and lateral flow capacity, while other soil surface characteristics, macropores and preferential lateral flowpaths are not considered explicitly.

2.5 Runoff process research at ETH

Naef (1977 and 1981) stated that only better understanding of flood formation processes can improve estimation of flood discharge in rivers. This need governed research of the engineering hydrology group first at the Laboratory of Hydraulic, Hydrology and Glaciology (VAW) and later at the Institute of Hydromechanics and Water Resources Management (IHW), ETH.

Scherrer (1997) and Faeh (1997) conducted sprinkling experiments on 18 grassland hillslopes with varying slopes, geology and soils throughout Switzerland. They applied between 50 and 100 mm/h of rainfall for 3 to 5 h over plot areas of 60 m² and measured surface and subsurface flow from the irrigated plots as well as soil water levels, soil water content and soil water tension in the plot. The experimental sites showed large differences regarding amount of surface and subsurface runoff, timing of runoff and flow paths. These differences could be explained with the occurrence of different runoff forming processes (e.g. on some plots Hortonian overland flow could be observed while on others subsurface flow processes dominated). To identify the runoff processes in detail, the model Qsoil was used (Faeh et al., 1997). The experiments and the model applications showed the crucial role of macropores in the runoff process. Therefore, Weiler (2001) investigated macropore flow and the mechanisms controlling it during infiltration more closely.

The above research showed that different runoff processes can occur on neighbouring plots and in one catchment, depending on the structure of the soil, the underlying geology, the vegetation cover or land-use and the topography. Even on one plot different processes occur depending on rainfall characteristics and antecedent conditions (Beven, 1989a). To understand the reaction of a whole catchment during heavy precipitation it is therefore necessary, to delineate the spatial distribution of areas with different dominant runoff processes.

2. FLAB: **F**lächen gleicher Dominanz bestimmter **A**blflussmechanismen (engl. Areas with same dominance of runoff mechanisms)

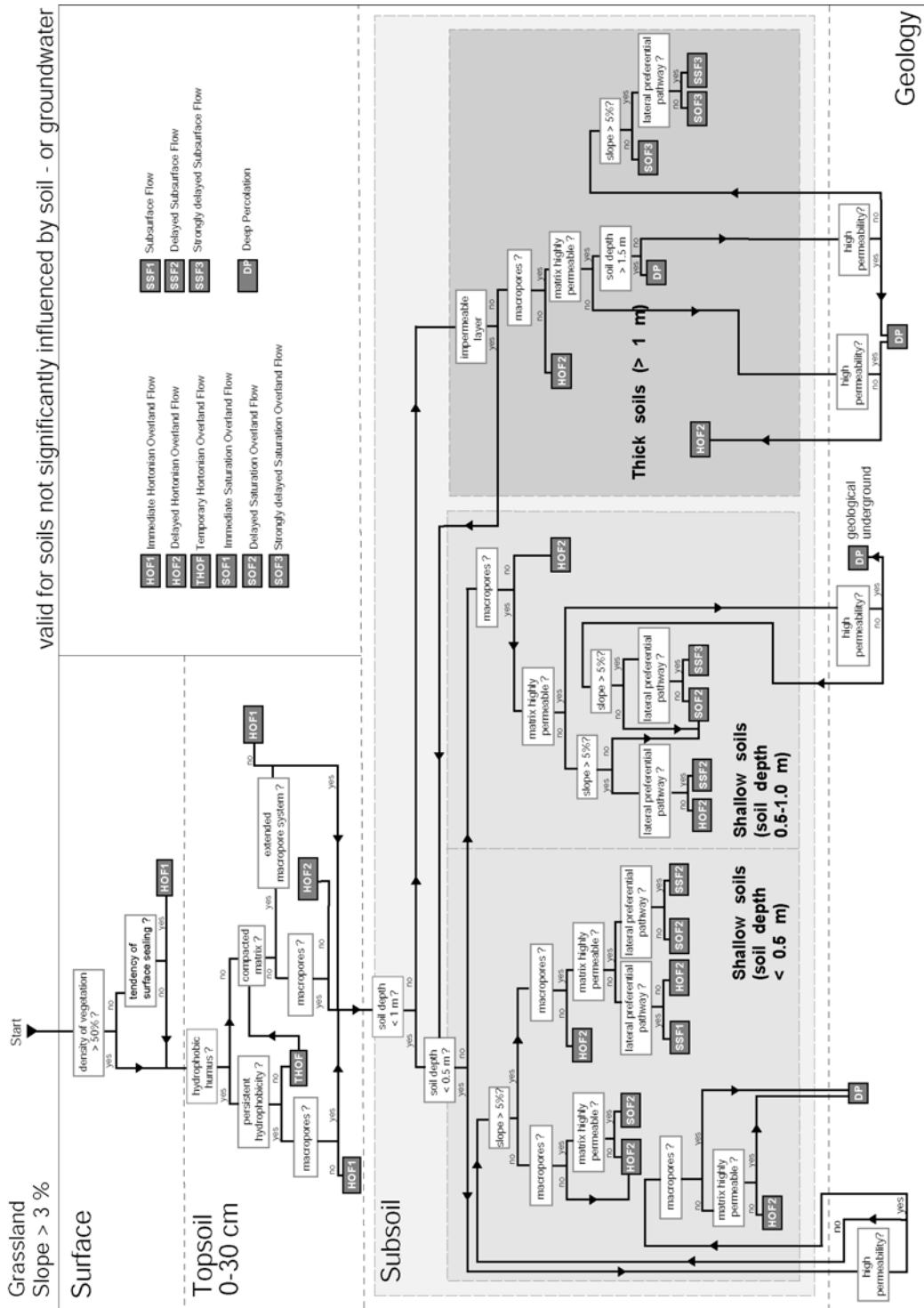


Fig. 2.2 Process decision scheme from Scherrer and Naef (2003)

Further work was undertaken to identify the factors that determine the process on a given site and to develop methods to map the dominant runoff processes out in the field (Naef et al., 2000; Scherrer and Naef, 2003). To this purpose decision schemes were developed that allowed the determination of the dominant runoff processes on the plot scale for different land-uses and

rainfall intensities. The classification bases on soil characteristics like macroporosity, matrix permeability, existence and depth of gleyey and impermeable layers and lateral flow paths. Figure 2.2 shows the process decision scheme for grassland. The schemes are very detailed reflecting the complexity of runoff formation.

2.6 Aim of this work

The process decision schemes of Scherrer and Naef (2003) were developed and tested on the plot scale. Additionally, methods to determine the key points for the process evaluation in the field were collected and the dominant runoff processes were delineated in three small catchments in Rheinland-Pfalz (Naef et al., 2000). However, no systematic testing of the methods to determine the key points in the field, the process decision scheme itself and the resulting runoff process map in a catchment has been done so far. Therefore, one aim of this project was to test and improve the methods and decision schemes to determine the runoff processes on the plot scale and the process delineation on the catchment scale.

Another goal of this project was the reduction of the amount of field work necessary for the process delineation. Therefore, information contained in soil maps and other spatial data was evaluated and hydrologically interpreted to allow an automated or at least partly automated process determination. To this effect the original process decision trees had to be generalized and condensed into one new process decision scheme.

Finally, a rainfall-runoff model was developed using the runoff process maps. Each runoff process is modelled separately and with as few model parameters as possible. The aim was to develop a tool that allows the simulation of single flood events based on the field investigations and the dominant runoff process map and without the need of calibrating model parameters using rainfall and runoff.

3 Experimental setup

3.1 Introduction

The neighbouring Ror and Isert catchments were selected as experimental catchments. They were chosen, because: (1) The Isert catchment reacts hydrologically very differently from the Ror catchment, (2) discharge during a major flood in May 1999 was measured in both catchments and (3) Leu (2003) conducted a pesticide transport study there, the data of which is at our disposal.

In both catchments, runoff processes were investigated on the plot scale using soil profiles, sprinkling and infiltration experiments (Chapter 4) and the dominant runoff processes were delineated on the catchment scale (Chapter 6). In the Ror catchment, soil water levels, runoff from several sub-catchments and EC in runoff were measured additionally.

In the following, the two experimental catchments are introduced, the field work done during the mapping is described and the hydrometric measurements conducted in the Ror catchment are specified.

3.2 Experimental catchments

The two catchments are located on the Swiss Plateau, about 30 km southeast of Zurich (Figure 3.1).

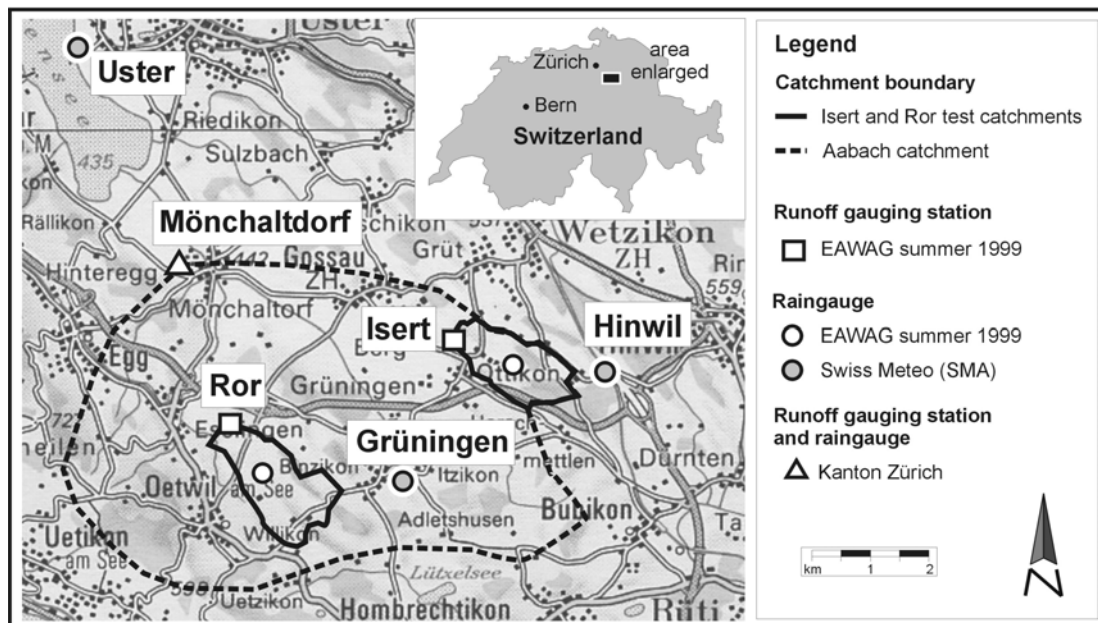


Fig. 3.1 Ror and Isert catchment and location of rain and runoff gages in the proximity.

In this region, the underlying bedrock is composed of sandstone, marl and conglomerates of the Upper Freshwater Molasse (OSM) and is partially overlain by glacial till of the Würm ice age and fluvial gravel deposits (Hantke et al., 1967). Major groundwater bodies with high hydraulic permeabilities are found in the fluvial gravel deposits, while the molasse and glacial till have low permeabilities (Haering et al., 1993). Drumlins and roche moutonnées form the elevations in this rolling countryside. In the depressions and valleys between the hills, swamps developed, most of which were artificially drained in the middle of the 20th century. The main land use in the watersheds is livestock farming with a dominance of meadows and pastures followed by agricultural fields (corn and grain). Only small parts of the catchments are forested or sealed (settlements and streets). Table 3.1 summarizes more catchment characteristics.

Table 3.1 Catchment characteristics.

		Ror catchment	Isert catchment
Area		2.1 [km ²]	1.7 [km ²]
Elevation range		490 - 550 [m a.s.l.]	514 - 575 [m a.s.l.]
Geology		Sandstone, marl and conglomerates of OSM ¹ , overlain by glacial till in the north-eastern part.	Interglacial fluvial gravel, overlain by glacial till in the northern part.
Groundwater		Low permeability Only small scale aquifers with low storage capacity.	High permeability Area wide aquifer with moderate storage capacity.
Land use	grassland	60%	42%
	fields	25%	33%
	forest	8%	15%
	settlements and streets	7%	10%
drained area		21%	14%

¹ OSM Upper freshwater molasse

Mean annual precipitation is 1370 mm at Grüningen SMA weather station, 1-2 km from the study areas (location see Figure 3.1). Mean annual temperature is 7°C, and mean annual evapotranspiration is about 40% of annual rainfall (Swiss Meteo, SMA). Precipitation has a slight peak in summer (May to September). Mean annual runoff of the Aabach at Mönchaltdorf station (46 km²) is 740 mm (Hydrologisches Jahrbuch Kanton Zürich, 2000).

3.3 Mapping of dominant runoff processes

To map the dominant runoff processes in the Ror catchment, 36 soil profiles were investigated. Fifteen soil pits were excavated (P 1 to P 15) and 21 soil core samples taken (S 1 to S 10 and GW 1 to GW 15). In the Isert catchment, six soil pits were excavated (PI 1 to PI 6) and two soil core

samples (SI 1 and SI 2) taken. The location of the soil profiles is shown in Figure A.x. Most of the profiles lie along hillslope transects (catena mapping approach). In addition, soil profiles on special soil map units and on areas with special surface or land-use characteristics were investigated. Near some of the profiles, sprinkling or infiltration experiments were conducted to further investigate infiltration capacity. 15 piezometers were installed to measure soil water levels. Table 3.2 lists the evaluated soil properties and parameters. The methods used for their determination are given in Chapter 4 and Appendix A. The data sampled for each soil profile and the results of the sprinkling experiments are summarized in Appendix A.

Table 3.2 Soil properties and parameters determined for the soil profiles.

	For all soil profiles	For soil pits only
Sample site	<ul style="list-style-type: none"> • Location • Elevation • Slope • Topography and exposition • Geology • Land-use • Lateral flowpaths 	
Soil surface	<ul style="list-style-type: none"> • Vegetation • Percentage of vegetation cover • Degree of hydrophobicity • Distinctive features (e.g. signs of erosion, soil surface sealing) 	
Top soil (0 - 30 cm)	<ul style="list-style-type: none"> • Aggregate stability 	<ul style="list-style-type: none"> • Macroporosity
For each soil horizon	<ul style="list-style-type: none"> • Thickness • Soil Colour • Soil texture • Shape of aggregates • Organic content • pH • Carbonate content • Water content • Hydromorphic features 	<ul style="list-style-type: none"> • Bulk density • Packing density • Content of coarse fragments

3.4 Hydrometric instrumentation

At the outlet of the Ror and the Isert catchment, discharge (in 10 min time interval) and the concentration of the pesticide atrazine (in 10 min time interval during flood events) were measured from May 1999 to July 1999 by EAWAG³ (Leu, 2003). During this period, on the 14.05.1999, a major flood was recorded in both catchments. From May 2000 to July 2000, discharge

3. EAWAG: Swiss Federal Institute of Environmental Science and Technology

and pesticide concentrations were measured at the outlet of the Ror experimental catchment (station Ror) and at two points within the catchment (stations Summerau and Rinderholz) (Figure 3.2). We continued measuring at these stations until December 2000.

Table 3.3 Area of sub-catchments in the Ror experimental catchment.

Catchment	Area [km ²]
Ror	2.102
Rinderholz	0.664
Poesch	0.128
Summerau	0.729
Lindist	0.386

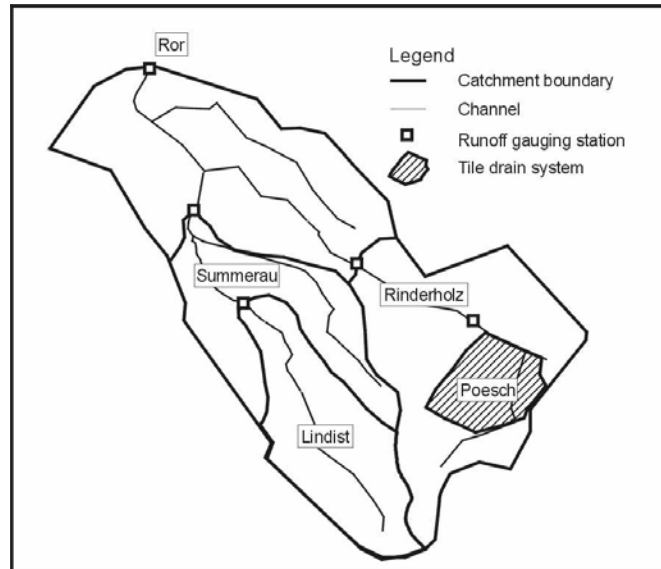
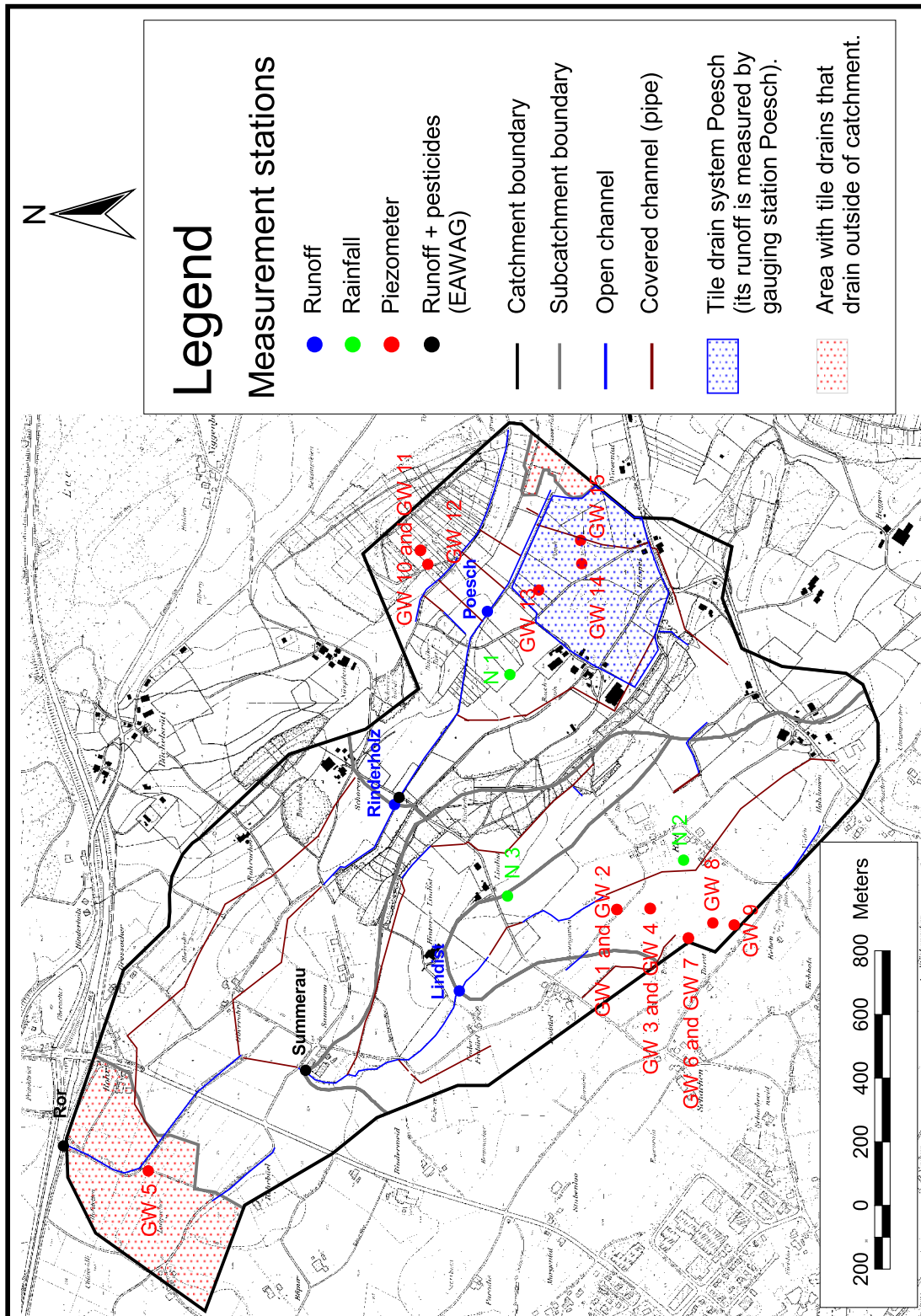


Fig. 3.2 Ror catchment and sub-catchments

In spring 2001, a hydrometric network was installed in the Ror catchment to observe the reaction of areas with different dominant runoff process. The discharge measurements at station Rinderholz were continued. The Rinderholz sub-catchment is dominated by natural and artificial subsurface flow (tile drains). Three piezometers (GW 10 - GW 12) were installed on a hillslope where subsurface flow was expected. Runoff from a tile drain system (Station Poesch) and the groundwater levels in the tile drain system (GW 13 to GW 15) were measured as well. In the saturated overland flow dominated sub-catchment Lindist, runoff (Station Lindist) and the groundwater levels along a hillslope transect (GW 1 to GW 9) were recorded. Rainfall was measured at station N 1 in the Rinderholz sub-catchment and at stations N 2 and N 3 in the Lindist sub-catchment. All measurements have a temporal resolution of 10 min. The location of all stations can be seen in Figure 3.2, additional information about the stations is given in Appendix B.



Hintergrundplan reproduziert mit Bewilligung des Amtes für Raumordnung und Vermessung, Baudirektion Kanton Zürich.

Fig. 3.2 Hydrometric instrumentation of the Ror catchment.

Several rain gauges of Swiss Meteo (SMA) are located near the catchments (location see Figure 3.1). In Grüningen, 1 km northeast of the Ror catchment, daily rainfall has been measured since 1900. The two experimental catchments are part of the 46.0 km² Aabach catchment (Figure 3.1) where the Kanton Zürich (AWEL) measures the runoff of the Aabach as well as rainfall in Mönchalt Dorf since 1980.



Fig. 3.3 Aerial photograph of Ror catchment and Swiss plateau. Lake Zurich and the Alps can be seen in the background.

Fig. 3.4 Aerial photograph of Isert catchment and Swiss plateau. Lake Greifensee can be seen in the background.



4 Process identification on a soil profile

4.1 Introduction

To identify the runoff process on a soil profile, the structure of the soil and the underlying geology, as well as land use and topography have to be considered. The structure of the soil is of major importance for the process determination and can be described with soil properties like matrix permeability, macroporosity, soil layering and soil surface characteristics. In this chapter, it is described which soil properties and parameters are important for the hydrological reaction of the soil and how these soil properties and parameters can be identified in the field or in the laboratory.

On over 40 soil profiles in the Ror and Isert catchment, the soil properties and other relevant parameters were determined. The process decision scheme of Scherrer and Naef (2003) was used to evaluate the dominant runoff process for each soil profile. Knowledge gaps about processes or parameter determination were identified and, if possible, closed with the collected experience and data. A new, simplified version of the decision scheme is introduced that allows an automated determination of the dominant runoff process.

4.2 Runoff formation on the plot scale

Runoff formation on the plot scale is complex, as the schematic representation of the relevant factors and processes show (Figure 4.1).

Infiltration capacity is a key factor governing runoff formation. If rainfall intensity exceeds infiltration capacity, Hortonian overland flow occurs and contributes to storm runoff. Infiltration into the soil matrix depends on soil texture, bulk density and soil moisture of the soil matrix. Macropore infiltration can be initiated on the soil surface or from a saturated layer near the surface (e.g. permeable A-horizon on a less permeable B-horizon). Macropore infiltration capacity depends on the amount of water that can enter the macropores and how easily water can flow from the macropores into the surrounding soil matrix. On macroporous soils, macropore infiltration normally exceeds matrix infiltration and is therefore of major importance for the infiltration process. Factors that reduce matrix permeability or the number of macropores like soil surface sealing, compaction of top soil and hydrophobicity of the soil surface, also reduce the infiltration capacity

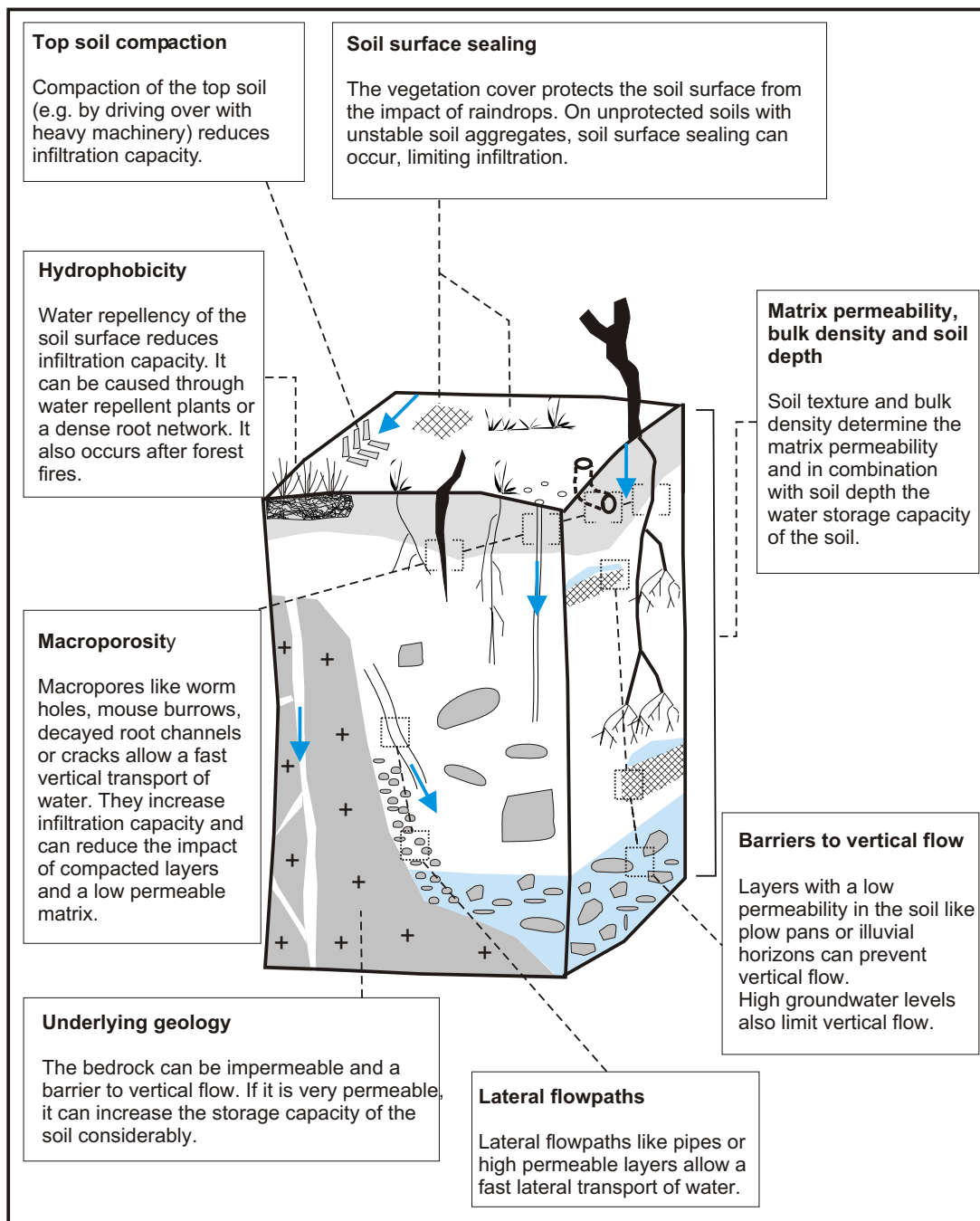


Fig. 4.1 Schematic representation of runoff formation on a soil profile (after Naef and Scherrer, 2003).

The vertical flow of the infiltrated water is stopped if it encounters a layer with significantly lower matrix permeability or macroporosity. In this case the water ponds in the soil above the layer with low permeability and either starts to saturate the soil profile or drains laterally through preferential flowpaths. A significant decrease in permeability and macroporosity often occurs at the soil - bedrock interface, if the soil stratum changes (e.g. soil textural changes in alternating deposits) or

through the compaction of deeper soil layers caused by agricultural practices (e.g. plow pans). Macropores of biogen origin (e.g. animal burrows and root channels) have a distinct distribution with soil depth and cannot be found below a certain depth. Permanently high ground- or soilwater levels also limit vertical flow.

Lateral preferential subsurface flow occurs in pipes, high permeable layers and tile drains. These structures bypass the soil matrix and allow a fast lateral transport of water. An efficient system of lateral flowpaths can prevent soil saturation even during heavy rainfall events. In this case fast subsurface flow or tile drain flow is the dominant runoff process.

4.3 Important parameters for the process evaluation and their determination in the field

4.3.1 Matrix permeability

Flow velocities in the soil matrix depend on the soil texture, bulk density and water content of the soil. Velocities increase with increasing sand and soil water content and decreasing bulk density, and are for saturated soils between < 1 cm/d (compacted clay) and 350 cm/d (uncompacted sand) (AG Boden, 1994).

Evaluation in the field. A soil sample was taken from each horizon of the soil profiles investigated in the Ror and Isert catchment. Its soil texture was analysed in the laboratory and its soil textural class defined according to AG Boden (1994). If possible, bulk density of the soil was also determined. Five classes of matrix permeabilities were established depending on the soil textural classes and the bulk density. The soil textural classes and the classes of matrix permeabilities are displayed in Figure 4.2. Class A encompasses clay rich soils with low k_{sat} , in class E on the other end of the spectrum are the sandy soils with high to very high k_{sat} values. The matrix permeability of both classes is not sensitive to soil compaction. Only class C is very susceptible to soil compaction. The silt rich soils of class C have high k_{sat} values in uncompacted soils but low values in compacted soils.

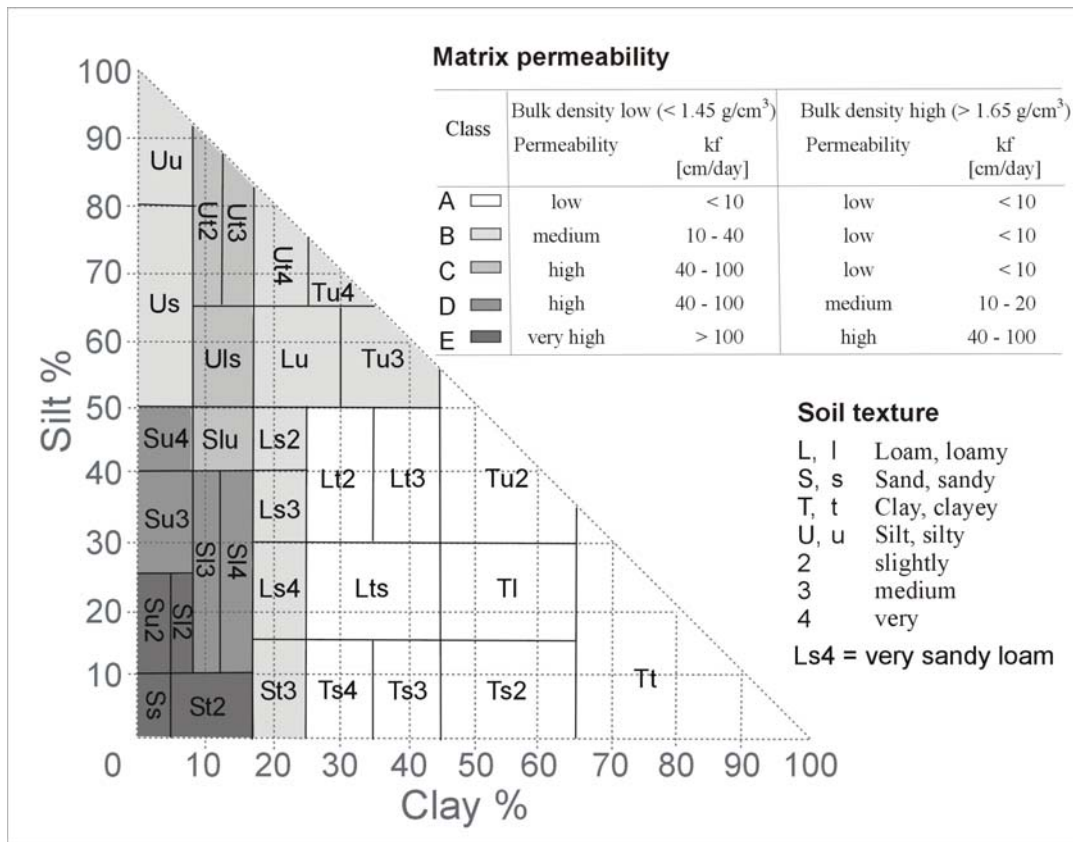


Fig. 4.2 Soil textural classes (data from AG Boden, 1994) and derived classes of matrix permeability. Soils of class D and E have a high permeability, while soils of class A and B have a low permeable matrix. The permeability of the class C soils depends on the degree of soil compaction.

In Figure 4.3 the soil texture of the samples taken in Ror and Isert in the top soil (A- horizon), in the sub-soil (B-horizon) and in the soil below 1 m depth are displayed. The top soils are of soil texture clayey loam to sandy loam with low to medium matrix permeabilities. These soil texture classes also dominate the subsoil above 1 m, while the sand content is higher in the subsoil below 1 m. However, due to high bulk densities measured in the subsoil, matrix permeabilities are low to medium. With increasing soil depth, the range of soil texture classes increases as well. These soil texture variations are caused by alternating sediment layers in the alluvial deposits found in the valley floor. No significant difference in soil texture between the two catchments was found.

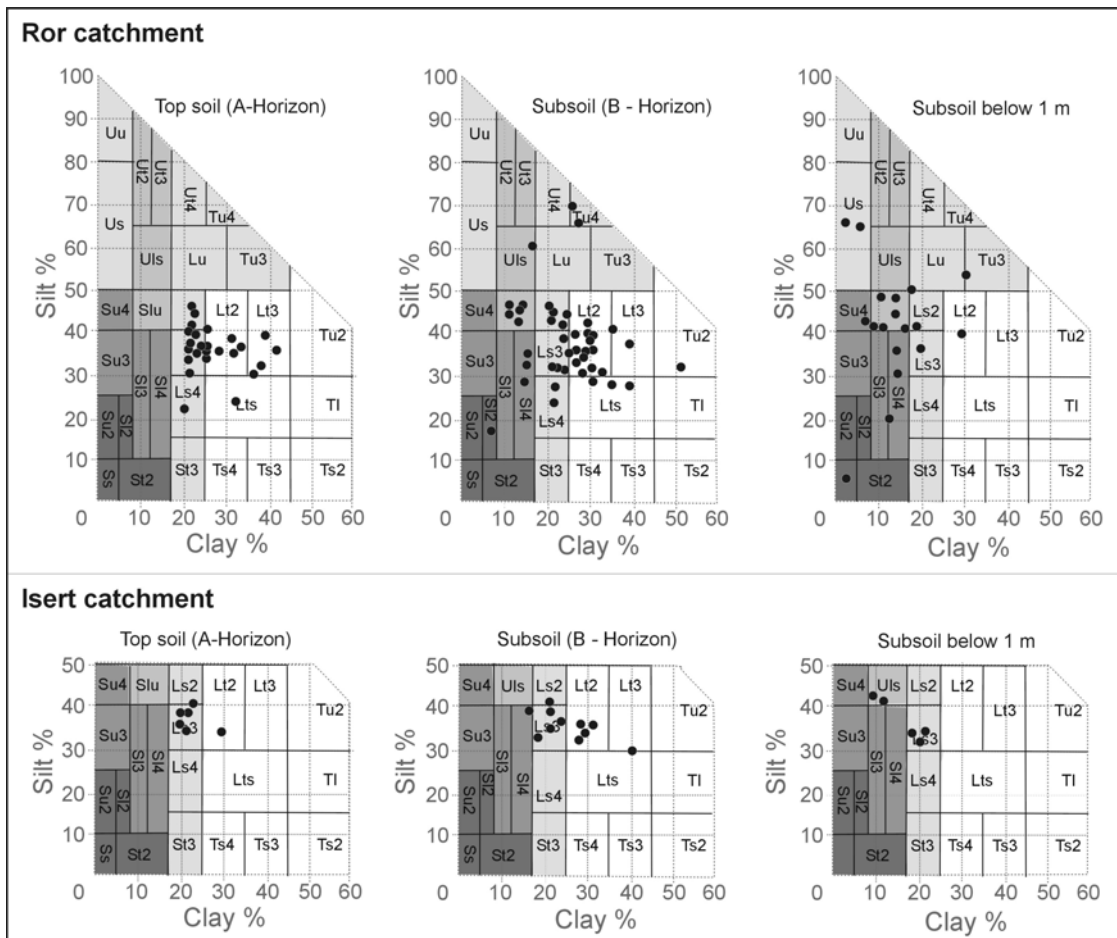


Fig. 4.3 Soil texture of the samples taken in the top soil (A-horizon), in the sub-soil (B-horizon) and in the soil below 1 m depth in the Ror and Isert catchment. Each black dot represents one sample.

4.3.2 Macroporosity

Macropores play a crucial role in the infiltration process. They allow high infiltration rates and fast vertical movement of the infiltrated water even in soils with a low permeable soil matrix. According to Weiler (2001) 100 macropores/m² can capture over 70 % of the overland flow and the capacity of such a macropore system is sufficient to transport 360 mm/h. Macropore flow is either initiated at the soil surface or from a saturated soil layer at depth (Weiler and Naef, 2003).

In Switzerland, mainly vertically orientated, continuous macropores formed by anecic earthworm species like *Lumbricus terrestris* are relevant. They can have a maximum diameter of 11 mm and transport water to a depth of more than 2 m (Ehlers, 1975). Flow velocities of up to 7 cm/s were measured in such pores by Weiler, (2001) and between 1 and 25 cm/s by Bouma et al. (1982). Wormhole densities of up to 700 to 900 wormholes/m² have been reported in non-tilled soils

which are ecologically suitable for earthworms. In tilled soils up to 230 wormholes/m² could be found, though the macropores were often disconnected by the tilling process and therefore less efficient for water transport (Ehlers, 1975). In Table 4.1 macropore densities measured in the field and the laboratory are listed.

Table 4.1 *Macropore densities measured in field and laboratory studies.*

Number of macropores	Diameter	Land-use	Number of soil profiles	Sampling depth and vertical distribution of macropores	Author
Mp/m ²	mm				
70 - 330	3.5 - 11.3	grassland	4	0-60 cm max at 40 cm	Weiler 2001
180 - 900	all wormholes	grassland	4	0-60 cm	Weiler 2001
300 - 700	> 3.5	pasture		with computer tomography in soil cores	Warner and Nieber, 1991
250 - 600	> 3.5	tillage		with computer tomography in soil cores	Warner and Nieber, 1991
100					Kretzschmar 1988
21 - 174	2 - 5	no-till	1	0-60 cm, increase with depth	Ehlers, 1975
6 - 174	5 - 11	tillage	1	0-60 cm, increase with depth	Ehlers, 1975
0 - 230	all macropores	arable land	3	decrease with depth	Zehe and Flühler, 2001
4 - 12	> 5 mm	different tillage management practices	20	0 - 40 cm	Trojan and Linden, 1998
100 - 200	2 - 5 mm		20	0 - 40 cm	
270 - 560	> 2	grassland	6	0-90 cm decrease with depth	Munyankusi et al. 1994
145 - 205	> 5	no-till corn	1	top 30 cm	Edwards et al., 1990
367 - 644	2 - 5	no-till corn	9	top 30 cm	Edwards et al., 1992
33 - 189	> 5	no-till corn	9	top 30 cm	Edwards et al., 1992

Besides macropore density, the size of the macropores is also important. Ehlers (1975) found that macropores with a diameter of over 5 mm constitute only 10 % of the total porosity but account for more than 60 % of the infiltration. Weiler (2001) also observed that large macropores can drain several dm². Some researchers like Ehlers (1975) found an increase of macropore density, others a decrease with depth (e.g. Zehe and Flühler, 2001), while a third group found a maximum somewhere in between (e.g. Weiler, 2001).

Evaluation in the field. Infiltration and vertical flow is enhanced by (1) a high macropore density, (2) large macropores, (3) a high percentage of vertically orientated pores, (4) continuity of the pores and (5) good interaction between macropores and matrix. Macropore density was assessed in the field by counting the number of macropores in horizontal cross sections in different soil depths (Figure 4.4) over an area of 200-2000 cm² (Smettern and Collis-George, 1985). To

obtain information about their continuity a dye tracer (e.g. Brilliant Blue) can be applied during an infiltrometer or sprinkling experiment before digging a trench (Flury et. al., 1994; Weiler, 2001). The density of macropores larger than 5 mm in diameter can be determined accurately while the density of smaller pores is often underestimated as they are partly destroyed or clogged during excavation.

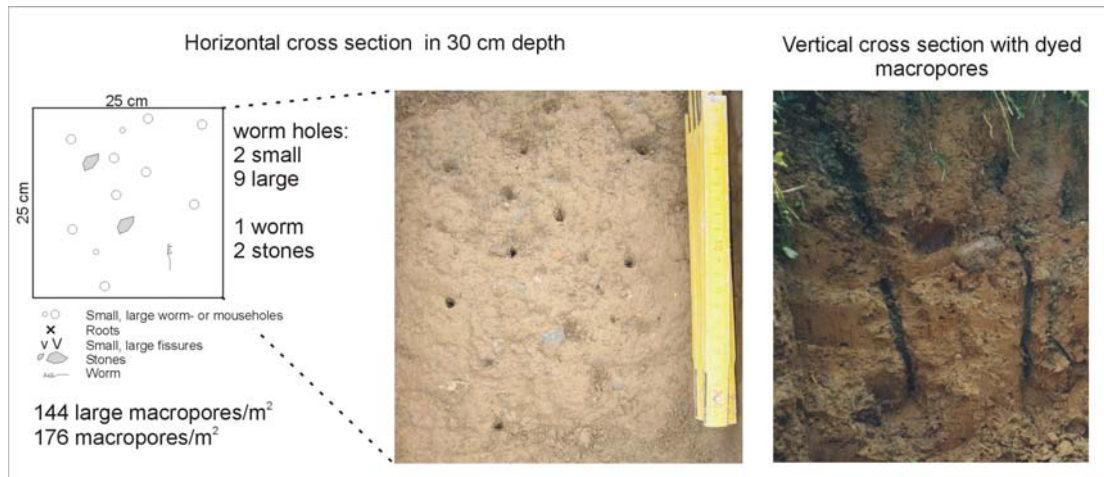


Fig. 4.4 Determination of macroporosity on the plot scale at a soil profile in the Ror catchment.

To find a relation between macropore density and infiltration rate, we conducted sprinkling and infiltration experiments on 16 plots. The experiments lasted for 1 h with sprinkling intensities of 60 - 75 mm/h over an area of 1 m². 10 experiments were conducted on meadow, 5 on agricultural fields and one in forest. The vegetation cover varied between 5 and 100 %. On all plots but one top soils were of soil texture sandy loam or clayey loam. No relationship between final infiltration rate and land use, vegetation cover or soil texture of the top soil could be found (Figure 4.5)

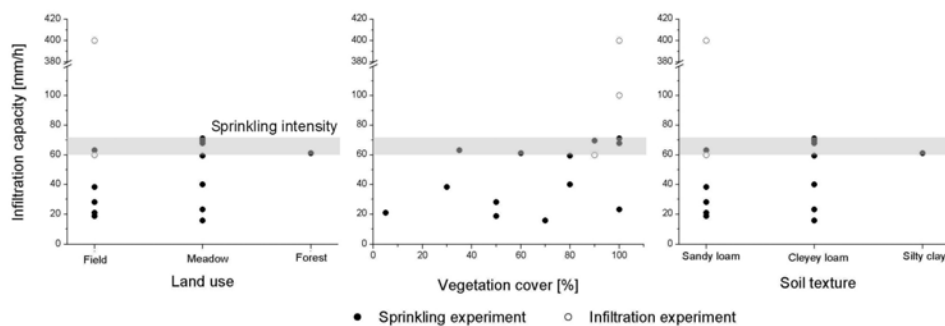


Fig. 4.5 The influence of land use, vegetation cover and soil texture on infiltration rate obtained from sprinkling and infiltration experiments (grey bars show range of sprinkling intensity).

In Figure 4.6 the final infiltration rate (left) and the volumetric runoff coefficient (right) are plotted against the average wormhole density ($d > 5$ mm) of the top 30 cm. For macropore densities over 30 Mp/m^2 no surface runoff occurred. The minimum observed macropore density of 8 Mp/m^2 still allowed infiltration rates of 20 mm/h .

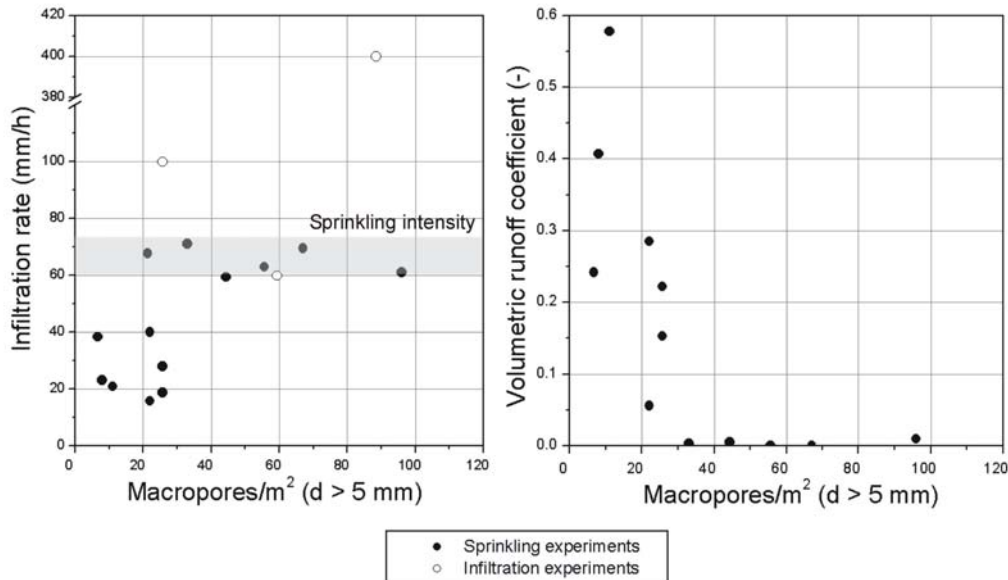


Fig. 4.6 The influence of wormhole density on infiltration. The final infiltration rate (left) and the volumetric runoff coefficient (right) obtained from sprinkling experiments ($60 - 75 \text{ mm/h}$ for 1 h) are plotted against wormhole density ($d > 5 \text{ mm}$). The wormhole density is the mean of wormhole densities in different depths of the top 30 cm of the soil.

Based on these experiments, soils with a macroporosity of more than 40 Mp/m^2 are classified as having a high macroporosity and no Hortonian overland flow should occur for high intensity rainfall ($> 20 \text{ mm/h}$). For low intensity rainfall ($< 20 \text{ mm/h}$), the number of macropores necessary to prevent Hortonian overland flow might even be smaller. On soils with a lower macroporosity surface runoff might occur. For such soils, infiltration and vertical flow capacity should be assessed with infiltration or sprinkling experiments.

4.3.3 Processes reducing infiltration and vertical flow capacity

4.3.3.1 Soil Compaction

Compacted soil layers have a reduced hydraulic conductivity and infiltration capacity. Prone to compaction are soils rich in silt and poor in clay, organic soils (Kuntze et al.1994) and poorly aggregated soils (Horn & Rostek, 2000). Soil compaction can occur close to the soil surface where the reduced infiltration capacity leads to Hortonian overland flow or in deeper soil layers that subsequently form barriers to vertical percolation. The effect of compacted soil layers can be compensated by macropores that allow water flow through the compacted layer. The areal extent and the spatial distribution of top soil compaction on a field is important. Traffic lines in the hillslope direction lead surface runoff effectively downslope, while traffic lines running perpendicular to maximum slope allow re-infiltration in uncompacted areas.

On arable land, compaction is mainly caused by repeatedly driving heavy farm equipment over fields. Compaction increases with increasing number of drive-overs, weight of the machinery and the water content of the soil during driving (Roth, 2002). The areal extent of compaction depends on the crops grown on a field. Frielinghaus et al. (1994) found that on potato and sugar beet fields practically the whole area was driven over at least once in a growing season, on corn and grain fields 60 - 70% were driven over. They also found that on highly compacted areas, the macropore volume was reduced by 50 - 75%. Top soil compaction on agricultural fields is removed with tillage and the areal extent therefore changes from year to year. Subsoil compaction (e.g. plow pans) is more permanent as it is often caused by conventional tillage practices.

On intensely used pastures, especially in mountainous regions, animal treading can compact the top layer of the soil (Horn, 1985; Scherrer, 1997). In forests soil compaction was observed following harvesting with heavy machinery (Hildebrand, 2002).

Compacted layers in the subsoil can also result from natural soil building processes, for example by translocation and accumulation of clay (secondary Pseudogley), of sesquioxides and organic compounds (Podzols) or alternating layers (primary Pseudogley) (Roth, 2002).

Table 4.2 summarizes soil properties and land-uses favoring soil compaction and soil types where natural soil compaction can occur.

Table 4.2 Factors favoring soil compaction

Soil properties	<ul style="list-style-type: none"> • Soils rich in silt and poor in clay, • Low aggregate stability, • Low natural bulk density, • High soil water content during compaction.
Land-use	<ul style="list-style-type: none"> • Agricultural fields, esp. potatoes, sugar beet, corn and grain, • Intensely used pastures, esp. in alpine regions, • Forests where heavy harvesting machinery is used.
Soil type	<ul style="list-style-type: none"> • Podzol, • Pseudogley, • Organic soils.

Table 4.3 Classification of bulk density (after AG Boden, 1994).

Bulk density [g/cm ³]	Degree of compaction
< 1.25	very low
1.25 - 1.45	low
1.45 - 1.65	medium
1.65 - 1.85	high
> 1.85	very high

Evaluation in the field Soil compaction can be determined from bulk density or soil resistance measurements. We measured bulk density from undisturbed core tube samples of a 100 cm³ volume. Three samples were taken from every horizon of all soil pit profiles. Classes of bulk densities and the corresponding degree of soil compaction are listed in Table 4.3. Soil resistance is measured with cone penetrometers. Hand penetrometers or pocket knives allow a fast identification of compacted layers like plow pans.

In the Ror and Isert catchment top soils showed very low to medium compaction. No difference was found between land-use “meadow” and “field” but top soils under “forest” had lower bulk densities (very low to low degree of compaction). Therefore compaction of the top soil is not a relevant factor in reducing infiltration capacity in the two catchments.

Bulk densities were higher in the sub-soil (B-horizon) with dominantly medium degree of compaction. Only in forested soils very low or low compaction was found in the sub-soil while on land-use “meadow” occasionally even high to very high compaction occurred. The two core tube samples taken below 1 m soil depth had a bulk density of 2 g/cm³ and therefore a very high degree of compaction. No significant difference in bulk density distribution was found between the two catchments.

4.3.3.2 Soil surface sealing

On soils with low vegetation cover, the kinetic energy of raindrops can disintegrate unstable soil aggregates. The disintegrated particles form a thin crust of low porosity and conductivity on the soil surface and/or are clogging soil macropores. Both processes can reduce infiltration significantly in otherwise well permeable soils. This process is called soil surface sealing. Roth (2002) gives an extensive overview over the processes leading to soil surface sealing and the governing parameters (Table 4.4).

Table 4.4 Processes and parameters leading to soil surface sealing

Soil surface sealing originates from	Parameters enhancing soil surface sealing
Kinetic energy of raindrops on soil particles	<ul style="list-style-type: none"> • High rainfall intensity, • Low vegetation cover (< 50%), • Smooth surface.
Instability of aggregates	<ul style="list-style-type: none"> • Clay content < 25%, • $C_{org} < 2\%$, • Low content of exchangeable Ca and sesquioxides, • Low microbiological activity, • Dry soil aggregates, • High Na content.

Evaluation in the field. A widely used approach to estimate aggregate stability is the wet sieve method (e.g. Kemper and Koch, 1966; Murer et al. 1993). A soil sample is shaken up in water and sieved. The part of the initial sample remaining as aggregates larger than 2 mm in diameter is a measure of aggregate stability.



Fig. 4.7 Surface crust formed by soil surface sealing in Isert catchment.

The aggregate stability can also be assessed by placing the soil aggregates in a water filled bucket and observing the decay of the samples. Very stable aggregates do not decay at all, while unstable aggregates totally decay (Mückenhausen, 1975). Soil surface sealing can be detected in the field after intense rainfall events (Figure 4.7). If soil parameters, aggregate stability tests or visual observations suggest soil surface sealing, sprinkling experiments should be conducted. The last two methods were used during the mapping. In the Ror catchment, only one profile with a low

aggregate stability was found and no surface sealing was detected in the catchment after rainfall

events. In the Isert catchment, very low aggregate stability was found on some fields with soil type Parabraunerde. On those fields, a surface crust formed after a heavy rainfall event and Hortonian overland flow can be expected during high intensity rainfall.

4.3.3.3 Soil hydrophobicity

Soil water repellency (hydrophobicity) reduces the infiltration capacity. Hydrophobicity of the soil surface or of the plant cover can lead to Hortonian overland flow. Hydrophobic layers in the soil can form a vertical percolation barrier. The efficiency of hydrophobic layers depends on their spatial continuity and whether macropores bypass them or not.

Water repellency is caused by organic compounds that are bound to soil particles. The compounds originate from water repellent parts of plants or microorganisms like bacteria, fungi, algae but also from higher plants like pine trees, eucalyptus, other evergreen trees, some shrubs, grasses and crops. Doerr et al. (2000) gives a summary of higher plant species associated with water repellency. In middle Europe, water repellency can occur on mat grass (*Nardus stricta*) (Markart and Kohl, 1996) and on heath vegetation with *Calluna vulgaris*, *Erica sp.* and *Vaccinium sp.* Scherrer (1997) also observed water repellency on alpine meadows with a dense near surface root network. Sandy soils (clay content <10%) are most susceptible to soil water repellency (DeBano, 1991). Water repellency often occurs after forest fires or when the soil is very dry. Hydrophobicity in soils is often transient and ceases during the wetting process. Doerr et al. (2000) gives a review of causes and characteristics of soil water repellency and its hydrological consequences.

Evaluation in the field. The WDPT-test (Water Drop Penetration Time) (Letey, 1969) was used to assess soil hydrophobicity. A water drop is placed on a soil surface and the time until its complete penetration is recorded. The soils are classified into different repellency classes according to their WDPT times. The classification of Bisdom et al. (1993) shown in Table 4.5 was used. The

Table 4.5 Classes of water repellency of soils and the corresponding threshold values of WDPT (after Bisdom et al., 1993)

Class	Degree of hydrophobicity	WDPT* [s]
1	Hydrophilic	< 5
2	Slightly hydrophobic	5 - 60
3	Strongly hydrophobic	60 - 600
4	Severely hydrophobic	600 - 3600
5	Extremely hydrophobic	> 3600

* Water drop penetration time

hydrophobicity of class 4 and 5 is persistent. For class 3 the transient hydrophobicity might cause temporary HOF at the beginning of an event. Hydrophobicity was observed neither in the Ror nor in the Isert catchment.

4.3.4 Hydromorphic features

Above layers with reduced permeability, saturated zones might develop and persist for some time. Therefore layers with reduced permeabilities might be inferred from the existence of temporary saturated zones in a soil profile.

Permanent water tables close to the surface can be seen directly in soil profiles or soil cores (water emerging from profile, building of a water table in the profile or loss of soil core during drilling), while periodically saturated horizons have to be identified indirectly through hydromorphologic features.

In most cases, often or permanently saturated soil horizons suffer a shortage in oxygen, resulting in chemical reduction of iron- and manganese oxides and changes of soil colour. Soil horizons with a permanent shortage of oxygen are either bleached because of depletion of iron and manganese or are grey with blueish and greenish mottles originating from different ferric compounds. Occasionally they can be black due to formation of iron sulfides. A low chroma matrix (Munsell chroma < 3) is typical for such horizons (Veneman et al., 1998).

In temporarily saturated horizons, chemical reduction alternates with oxidation. Concentrations of iron and manganese (black and rusty mottles) are surrounded by a bleached matrix, the resulting mixture of grey and yellow colours is known as mottling. In soils with low hydraulic conductivity, the iron and manganese concentrations are small and widespread, while in highly permeable soils large concentrations (from several mm to cm in diameter up to ironpan horizons) can be found (Schachtschabel et al., 1998). The concentrations and rusty mottles are deposited mainly on the surface of soil aggregates if the saturation is caused by rising groundwater levels (soil type “Gley”) and inside the soil aggregates if the saturation occurs in impervious layers in which drainage is restricted (soil type “Pseudogley”).

There are some limitations to identify the present soil saturation regime from soil colour. Natural soil colour (e.g. grey bedrock material) sometimes makes it difficult to identify hydromorphological features. If the groundwater is oxygen rich, strong mottling can occur in permanently saturated layers. Also if iron and manganese are not present, soils do not show hydromorphologic features although they are often saturated. And finally hydromorphologic features may be relicts from previous periods and do not reflect present hydrology.

Frequently or permanently saturated areas can also be identified by water loving plant communities. The wetness index of Ellenberg (1991) may be used to identify water loving plant species. Plant species with a wetness index of 8 or 9 for example, grow on often saturated soil.

Evaluation in the field. Hydromorphologic features and soil colour indicate how often a soil layer is saturated (e.g. Moore, 1974) and help to identify impervious layers with restricted drainage. In Table 4.6 different classes of soil saturation and the corresponding hydromorphological features are listed.

Table 4.6 *Hydromorphological features (changed from BGS, 1992)*

Degree of saturation	Horizon symbol	Hydromorphological features
Always saturated	r	<ul style="list-style-type: none"> • Grey, grey-blueish or black colour, • Rusty mottles only as pore linings.
Often saturated	gg	<ul style="list-style-type: none"> • Strong rusty mottling, • > 3% area of rusty mottles, • Matrix between mottles is grey (chroma 1 - 2).
Sometimes saturated	g	<ul style="list-style-type: none"> • Moderate rusty mottling, • < 3% area of rusty mottles, • Matrix between mottles is brownish (chroma 3 - 4).
Seldom saturated	(g)	<ul style="list-style-type: none"> • Weak rusty mottling, • Rusty mottles often only inside aggregates.
Rarely or never saturated		<ul style="list-style-type: none"> • No rusty mottling.



Fig. 4.8 *Soil profile P 23 in Ror catchment. Grey colour and rusty mottles indicate frequent saturation of subsoil.*

In the Ror catchment hydromorphological features were found in most soil profiles. Those features were used as a key parameter to determine the depth of the impervious layer and the storage capacity of the soil. In the Isert catchment most soils did not show any hydromorphological features. An exception are the mostly drained soils in the riparian zone influenced by groundwater. Figure 4.8 gives an example of a soil profile in the Ror catchment, where the grey colour of reduction and rusty mottling was found below 20 cm soil depth.

4.3.5 Soil morphology

Instead of determining matrix permeability from soil texture, bulk density and macroporosity which is time consuming, some researchers suggest to look at the morphology of large soil blocks or aggregates instead. In most soils individual mineral grains are bound together as aggregates. Soil morphology describes the shape, size and bedding of these aggregates as well as the micro- and macropores between the aggregates and so contains much information about matrix properties, soil porosity and degree of soil compaction. Since soil morphology characterizes water flow through the soil, some workers tried to quantify soil morphology and relate it to hydraulic properties (e.g. Lin et al., 1999 a, b; Tenholtern et al., 1993).

Evaluation in the field. Harrach (1984) introduced the term packing density to quantify soil morphology. Packing densities range from (1) very loosely packed (very high k_{sat}) to (5) very densely packed (very low k_{sat}). The classification depends on (1) size of aggregates, (2) aggregate stability, (3) bedding of aggregates, (4) resistance to penetration and (5) amount of macropores. Root distribution and shape of aggregates can be used as additional information. The method is described in more detail in Tenholtern et al. (1993) and DIN 19682-10.

It was difficult to accurately estimate the packing density for each horizon in the soil profiles in Ror and Isert. Packing density is easily underestimated in wet and overestimated in dry soils. No close relationship between packing density and macroporosity was found. Therefore this method was not used for the process determination.

4.3.6 Sprinkling and infiltration experiments

Sprinkling and infiltration experiments allow a direct determination of infiltration or vertical flow capacities.

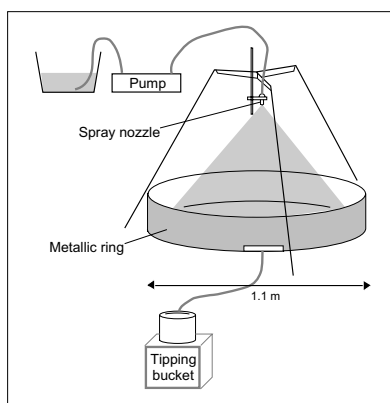


Fig. 4.9 The IHW sprinkling device.

Sprinkling experiments. The IHW sprinkling device (Figure 4.9) allows continuous sprinkling with intensities between 50 and 150 mm/h of a 1 m² circular area. A metallic ring is driven 10 cm deep into the soil to enclose the sprinkling area. The transition between soil and the ring is sealed with clay. Surface runoff leaves the ring through an outlet at the lowest point and is measured with a tipping bucket. Soil moisture is measured with a TDR probe and dye tracer can be added to the sprinkling water to visualize flow paths.

Infiltration experiment. On flat areas, the infiltration rate can be estimated with a double-ring infiltrometer (Figure 4.10). An inner ($d = 30$ cm) and an outer ring ($d = 50$ cm) are driven into the soil and filled with water. Changes in water level in the inner ring allow the estimation of the infiltration rate. Natural infiltration rates are largely overestimated with this method but it allows a fast comparison between different sites.



Fig. 4.10 Double-ring infiltrometer.

4.3.7 Lateral flow capacity

On inclined areas the infiltrated water can flow laterally in the soil if there is a layer with a reduced vertical permeability. If the lateral flow capacity is high, fast subsurface flow will occur and contribute to flood runoff. This lateral drainage can be so effective that even during extreme rainfall events the soil will not saturate. If the lateral flow capacity of the soil is lower, the soil saturates up to the surface during flood events and overland flow occurs. However, lateral flow can influence the drainage of such areas.

A high lateral flow capacity requires preferential lateral flowpaths, like pipes and highly permeable layers sufficient in length to influence the flow process on the hillslope scale. Jones (1990) gives an overview of the processes leading to pipe formation by subsoil erosion in humid lands and their hydrological effects. Pipes are often formed in a layer with a lateral permeability and a hydraulic gradient high enough to permit significant amounts of lateral throughflow above a layer with marked reduction in vertical permeability. Pipe initiation is further enhanced in horizons with low aggregate stability and soils with vertical flow (e.g. through cracks). Podzol soils are susceptible to piping. Pipe formation is enhanced in humid regions where frequent high intensity rainfall events occur.

Layers in the soil or geological underground with a higher permeability than layers below or above can occur in alternating deposits, at the soil bedrock interface or through bedrock weathering processes (Scherrer, 1997).

Subsurface flow occurs also in man-made drainage systems. These systems react fast and strong to precipitation.

Evaluation in the field. Preferential lateral flowpaths are difficult to find. They can sometimes be identified at the hillslope scale by depressions of collapsed pipes or by observing return flow during or after rainfall events. Well suited for the identification but time consuming are large scale sprinkling and tracer experiments. Geophysical methods might also be useful for the identification. Preferential lateral flowpaths in the bedrock can sometimes be found in geological outcrops located in or near the catchment. Table 4.7 lists parameters giving evidence of preferential lateral flowpaths.

Table 4.7 Type of preferential flowpaths and parameters indicating their existence.

Flow path	Parameters indicating preferential flowpaths
Pipes	<ul style="list-style-type: none"> • Surface near animal burrows, moleholes, etc., • Depressions caused by collapse of eroded pipes, • Soil with easily erodible horizon over horizon with reduced vertical permeability and soils with very preferential infiltration, • Soil type Podzol, • Forest with many decayed root channels.
High permeable layers	<ul style="list-style-type: none"> • Geological outcrops, • Geophysical methods, • Bedrock with coarse grained weathering products.
Tile drains	<ul style="list-style-type: none"> • Plans of drainage system, • Information from land owner, • Shaft-covers, exit of tile drains in river, etc.
All	<ul style="list-style-type: none"> • Observation of return flow during an event, • Observation of return flow after an event (esp. at base of hillslopes), • Springs, • Tracer and sprinkling experiments on the hillslope scale.

In the Ror and Isert catchment tile drains are the most important lateral flow paths. No large pipes or highly permeable layers were identified. Smaller pipes were found on the steep slopes of the drumlins, especially when forested. Whether the capacity of these pipes is high enough to prevent the soil from saturating could not be determined directly from the soil profiles, but only from soil water table measurements or large scale sprinkling experiments.

4.4 Dominant runoff processes

On a given site more than one of several runoff processes can occur; the dominant runoff process is the process that contributes most to runoff during a storm event. It is distinguished between high intensity, short duration and low intensity, large amount rainfall events, which might lead to different dominant runoff processes. For the Ror and Isert catchments a rainfall intensity of 20 mm/h was chosen as the boundary intensity between the two types of rainfall events. Other workers found a change in runoff process at higher intensities (e.g. Buttle et al. 2004 at 50 mm/h).

The following dominant runoff processes are distinguished: Hortonian Overland Flow **HOF**, Saturated Overland Flow **SOF**, fast Subsurface Flow **SSF** and slow subsurface flow or Deep Percolation **DP**. This classification accounts for the flow paths of rainwater to the stream as well as its contribution and timing to the storm hydrograph. The fast subsurface flow is further divided into natural subsurface flow on hillslopes and tile drain flow **D** (Figure 4.11).

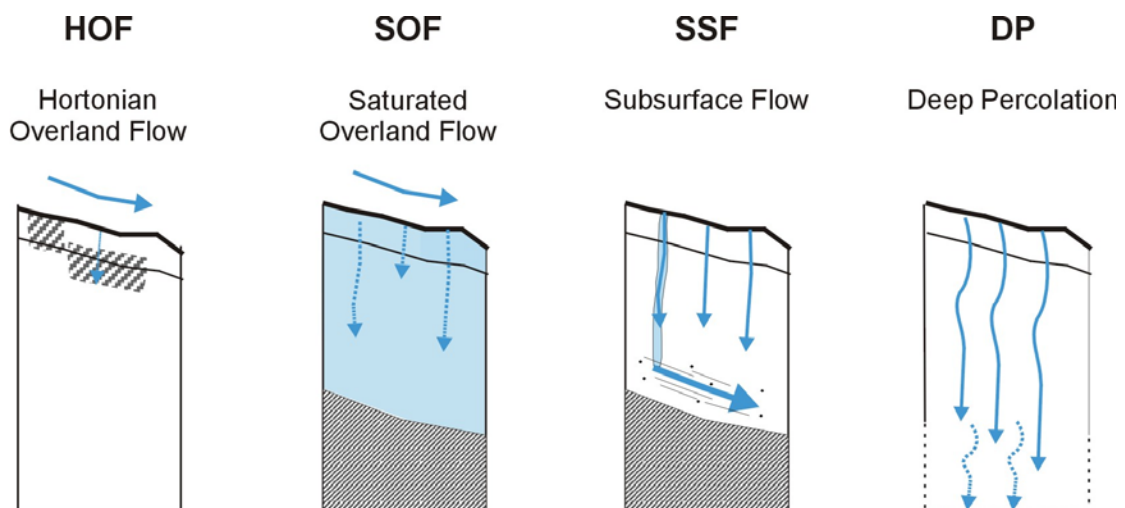


Fig. 4.11 Dominant runoff processes and the corresponding reaction during flood events.

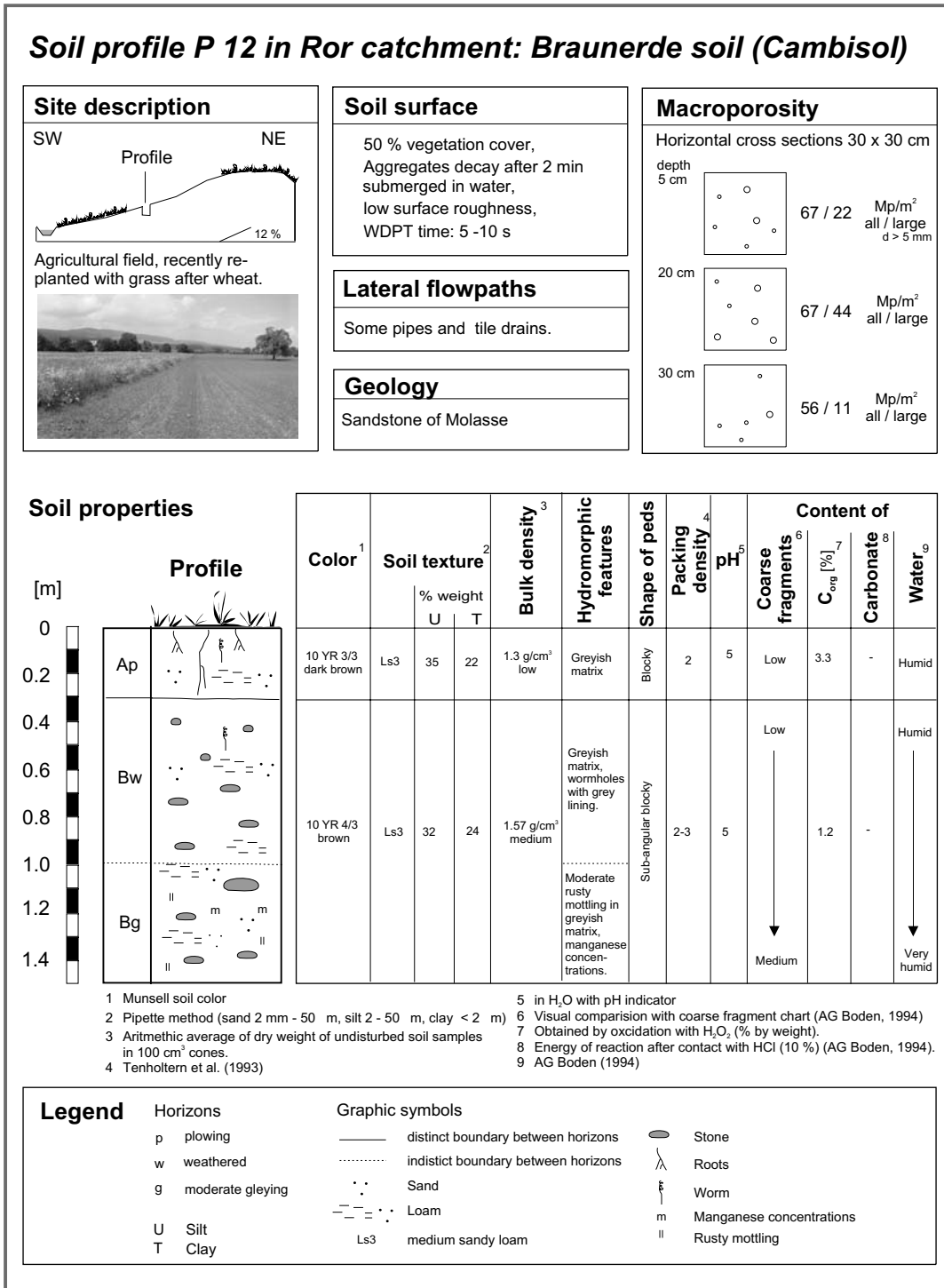
The dominant runoff processes can occur with different process intensities. The storage capacities of the different process intensities have to be defined previous to the mapping (Table 4.8).

Table 4.8 Dominant runoff processes and process intensities.

Process and process intensity		Assigned storage capacity
Hortonian overland flow (infiltration excess overland flow)		
HOF 1	no infiltration is possible (sealed areas)	0 mm
HOF 2	limited infiltration is possible	0 mm
Saturated overland flow due to saturation of the soil. Storage capacity of soil is		
SOF 1	low	0 - 40 mm
SOF 2	medium	40 - 100 mm
SOF 3	large	100 - 200 mm
Flat or gently sloped tile drained areas. Storage capacity of soil is		
D 1	low	0 - 40 mm
D 2	medium	40 - 100 mm
D 3	large	100 - 200 mm
Fast subsurface flow in hillslopes. Lateral flow capacity is high and storage capacity of soil is		
SSF 1	low	0 - 40 mm
SSF 2	medium	40 - 100 mm
SSF 3	large	100 - 200 mm
DP	Slow subsurface flow or groundwater recharge and very large storage capacity of soil.	> 200 mm

4.5 Determination of the dominant runoff processes on a soil profile

The dominant runoff processes were determined for all soil profiles, based on the insight and the methods introduced in the previous chapters. For the soil profile P 12 (location see Figure A.1) in the Ror catchment, the determination of the dominant runoff process from soil structural features and soil properties will be demonstrated. All data sampled for the profile is summarized in Figure 4.12



Soil properties

Color ¹	Soil texture ²		Bulk density ³	Hydromorphic features	Shape of peds	Packing density ⁴	pH ⁵	Content of			
	U	T						Coarse fragments ⁶	C _{org} [%] ⁷	Carbonate ⁸	Water ⁹
10 YR 3/3 dark brown	Ls3	35 22	1.3 g/cm ³ low	Greyish matrix	Blocky	2	5	Low	3.3	-	Humid
10 YR 4/3 brown	Ls3	32 24	1.57 g/cm ³ medium	Greyish matrix, wormholes with grey lining.	Sub-angular blocky	2-3	5	Low	1.2	-	Humid
				Moderate rusty mottling in greyish matrix, manganese concentrations.				Medium			Very humid

1 Munsell soil color
 2 Pipette method (sand 2 mm - 50 μm, silt 2 - 50 μm, clay < 2 μm)
 3 Arithmetic average of dry weight of undisturbed soil samples in 100 cm³ cones.
 4 Tenholtern et al. (1993)
 5 in H₂O with pH indicator
 6 Visual comparison with coarse fragment chart (AG Boden, 1994)
 7 Obtained by oxidation with H₂O₂ (% by weight).
 8 Energy of reaction after contact with HCl (10 %) (AG Boden, 1994).
 9 AG Boden (1994)

Legend

Horizons	Graphic symbols	
p plowing	— distinct boundary between horizons	● Stone
w weathered indistinct boundary between horizons	√ Roots
g moderate gleying	••• Sand	⋈ Worm
U Silt	— — — Loam	m Manganese concentrations
T Clay	Ls3 medium sandy loam	Rusty mottling

Fig. 4.12 Field and laboratory data for soil profile P 12 in the Ror catchment.

Estimation of infiltration capacity. As the soil profile is located in an agricultural field, recently planted with grass after wheat, top soil compaction cannot be excluded. With a vegetation cover below 50%, soil surface sealing might occur. In Table 4.9 all processes hindering infiltration are listed and evaluated.

Table 4.9 Evaluation of processes hindering infiltration in example of profile P 28.

	Parameters that		leading to HOF as dominant runoff process if rainfall intensities are	
	decrease infiltration	increase infiltration	low < 20 mm/h	high > 20 mm/h
Macroporosity and matrix permeability		<ul style="list-style-type: none"> • Macroporosity: "high macroporosity". • Matrix permeability medium, • Low bulk density. 	no	no
Soil surface sealing	<ul style="list-style-type: none"> • 50 % vegetation cover, • Low aggregate stability, • < 25 % clay, • Low surface roughness, • < 1 % carbonate. 	<ul style="list-style-type: none"> • $C_{org} > 2.5 \%$, • Macroporosity high, • No visible surface crust. 	no	possible
Compaction of top soil	<ul style="list-style-type: none"> • Low aggregate stability, 	<ul style="list-style-type: none"> • Low bulk density, • Packing density 2. 	no	no
Hydrophobic surface		<ul style="list-style-type: none"> • Slightly hydrophobic, • No hydrophobic plants. 	no	no

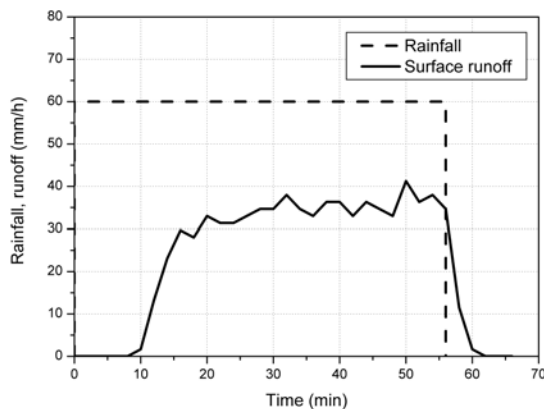


Fig. 4.13 Sprinkling experiment.

Table 4.9 shows that low intensity rainfall will infiltrate. Surface sealing and HOF 2 might occur during high rainfall intensities if the vegetation cover is low. No top soil compaction was observed but under different crops (e.g. corn) and in wet years compaction might occur. The plot was sprinkled for 1 h with an intensity of 60 mm/h (Figure 4.13).

In less than 10 min surface runoff occurred with a runoff coefficient rising fast to 0.5 - 0.6. The final infiltration rate was 25 mm/h. Therefore, during high intensity rainfall HOF 2 can occur.

Estimation of vertical flow capacity. In 1 m depth, rusty mottling and a greyish soil matrix indicate periodic saturation of the soil. At this depth, permeabilities are low and vertical percolation is inhibited. A first, but less effective barrier to vertical percolation is the plow horizon at 30 cm depth. Although no actual plow pan exists, bulk densities increase and macroporosity is reduced. For high intensity rainfall and wet antecedent conditions this horizon will be the actual barrier to vertical percolation.

Storage capacity of soil. The A-horizon (top 30 cm) is of soil texture “medium clayey loam” and has a low bulk density. According to AG Boden (1994), this corresponds to a porosity of 7 %, which is available for fast drainage of water and the storage of ground- or stagnic water in the soil (soil moisture is assumed to be at field capacity before event). Therefore 21 mm of rainfall can be stored in the A-horizon. The B_w horizon (30 -100 cm) is of soil texture “slightly sandy loam” with a medium bulk density. This corresponds to 6.5 % porosity or 45.5 mm of water storage capacity. Part of the slow drainable porosity might also be available for water storage during dry antecedent conditions in the top soil. For high intensity rainfall, the storage capacity of the soil is around 20 mm, for low intensity rainfall around 67 mm.

Lateral Flow paths. The field is not systematically drained but single tile drains exist. Also some animal burrows can be found. The lateral flow capacity can be classified as moderate.

The final process evaluation for Profile P 12 is given in Table 4.10.

Table 4.10 Process evaluation.

Rainfall intensity	Process evaluation	
low	All the water infiltrates during low intensity rainfall. Barriers to vertical percolation exist and the lateral flow capacity is only moderate. Therefore SOF is the dominant process with an estimated storage volume of the soil of 60 - 70 mm. Therefore the process intensity is 2.	SOF 2
high	If vegetation cover is low, HOF 2 might occur during high intensity rainfall, otherwise the water infiltrates resulting in SOF 1.	HOF 2 or SOF 1

4.6 Process decision scheme

In the previous chapter (Ch.), it was shown that the dominant runoff process can be determined on the plot scale. Scherrer and Naef (2003) developed process decision schemes where all the necessary steps and decisions for a systematic determination of the dominant runoff process are summarized. Different decision schemes for different land-use types, rainfall intensities and soils influenced by groundwater were developed. The schemes capture in detail the very complex nature of runoff formation. Key points are soil parameters like macroporosity, matrix permeability or the existence of lateral flow paths.

As one aim of this study is to automate the process determination using soil maps and other spatial data, the complex schemes had to be generalized (Figure 4.14). Hydrological interpretations were used as key questions like: “Is infiltration inhibited”. Then a description of the factors influencing infiltration capacity is given. For the process determination with the generalized schemes still all information and data contained in the complex schemes can be used. However, key questions of the new schemes can also be answered from available spatial data only. The quality of the process determination then depends on the quality of the available spatial data. Additionally, the insight gained into the runoff formation might be less detailed.

Other advantages of the generalized scheme are that the process determination is easier to understand for workers from neighbouring fields, that new process knowledge can be introduced more easily and that an adaption to different hydrological problems or climatic regions is facilitated. Additionally, the runoff process “drainage from tile drained fields” was introduced into the new scheme.

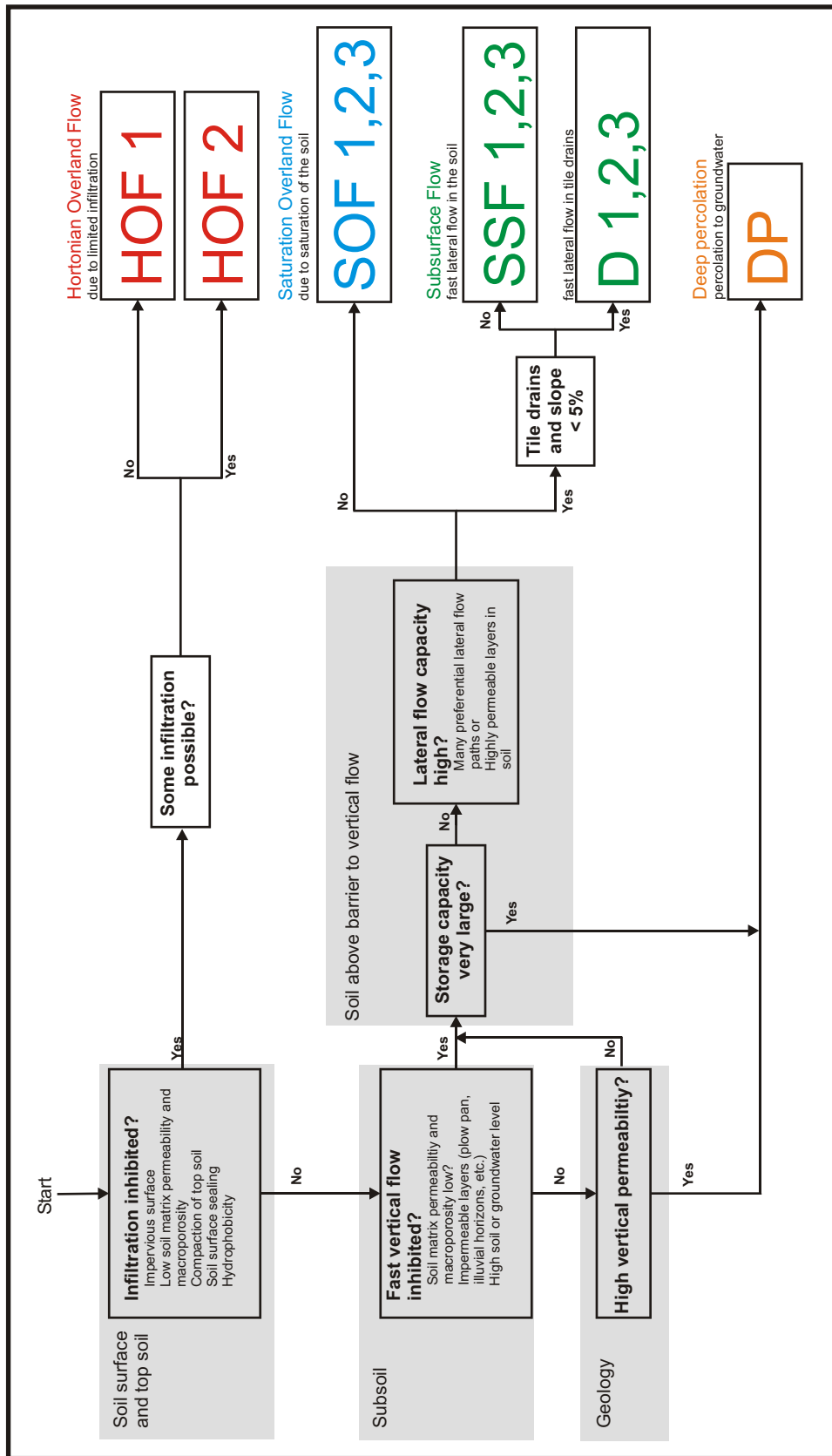


Fig. 4.14 Generalized decision scheme to determine the dominant runoff process on a soil profile.

The first key question that has to be answered for the process determination is: “Is infiltration inhibited?” If the question is answered with “yes”, Hortonian overland flow is the dominant runoff process. The differentiation between HOF 1 and HOF 2 is done according to the amount of water that can still infiltrate. On HOF 1 areas, no water infiltrates, while on HOF 2 areas some infiltration is possible.

If all rainfall can infiltrate, the next key question is: “Is fast vertical flow through the soil profile inhibited?”. If vertical flow is not inhibited and the underlying bedrock is permeable as well, deep percolation to groundwater is the dominant runoff process. If either vertical flow is inhibited or the geology impermeable, the soil above the barrier to vertical flow determines, which runoff process occurs. In soils with a very large storage capacity, deep percolation is the dominant runoff process. If the storage capacity of the soil is not large, the water will either saturate the soil or drain laterally through preferential flow paths. In soils with a low lateral flow capacity, saturated overland flow is the dominant runoff process. A high lateral flow capacity leads to subsurface flow as dominant runoff process. Subsurface flow is further divided into tile drain flow if the lateral flow paths are tile drains and slope is below 5 % and natural subsurface flow on hillslopes.

Each soil profile has to be assigned to one dominant runoff process and process intensity. To account for the spatial variability within on runoff process each process intensity covers a range of storage capacities of the soil (e.g. SOF 1 0 to 40 mm). Differently expressed, soils of process SOF 1 have a mean storage capacity of 20 mm with a deviation of ± 20 mm.

The process determination on the plot scale does not consider influences through neighbouring process areas or whether the area is connected to a stream or channel or not. The determined dominant runoff process during a flood event therefore corresponds to the active area of Ambrose (2004). However, the “active” area need not necessarily also be the contributing area. Ways around this problem are:

(1) In small, well drained catchments with a favourable runoff process distribution (e.g. no HOF 1 area upslope of a DP area) the difference between active and contributing area is very small during large flood events and can therefore be ignored. This assumption is valid for the two experimental catchments investigated in this study.

(2) During the delineation of the dominant runoff processes on the catchment scale, the influence between neighbouring areas is considered using the process catena approach (see Chapter 6.4). This can lead to a re-classification of process areas and a deviation between the actual process determined on the plot scale from soil data and the mapped process on the catchment scale. For practical purposes like flood discharge estimations, this approach works quite well. However,

since one aim of this study was to automate the process determination using soil maps, the approach of re-classification was used very restrictively.

(3) The interaction between neighbouring process areas is captured using a distributed rainfall runoff model. This approach was not used or tested in the framework of this study.

5 Automated process identification

5.1 Introduction

The determination of the dominant runoff processes on a soil profile in combination with sprinkling and infiltration experiments is time consuming. This work is substantially reduced if the dominant runoff process or important parameters for the process identification can be determined directly from maps and digital spatial data. Soil maps are the most important source of data for the determination of dominant runoff processes, followed by maps of geology, land-use and topography. To this purpose the available data from the Ror catchment was hydrologically interpreted and transformed into a body of rules that allows an automated determination of the dominant runoff processes using GIS.

5.2 Hydrological interpretation of soil maps and other spatial data

5.2.1 General information

The dominant runoff processes in a catchment can change within short distances depending on relief, parent material, land-use, etc. Therefore highly resolved data is needed. For Kanton Zürich an excellent soil map for agricultural areas with a scale of 1:5'000 (FAL, 1997) exists, containing information about soil types, soil water regimes, sub-soil types, soil texture and other parameters. How this information was transformed into a body of rules is described in the following. For the transformation a hydrological interpretation of the available data, especially the soil map, had to be conducted. The hydrological interpretation bases on observations made and experiences gained during the process determination on the soil profiles in the Ror and Isert catchment.

5.2.2 Soil type

Soil maps are usually soil type maps. The soil types displayed in soil maps are not standardized, the classification system and nomenclature of soil types differ considerably between countries. Soils are classified according to factors influencing soil formation (e.g. climate, vegetation zones), soil-forming processes (e.g. humus accumulation, translocation of minerals) or soil properties (e.g. diagnostic horizons, colour, soil chemical and physical properties). The "Soil Taxonomy" used in the USA (USDA, 1975) is based on soil properties only, while the FAO (FAO/UNESCO, 1988) and the Swiss / German (BGS, 1992 / AG Boden, 1994) classification systems incorporate all the three parameters. Here Swiss soil types are used, the corresponding soil types of the German, the

FAO and the Soil Taxonomy classifications also are given. Due to the totally different classification concepts, an exact assignment is not always possible.

The Swiss classification system has four levels. The highest level defines the soil water regime and distinguishes between percolated soils, soils with poor drainage, and soils influenced by groundwater. The second level differentiates between the amount of relicts of parent material, organic matter and secondary minerals. The third level bases on chemical and mineralogical components of the parent material and of the newly formed secondary minerals in the soil. On the lowest level special soil-forming processes like clay translocation or aluminium leaching are used for the classification. The information contained in the soil type classification is used for the process evaluation. An overview of the most important soil types in Switzerland and their hydrological reaction is given in Table 5.1.

Table 5.1 The most important soil types in Switzerland and their hydrological reaction. Corresponding soil types of the German (G), the FAO (F) and Soil Taxonomy (S) classification are given as well.

Soil group and general description			
Soil type	Soil description	Hydrological Interpretation	Nomenclature
(A)-C soils, beginning of soil formation, A horizon very thin or missing.			
Gesteinsboden (Silikat-, Misch-, Karbonat-, etc.)		Very low storage volume of soil. Underlying geology determines runoff process.	G: Rohböden, Syrosem F: Lithic Leptosol, Arenosol S: Entisol
A-C soils are poorly developed soils. A horizon over poorly or unweathered bedrock.			
Ranker	Bedrock without carbonate.	Low storage volume of soil. A Horizon often very permeable and with lateral flowpaths. If the underlying geology is impermeable A horizon either saturates and SOF1 occurs or water flows laterally as SSF1. If the underlying geology is permeable the water flows as DP or SSF in the bedrock.	G: Ranker (consolidated bedrock) and Regosol (unconsolidated bedrock) F: Leptosol, Regosol S: Inceptisols with prefix "hapl",
Regosol	Bedrock containing some carbonate.		G: Pararendzina, Ranker-Rendzina
Rendzina	Bedrock rich in carbonate.		G: Rendzina F: Rendzic Leptosol S: Rendoll
Ah-Bw-C soils, Bw horizon is weathering product and its brown colour is caused by fine spread ironoxides.			
Braunerde	A and B horizon carbonate free, neutral to slightly acidic and have a high base saturation.	Soil with medium to large storage capacity. Suitable for earthworms and for every type of land-use. All runoff processes possible.	G: Braunerde F: Eutric Cambisol S: Ochrepts
Kalkbraunerde	Secondary carbonates in B and sometimes A horizon.	Carbonate content enhances aggregate stability.	G: Kalkbraunerde F: Calcaric Cambisol
Saure Braunerde	pH < 5, lower base saturation, higher Al- activity.	Acidity makes it less suitable for earthworms.	G: Braunerde

Table 5.1 The most important soil types in Switzerland and their hydrological reaction. Corresponding soil types of the German (G), the FAO (F) and Soil Taxonomy (S) classification are given as well.

Soil group and general description			
Soil type	Soil description	Hydrological Interpretation	Nomenclature
A-AE-It...soils with illuvial horizon in which silicate clays have accumulated under eluvial horizon with clay and carbonate depletion.			
Parabraunerde		Like Braunerde but often low aggregate stability in top soil due to clay and carbonate depletion. Soil surface sealing leading to HOF2 can occur. Illuvial horizon can be barrier to vertical percolation, limiting the storage volume of the soil.	G: Parabraunerde, Lessivé F: Luvisol, Podzolvisol S: Boralf, Udalf
O-Ah-E-lfe... soils with illuvial horizon in which organic matter and oxides of aluminium and or iron oxides have accumulated under an eluvial horizon which is light in colour. They form mostly on coarse-texture, acid, parent materials subject to ready leaching.			
Humuspodzol	Translocation of organic matter only.	Permeable to very permeable soil matrix but reduced suitability for earthworms due to acidity. Dominant land-use is forest. Root channels build macropore system and preferential flow paths. SSF or DP occur.	G: Humuspodsol
Braunpodzol	Eluvial horizon barely visible, subsoil like Saure Braunerde.		G: Braunerde-Podsol
Eisenpodzol	Translocation of iron and organic matter.	Illuvial horizon (e.g. Ortstein) can be barrier to vertical percolation.	G: Eisenhumuspodsol F: Podzol S: Spodsol (Orthod)
Ah-...-Bgg-... soils with poor drainage. A horizon with very low permeability (G:Sd) prevents percolation of water. During wet periods water table builds above this layer (G:Sw). No groundwater is present. Diagnostics Bgg horizons shows rusty and grey mottling.			
Braunerde-Pseudogley	Upper limit of Bgg horizon below 40 cm and above 60 cm depth.	Barrier to vertical percolation exists and saturation of soil with SOF occurs. In case of lateral flowpaths above Sd SSF can occur. Low to medium storage volume of soil. Soil sometimes saturated.	G: Braunerde-Pseudogley
Pseudogley	Bgg horizon above 40 cm depth.	Very low storage volume of soil and soil often saturated.	G: Pseudogley F: Planosol, Gleysol S: Prefix "Aqu"
Ah-...-Bgg-Br...soils influenced by the varying groundwater level (G: Ah-Go-Gr profile).			
Braunerde-Gley	Periodical saturation of subsoil. Soil matrix brown, rusty mottling increases with depth. Top 40 cm like Braunerde.	Soils with shorter or longer periods of saturation. SOF dominates. Soil types differ in storage volume and duration of saturation.	G: Braunerde-Gley F: Gleyic Cambisol
Buntgley	Periods of saturation of soil alternate with lower water tables. Soil matrix grey, rusty mottling in zone of fluctuation of water table. Upper limit of Bgg horizon below 40 cm and above 60 cm depth.		G: Gley F: Gleysol S: Prefix "Aqu"
Fahlgley	Soil most of the time saturated. Grey, green and blue colours of reduction dominate. Br horizon above 60 cm depth.		G: Nassgley

5.2.3 Soil water regime and storage capacity

The Swiss classification scheme distinguishes between three classes of soil water regimes that are further divided according to the characteristic and depth of hydromorphic layers. In addition, different soil depths usable for plants are allotted, resulting in 28 sub-groups of soil water regimes and storage capacity. Table 5.2 summarizes the sub-groups and their hydrological interpretation.

Table 5.2 Sub-groups of soil water regimes (a to z) defined in the soil map of the Kanton Zürich (FAL, 1997) and our hydrological interpretation. Dark grey indicates SOF 1, medium grey SOF 2 and light grey colour SOF 3. These processes occur if no preferential lateral flowpaths are present and no HOF 2 occurs.

Soil water regime		Soil depth usable by plants ¹ [cm]				
		> 100	70 - 100	50 - 70	30 - 50	< 30
Vertically percolated soils.	Normal permeability.	a	b	c	d	e
	Slightly poor drainage		f	g	h	i
	Slightly influenced by groundwater		k	l	m	n
Soils with poor drainage	Seldom saturated		o	o	p	p
	Often saturated				q	r
Soils influenced by groundwater	Seldom saturated		s	t	u	u
	Often saturated			v	w	
	Most of the time saturated				x	y
	Permanently saturated					z

¹Total soil depth minus content of coarse fragments minus compacted or permanently saturated zones

5.2.4 Soil sub-types

The Swiss classification further divides the soil types in soil sub-types. Table 5.7 lists the parameters used for this soil sub-type classification that are relevant for the DRP mapping. Not all parameters are determined for all soil map units. Sometimes soils were allocated to the closest soil sub-type, even if not all of the soil sub-type parameters did match, instead of creating a new soil map unit.

Table 5.3 *Hydrological Interpretation of parameters used for the soil sub-type classification of the soil map of the Kanton Zürich 1:5'000.*

Parameter	Values	Hydrological interpretation
Layering	<ul style="list-style-type: none"> Eroded, Extremely permeable underground, others. 	<ul style="list-style-type: none"> Occurrence of surface runoff, DP possible.
Type of weathering, extreme soil texture	<ul style="list-style-type: none"> Karstic, Extremely sandy, Extremely clayey, others. 	<ul style="list-style-type: none"> DP possible, High matrix permeability, Very low matrix permeability.
pH	<ul style="list-style-type: none"> 6 classes (alkaline to very acidic). 	<ul style="list-style-type: none"> Ecological suitability for earthworms.
Carbonate content	<ul style="list-style-type: none"> 6 classes (partly decarbonated to containing Na). 	<ul style="list-style-type: none"> Aggregate stability and ecological suitability for earthworms:
Soil Peds	<ul style="list-style-type: none"> Unstable aggregates, others. 	<ul style="list-style-type: none"> Aggregate stability.
Bulk density	<ul style="list-style-type: none"> 4 classes (loose to very compacted). 	<ul style="list-style-type: none"> Degree of soil compaction.
Poor drainage	<ul style="list-style-type: none"> 4 classes (slightly to very poorly drained). 	<ul style="list-style-type: none"> Barriers to vertical percolation.
Groundwater changing	<ul style="list-style-type: none"> 6 classes (subsoil humid to extremely gleyic). 	<ul style="list-style-type: none"> Degree of periodical saturation of soil.
Groundwater permanent	<ul style="list-style-type: none"> 5 classes (subsoil wet to swamp). 	<ul style="list-style-type: none"> Degree of permanent saturation of soil.
Tile drains	<ul style="list-style-type: none"> Drained. 	<ul style="list-style-type: none"> Artificial lateral flow paths.

5.2.5 Other information contained in soil map

Soil texture. Soil texture is usually estimated with the finger method. Due to the uncertainties of this method, the soil texture classification in the soil map of the Kanton Zürich (Table 5.4) is relatively coarse. For the texture classes sand and loamy sand, high to very high matrix permeabilities can be expected while for clayey loam to clay the matrix permeabilities are very low (see Chapter 4.3.1). To estimate the matrix permeabilities for the classes sandy loam and loam, a finer differentiation would be necessary.

Table 5.4 Texture classes of the soil map of the Kanton Zürich 1 : 5'000 and the derived matrix permeabilities.

Texture class	Silt [%]	Clay [%]	Matrix permeability
Sand	< 50	< 5	High to very high
Loamy sand		5 - 10	
Sandy loam		10 - 20	Medium to very high
Loam		20 - 30	Low to medium
Clayey loam		30 - 40	
Loamy clay	> 50	40 - 50	Low
Clay		> 50	
Clayey silt		30 - 50	Low to high, depending on soil compaction.
Loamy silt	10 - 30		
Silt	< 10		

Table 5.5 Classes of coarse fragment content.

Coarse fragments class	Vol. %
1	< 5
2	5 - 10
3	10 - 20
4	20 - 30
5	30 - 50
6	> 50

Content of coarse fragments. The soil map of the Kanton Zürich distinguishes between six classes of coarse fragments ($d > 2$ mm) with volumetric percentage between < 5 % to > 50 % (Table 5.5). Coarse fragments limit the storage capacity of the soil, and might enhance the formation of preferential flowpaths.

Biological activity. The biological activity ranges from high to very low (Table 5.6). The worm density contained in the classification is relevant because a high worm density implies a high macroporosity of the soil.

Table 5.6 Classes of biological activity and corresponding worm density.

Biological activity	Worms per m ²
1 high	> 100
2 normal	30 - 100
3 low	10 - 30
4 very low	< 10

5.2.6 Geology, land-use and other information

The dominant runoff processes are also influenced by geology, topography and land-use. Table 5.7 lists the sources of such information.

Table 5.7 Additional information used for the delineation of a dominant runoff process.

Source	Hydrological relevant information
Geological maps	Geological layers, bedrock properties like permeability, strike and fall of layers, position within stratum.
Hydrogeological maps	Permeability of bedrock, depth to groundwater.
Topography	Relief (hillslopes, hollows, flat areas, riparian zones), slope.
Land-use maps	Sealed surfaces, agricultural fields and parameters like crops grown or intensity of use.
Vegetation maps	Plant communities as indicators (e.g. humidity- or wetness indicators).
Forest maps	Vegetation and soils in forested areas.
Historical maps	Former swamps or rivers, land-use changes.
Drainage plans	Tile drains, open ditches and channels, sewer system.
Aerial photography	Actual land-use, soil properties (e.g. colour, wet areas), signs of erosion, gullies, brooks, signs of deposition.

5.3 Set of rules to estimate the DRP from soil map data

The developed set of rules to determine the dominant runoff process consists of two parts. First the susceptibility of the soil to HOF 2 due to limited infiltration is assessed (Table 5.8). Factors limiting infiltration are low matrix permeability in combination with low macroporosity, soil surface sealing, top soil compaction or hydrophobicity. If the soil is susceptible to HOF 2, its actual occurrence depends on additional factors like unfavourable land use, agricultural practises, vegetation cover and high rainfall intensities.

If HOF 2 is not expected, the decision tree introduced in Figure 5.1 has to be used. The first criterium is the soil water regime, followed by the soil sub-type information about soil drainage and groundwater characteristics. Then the existence of tile drains and the permeability of the underlying bedrock is checked.

The set of rules defines the occurrence of HOF, DP, D and SOF or SSF. As it was not possible to infer the existence of natural preferential flowpaths from the soil or geological maps in the Ror catchment, we cannot differentiate between the SOF and SSF process.

Table 5.8 Rules to estimate the susceptibility of the soil to soil surface sealing, top soil compaction, hydrophobic surface and a generally low infiltration capacity. A soil is susceptible to HOF 2 if at least one parameter or a parameter combination given in column 2 to 4 occurs and the parameters in columns 6 and 7 do not occur. Even if the soil is susceptible to HOF 2, it only occurs if land use is unfavourable and rainfall intensities are high.

Process limiting infiltration	Soil type	Soil texture of top soil	Soil sub-type		Soil texture of top soil	Soil sub-type
Soil surface sealing	[T or	IU or U or	ZL ZT or MA or KA]	and not	[tL or IT or T or	ML or MF or MM or MH or O]
Top soil compaction		[cU or IU or U or	L2 or L3 or L4 or ZL]			
Hydrophobic surface			[ML or VS]			
Low infiltration capacity		[L or cL or IC or C]	and [BA 3 or BA 4]	and not		O

Legend		
Soil texture	Organic material	Bulk density
L Loam	ML Mor humus (Rohhumus)	L2 Compacted
U Silt	MF Moder humus	L3 Very compacted
C Clay	MA Low humus content	L4 Extremely compacted
IU Loamy Silt	MM Mull humus	
IC Loamy Clay	MH Rich in humus	Soil aggregates
cL Clayey Loam	O Hydromorph organic material	ZL Unstable aggregates
cU Clayey Silt		ZT Clay skins (cutans)
VS extremely sandy	Soil water	Carbonate content
Soil type	I1 Slightly stagnic	KR Rich in carbonate
T Parabraunerde	G1 Very slightly gleyic	KA Rich in sodium
	G2 Slightly gleyic	

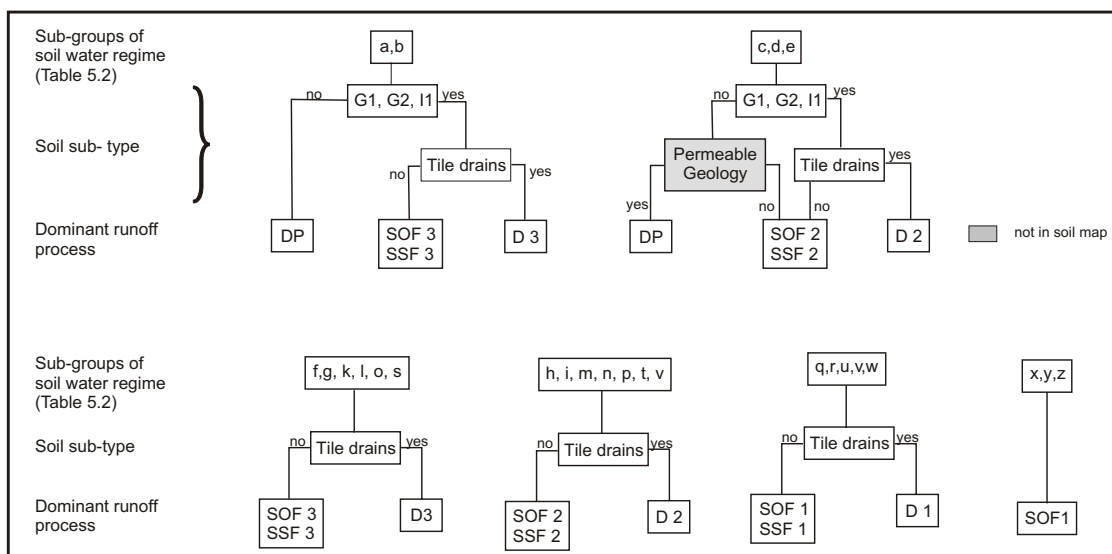


Fig. 5.1 Set of rules to estimate the dominant runoff process from soil map information, if infiltration capacity is sufficient and no HOF 2 does occur.

5.4 Evaluation of DRP set of rules

The dominant runoff process was assessed manually for the 43 soil profiles in the Ror and Isert catchments as described in Chapter 3. They were also determined with the described set of rules. In Table 5.9 the results of the two methods are compared.

Table 5.9 Comparison of process determination on soil profiles in the field and with the set of rules. Gray background indicates matching process determination.

		Dominant runoff process determined from body of rules							
		HOF 2	SOF 1 SSF 1	SOF 2 SSF 2	SOF 3 SSF 3	D 1	D 2	D 3	DP
Dominant runoff process determined from soil profile	HOF 2	2							
	SOF 1		4	2	1				
	SOF 2			7					
	SOF 3			1	5				1
	SSF 1			1					
	SSF 2								
	SSF 3			3	5				
	D 1					5	1		
	D 2						2		
	D 3						1	1	
	DP		1						1

For 76 % of the soil profiles, the set of rules determined the correct process. Deviations were mostly in process intensity. Only in two cases the process determination was wrong. The current set of rules does not yet differentiate between the SOF and SSF process. These results encourage research to design advanced DRP sets of rules.

6 Process delineation in catchments

6.1 Introduction

Methods to determine the dominant runoff processes on the plot scale were introduced in Chapter 4 and 5. The next step is now to determine the spatial distribution of the dominant runoff processes in a catchment. To get a map of dominant runoff processes, spatial data has to be incorporated and the interactions between neighbouring process areas, for example along a hillslope, as well as the topographic control on runoff have to be considered. Figure 6.1 gives a schematic overview of the mapping procedure.

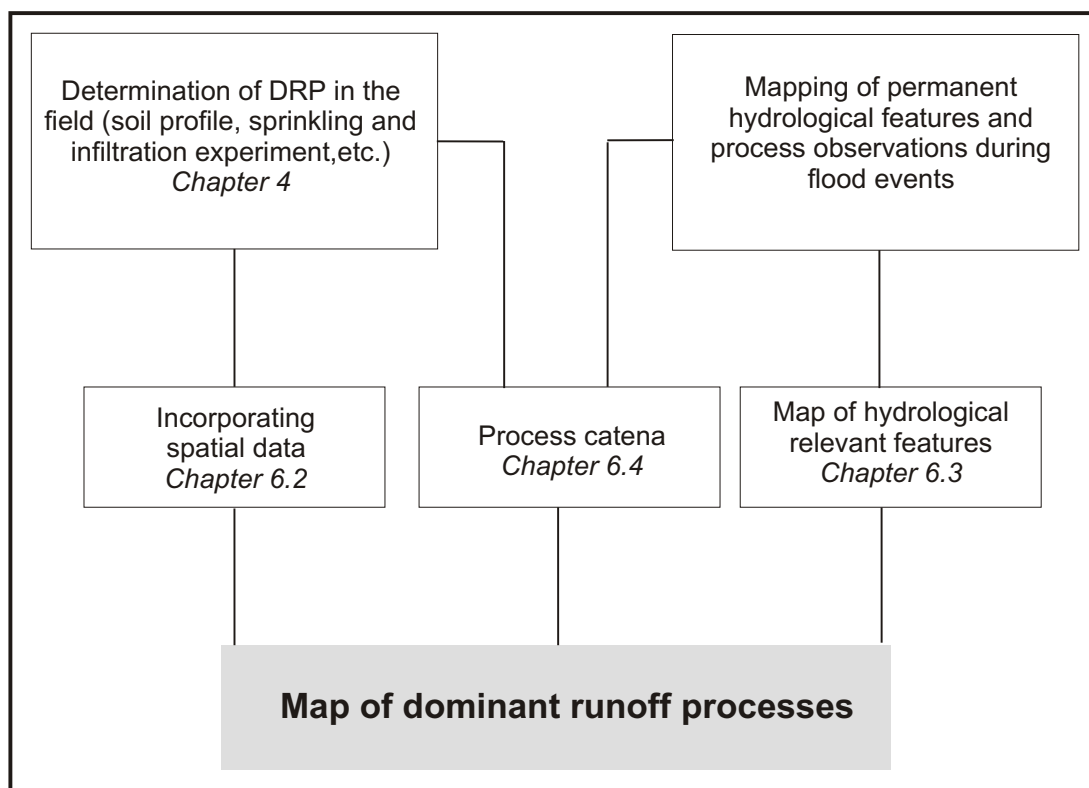


Fig. 6.1 Steps necessary to delineate the dominant runoff processes in a catchment.

On the example of a 500 m x 500 m square within the Ror experimental catchment it will be illustrated, how a DRP map is delineated. Steps necessary to do so after determining the DRP in the field on typical soil profiles are (1) incorporating spatial data, (2) mapping of hydrologically relevant features and (3) incorporating information about the interaction between neighbouring process areas and the topographic control on runoff formation by drawing a process catena. The described mapping approach was then applied to the whole Ror and Isert catchment. These maps

derived manually are then compared to maps automatically delineated with a GIS using the DRP set of rules.

6.2 Incorporating spatial data

For the test square spatial data about geology, soils, land use and tile drains are available (Figure 6.2).

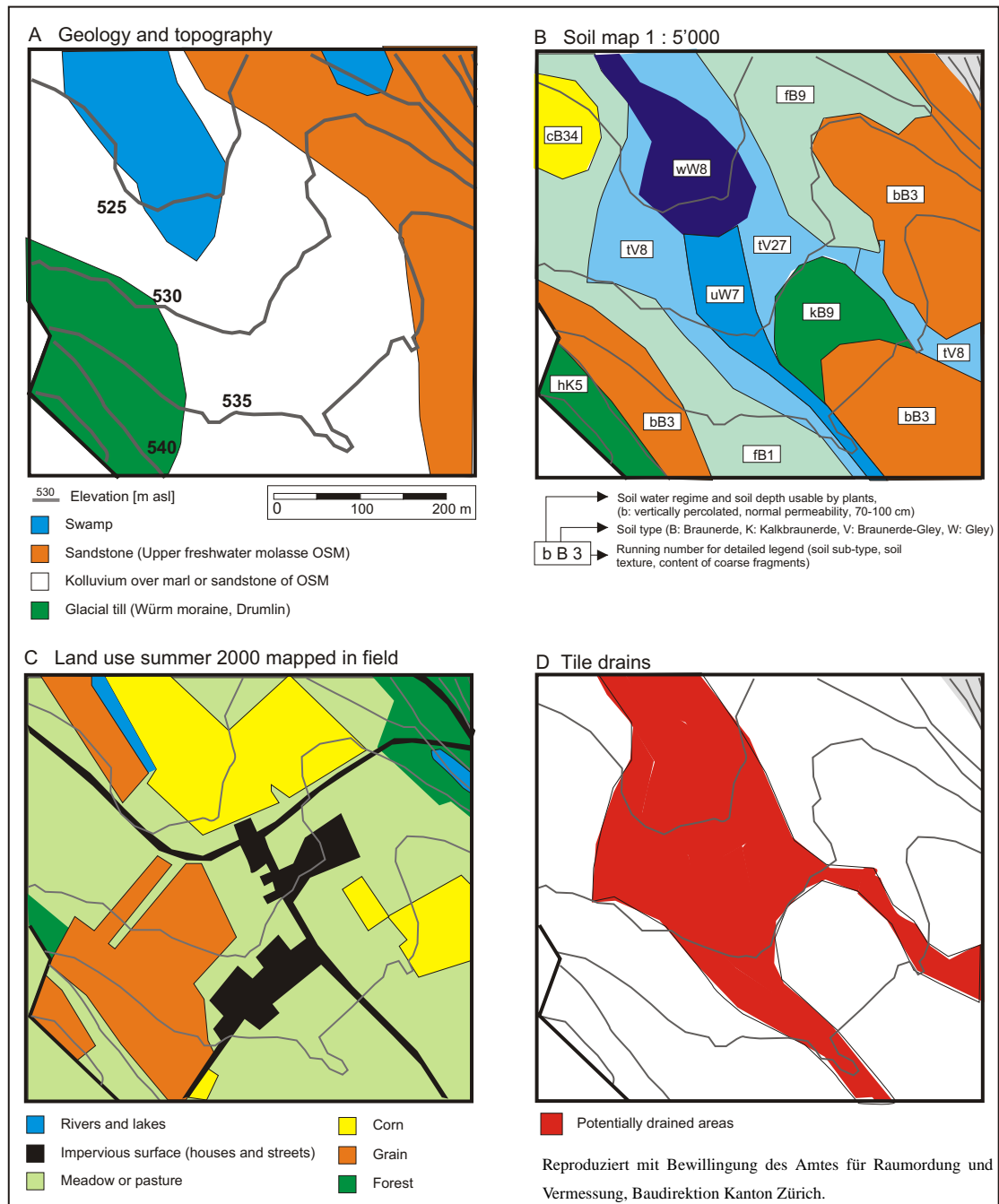


Fig. 6.2 Spatial data available in the test area (A geology and topography, B Soil map, C Land use, D potentially drained area).

The underlying bedrock of the test units consists of alternating layers of sandstone and marl of the Upper Freshwater Molasse and is partially overlain by colluvium in the middle part and glacial till of the Würm ice age in the south-western part of the area. The marl can be considered as practically impermeable while the sandstone has a low permeability with locally higher permeabilities in connection with fissures. Since the layering is nearly horizontal and was not under tectonic stress, fissures are not frequent. The permeability of the glacial till is rather low, due to its high clay and silt content. No deep or extended groundwater bodies and springs exist. During flood events, the underlying geology can therefore be regarded as impermeable.

The area was not systematically drained during the melioration campaign in the 1930s. However, information from land owners and the existence of shaft pits and pipes indicate that some tile drains exist in part of the area. In Figure 6.2 D the potentially drained area is displayed.

For the soil map units wW8 and fB9 the process determination will be described in more detail using the information from geology, land use and tile drain information (Figure 6.2):

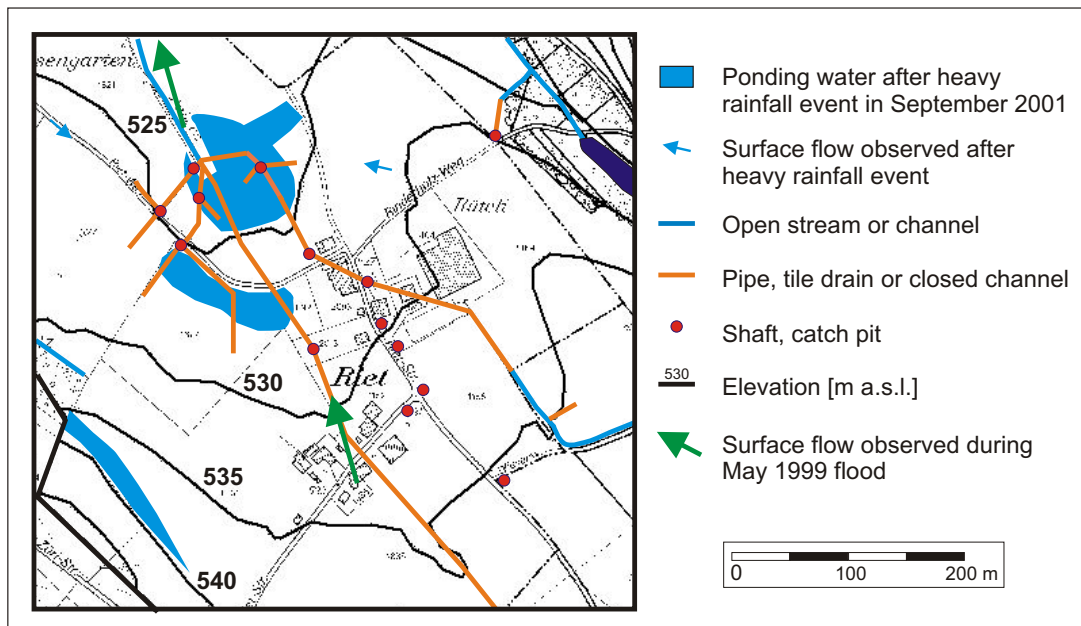
Soil map unit wW8 can be found in the valley floor and in a small strip along the brook with slopes below 10 %. The soil map code wW stands for an often saturated, 30 - 50 cm thick Buntgley. The sub-soil type information indicates an extremely gleyic soil. The soil map legend states that the humus type is mor, the parent material alluvium, the soil texture loamy clay and that the content of coarse fragments is smaller than 5 Vol.%. This indicates that wW8 used to be a flood plain with periodic sedimentation of fine grained material and permanently high groundwater tables. Part of the area is used for agriculture. The low storage capacity of this shallow soil and the frequent saturation indicates SOF 1 as dominant runoff process.

Soil map unit fB9 covers part of the sandstone ridge and its convex and gentle sloping hillslopes. The Braunerde soil has slightly poor drainage and reaches a depth of 70 to 100 cm. The soil sub-type indicates a stagnic soil and therefore a limited vertical percolation, thus SOF might occur. The soil texture of the topsoil is loam with low to medium matrix permeabilities and clayey loam to loamy clay of the subsoil with low matrix permeabilities. The aggregates are classified as unstable. Corn is grown on part of this area and therefore the vegetation cover is low at least for part of the year. The frequent driving over with heavy machinery in combination with low aggregate stability and low vegetation cover might result in soil surface sealing or top soil compaction. Both processes reduce infiltration capacity leading to HOF 2. If HOF 2 does not occur SOF 3 is the dominant runoff process.

Apart from soil map unit fB9 soils are not susceptible to HOF 2 in the rest of the test square. The impervious surfaces (houses and streets) were classified as HOF 1.

6.3 Mapping of hydrological relevant features

Permanently wet areas, swamps, springs, spring horizons, small rivers and brooks can be mapped in the field or from aerial photographs. Ditches, channels, drain pipes exiting to rivers, man-holes or shafts allow the identification of artificially drained areas, even when no drainage plans are available. Observations during or directly after flood events of surface runoff, signs of erosion, ponding water or return flow are valuable. Farmers can usually identify frequently wet areas and points where return flow or erosion occur. Sometimes information can be obtained where water was flowing during past floods. The identified features are shown in Figure 6.3.



Hintergrundplan reproduziert mit Bewilligung des Amtes für Raumordnung und Vermessung, Baudirektion Kanton Zürich.

Fig. 6.3 Mapped hydrologically relevant features.

The test area was partly drained in the 1940s (Figure 6.2 D), however ponding water during flood events indicates that the tile drain system can not prevent saturation of the soil. The ponding water in the southwest of the area indicates SOF 1, which could not be determined from the soil map done. Surface flow observed during floods in September 2001 and May 1999 point to SOF or HOF 2 on the respective areas.

6.4 Hillslope interactions between DRP - The process catena

The catena mapping approach considers the interaction an upslope process might have on the downslope process. Figure 6.4 shows a process catena in the test area (location see Figure 6.5). On top of the drumlin hillslope, SOF 2 occurs because the low permeable moraine is a barrier to vertical percolation and the lateral flow capacity is low to medium. At profile GW 8 there is a change in slope, the soil thickness decreases and return flow emerges. The two factors lead to a fast saturation of the soil and to SOF 1. Further downslope (GW 6), the moraine and molasse material is overlain by more permeable colluvium. The water infiltrates into the thick soils and flows laterally in the colluvium. Saturation was observed at GW 6 only after large rainfall events. The process in this area is either SOF 3 or SSF 3. After a second change in slope return flow out of the colluvium occurs and a small strip of SOF 1 can be found. Downslope the colluvium decreases in thickness and grain size. Slopes are now more gentle and bedrock is molasse, overlain with a thin layer of loamy colluvium with low permeability at GW 3. Here SOF 2 is the dominant runoff process. Since runoff from the small SOF 1 strip flows over the larger SOF 2 area below where it can re-infiltrate it was classified as SOF2. Close to the river (GW 1) groundwater levels are high and soils often saturated. Observed water levels suggest that the existing tile drains are not efficient enough to drain the soil during flood events, resulting in SOF 1 as DRP.

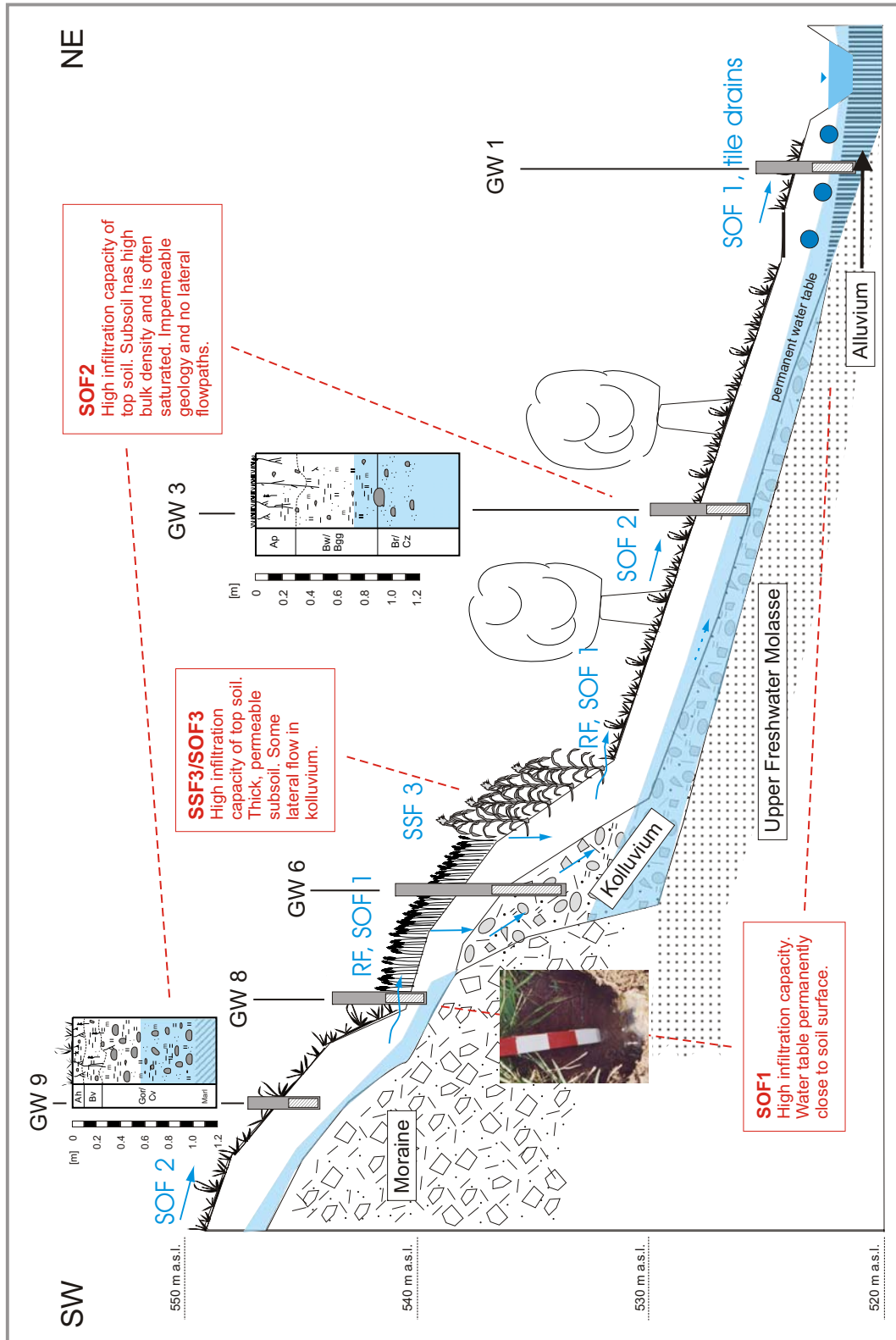
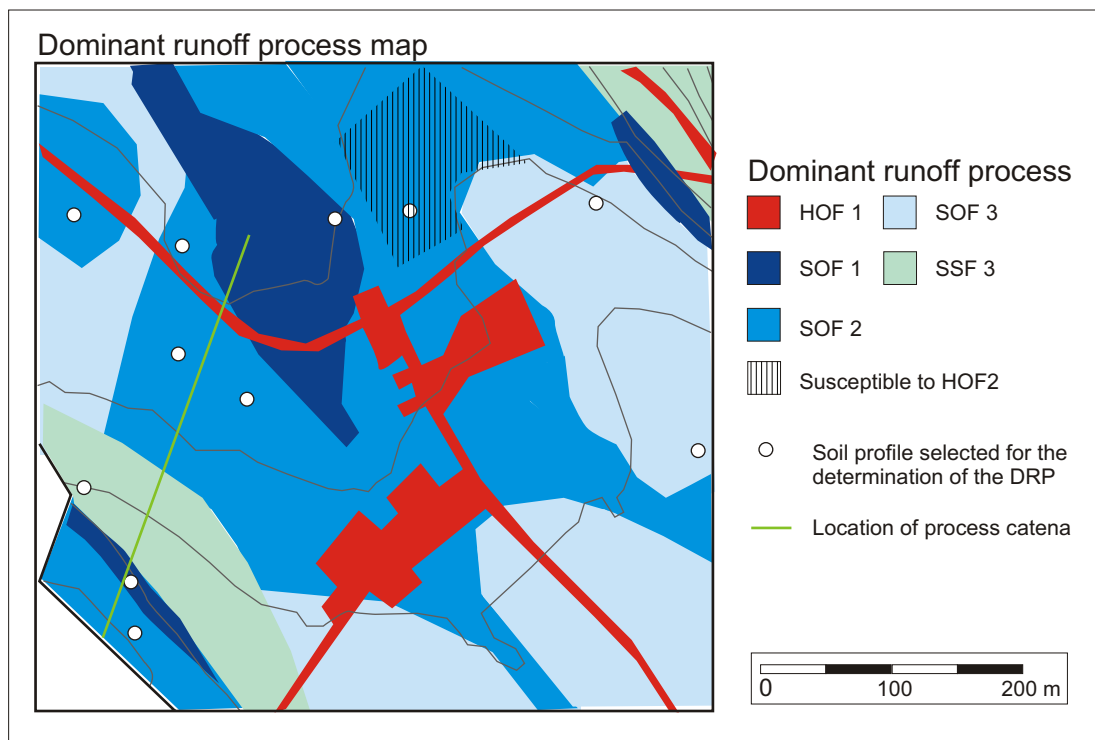


Fig. 6.4 Process catena in 500 x 500 m square in Ror catchment (Location see Figure 6.5)

6.5 Dominant runoff process maps

6.5.1 Dominant runoff process map of test area

Considering the information about topographic control on runoff formation, the observed soil water levels and results from field work a DRP map can be drawn (Figure 6.5). The process type D (tile drained) does not occur, since the existing few tile drains are not efficient enough to prevent saturation of the soil during flood events. Nevertheless, their influence was considered by reducing the SOF 1 area in the valley floor to that part that lies in a pronounced depression close to the channel.



Reproduziert mit Bewilligung des Amtes für Raumordnung und Vermessung, Baudirektion Kanton Zürich.

Fig. 6.5 The dominant runoff process map of the test area in the Ror catchment.

6.5.2 Dominant runoff process map of Ror catchment

The same procedure as illustrated for the test area was used to delineate the dominant runoff processes in the whole Ror catchment (Figure 6.6).

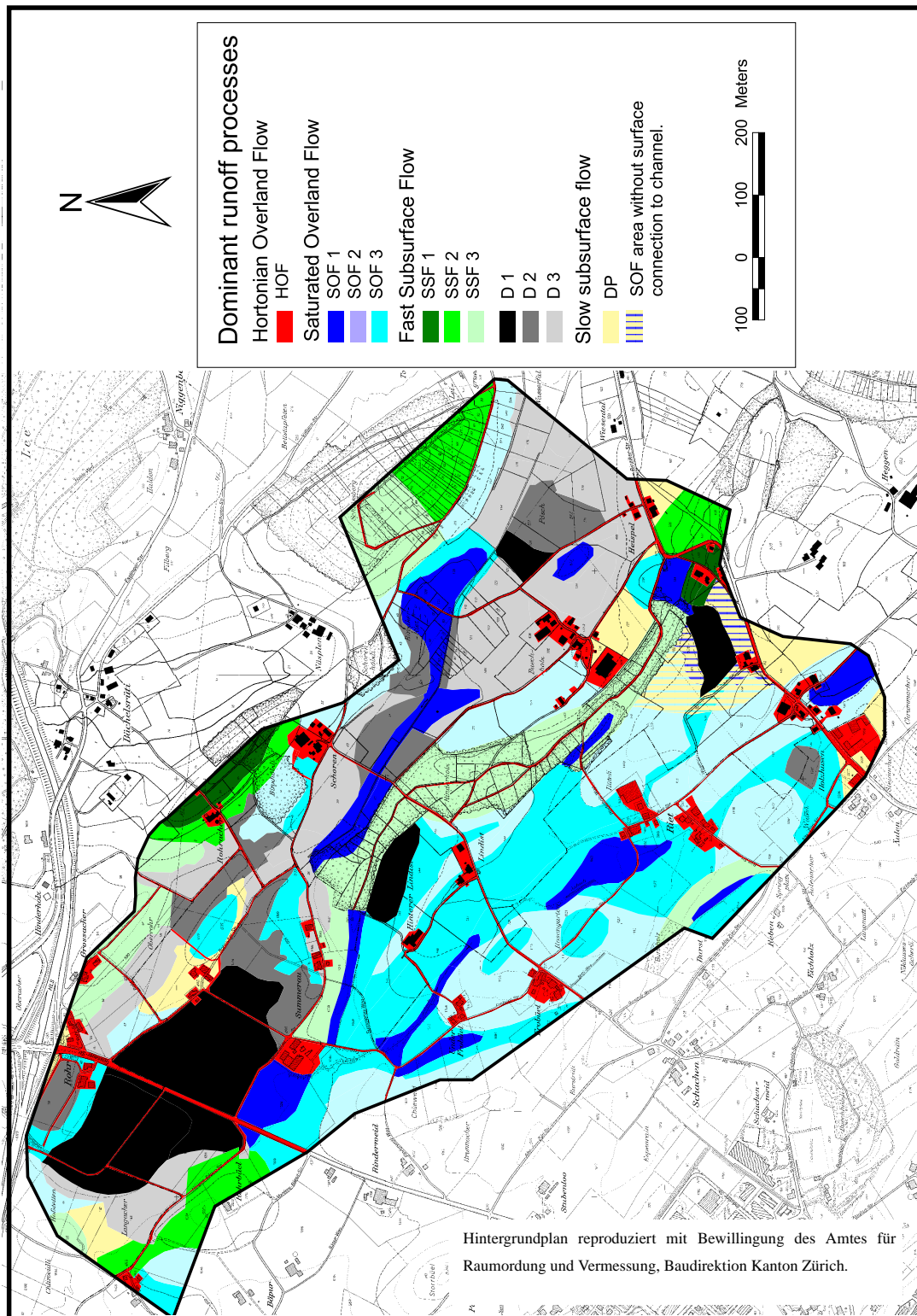


Fig. 6.6 Map of dominant runoff processes for rainfall intensities up to 20 mm/h in the Ror catchment.

In the Ror catchment two main soil groups can be distinguished: (Kalk-) Braunerde (Eutric and Calcaric Cambisol) and Gley (Gleysols). The Braunerde are located on the hillslopes and ridges both over moraine and molasse bedrock. The soil texture in the top soil is sandy loam to loam and the soil pH is slightly acidic to neutral depending on the carbonate content. Therefore they are ecologically suitable for earthworms. Under forest and permanent grassland, high macropore density and infiltration capacities can be expected. This is also valid for arable land with the exception of small areas susceptible to top soil compaction and surface sealing. There HOF 2 might occur during high intensity rainfall. Clay and silt content increases with soil depth, leading to a reduced matrix permeability in the subsoil. The bedrock has a low permeability. Therefore practically all Braunerde soils in the catchment are influenced by water in the subsoil and show stagnic or gleyic features. Large rainfall events saturate the soil and SOF occurs in 41 % of the area. In the Ror catchment, the lateral subsurface flowpaths are of biological origin (mouse borrows or root channels under forest). No highly permeable layers on the soil bedrock interface or in the bedrock was found. Therefore, only some steep, forested or extensively used hillslopes were classified as SSF areas. Since the lateral subsurface flow capacity is limited the DRP can switch to SOF during high intensity rainfall events on non forested hillslopes. DP occurs only on 6 % of the areas with thick Braunerde soils and deep groundwater tables.

Gley soils can be found in the lower flat part of the catchment and in the valleys over alluvial or kolluvial deposits or former swamps. Soil texture of the top soil ranges between loam and loamy clay and the humus content is high. In the subsoil all soil texture classes from sand to clay with a high spatial variability can be found. In the alluvial plains, the soils show horizontal layering. Groundwater levels are high and reach the soil surface during heavy rainfall events. At many places though, artificial drainage systems prevent the top 50 to 100 cm of the soil from being permanently saturated. Therefore the soil is suitable for earthworms and many macropores exist. Infiltration capacity is good. All the flat, drained gleys were classified D (subsurface flow, artificially drained). When the drainage system can not prevent saturation of the soil, overland flow occurs or the water is stored behind topographic barriers and infiltrates later. 21% of the catchment area are systematically drained. Gleys on steeper slopes and with a less efficient drainage system were allocated to the dominant runoff process SOF.

6.5.3 Dominant runoff process map for Isert catchment

The dominant runoff process map of the Isert catchment can be seen in Figure 6.7.

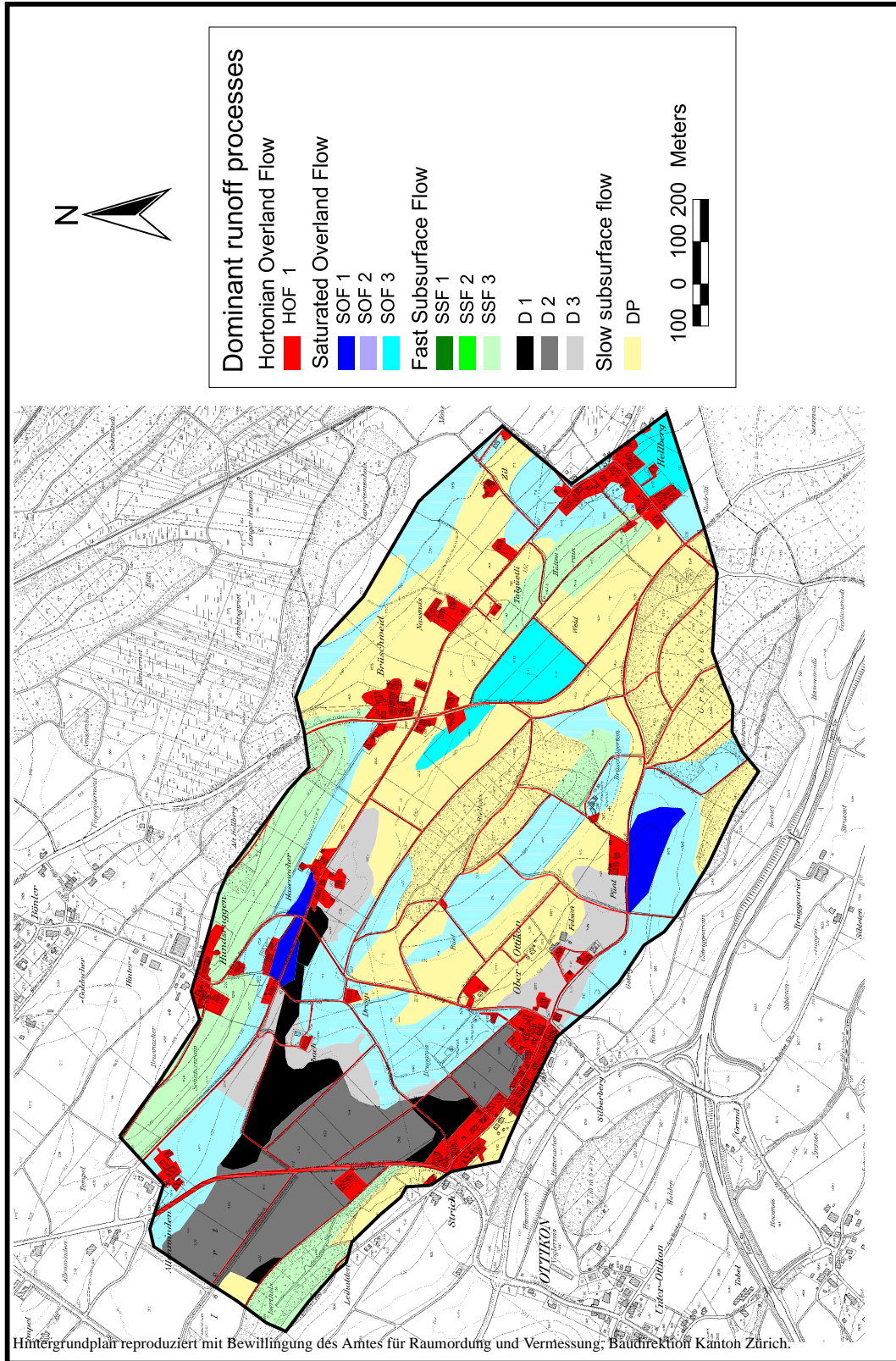


Fig. 6.7 Map of dominant runoff processes for rainfall intensities up to 20 mm/h in the Isert catchment.

In the Isert catchment, three soil types can be distinguished: (Kalk-) Braunerde, Parabraunerde and Gley. Kalkbraunerde (Calcaric Cambisol) is found on steep hillslopes of the drumlins where due to erosion no decarbonated horizon formed. The high pH and base saturation of the soil as well as the extensive land use (pasture or forest) provide ideal living conditions for soil animals like earthworms or mice. Aggregates are stable, soil texture is sandy loam to loam and macroporosity is high. Therefore infiltration capacity is high and SSF is the dominant runoff process for 18% of the catchment area.

The Braunerde soils are located on kolluvial deposits on the foot of the drumlins. The top soil and infiltration behaviour is similar to Kalkbraunerden but the subsoil has a higher clay and silt content (loam to clayey loam). About half of the Braunerde area shows gleyic features in the subsoil. For those areas, SOF is the dominant runoff process. SOF is expected on 26% of the catchment area. Where the Braunerde formed directly over permeable gravel deposits or moraine, DP occurs.

About half of the catchment area is covered with Parabraunerde (Luvisol, Podzoluvisol). Parabraunerde are soils with an illuvial horizon in which silicate clays have accumulated under an eluvial horizon with clay and carbonate depletion. Parabraunerde soils only form when vertical percolation is good; in the Isert catchment they are found over the permeable fluvial gravel deposits and gravel rich till. Since no prevention of infiltration and percolation occurs and the geological underground is permeable, DP is the dominant runoff process on many Parabraunerde areas covering 20% of the Isert catchment. However, if the clay and carbonate depletion in the top soil advances, the aggregates become unstable. Such soils are susceptible to soil surface sealing on arable land with low vegetation cover leading to HOF 2 during high intensity rainfall. An illuvial horizon with high clay content might also restrict vertical percolation and limit the storage volume of the soil. If the macropores bypassing this illuvial layer are destroyed or disrupted by ploughing, SOF occurs. 14 % of the catchment are covered with such well developed Parabraunerden under agricultural fields where HOF 2 or SOF are expected during high rainfall intensity. Gley soils formed in the lower part of the catchment which was a former swamp. This area is now artificially drained and the dominant runoff process is D, covering 17%.

6.6 Comparison of mapped and automatically delineated DRP map

With the set of rules to determine the dominant runoff processes, DRP maps were automatically produced for the Ror and Isert catchment from digital soil, geological, land use and tile drain maps using GIS. The maps were then compared with the manually produced maps. The results are shown in Figure 6.8 and Figure 6.9

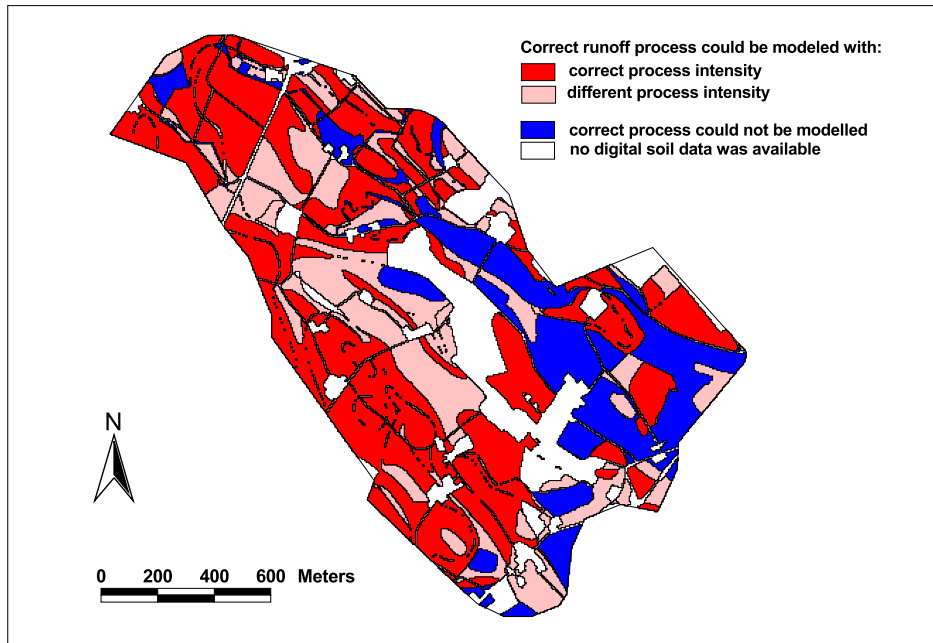


Fig. 6.8 Comparison between the manually derived DRP map and the DRP map produced in a GIS using the DRP body of rules for the Ror catchment.

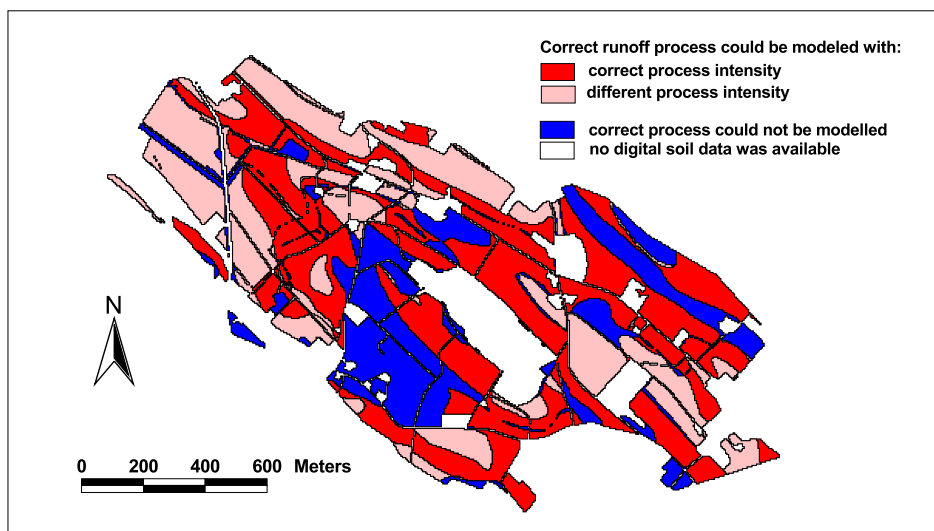


Fig. 6.9 Comparison between the manually derived DRP map and the DRP map produced in a GIS using the DRP body of rules for the Isert catchment.

For 17 % of the Ror and 28 % of the Isert catchment area no digital soil data was available and an automated process determination was not possible. The following percentages therefore refer to the investigated and not to total catchment area.

In Ror, the automated, GIS based process determination was correct for 52 % of the area. In another 27 % the runoff process was determined correctly but the process intensity differed one step. The runoff process was not determined correctly on 21 % of the area, mainly in the Rinderholz sub-catchment. In most cases, the DRP set of rules identified SOF 3 as runoff process and the mapping D 3. In the digital data set used in the GIS these areas are classified as not drained, while field surveys suggest that many of them probably are drained.

In the Isert catchment, on 47 % of the area the runoff process and intensity were determined correctly, while on 32 % the process was correct but the process intensity differed one step. For 21 %, the process was not correctly determined. The model identified SOF 3 or D 3 while the manual mapping identified DP.

The automated process determination in the two catchments, the SOF dominated Ror and the DP dominated Isert catchment was successful. Some of the deviations are due to inconsistencies in the digital data used in the process. Another reason is that the automated process determination cannot yet differentiate between SOF and natural SSF. It also does not consider the influence of the topography on runoff formation. These factors shall be included into the automated process determination in the near future.

7 Hydrological consequences of the different runoff processes

7.1 Introduction

Runoff processes differ in the amount of water that is stored in the soil and the dominant flow paths it takes. Therefore, each runoff process has a distinct hydrologic response to precipitation in the way the soil is saturated or drained and in relative amount of surface, fast or slow subsurface flow in runoff.

To investigate the characteristics of the filling and draining of the soil, wells were installed and soil water levels recorded on areas which differ in the dominant runoff processes. The contributions of the different flow paths to total runoff depends on the distribution of runoff processes in a catchment. Therefore, runoff reactions from the SOF dominated Lindist sub-catchment, the subsurface flow dominated Rinderholz sub-catchment and the tile drain system Poesch were measured and compared. Different residence times and flow paths of water might influence the water chemistry. Therefore, electric conductivity in runoff from the three sub-catchments was compared as well.

The hydrometric measurements allowed to test the results from the process mapping and to better understand the hydrology of the different runoff processes.

7.2 Soil water levels

Groundwater wells were installed on areas, where saturated overland flow, subsurface flow and tile drain flow was expected. The location of the wells can be seen in Figure 7.1. Figure 7.2 a shows the soil water level fluctuations during the September 2002 flood on a SOF dominated hillslope (GW 3, 6 and 8), on a SSF 3 hillslope (GW 10 and 11) and on tile drained field (GW 13 and 15). The soil water levels are also plotted against the cumulated rainfall for the same event (Figure 7.2 b) and against the respective sub-catchment runoff (Figure 7.3).

On the SOF 1 area, the water level reaches the surface after only 20 mm, on the D 1 area after 40 mm of rainfall. On the SOF 2 area however, 80 mm are needed, on the SOF 3/SSF 3 area 140 mm and on the SSF 3 hillslope 100 mm until the water level reaches the surface.

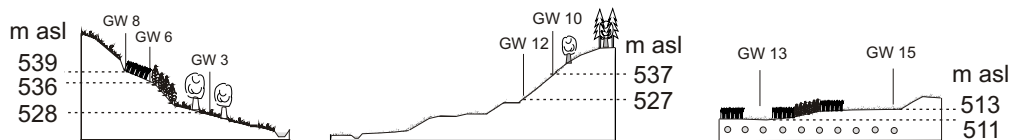
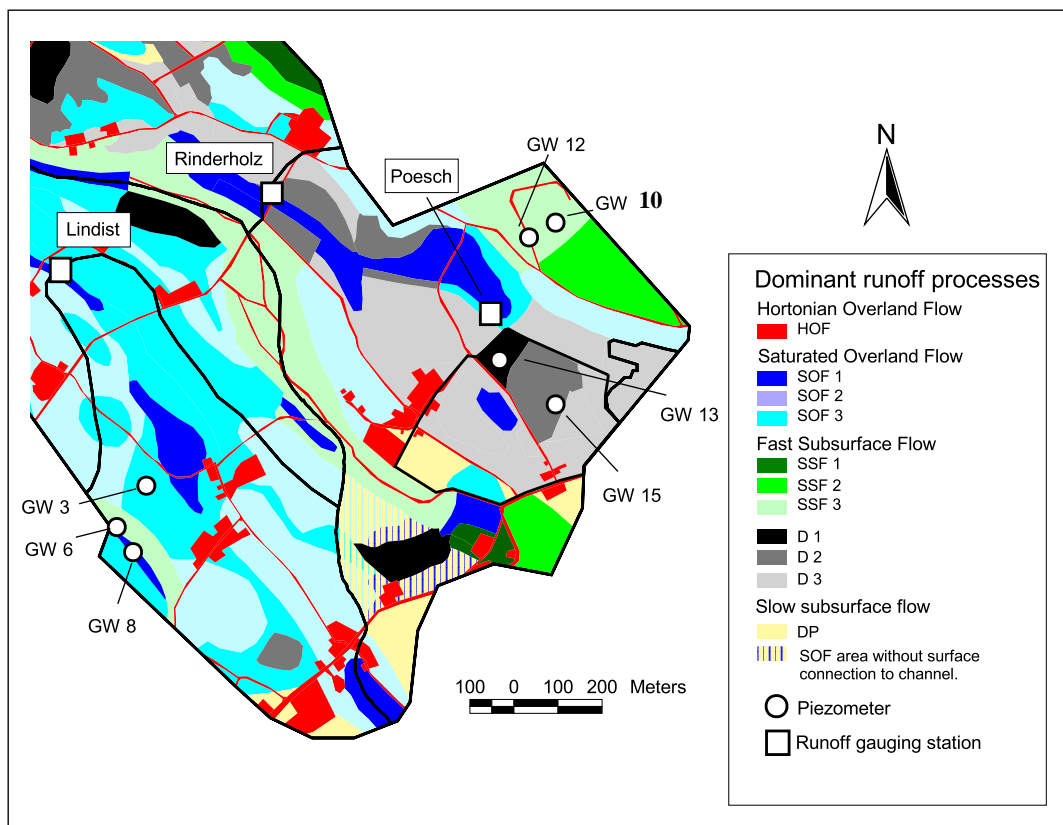


Fig. 7.1 Location of groundwater wells in the Ror catchment.

The recession of the water levels are typical too. The water level in the SOF 2 well dropped to nearly pre-event levels within 2 days after the rainfall ended. The same can be observed in well GW 6 on a SOF 3/SSF 3 area. Only the SOF 1 area stayed saturated for several days after the event.

On the subsurface flow hillslope, water levels rise faster and fall slower in the downslope well than in the upslope one. And unlike the SOF wells, they show continuous saturation of the soil during the two days of the main event. These observations indicate lateral flow of water downwards in the hillslope.

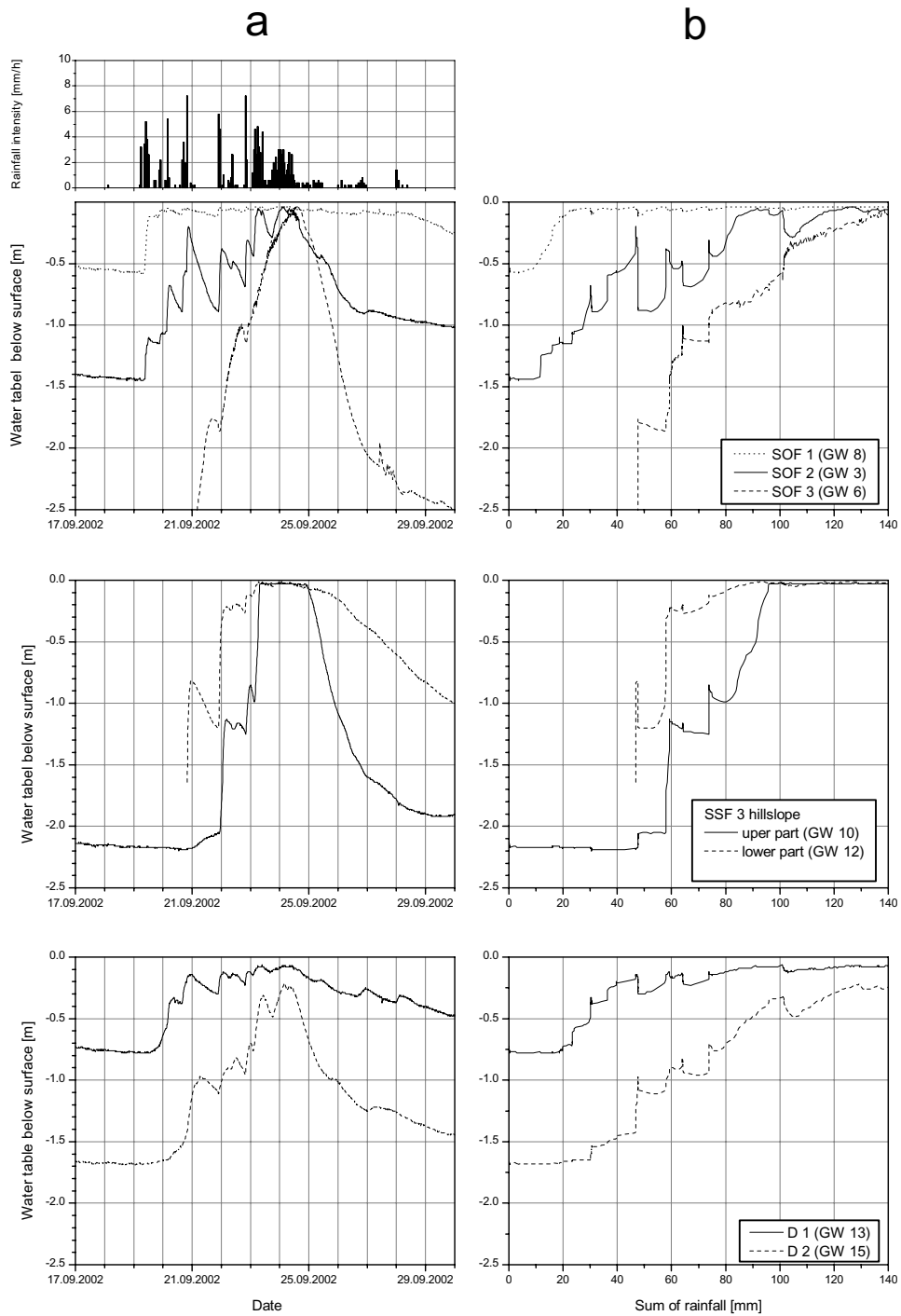


Fig. 7.2 Soil water levels measured in groundwater wells installed on different process areas during the September 2002 flood event. (a) Soil water hydrograph and (b) soil water levels plotted against sum of rainfall. In the first row, data from SOF 1 to 3 areas are displayed, in the second row data from two positions of a SSF 3 hillslope and in the bottom row data from D 1 and 2 areas. In brackets number of the groundwater well.

During the event, the water level in well GW 15 on the tile drained field does not reach the surface due to the efficient drainage system. The well GW 13 on the D 1 area however, reacts like the SOF 1 well. Both D wells are located in alluvial deposits which were artificially drained in the 1930s. The efficiency of this system might be reduced nowadays. Together with the large variations in soil texture of the alluvial deposits, large differences in drainage rate result, ranging from SOF like reactions to a very efficient drainage.

In Figure 7.3, soil water levels are plotted against runoff from the respective sub-catchment. The water level in GW 8 on the SOF 1 area reaches the surface rapidly while runoff in Lindist is still low and stays there during the event. Water levels in the wells on the SOF 2 and SOF 3/SSF 3 area rise much slower. These areas contribute to runoff only after the soil is saturated (Figure 7.3 a-c), first on the SOF 2 area then on the SOF 3 area.

The water levels in the SSF 3 hillslope are compared to runoff from the Rinderholz sub-catchment (Figure 7.3 d and e). At the beginning of the event, soil water levels show no reaction to precipitation and rise two days after the water levels in the SOF wells. Then water levels rise rapidly and reach the soil surface within one day and remain there during the main event. The soil water levels and runoff seem to be correlated during the rising runoff hydrograph. The loops in the rising limb and the pronounced recession in the falling limb suggest a fast soil drainage. However, additional measurements would be necessary to allow a further interpretation of the complex SSF system.

A strong correlation exists between the water level and the runoff from the tile drain system (Figure 7.3 f). A change in slope above 0.5 m soil depth indicates a change in drainage process or soil storage capacity.

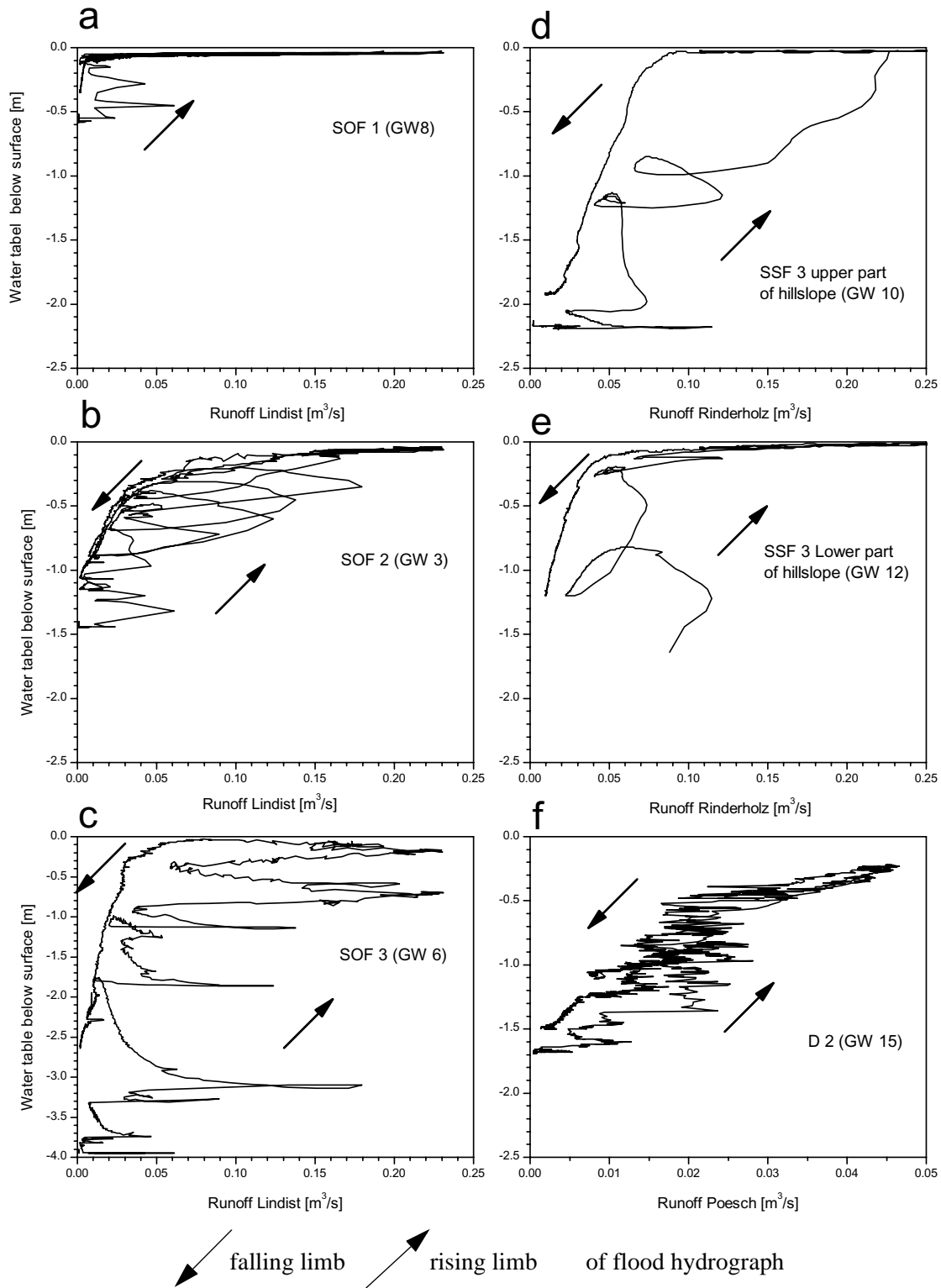


Fig. 7.3 Measured soil water levels on different process areas plotted against discharge of the respective sub-catchment for the September 2002 flood. The measurements on SOF areas of different intensities in the Lindist sub-catchment (a - c), on a SSF 3 hillslope in the Rinderholz subcatchment (d and e) and on a D 2 area of the tile drain system Poesch (f). Number of the wells in brackets.

To quantify the correlation between groundwater levels and runoff in the respective sub-catchment during the September 2002 flood event, the Kendall rank correlation coefficient (Appendix C) was calculated for each well and plotted against distance of the groundwater wells from open streams and channels (Figure 7.4 a), open and covered streams and channels (e.g. pipes) (Figure 7.4 b) and the process intensities of the areas on which the groundwater wells were installed (Figure 7.4 c).

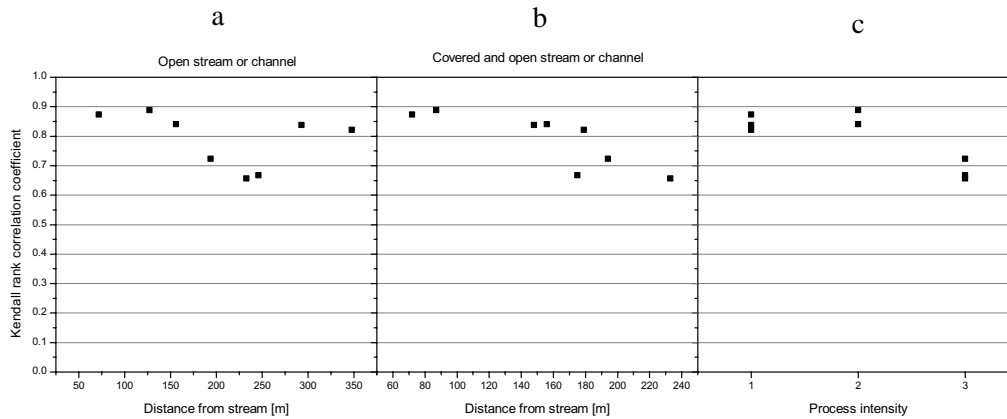


Fig. 7.4 Rank correlation between groundwater levels and runoff versus distance from open streams (a), distance from open and covered streams (b) and process intensity of the area on which the groundwater well was installed (c).

All calculated rank correlation coefficients lie between 0.6 and 0.9 and do not decrease with increasing distance to an open stream or channel. If the correlation coefficients are plotted against distance to open and covered streams or channels it appears that water levels in the individual groundwater wells are less correlated to runoff in the more distant wells. However, the decrease of correlation can best be explained with the process intensity. During the September 2002 flood, areas with process intensity 1 and 2 contributed to runoff. All wells on these areas have correlation coefficients higher than 0.8. The areas of process intensity 3 did only contribute partly and at the end of the event to runoff. Wells on these areas have correlation coefficients around 0.7. The correlation coefficients of the process intensity 3 wells and wells with large distance to the stream are still very high compared to values found in literature.

Seibert et al. (2003), for example, calculated rank correlation coefficients between groundwater levels and runoff in a subsurface flow dominated 0.5 km² Swedish catchment (no Hortonian or saturated overland flow could be observed). They found correlation coefficients of around 0.9 for wells closer than 35 - 60 m to the channel which dropped abruptly to values around 0.3 for wells further away. They explained their findings with two distinct hydrological zones, the riparian zone with high correlation coefficients actually contributing to runoff and an upslope zone where water levels lag behind runoff.

7.3 Catchment runoff

As the different dominant runoff processes react differently to intense precipitation, the magnitude of flood discharge depends on the aerial extent of each process in a catchment. This is illustrated by Figure 7.5. Peak discharges are higher in Lindist where fast and strongly reacting SOF 1 and 2 areas dominate, while in Rinderholz the delayed processes SSF, D or DP cover close to 70% of the area (Figure 7.6).

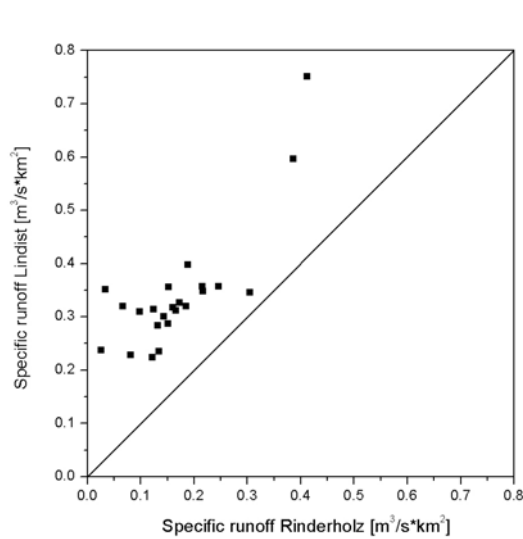


Fig. 7.5 Specific runoff measured at Lindist and Rinderholz stations for runoff events with specific discharge larger than $0.2 \text{ m}^3/\text{s}\cdot\text{km}^2$.

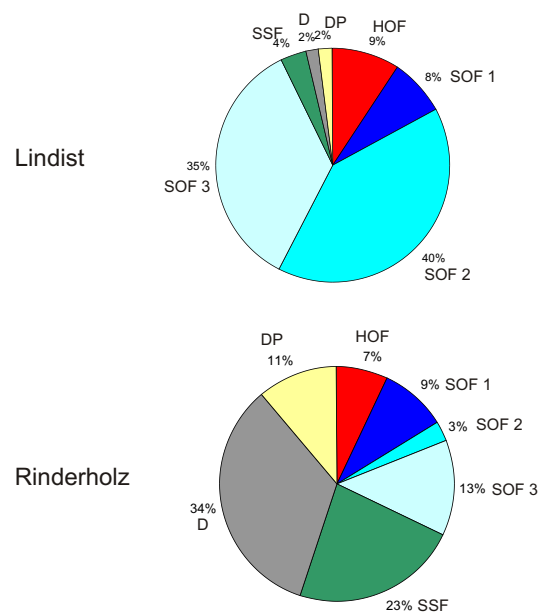


Fig. 7.6 Distribution of dominant runoff processes in the Lindist and Rinderholz catchment.

Figure 7.7 displays rainfall and runoff in the Lindist and Rinderholz sub-catchments and in the tile drain system Poesch during the September 2002 flood. Within 6 days (19.09 - 25.09.02) 130 to 140 mm of rainfall with a maximum intensity of 7 mm/h were recorded. In Lindist 80 mm or nearly 60 % of rainfall was running off, in Rinderholz only 60 mm or 44 %. Specific discharge (Figure 7.7 c) in Lindist is higher than in Rinderholz during peak flow times, during recession Lindist contributes less. In both catchments peak flows increase with increasing rainfall amounts and saturation of the soil. The SSF 3 and D areas in Rinderholz attenuate rainfall peaks by storing water and releasing it retarded as subsurface flow. The tile drain system Poesch reacts like the Rinderholz catchment.

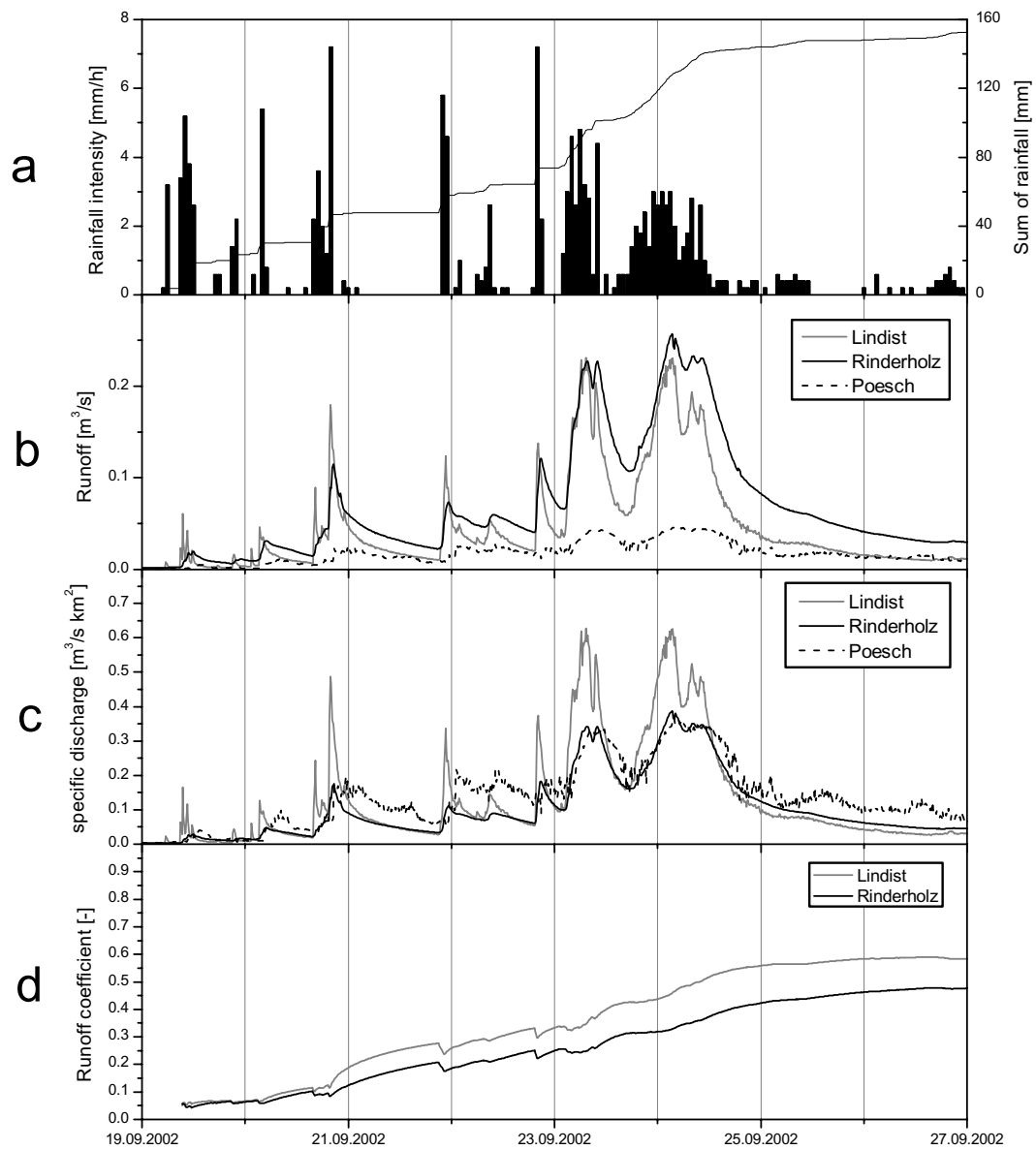


Fig. 7.7 The September 2002 flood event in the Lindist, Rinderholz and Poesch sub-catchments. Displayed are rainfall intensity and sum of rainfall (a), runoff (b), specific runoff (c) and volumetric runoff coefficients (d).

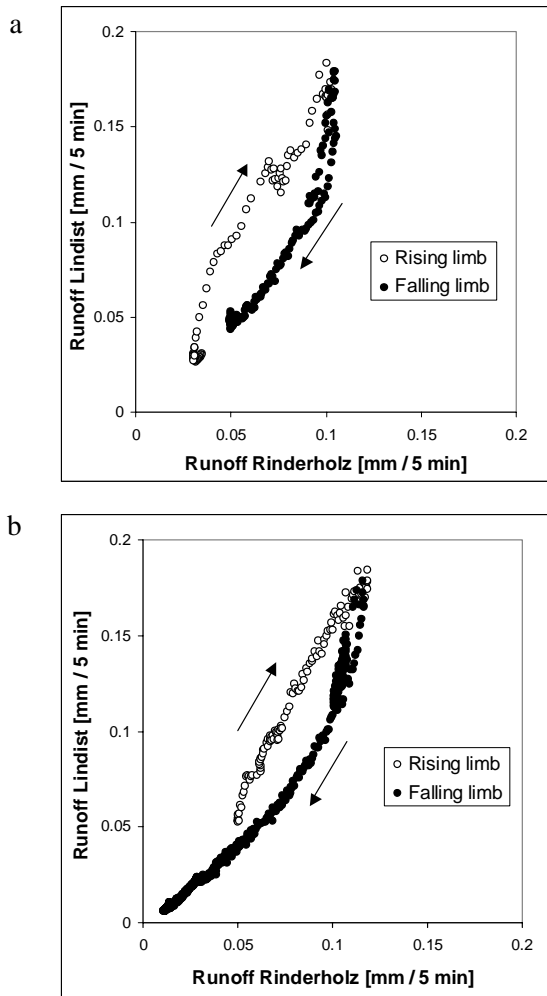


Fig. 7.8 Gauged Lindist runoff versus Rinderholz runoff a) for flood peak 1 on the 23.09.2003 and b) flood peak 2 on the 24.09.2003 during the September 2002 event.

In Figure 7.8 specific runoff in the Lindist sub-catchment is plotted against specific runoff in the Rinderholz sub-catchment for the two flood peaks during the September 2002 event. During the rising limb of the flood hydrograph the SOF dominated Lindist catchment contributes proportionally more to runoff as compared to the subsurface flow dominated Rinderholz catchment and less on the falling limb, resulting in clockwise hysteresis. The same could be observed between riparian zone runoff and hillslope runoff by McGlynn and McDonnell (2003b). This further confirms the process evaluation in the two sub-catchments.

7.4 Electric conductivity

In all three sub-catchments, electric conductivity (EC) of the runoff was measured in 10 min intervals (Figure 7.9 a). While rainfall at nearby Taenikon station has a conductivity of around 10 $\mu\text{S}/\text{cm}$, with small variations during storm events (NABEL, 2002), the EC in runoff reached values of $710 \pm 30 \mu\text{S}/\text{cm}$ in Lindist and $660 \pm 20 \mu\text{S}/\text{cm}$ in Rinderholz and Poesch during low flow periods in summer 2002. During peak discharge of the September 2002 flood event, the EC decreased to 200 $\mu\text{S}/\text{cm}$ in Lindist and 300 $\mu\text{S}/\text{cm}$ in Rinderholz.

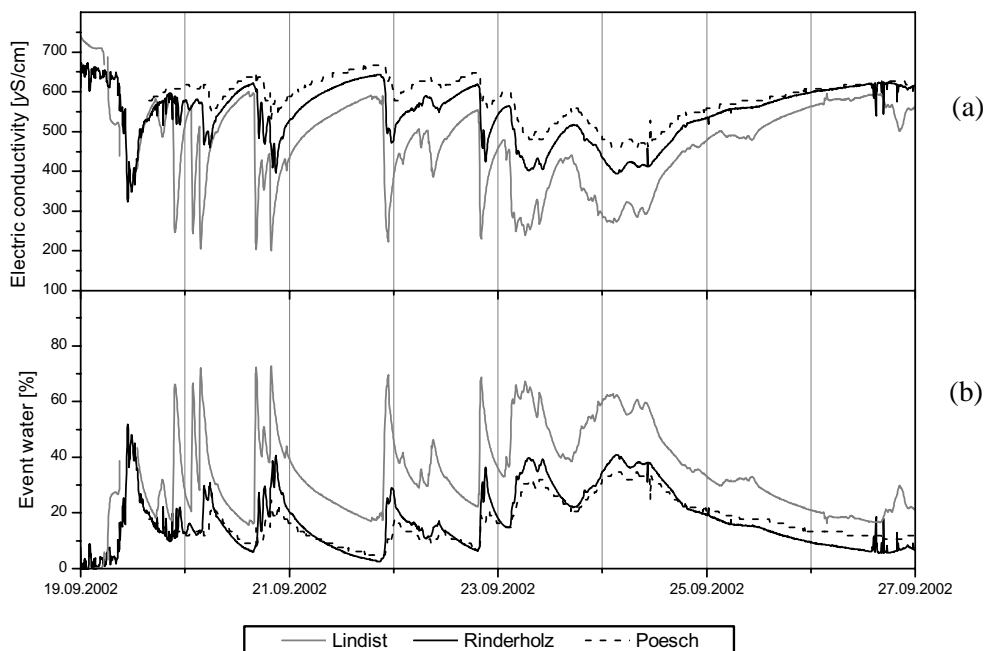


Fig. 7.9 Electric conductivity measured in the runoff in Lindist, Rinderholz and the tile drain system Poesch during the September 2002 flood event (a) and the percentage of event water calculated from the EC (b).

Figure 7.10 shows the relationship between runoff and EC during the two flood peaks on the 23. and 24.09.2002. In all three sub-catchments, runoff and EC are correlated. EC values are higher in the subsurface flow dominated Rinderholz and Poesch sub-catchments than in the surface flow dominated Lindist catchment

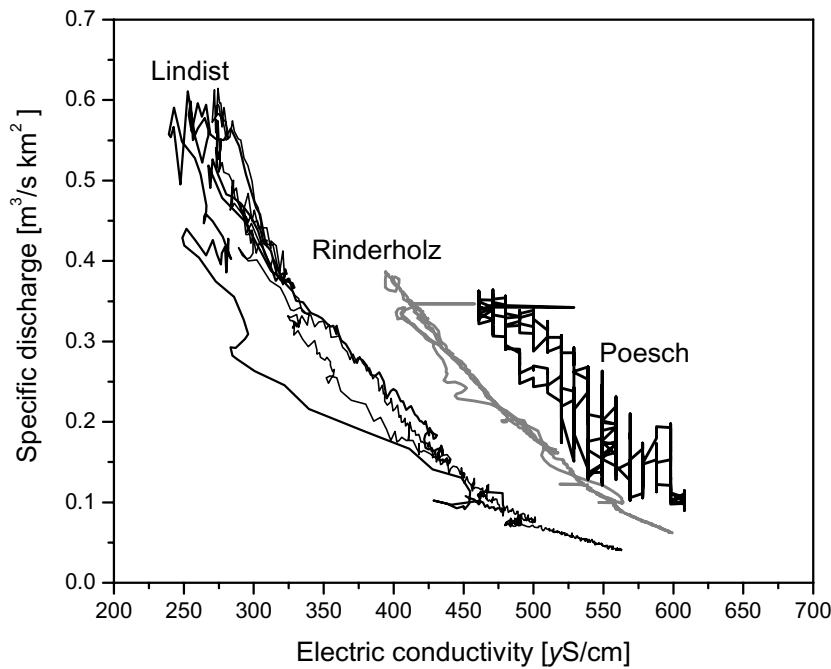


Fig. 7.10 Specific discharge plotted against electric conductivity during two flood peaks on the 23. and 24.09.2002 in the sub-catchments Lindist and Rinderholz and the tile drain system Poesch.

The constant EC in the rainfall input, the large difference in EC between rainfall and base flow and the strong correlation between EC and runoff during flood events allowed a two-component hydrograph separation with rainfall and base flow as components and EC as tracer according to Pearce et al., 1986:

$$q_e = q_t - q_p \quad 7.1$$

$$q_p = \frac{c_t - c_e}{c_p - c_e} \cdot q_t \quad 7.2$$

With q_t as measured discharge, q_e as event water (rainfall) and q_p as pre-event water. c_t , c_e , c_p are the corresponding EC values.

This approach does not consider that overland flow or shallow subsurface flow also take up solutes, resulting in an increase in EC. Wetzel (2003), for example, measured an EC of 99 $\mu\text{S}/\text{cm}$ in overland flow. Additionally shallow pre-event soil water might have a lower EC than base flow. After the event, on the 27.09.2002, the water in the shallow wells located on SOF areas had an EC between 250 and 350 $\mu\text{S}/\text{cm}$, while the EC values in the deep SSF and D wells ranged from 550 to 650 $\mu\text{S}/\text{cm}$. Next to this variability of the EC in pre-event water, a variable EC in event water (rainfall) might contribute to the uncertainty of the hydrograph separation (Genereux, 1998).

These limitations allow only a relative comparison of event water percentages between the three catchments,

Figure 7.9 b gives the result of this separation as percentage of event water of total runoff. The high percentage of event water in Lindist is consistent with the larger contribution of saturated overland flow to runoff. The higher pre-event water contributions in Rinderholz and the tile drain system Poesch indicate a higher contribution of subsurface flow to runoff. The event water calculations support the results of the dominant runoff process estimation.

7.5 Conclusions

The water level changes are characteristic for the runoff processes occurring. SOF 1 areas reach saturation after a low amount of rainfall, while SOF 3 or SSF 3 areas need much more rainfall to saturate. On the SSF 3 hillslope, saturation of the downslope area is further enhanced through lateral flow from upslope. Generally, water levels drop rapidly after an event, indicating fast drainage of the soil. This could also be observed in the SOF 2 and SOF 3 wells.

A comparison between water levels and the respective catchment runoff indicate that SOF areas contribute to runoff only after the soil is saturated. On the subsurface flow hillslope, the soil water levels seem to be correlated to catchment runoff during the rising runoff hydrograph. A strong correlation exists between the water level and the runoff from the tile drain system.

Peak discharges during flood events are higher in Lindist, where fast and strong reacting SOF 1 and SOF 2 areas dominate than in Rinderholz, where the delayed processes SSF, D or DP cover close to 70% of the area.

The higher percentage of event water in Lindist, calculated from electric conductivity, also reflect higher contributions of surface flow in Lindist.

The hydrometric measurements support the results of the dominant runoff process estimation and give insight into their hydrological reaction. The knowledge gained will now be implemented into rainfall - runoff modelling (Chapter 8).

8 Rainfall-runoff modelling based on process maps

8.1 Introduction

Rainfall runoff models calculate runoff from meteorological input data using catchment information and a concept of runoff formation.

The real processes of runoff formation are complex and usually are simplified to such a degree that they are no longer physical but rather conceptual (Beven, 1989b; Grayson et al., 1992; Naef, 1981). Such conceptual models have to be calibrated. Simulations from such models can give satisfactorily results when the simulations are conducted within the calibration range. However, the quality of simulations of extreme flood events outside the calibration range, the simulation for areas smaller or larger than the calibration area or for simulations with changed input conditions (e.g. climate change) or catchment properties (e.g. land-use change) cannot be assessed.

A more stable calibration and a reduction of the uncertainty in the extrapolation range can be expected, if a conceptual model adequately represents the important processes in a catchment and if catchment properties besides measured rainfall and runoff data can be included into the calibration process. A way to achieve this is the evaluation of runoff processes in a catchment.

In the model Qarea-pro presented here, each runoff process is conceptualized with a separate module. As the results from the hydrometric data interpretation (Chapter 7) indicate, the processes differ in the amount of water that is stored in the soil and the way the soil is filled and drained. Therefore, the process conceptualization should be able to correctly simulate soil water levels and drainage of the soil. Additionally, it should be possible to determine important model parameters from field data.

The model and modules were used to test assumptions made during the mapping and the process conceptualization. During model development and especially during its application, some gaps in process knowledge or problems of model parameter determination were discovered.

In the following chapter the process modules are introduced and the results of the simulations as well as the gaps in process knowledge are discussed. The process modules were developed using the September 2002 flood event data from the sub-catchment Lindist and the tile drain system Poesch. The model was then applied in Rinderholz, Ror and Isert and to other events without a change in calibration parameters.

8.2 Model structure

We developed the model Qarea-pro to allow water balance and peak discharge calculations during flood events based on the dominant runoff process maps. Figure 8.1 gives an overview of the structure of the Qarea-pro model, where each process is represented by a separate module. Runoff calculated for each process is multiplied with the respective process area in each sub-catchment.

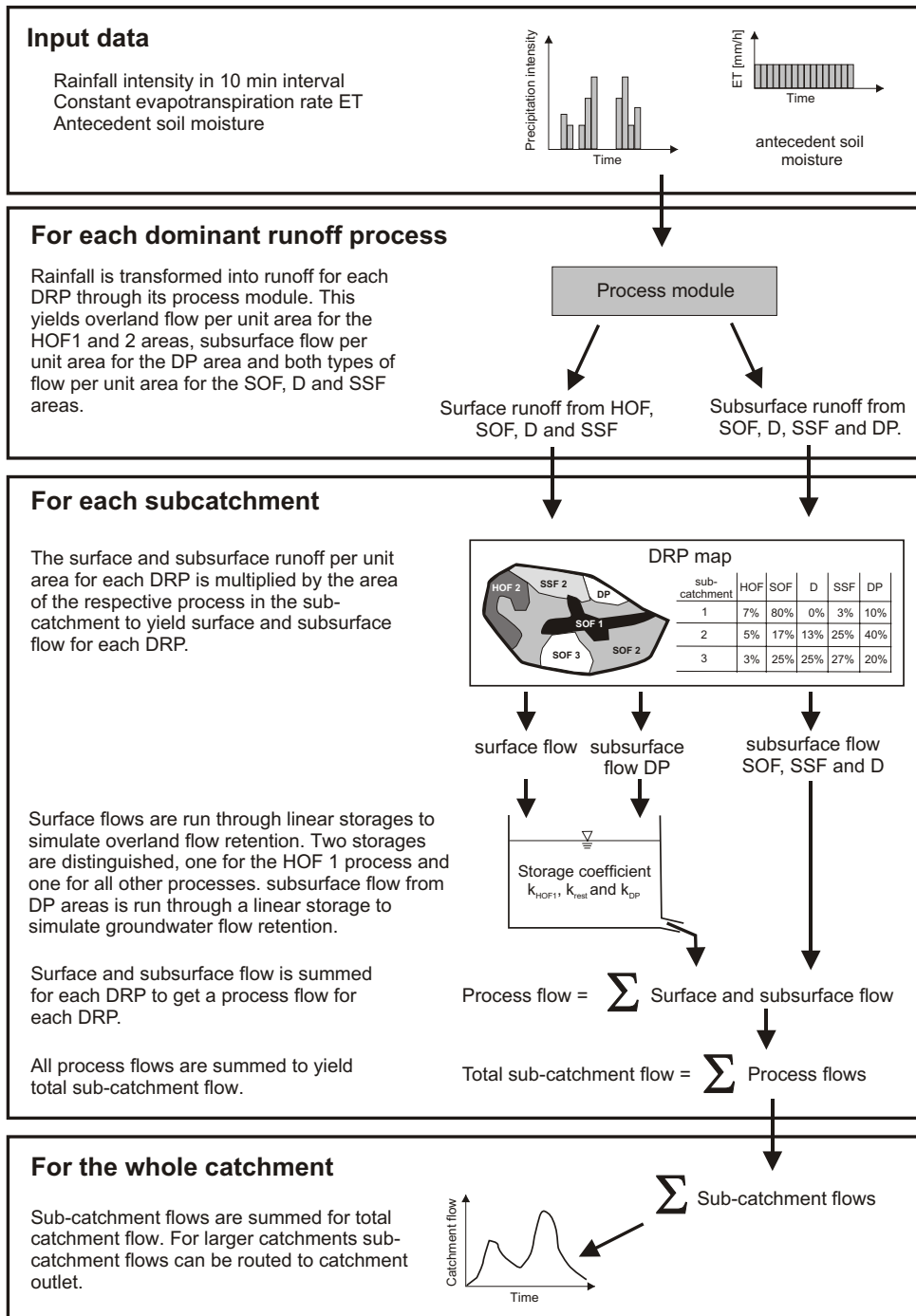


Fig. 8.1 Schematic representation of rainfall-runoff model Qarea-pro.

Total flow of a sub-catchment is the sum of the weighted process flows, catchment flow results from adding up sub-catchment flows. The size of a sub-catchment should not exceed 10 km², since the linear storage coefficients to calculate runoff concentration are scale dependent. Inputs into the model are rainfall intensities for each sub-catchment, a constant evapotranspiration rate and a factor to account for pre-event soil moisture. Interception losses and flood routing are not included in the model.

8.3 Process modules

The modules for the different dominant runoff processes were designed to represent the main features of the process with only a few parameters. If possible, the parameters should have some physical meaning and correlate to field data.

8.3.1 Hortonian overland flow

Hortonian overland flow $q(t)$ from sealed areas (HOF 1) is supposed to be directly proportional to rainfall $p(t)$ at time t with a as runoff coefficient.

$$q(t) = a \cdot p(t) \quad 8.1$$

Since the investigated catchments are rural and HOF hardly occurs, this parameter a is not very sensitive and was set to 0.5. In catchments with a higher percentage of sealed areas (e.g. many rock outcrops or settlements) a might be larger. It can be determined with sprinkling experiments, from literature values or has to be calibrated.

HOF 2 can be conceptualized by assuming either a constant infiltration rate or a soil moisture dependent infiltration function. The infiltration rate or function can be estimated from soil properties and with sprinkling experiments. At times, when rainfall intensity exceeds infiltration capacity, the excess water flows off as surface runoff. Such a conceptualization requires though, that a second dominant runoff process is mapped for all HOF 2 areas, to account for the infiltrated water.

8.3.2 Saturated overland flow

On saturated overland flow, as well as on SSF, D and DP areas the infiltration rate exceeds the rainfall rate. Runoff occurs, if the soil is saturated. The saturated overland flow process is conceptualized with a bucket. No runoff occurs until the bucket is filled and then all further rainfall becomes surface runoff. The main parameter is the storage capacity S_{map} of the bucket (soil) which is determined during the mapping.

The storage capacity is the product of the soil depth h_{max} and the effective porosity n . The effective porosity is the porosity that can be used for storage of water during a flood event. In the humid climate of Switzerland, soil moisture is often around or just below field capacity. Therefore the effective porosity was defined as the difference between saturated volumetric water content and volumetric water content at field capacity (60 cm soil water tension) and corresponds to the air capacity. The effective porosity was estimated on the soil profiles from soil texture and bulk density according to AG Boden (1994). An effective porosity of 8 % was calculated for the soils in the Ror catchment, which are dominantly of soil texture clayey loam to sandy loam with low to medium bulk density. Mapped soil depth h_{max} for the SOF 1 process is 0.5 m, for the SOF 2 process 1.3 m and for the SOF 3 process 2.5 m, corresponding to 40 mm, 104 mm and 200 mm storage capacity, respectively.

The infiltrated water continuously leaves the soil through drainage and evapotranspiration. Although these processes are slower than the filling of the soil during intense precipitation events, they become important during events of longer duration.

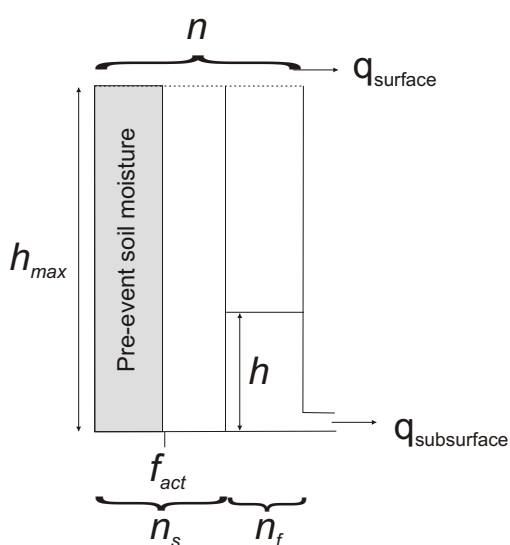


Fig. 8.2 SOF runoff process module.

The observed water levels in the piezometers did rise and fall surprisingly fast during rainfall events. To account for these fast movements of the water table a low drainable porosity or macropores were needed. In the soil drainage conceptualization, it was assumed that the effective porosity n is the sum of a fast drainable porosity n_f (e.g. macropores) and a slowly drainable porosity n_s (Figure 8.2).

On similar soils like those found in the Ror catchment (similar soil texture and

bulk densities over bedrock moraine and under land use grassland) Weiler (2001) counted macropore densities of 400 to 700 macropores/ m^2 of macropores with an area of 10 to 100 mm^2 . Assuming a mean macroporosity of 550 Mp/m^2 and a mean macropore area of 55 mm^2 , this corresponds to a macroporosity of 3 %. The effective porosity of 8 % was therefore divided into a fast drainable porosity of 3 % and a slowly drainable porosity of 5 % in the model. To account for pre-event rainfall, the slowly drainable porosity can be partly filled. Factor f_{act} determines the degree of filling of the slowly drainable porosity and has to be calibrated or estimated from pre-event rainfall (see Ch. 8.4.3). The actual soil storage capacity S_{act} for each process intensity i (e.g. SOF 1 to SOF 3) is then calculated as

$$S_{act}(i) = (n_s \cdot (1 - f_{act}) + n_f) \cdot h_{max}(i) \quad \text{with } 0 \leq f_{act} \leq 1 \quad 8.2$$

All infiltrated water is stored in the slow drainable pore volume until it is saturated. Then rainfall infiltrates into the fast drainable pore space and a water table develops. Saturated overland flow starts as soon as the water table reaches the soil surface. In the SOF module, the soil drainage $q_{subsurface}$ is assumed to be proportional to the square of water level h above an impermeable layer in the soil (Equation 8.3).

$$q_{subsurface} = c_{SOF} \cdot h^2 \quad 8.3$$

This correlation was empirically derived from the observed water level recession in our groundwater wells located on SOF areas. The minimal value of c_{SOF} is zero (no drainage of SOF areas), the maximum value of c_{SOF} should be selected in a way that subsurface flow from SOF areas does not exceed subsurface flow from D or SSF areas.

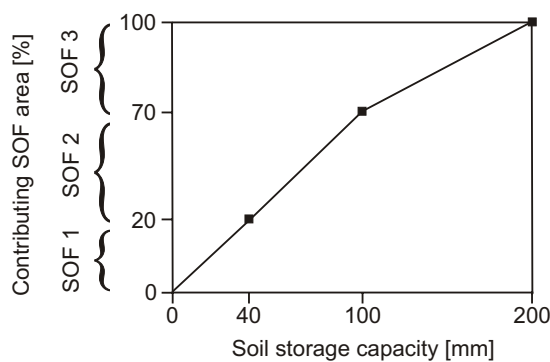


Fig. 8.3 Relationship between soil storage capacity and contributing SOF area. Squares were determined during the mapping, in between points linear interpolation.

Each process intensity encompasses areas with different storage capacities of the soil (e.g. 20 % SOF 1 area with 0 to 40 mm of storage capacity). To allow for a gradual expansion and shrinking of the saturated areas, a linear relationship between storage capacity of the soil and contributing area within one process intensity was assumed (Figure 8.3).

8.3.3 Tile drain flow

The soil water levels in the drainage module are calculated in the same way as in the SOF module and model parameters are determined correspondingly. The conceptualization of the soil drainage is different though. Subsurface flow from the tile drains $q_{subsurface}$ is based on the one-dimensional steady-state flow Hooghoudt's equation (e.g. Dieleman and Trafford, 1976, Khan and Rushton, 1996) (Equation 8.4).

$$q_{subsurface} = \frac{8 \cdot k_{sat} \cdot D_e \cdot h + 4 \cdot k_{sat} \cdot h^2}{S^2} \quad 8.4$$

k_{sat} is the saturated hydraulic conductivity, D_e the equivalent depth, S the drain spacing and h the depth of water table above the tile drain at half the drain spacing.

The equation is based on the Dupuit assumptions that (i) flow to the tile drain is one-dimensional and horizontal, (ii) streamlines are horizontal, (iii) equipotentials vertical, (iv) the flow velocities are proportional to water table slope and depth and (v) the water table intersects the tile drain.

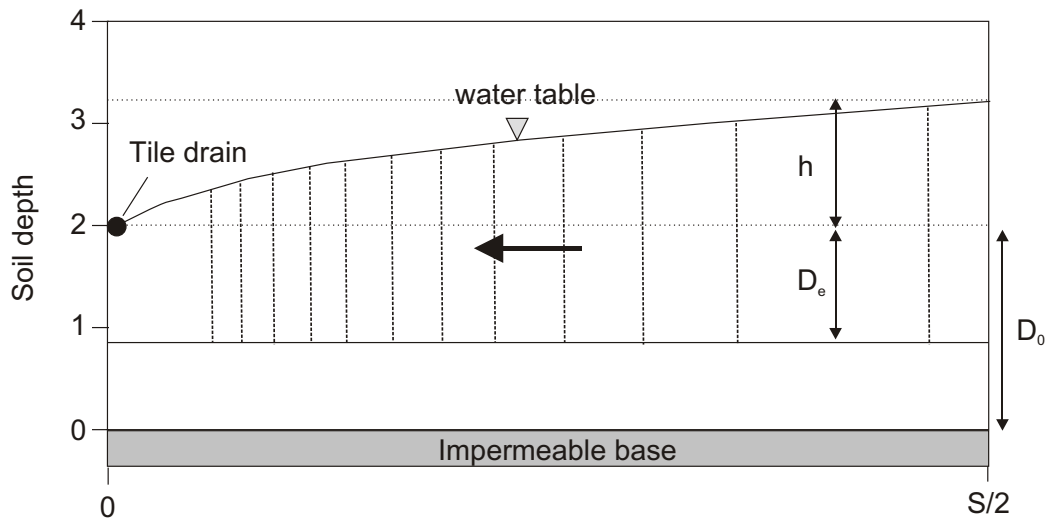


Fig. 8.4 Structure of drainage module with water table position, equipotentials and model parameters (changed from Khan and Rushton, 1996).

Hooghoudt (1944) introduced the equivalent depth D_e in the place of the distance between tile drain and impermeable base of the aquifer D_0 , to allow for radial flow close to small diameter tile

drains. Moody (1966) simplified Hooghoudt's expression for radial flow which allows the calculation of D_e using Equation 8.5 (r_d is the radius of the drain).:

$$D_e = \frac{D_0}{\left(1 + \frac{D_0}{S} \cdot \left(2.55 \cdot \ln \frac{D_0}{r_d} - c\right)\right)} \quad \text{for } 0 < D_0 \leq 0.31 S \quad 8.5$$

$$c = \left(3.55 - 1.6 \frac{D_0}{S} + 2 \cdot \left(\frac{D_0}{S}\right)^2\right)$$

$$D_e = \frac{S}{2.55 \cdot \left(\ln\left(\frac{S}{r_d}\right) - 1.15\right)} \quad \text{for } D_0 > 0.31 S$$

The parameters that have to be determined are k_{sat} , S , r_d and D_0 . In the Ror catchment the value for $S = 20$ m and $r_d = 3$ cm were taken from a map of the tile drain system, $k_{sat} = 100$ mm/d was estimated from soil texture and bulk density and D_0 is larger than 1 m (determined from soil cores). Using Equation 8.5 values for D_e therefore lie in the range between 0.68 m and 1.2 m.

If the soil water table reaches the surface, surface runoff occurs. This runoff can reach the channel as overland flow or re-infiltrate on highly permeable areas or be stored on the surface behind topographic barriers. All these effects occur on tile drained fields in the Ror catchment. However, in the drainage module, all surface runoff flows overland into the channel.

8.3.4 Subsurface flow

In the subsurface flow module, the soil model of the SOF module was used as well. Transient lateral saturated subsurface flow was routed downslope with a 1-dim approach (Wigmosta and Lettenmaier, 1999; Weiler and McDonnell, 2004). The hillslope is represented as a 1-dim hillslope slice of mean length, slope and soil depth h_{max} (Figure 8.5). The hillslope is divided into cells and the flow from the upslope to the downslope cells is calculated using the Dupuit-Forchheimer assumption (Freeze and Cherry, 1979). Subsurface flow $q_{subsurface}$ through a unit width is a function of the saturated hydraulic conductivity k_{sat} , the water table slope β and the saturated thickness h (Equation 8.6).

$$q_{subsurface} = k_{sat} \cdot \beta \cdot h \quad 8.6$$

The water table slope β between two cells is calculated from the length l and slope i of the hillslope, the number n_c of cells and the difference of the saturated thickness dh between the upslope and downslope cells (Equation 8.7).

$$\beta = \frac{dh \cdot n_c}{l} + i \quad 8.7$$

As SSF occurs in the Ror catchment on hillslopes of similar slopes and length, a mean hillslope length of 70 m and a slope of 18 % could be used in the model. The hillslope was divided into 30 cells, the saturated hydraulic conductivity was determined with a large scale sprinkling experiment.

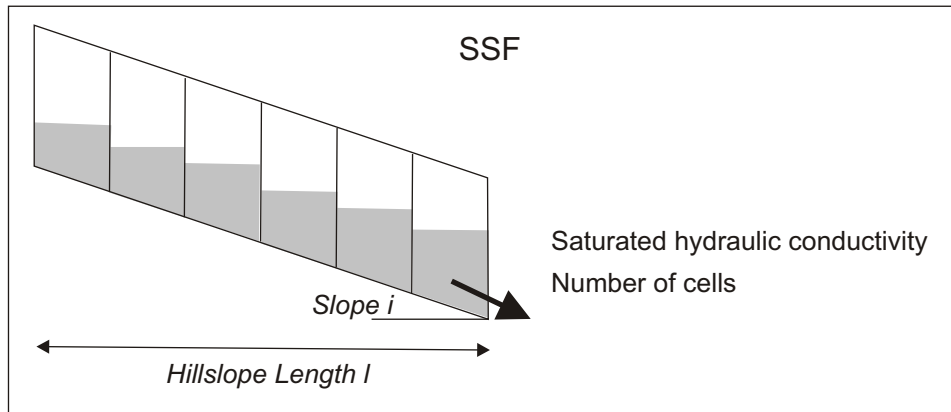


Fig. 8.5 Structure of SSF module.

8.3.5 Deep percolation

In the deep percolation module, the rainfall entering the drainable pore space flows into a groundwater storage, represented by a single linear storage (Figure 8.6 and Equation 8.8).

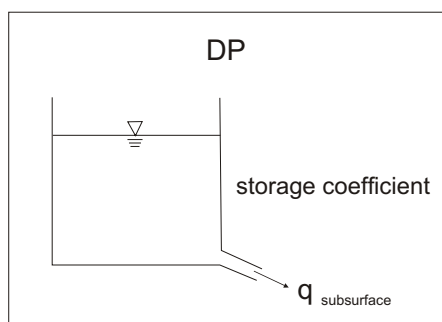


Fig. 8.6 Structure of DP module

$$q(t) = \frac{1}{k_{DP}} \cdot V(t) \quad 8.8$$

$V(t)$ is the volume of the storage and k_{DP} the storage coefficient. The storage coefficient can be estimated from the measured base flow recession curve.

8.4 Model parameters

8.4.1 Determination of model parameters

The model needs a set of 19 parameters for the simulation (Table 8.1). Half of these model parameters (10) can be determined through the DRP mapping and from field data only, among other things the most important parameters for the model calculations: the areal extent and the storage capacity of the different dominant runoff processes. Another model parameter is estimated from pre-event rainfall and two model parameters are set to a constant value prior to model calibration, since they are of minor importance. This leaves six parameters that could not be determined from catchment properties only, because the governing processes are not yet fully understood or are of minor importance. This concerns the three parameters governing the drainage of the soil, as well as the three parameters describing the surface retention of surface runoff and the subsurface retention of DP flow.

However, an upper and lower boundary of the parameter values could be defined from catchment properties for the three soil drainage parameters D_e , k_{sat} , and c_{SOF} . The final parameter values were then determined using the measured soil water levels on the respective process areas and in the case of the SSF parameter additionally with data from a large scale sprinkling experiment (see Ch. 8.5).

Storage coefficients can be determined from the falling limb of a measured flood hydrograph or they can be calibrated. The parameter value range for the three storage coefficients was estimated from values determined or calibrated in other catchments of about the same size and topography. However, the exact values for the storage coefficients have to be found through calibration to observed catchment runoff.

Table 8.1 All model parameters, how they are determined and the parameter values determined prior to simulation.

	Model parameter	Determined from	Parameter value determined prior to simulation
Determined from catchment properties only	Areal extend of each runoff process in catchment	<ul style="list-style-type: none"> DRP map 	
	Storage capacity of the soil for each DRP and process intensity h_{max} n	<ul style="list-style-type: none"> DRP map Soil texture Bulk density 	<i>Process intensity</i> 1: $h_{max} = 500$ mm 2: $h_{max} = 1300$ mm 3: $h_{max} = 2500$ mm $n = 0.08$
	The soil model parameters fast and slow drainable porosity n_f n_s	<ul style="list-style-type: none"> Macroporosity Soil texture 	$n_f = 0.03$ $n_s = 0.05$
	Saturated hydraulic conductivity of drainage module k_{sat}	<ul style="list-style-type: none"> Soil texture Bulk density 	100 mm/d
	Mean length of hillslope l	<ul style="list-style-type: none"> Topography 	70 m
	Mean slope of hillslope i	<ul style="list-style-type: none"> Topography 	18 %
	Tile drain spacing S	<ul style="list-style-type: none"> Plan of tile drain system 	20 m
	Tile drain radius r_d	<ul style="list-style-type: none"> Plan of tile drain system 	0.03 m
Determined from pre-event rainfall	Actual filling of soil storage f_{act}	Pre-event rainfall: 50 - 100 mm 100 - 150 mm	0.75 0.80
Set to a constant value	HOF 1 runoff coefficient a		0.5
	Evapotranspiration ET		1 mm/d
Parameter value range can be determined from catchment properties	Actual value is determined using soil water levels and sprinkling experiments	Saturated hydraulic conductivity of SSF module k_{sat}	<ul style="list-style-type: none"> Sprinkling experiments Soil water levels Logical deduction Soil depth
		Constant for soil drainage in SOF module c_{SOF}	
		Thickness of equivalent layer in drainage module D_e	
	Actual value is determined using outflow hydrograph	Storage coefficients for <ul style="list-style-type: none"> HOF 1 surface runoff, k_{HOF} Surface runoff from all other process areas k_{rest} DP subsurface runoff k_{DP} 	<ul style="list-style-type: none"> Transfer from catchments of about same size and topography Catchment runoff

Table 8.2 lists the six parameters which could not be determined prior to model simulation, their value ranges and the values used for the model simulations.

Table 8.2 Model parameters that could not be determined prior to simulation, their ranges of possible parameter values determined from catchment properties and the final value used for the simulations.

Process module	Parameter	Value range	Value used for simulation
SOF	• Constant c_{SOF} for soil drainage	0 - $1 \cdot 10^{-6}$ 1/s	$1 \cdot 10^{-6}$ 1/s
Drainage	• Thickness of equivalent layer D_e	6800 - 12000 mm	6800 mm
SSF	• Saturated hydraulic conductivity k_{sat}	> 100 mm/d	2000 mm/d
Runoff concentration	Storage coefficient for		
	• HOF 1 surface runoff,	• 1- 5 h	• 1h
	• Surface runoff from all other DRP	• 1 - 10 h	• 5 h
	• DP subsurface runoff	• 100 - 1000 h	• 500 h

8.4.2 Sensitivity analysis

A sensitivity analysis was conducted for the soil drainage and runoff concentration parameters using three objective functions: (1) the Nash model efficiency (Nash and Sutcliff, 1970), (2) the model water balance as simulated sum of runoff divided by measured sum of runoff and (3) the peak discharge as simulated peak discharge divided by measured peak discharge. For the sensitivity analysis catchment runoff of the Lindist, Rinderholz or Poesch catchment during the September 2002 flood event was used. Shown are the results of the catchment, in which the parameter investigated was most sensitive.

The values of the objective functions for different values of the three soil drainage parameters are displayed in Figure 8.7. Within the pre-defined parameter value range, all three parameters are very insensitive. Therefore, they can not be calibrated using catchment runoff.

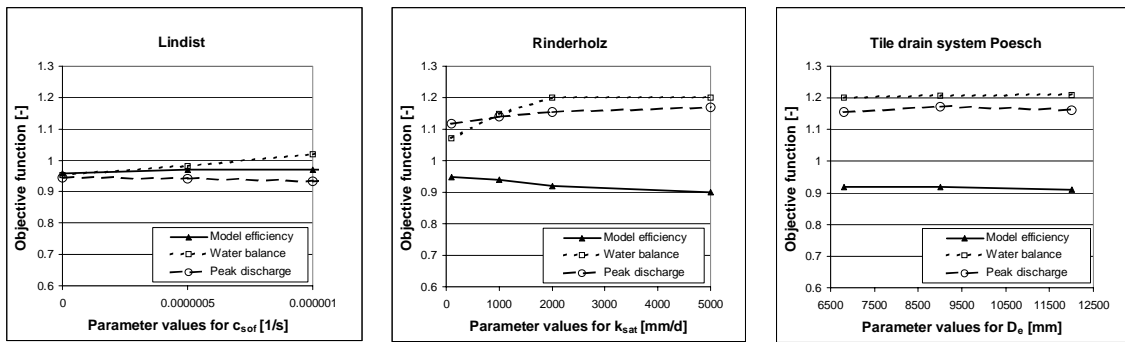


Fig. 8.7 Values of objective functions for different values of the three soil drainage parameters c_{sOF} , k_{sat} and D_e in the Lindist, Rinderholz and Poesch sub-catchment respectively. The objective functions used are (1) the model efficiency (Nash and Sutcliff, 1970), (2) the model water balance as simulated sum of runoff divided by measured sum of runoff and (3) the peak discharge as simulated peak discharge divided by measured peak discharge.

The sensitivity analysis showed that the storage coefficients for HOF 1 surface runoff and for the DP base flow are not sensitive either (Figure 8.8). The reasons for this are that HOF 1 only contributes little to runoff, while the time scale of the DP contribution to runoff is much larger than the duration of a single flood event. This leaves the storage coefficient for surface runoff from non-sealed areas as only sensitive model parameter that has to be calibrated using rainfall and runoff. It was determined from measured runoff in the Lindist sub-catchment ($k_{rest} = 5$ h).

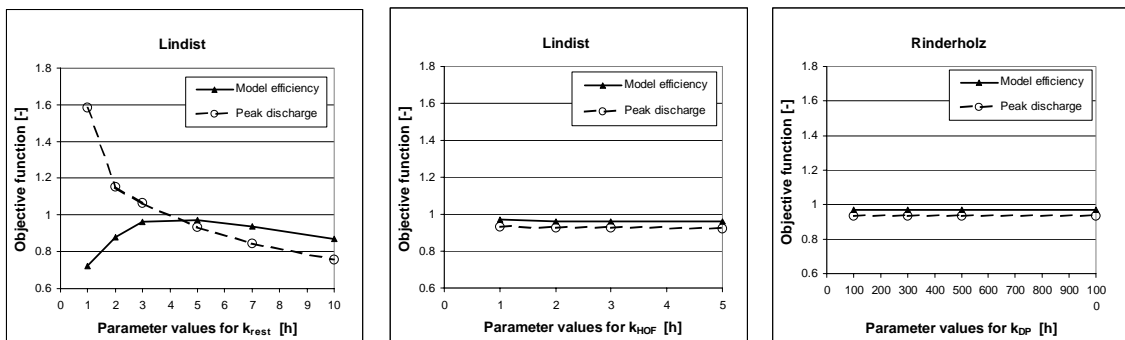


Fig. 8.8 Values of objective functions for different values of the three storage constants in the Lindist and Rinderholz sub-catchment. The objective functions used are (1) the model efficiency (Nash and Sutcliff, 1970) and (2) the peak discharge as simulated peak discharge divided by measured peak discharge.

Since only one sensitive parameter is calibrated to runoff, while all other model parameters are either determined directly from field data or calibrated independently using soil water levels of the respective DRP area, the problems of parameter inter-correlation and identifiability do not arise.

The sensitivity analysis was conducted in the Ror catchment, which is a small, agricultural catchment with a low percentage of HOF 1 area and a surface near impermeable layer (only shallow groundwater bodies can be found). Additionally, natural subsurface flow is of minor

importance and not very preferential. In a catchment with different catchment properties (e.g. a higher percentage of HOF 1 areas) some of the above insensitive parameters might be sensitive.

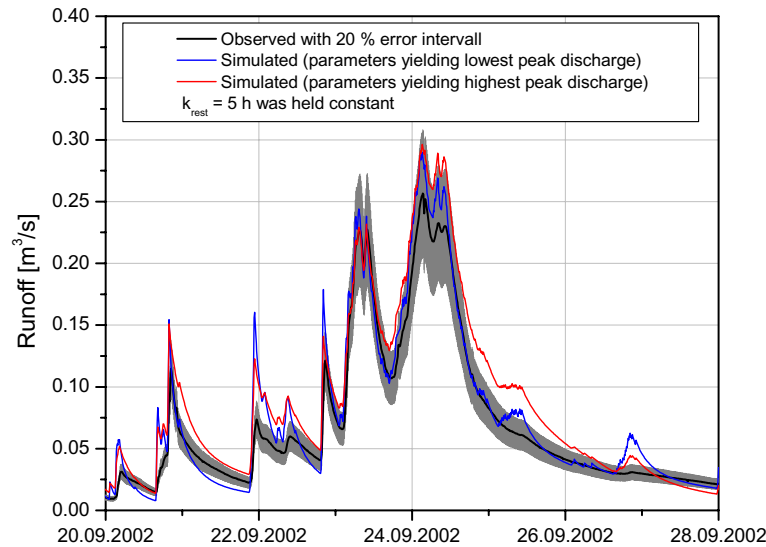


Fig. 8.9 Simulated runoff in the Rinderholz sub-catchment during the September 2002 flood using parameter values for the model parameters listed in Table 8.2 yielding the lowest (blue) and largest peak discharge (red) possible. Only the storage coefficient k_{rest} was held constant. Black line is observed runoff and grey is the 20% runoff measurement error.

In Figure 8.9 simulated runoff is displayed, using parameter values for the model parameters listed in Table 8.2 that yield the lowest (blue line) and highest (red line) peak discharge (only $k_{rest} = 5$ h was held constant). Observed runoff (black) with a 20% runoff measurement error (grey) is shown as well. For the two main flood peaks, simulated runoff lies within the 20% error interval of the runoff measurements for both scenarios.

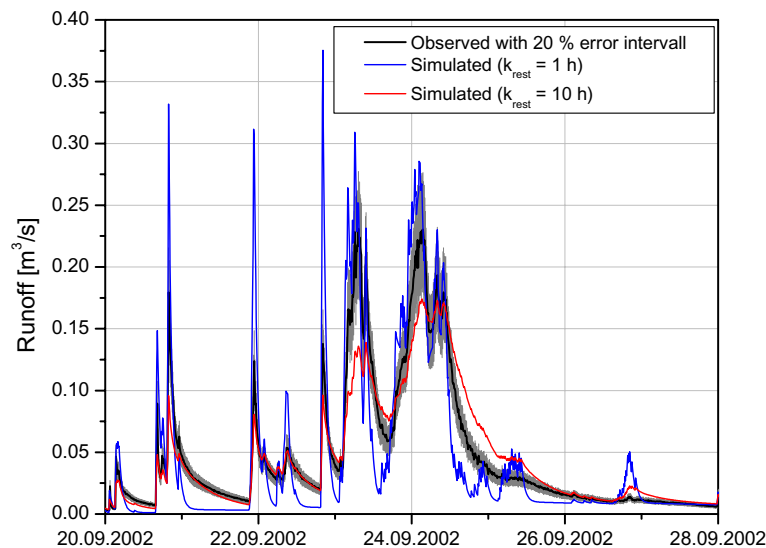


Fig. 8.10 Simulated runoff in the Lindist sub-catchment during the September 2002 flood using the optimised parameter values for all model parameters listed in Table 8.2 except the storage coefficient k_{rest} which was varied. Black line is observed runoff and grey is the 20% runoff measurement error.

In Figure 8.10 simulated runoff for two values of k_{rest} (1 h and 10 h) are shown. All other model parameters were held constant. For the very small storage constant of 1 h, especially the small flood peaks at the beginning of the flood event are overestimated while runoff during recession is underestimated. However, during the large flood peak simulated runoff again is within the 20 % error interval of the runoff measurements.

Peak discharge and runoff volume during a large flood event can be simulated quite accurately with the model, even if no measurements of soil water levels or runoff are available. Simulation results improve tremendously, if the storage coefficient k_{rest} can be calibrated to runoff. To do so, one measured flood event might already be sufficient. However, if also the flow paths of the water (percentage of surface and subsurface flow) are of interest, measurements of soil water levels on the different process areas are needed, to calibrate the soil drainage parameters.

8.4.3 Initial conditions

Pre-event rainfall and soil moisture have an influence on flood formation and should also be considered in the model simulations. One way to do so is to start simulations a long time period prior to the flood event, so that pre-event rainfall is captured and the initial soil moisture conditions are negligible. Figure 8.11 gives the results of the September 2002 flood event simulations. Simulations started one month before the main flood event with empty soil storages. Runoff is underestimated for the first flood peaks in the Rinderholz and for all flood peaks in the Lindist catchment. Nevertheless simulation results are satisfactory, especially for the main flood peak in the Rinderholz catchment

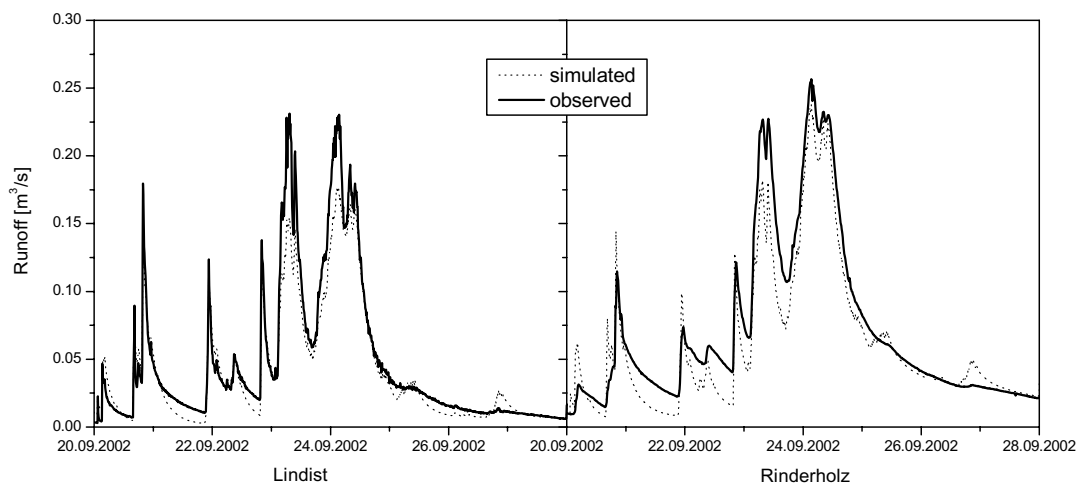


Fig. 8.11 Observed and simulated runoff for the Lindist (right) and Rinderholz (left) catchments during the September 2002 flood event. Simulation started one month before the main flood event with empty soil storages ($f_{act} = 0$).

However, the model was neither designed (e.g. ET) nor parametrized (e.g. base flow and soil drainage) for long term simulations. Therefore, this approach was not used to account for pre-event rainfall. Instead the factor f_{act} was introduced that allows for a partial filling of the slow draining soil storage (Equation 8.2 in Ch. 8.3.2). The slow draining soil storage capacities differ between runoff process intensities and therefore also between catchments with different process distributions. Its values for the Lindist and Rinderholz catchments are 50 mm and 95 mm respectively. The 30 d net pre-event rainfall (measured rainfall minus 30 mm evapotranspiration) for the September 2002 flood event is 70 mm, resulting in values of $f_{act} = 1.0$ for the Lindist and $f_{act} = 0.75$ for the Rinderholz catchment. Figure 8.12 gives the results of the model simulations using these values. Simulation results are very satisfactory.

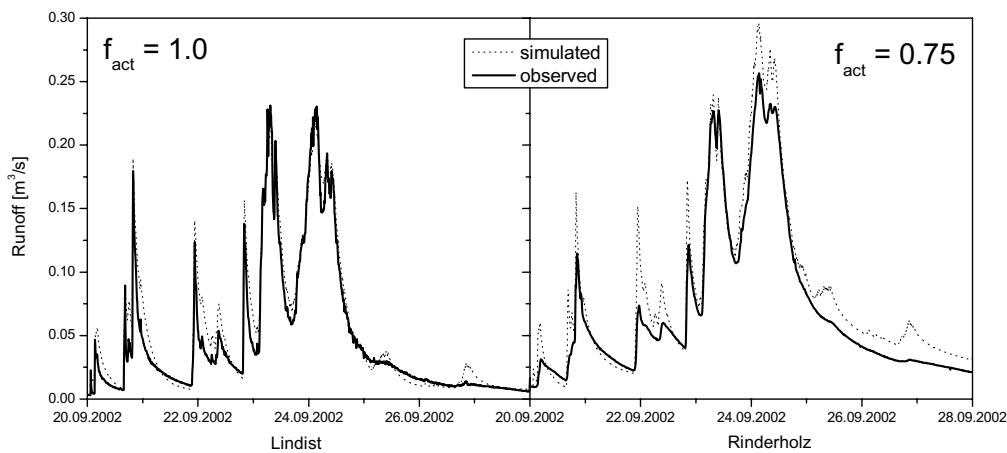


Fig. 8.12 Simulated and observed runoff in the Lindist and Rinderholz catchments using the corresponding values for f_{act} determined from 30 d pre-event rainfall.

However, using different values for f_{act} in the two catchments is not warranted from a process based point of view. Additionally, the value of $f_{act} = 1.0$ for the Lindist catchment is rather high. Therefore, the Rinderholz value of $f_{act} = 0.75$ was chosen for the model simulations, accepting that runoff is underestimated in Lindist during the beginning of the event (Figure 8.14). During the main flood peak though, simulation results are not influenced by f_{act} anymore.

Since all other flood events simulated in this study have similar or even higher amounts of pre-event rainfall, $f_{act} = 0.75$ was chosen as a lower boundary value. For events with a pre-event rainfall between 50 and 100 mm in 30 days, f_{act} was set to 0.75, for events with 100 to 150 mm of pre-event rainfall, f_{act} was slightly increased to 0.8, accepting the possible underestimation of runoff at the beginning of an event.

8.5 Performance of modules

8.5.1 SOF module

The parameters determining the storage capacity in the SOF module were estimated from field data. The parameters governing soil drainage were calibrated to groundwater levels recorded on the different SOF areas for the September 2002 flood. In Figure 8.13 the observed and simulated groundwater levels are displayed.

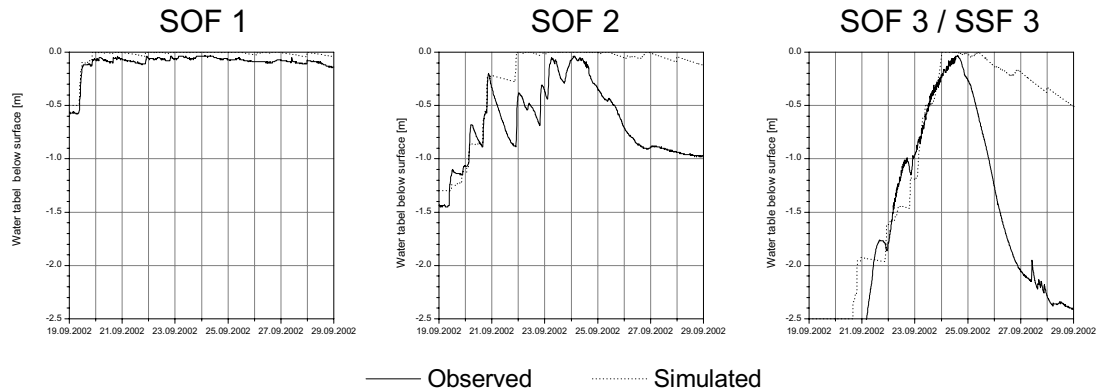


Fig. 8.13 Observed and simulated groundwater levels during the September 2002 flood.

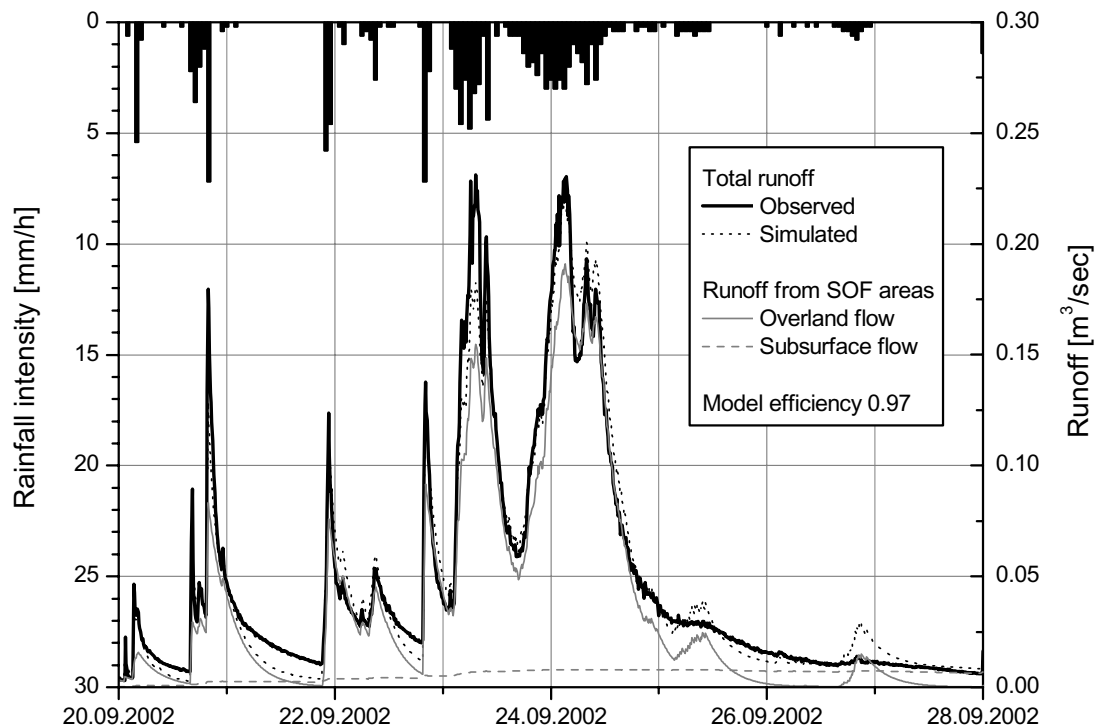


Fig. 8.14 Observed and simulated runoff in the Lindist sub-catchment during the September 2002 flood.

The simulated water levels on the SOF areas during the September 2002 flood agree to the observed ones with regard to time and duration of saturation. Differences occur during the drainage of the SOF areas. SOF 2 and SOF 3 areas drain faster than in the model. In Figure 8.14, the observed and simulated runoff in Lindist are displayed, together with surface and subsurface contributions from the SOF areas. Although the simulated groundwater levels are too high, the model rather overestimates runoff during recession, due to the subsurface flow contribution from the drainage of SOF areas.

Obviously, the fast drop of the water levels on the plot scale does not lead to a corresponding increase in the runoff. This might be explained by internal drainage of the soil (Figure 8.15). The concept assumes a permeable top soil over a subsoil with low matrix permeability and high macroporosity. During an event, the top soil starts to saturate and macropore flow is initiated. Due to a low interaction between macropores and the low permeable matrix, the water drains only slowly from the macropore into the matrix, resulting in a filling of the macropores and the top horizon. Surface runoff occurs, although the soil is not totally saturated. After the event, the water drains from the macropores into the unsaturated soil matrix of the subsoil, and does not contribute to runoff. However, further research is needed to better understand the process of soil drainage.

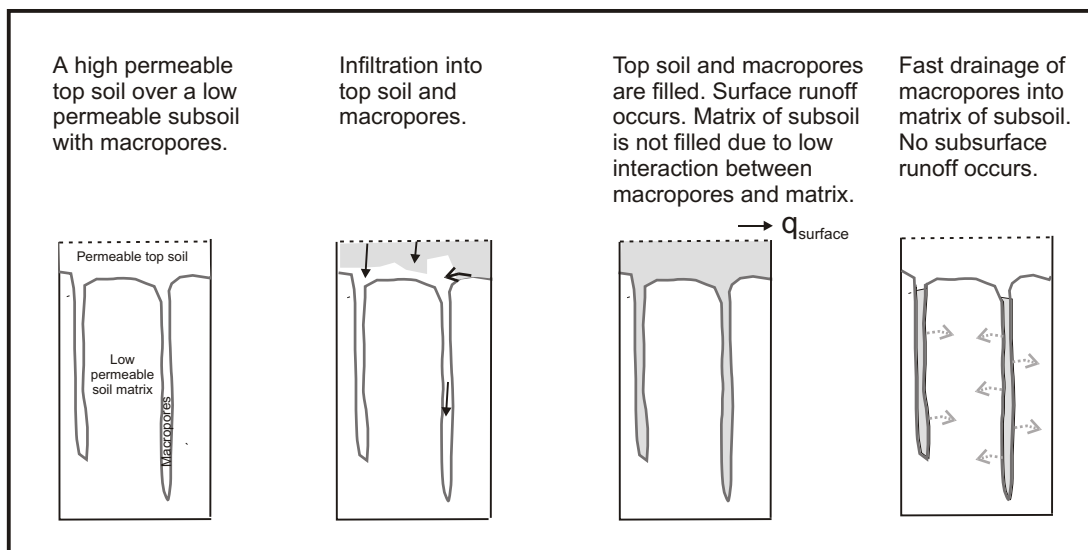


Fig. 8.15 Concept how SOF areas might be drained.

8.5.2 SSF module

The saturated hydraulic conductivity was calibrated using the measured soilwater levels in a SSF 3 hillslope (Figure 8.16) and the data from a sprinkling experiment on the same hillslope of Kienzler and Oberrauch in July 2003 (personal communication) (Figure 8.17).

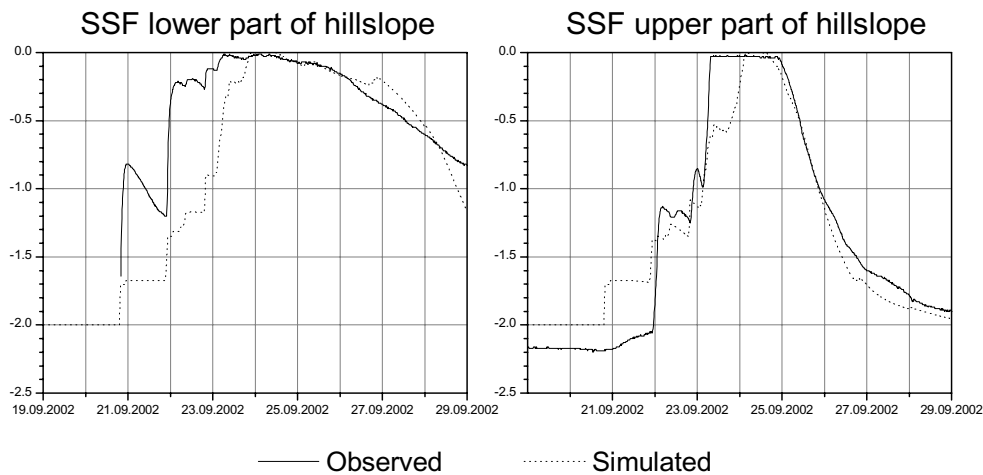


Fig. 8.16 Observed and simulated water levels on a SSF 3 hillslope in the Rinderholz sub-catchment during the September 2002 flood.

The water levels calculated with the SSF module rise slower than the observed ones during the September 2002 event. In the lower part of the hillslope, water levels rose 24 h before the model. In the upper part of the hillslope, the delay is less pronounced. Preferential flow, not considered in detail in the module, might be responsible for this.

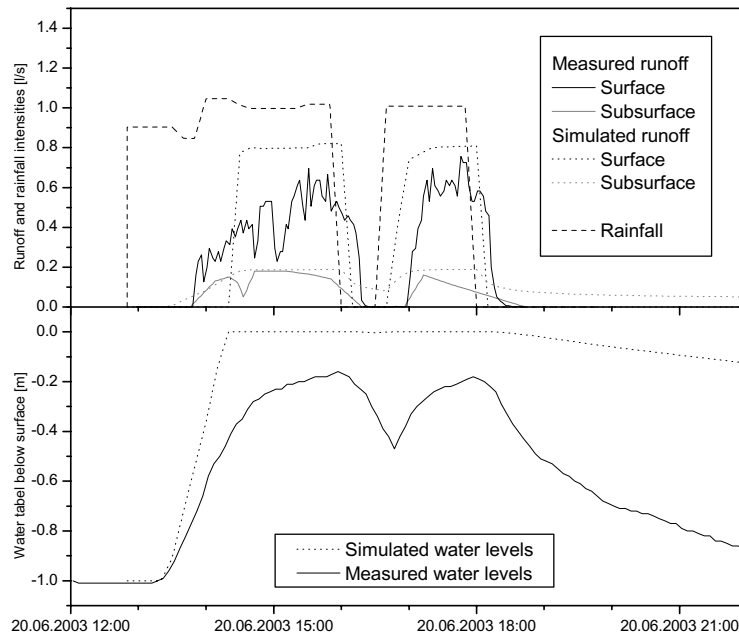


Fig. 8.17 Measured and simulated runoff and groundwater levels during a sprinkling experiment on a SSF hillslope in the Rinderholz catchment (Kienzler and Oberrauch, 2003, personal communication). 95 m^2 were sprinkled with an intensity of 1 l/s (38 mm/h) and surface and subsurface flow were measured in a ditch below the sprinkled area.

During a sprinkling experiment with intensities of 30 to 40 mm/h (Kienzler and Oberrauch, 2003, personal communication), the subsurface flow capacity of the hillslope was exceeded and surface flow occurred after one hour. Surface and subsurface flow ceased rapidly after sprinkling was stopped, the simulated runoff continued much longer. The SSF module simulated the onset and maximum flow rate of the subsurface flow quite accurately, the sudden stop of subsurface flow could not be described with the concept of filling and emptying storages.

8.5.3 Drainage module

The drainage parameter was calibrated to the measured groundwater levels and runoff from the tile drain system Poesch. Observed and simulated water levels are similar (Figure 8.18) but contrary to the simulations soil saturation was not observed in the field on the D 2 area. The simulated subsurface flow from the tile drain system corresponds well to observed runoff during recession (Figure 8.18).

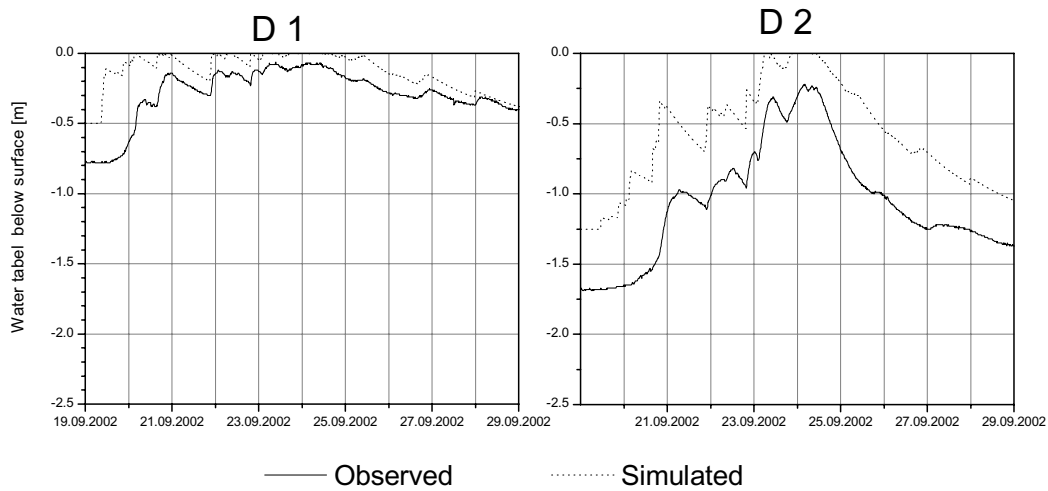


Fig. 8.18 Observed and simulated soil water levels in the tile drain system Poesch

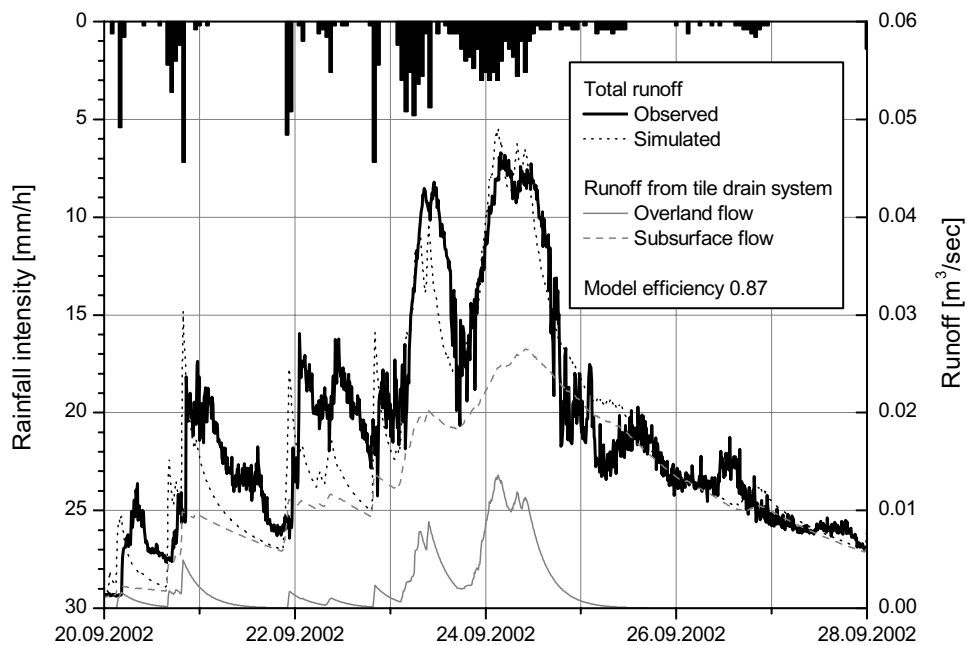


Fig. 8.19 Observed and simulated runoff of the tile drain system Poesch during the September 2002 flood event.

During peak flow though, measured runoff reacts fast and strong. This behaviour can only be reproduced if all the surface runoff occurring from the saturated tile drained field is added. The measurements and simulations indicate that the runoff reaction of tile drained areas is as fast as on SOF areas, although flow paths are quite different.

8.5.4 Performance on the catchment scale

As mentioned earlier (Chapter 7.3) the distribution of the dominant runoff processes in Rinderholz differs from Lindist. Total runoff and the contribution of the three runoff processes SOF, SSF and D were simulated for Rinderholz using the actual DRP distribution but without changing the calibrated parameters estimated for the Lindist catchment (Figure 8.20).

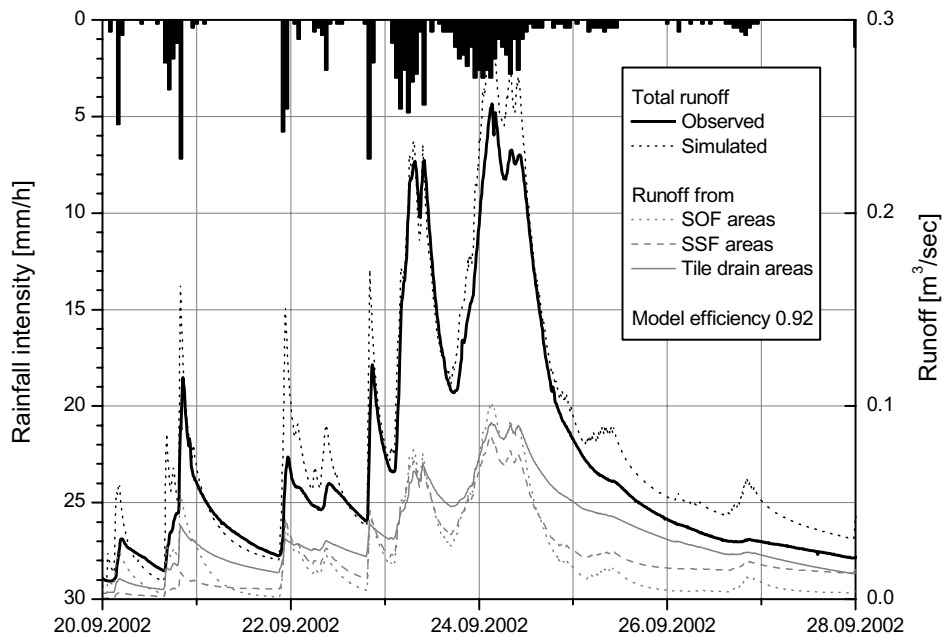


Fig. 8.20 Observed and simulated runoff in Rinderholz during the September 2001 flood and the contributions from SOF, SSF and D areas.

Runoff is slightly overestimated by the simulation, especially during recession. No significant difference between SOF and SSF flow during peak flow can be found. The overall performance of the model is satisfactory.

8.5.5 Evaluation of soil drainage concepts

The simulation of peak flows and runoff volume during single flood events depends mainly on the amount of water that can be stored in the soil before runoff occurs. The relevant parameters can adequately be defined by the mapping and modelling approach and do not have to be calibrated.

The soil drainage processes, which influence the long term behaviour of the model, could not be conceptualized without relying on calibrated parameters, since the processes of soil drainage are still not understood. In this context, especially the influence of preferential lateral flowpaths on soil and hillslope drainage should be investigated more closely.

8.6 Simulation of other floods

8.6.1 Catchment runoff

Two floods occurring in September 2001 and October 2002, which have not been used for the calibration, have been simulated without change in model parameters.

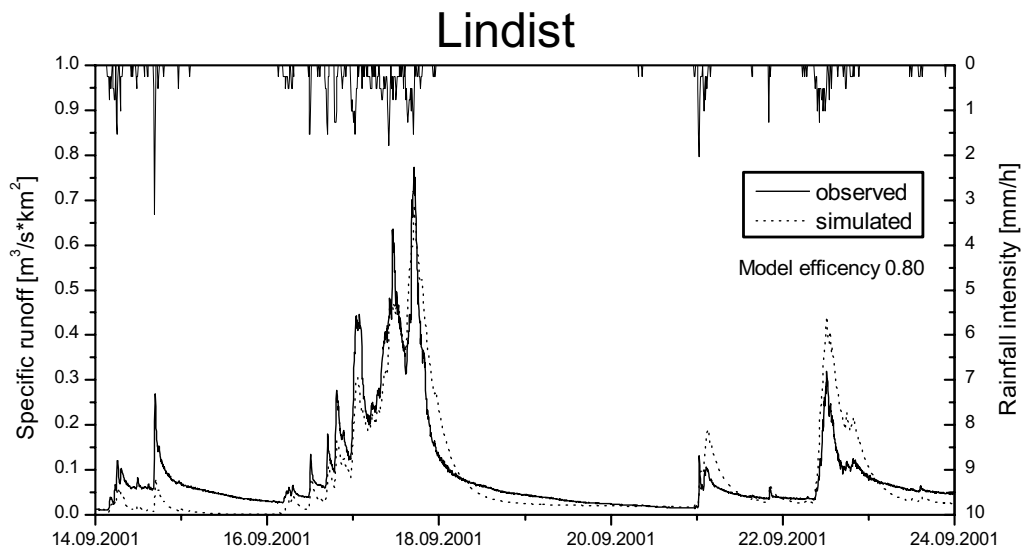


Fig. 8.21 Observed and simulated runoff in the Lindist catchment during the September 2001 flood.

Hydrograph, peak flow and runoff volume of the main flood event in september 2001 as well as of the two following small events could be simulated in Lindist by the model. Again flows during recession were slightly overestimated (Figure 8.21). Data for Rinderholz and the tile drain system Poesch were not available.

Hydrographs for the October 2002 event, which is smaller than the September 2001 and September 2002 events, are shown in Figure 8.22..

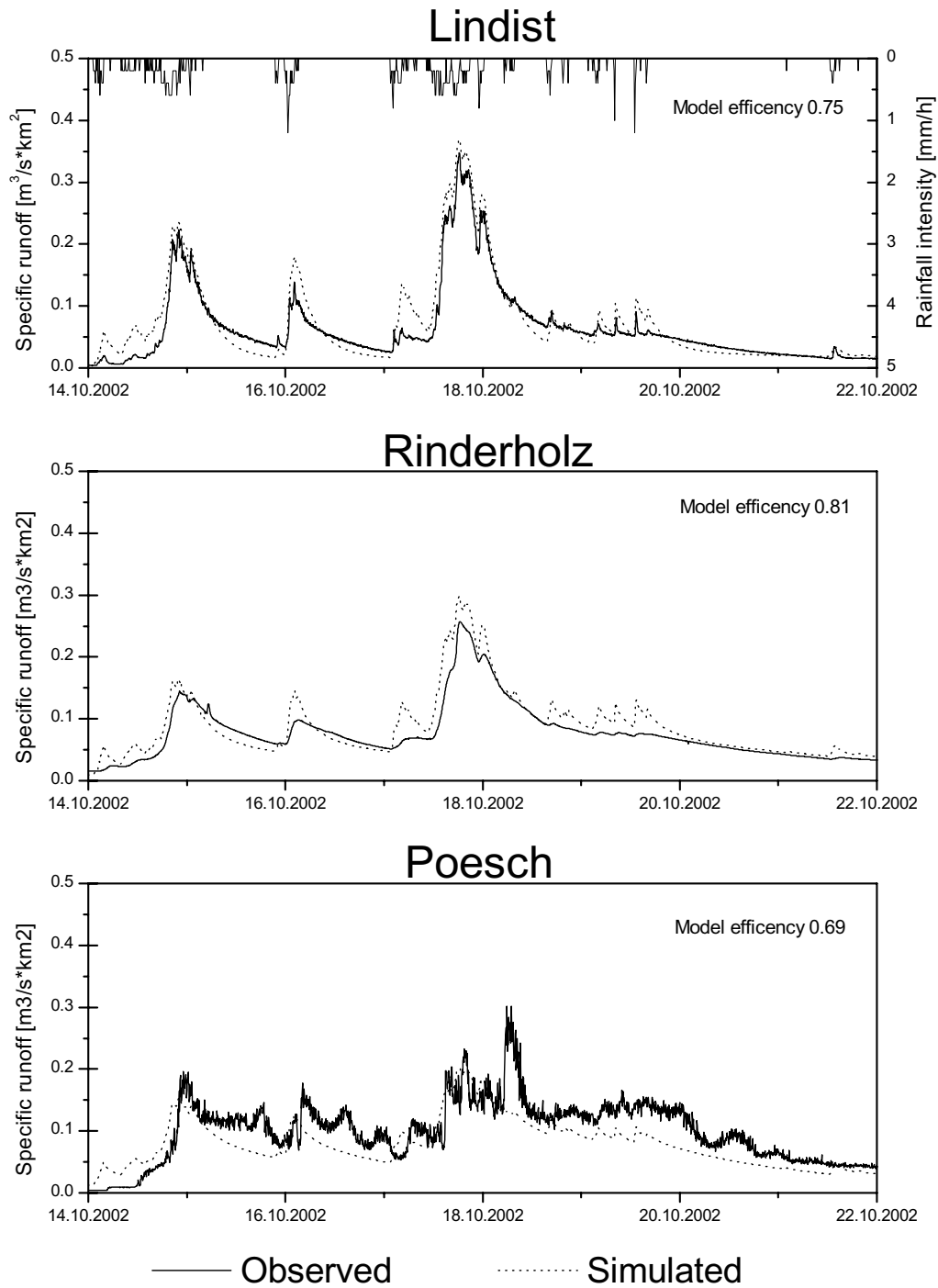


Fig. 8.22 Observed and simulated discharge in Lindist and Rinderholz and from the tile drain system Poesch during the October 2002 flood.

The hydrograph of the two flood events could be reproduced well by the model. Tile drain runoff in Poesch is underestimated by the model, probably because the catchment area of the tile drain system could not be defined exactly and the extremely fast reaction of the drainage system was surprising and might be underestimated by the model.

8.6.2 Event water

Event runoff calculated from EC is compared to the simulated surface runoff from HOF and SOF areas (Figure 8.23).

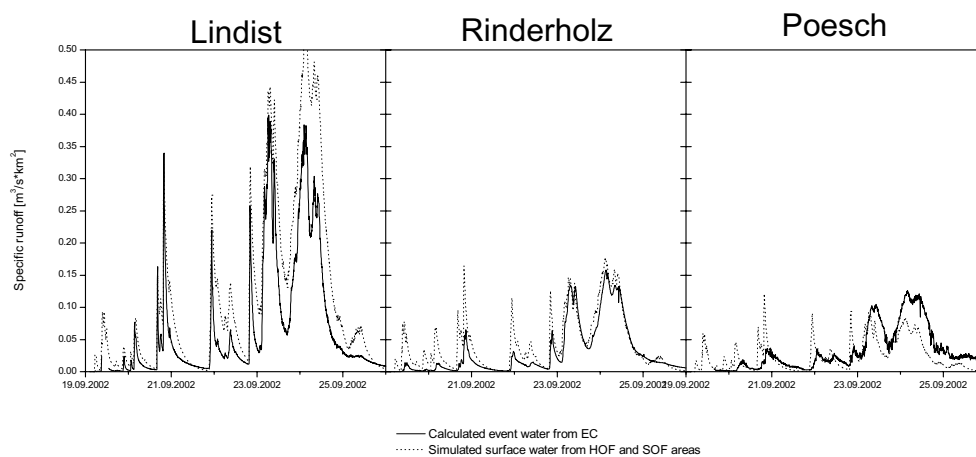


Fig. 8.23 From EC calculated event water and with model *Qarea-pro* simulated surface runoff for the two sub-catchments Lindist and Rinderholz and the tile drain system Poesch for the September 2002 flood event.

Calculated event water and simulated surface runoff from HOF and SOF areas correspond well in the Lindist and Rinderholz sub-catchments but not in the tile drain system Poesch. Interpretation of this data is difficult, last but not least because of the high uncertainties in the event water calculations. Nevertheless the following points can be stated: (1) model results in the Lindist sub-catchment do not oppose the high percentages of calculated event water and vice versa, (2) event water contributions are smaller than total simulated surface runoff in all three sub-catchments at the beginning of the event and (3) during peak discharge, event water contributions are higher than simulated surface runoff in the tile drain system Poesch. This might be explained with fast preferential subsurface transport of event water during storm runoff.

8.6.3 Extent of saturated areas

For the September 2002 flood event saturated areas during peak discharge on the 24.09.2002 (SOF, D and SSF with process intensity 1 and 2 and SSF 3) were determined with the model (grey areas in Figure 8.24). On the same figure the areas are shown on which ponding or flowing water could be observed in the field on the same day. Saturated areas on slopes where water was not ponding on the soil surface could not be identified.

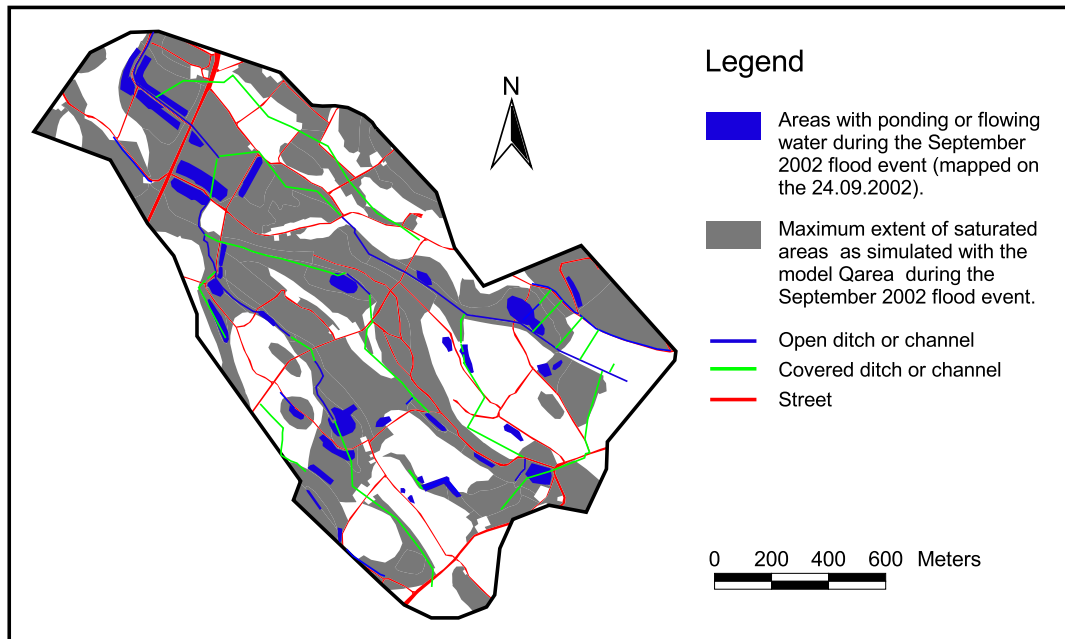


Fig. 8.24 Comparison of modelled areal extent of saturated areas with areas on which ponding or flowing water could be observed in the Ror catchment on the 24.09.2002.

To identify such areas, aerial infrared photographs were taken after the September 2001 flood (peak on the 17.09.2001) of the Ror catchment on the 19.09.2001 and on the 27.09.2001. Photographs were taken on two dates to infer the extent of saturated areas and the spatial pattern of the drying down. However, as the SOF areas drain exceedingly fast, the photographs have to be taken in a sequence of a few hours after a flood. Frequently saturated areas causing a change in vegetation could be identified (Figure 8.25).

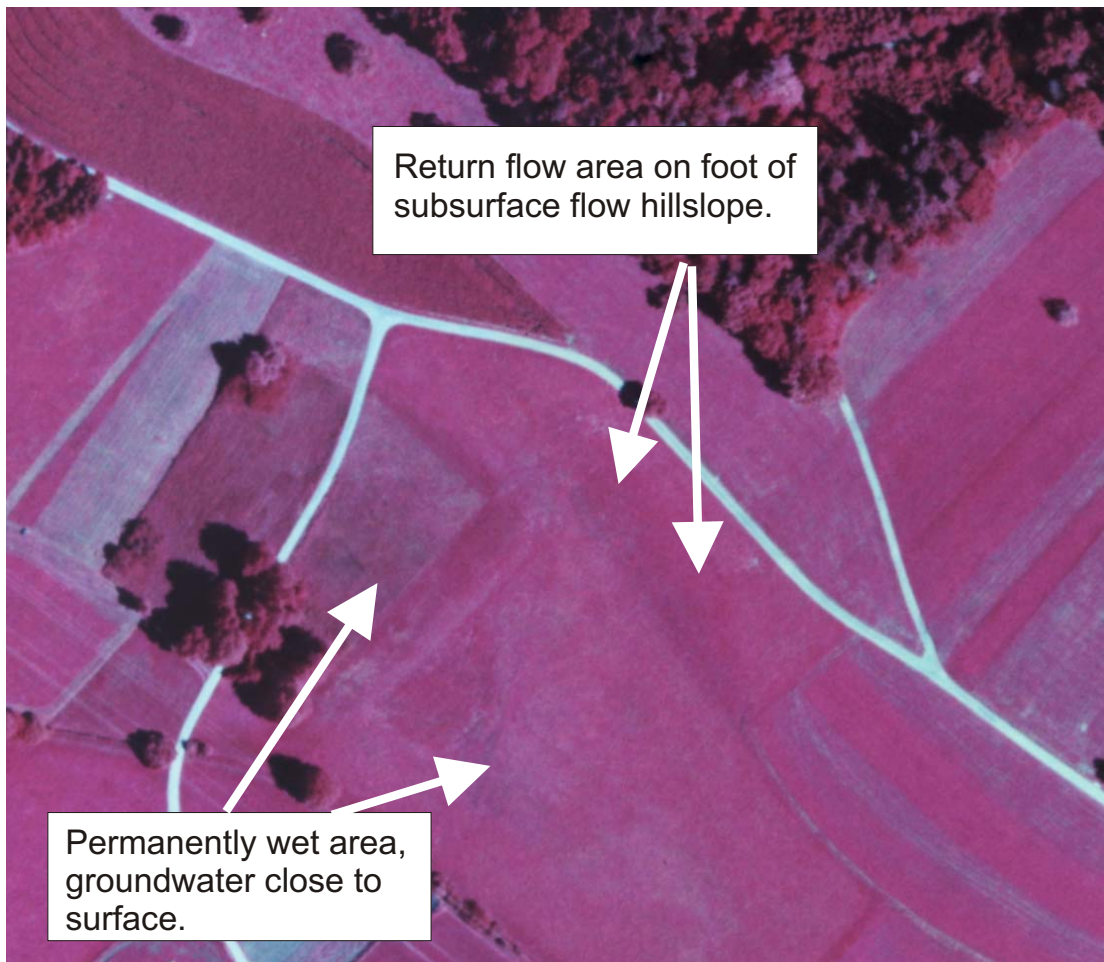


Fig. 8.25 Frequently saturated areas identified from infrared photography.

8.7 Model evaluation

The model could reproduce observed runoff and soil water levels. Most parameters could be determined directly from field data, only one parameter (k_{rest}) had to be calibrated using rainfall and runoff. A multi-criteria validation of the model is possible, using data like soil water levels, results from sprinkling experiments, event water calculations or process observations during flood events.

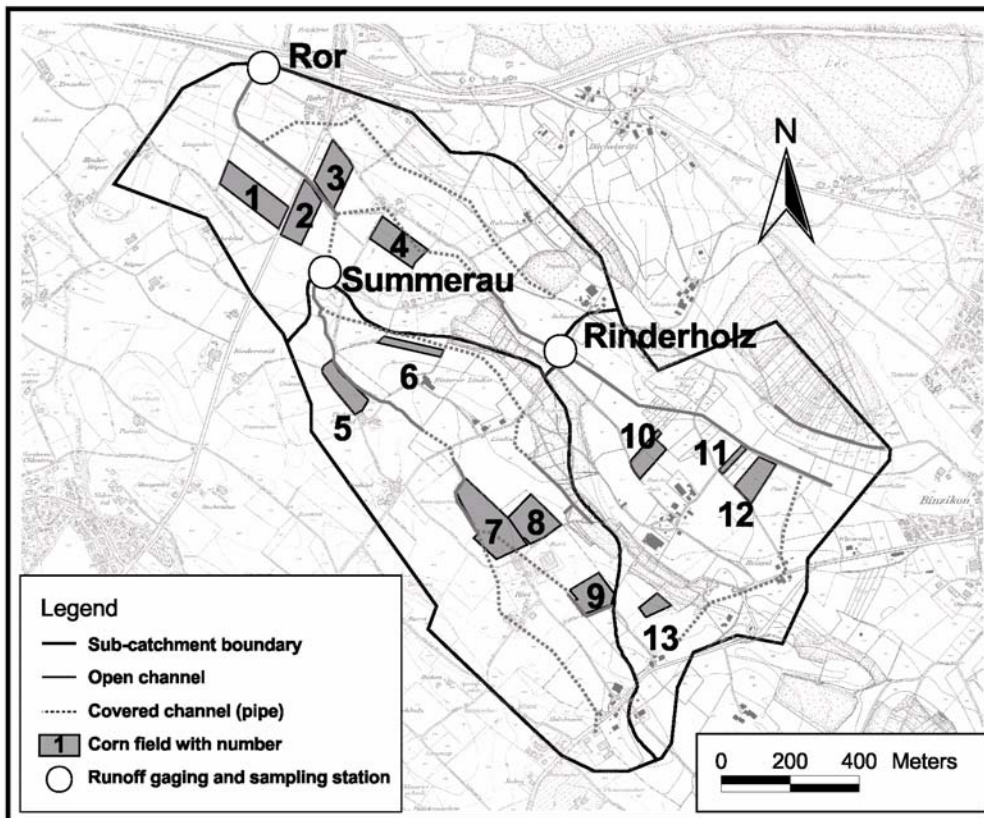
9 Testing mapping and modelling results using pesticides as tracers

9.1 Introduction

The group “process water and agriculture” of EAWAG investigates pesticide transport in the Ror catchment (Leu, 2003). They found that pesticides are transported from fields to surface waters mainly during flood events and dominantly in surface runoff and fast preferential subsurface flow. As the efficiency of the transport depends on runoff generation mechanism on the concerned agricultural fields, the pesticides measured in the brook can be used for an independent test of the DRP mapping and modelling. On the other hand the dominant runoff process maps and the model results help to interpret the solute transport measurements.

9.2 Pesticide study

The EAWAG (Leu, 2003; Leu et al. 2004a and Leu et al. 2004b) investigated herbicide and pesticide loss from agricultural fields to surface waters. To this purpose, the herbicides atrazine, dimethenamid and metolachlor, as well as one tracer pesticide per field were applied on 13 corn fields in the Ror catchment. Due to analytical problems with one tracer pesticide, fields # 6 and 13 had to be excluded from our study. The pesticide concentration in the runoff was measured at three sites with high temporal resolution during 67 days after the application of the pesticides. Figure 9.1 shows the location of the corn fields and the sampling stations.



Hintergrundplan reproduziert mit Bewilligung des Amtes für Raumordnung und Vermessung, Baudirektion Kanton Zürich.

Fig. 9.1 Location of corn fields and EAWAG sampling stations.

Herbicides and tracer pesticides were applied on the 8th of May 2000 after a relatively dry period. During the following 9 days no rainfall occurred, followed by 3 small rainfall events with a total of 50 mm of rainfall in the next 14 days. Those rainfall events caused no significant hydrologic response. On the 31st of May, 23 days after the pesticide application, a major rainfall event occurred with 46 mm in 24 h causing a small flood. High pesticide concentrations could be measured and depending on the herbicide, the event accounted for 69 to 93% of total loads in runoff during the 67 day measurement period (Leu, 2003). Table 9.1 summarizes information about the corn fields, the pesticides applied and the loads measured during this May 2000 event. The experimental setup, analytical method and load calculations are described in detail in Leu (2003).

Table 9.1 Characterization of the corn fields, the tracer pesticides applied and the pesticide loads measured in runoff during the May 2000 event (changed and complemented from Leu, 2003).

Field	Area [ha]	C _{org} ^a [%]	Soil texture top soil	Pesticide	Load [% of applied] ^b	Sorption coefficient K _{oc} [ml/g]	Field half life [days]	Source ^c
1	1.4	2.9 2.8-7.5	sandy loam Ls3	Alachlor	0.07	33 - 742	14 - 49	[1],[2],[3]
2	1.1	4.0 5.5-7.2	clayey loam Lt2	Terbutyl-azin	0.06	162 - 278	30 - 60	[2]
3	1.2	5.2 4.9	clayey sandy loam Lts	Dimet-achlor	0.13	63	8 - 43	[2]
4	1.1	7.2 3.2-5.2	clayey loam Lt2	Simazine	0.35	4 - 2000	28 - 149	[1],[2],[3]
5	0.7	3.6 3.4	sandy loam Ls3	Prometryn	0.05	400	6 - 360	[1],[2],[3]
7	1.9	5.6 4.2-5.4	clayey loam Lt3	Alachlor	0.17	33 - 742	14 - 49	[1],[2],[3]
8	1.3	3.3 2.9-3.7	sandy loam Ls3	Terbutyl-azin	0.26	162 - 278	30 - 60	[2]
9	1.0	2.0 3.9	sandy loam Ls3	Furalaxyl	0.05	?	31 - 65	[2]
10	0.3	12.2 4.0	clayey loam Lt3	Cyanacine		?	14 - 98	[3]
11	0.6	6.2 8.4	sandy loam Ls2	Furalaxyl	no tracer pesticide could be found in runoff	?	31 - 65	[2]
12	0.1	7.3 6.1	clayey loam Lt3	Metaza-chlor		?	3 - 9	[2]

^afirst row own measurements, second row measurements of Leu (2003)

^b Load measured from the 31.05.2000 4:30 am to 1.6.2000 11:00 am in runoff

^c Literature: [1] Wauchope et al. (1992)

[2] Tomlin (1997)

[3] EXTOWNET (1996)

The amount of pesticide mobilized by the rainfall depends on the chemical properties of the pesticide and the soil (especially organic content C_{org} and soil texture), weather conditions after application and the runoff processes occurring on the fields. The organic matter content as well as the soil texture in the top soil vary little on the investigated fields and cannot explain the differences in pesticides in runoff. The weather conditions were the same for all fields. This leaves the chemical properties of the pesticides and runoff processes on the fields as variables. The degradation, sorption and transport behaviour of the tracer pesticides in the field is not well known, K_{oc} and field half life found in literature vary widely and were mostly determined in the laboratory only. Therefore, a real quantitative comparison of measured pesticides loads is only

possible between fields on which the same tracer pesticide was applied (field pair 1 and 7, field pair 2 and 8 and field pair 9 and 11).

9.3 Results

Figure 9.2 shows the simulated and measured runoff in Ror and in Summerau for the May 2000 event. The model was then used to calculate the contributions to runoff from each corn field separately. The model results and the measured pesticide load for the tile drained fields 1 to 4 and 10, 11 and the SOF fields 5 to 9, as well as the distribution of runoff processes on the field can be seen in Figure 9.3 and Figure 9.4.

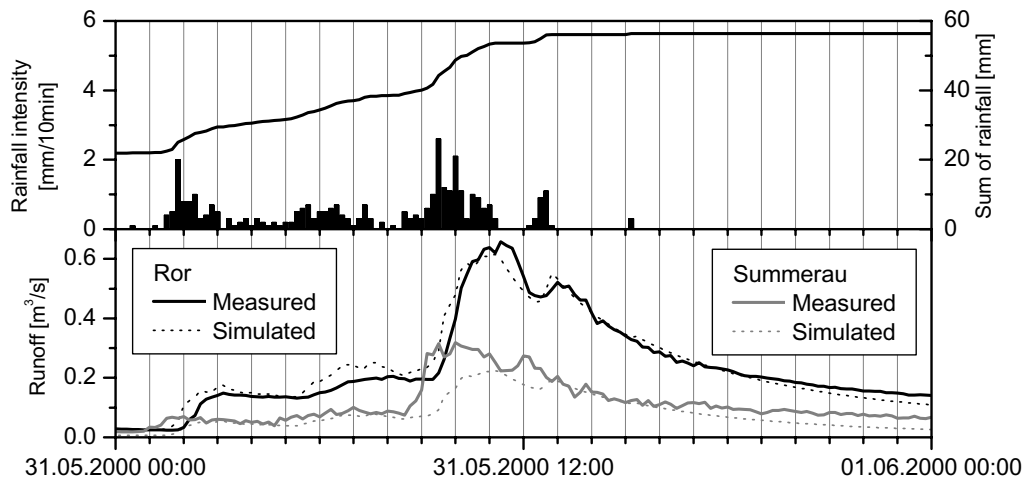


Fig. 9.2 Measured and simulated rainfall and runoff in Ror and Summerau for the May 2000 event.

Runoff from tile drained areas originates mainly from areas with runoff process D 1. D 2 areas contribute significantly less, while D 3 areas do not contribute. Runoff process D 1 is found on 57 % to 100 % of the area on fields 1 to 4. According to the model these fields react fast and strongly to precipitation. The pesticides in runoff showed the same, fast reaction. The pesticide measurements therefore support the rather surprising model assumptions of a fast contribution of tile drain flow to runoff.

The four fields with process D 1 and D 2 differ in the way surface runoff can reach the channel. On field 1, surface runoff can not flow into the channel directly, due to a topographic barrier. From the other fields, only a fraction of the surface runoff reaches the channel, while the rest is withheld in depressions. As the tracer pesticides reach the channel quickly, fast and efficient preferential transport into the tile drain system through macropores and pipes has to be assumed. On fields 10

and 11 process type D 3 dominates. During events, like in May 2000, only little runoff emerges from such areas. This is confirmed by the fact that no pesticides applied on these two fields were found in the runoff.

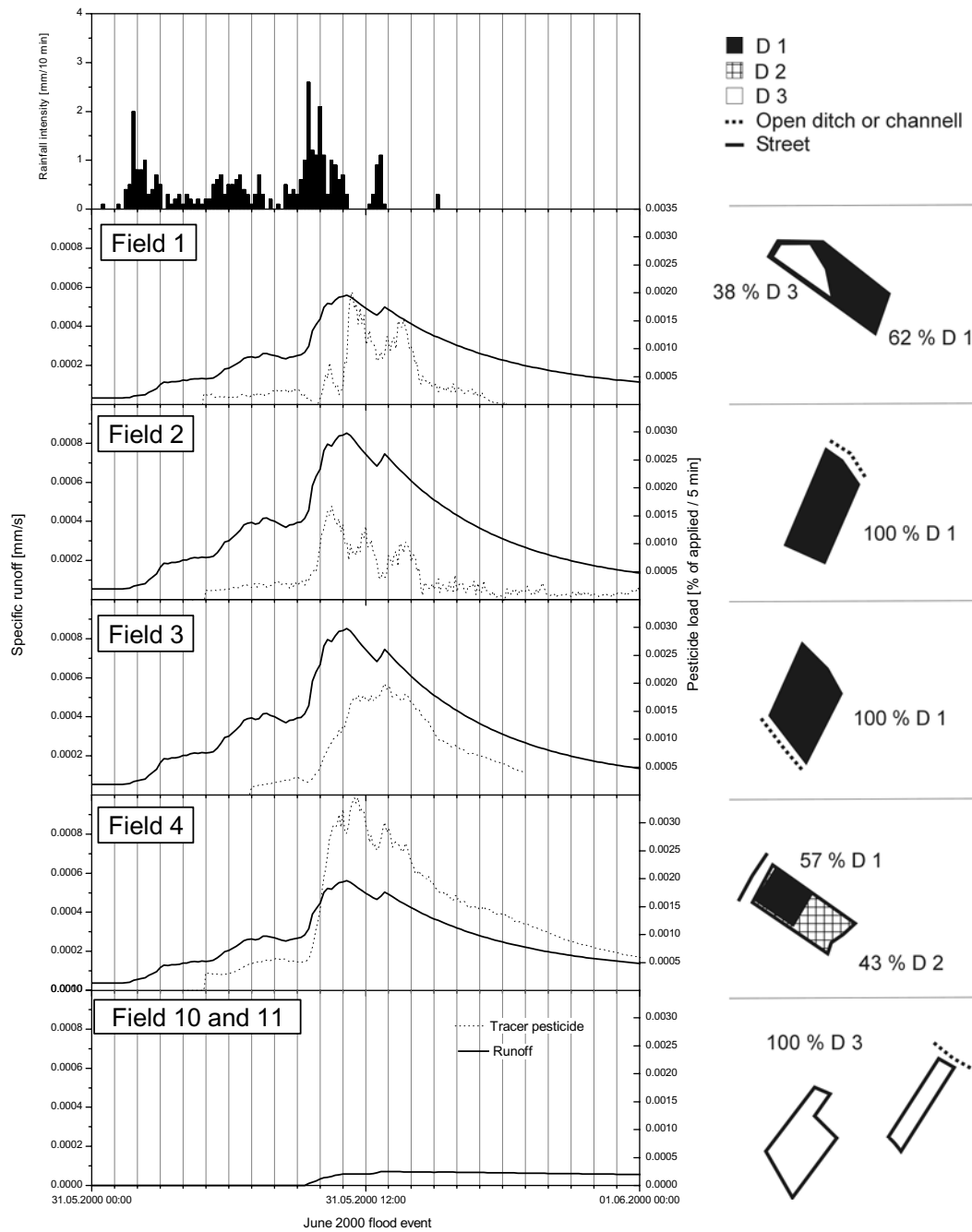


Fig. 9.3 Pesticide load in percent of applied for tile drained fields in the Ror catchment and simulated runoff from these fields (left). On the right side the runoff processes expected on these fields are shown.

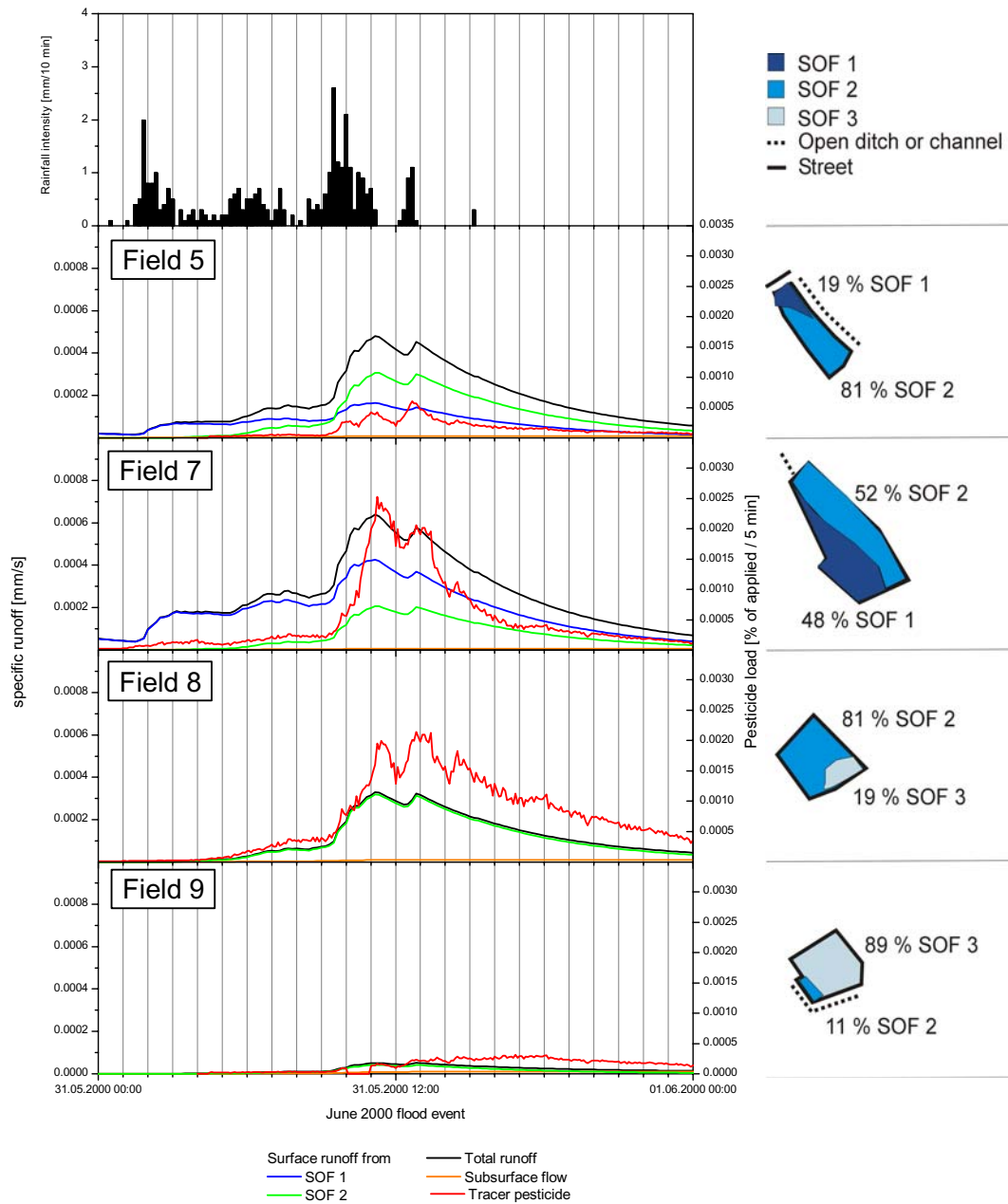


Fig. 9.4 Pesticide load in percent of applied on four SOF fields in the Summerau sub-catchment and simulated specific surface and subsurface runoff from the fields (left). On the right side the runoff processes expected on these fields are shown.

On the SOF fields 5 to 9, surface runoff could be observed during the event (only very little on field 9 though). Between 52 % and 81 % of the area of fields 5, 7 and 8 are of process type SOF 2. The pesticide concentrations in runoff start to rise and reach peak values at about the same time

as runoff from the SOF 2 areas. On 19 % and 48 % of fields 5 and 7 SOF 1 is expected. Runoff from these areas is faster than the pesticide tracers.

Field 9 with 89 % SOF 3 contributes little to runoff during the event. This corresponds to the small amount of pesticide found in runoff. On field 13 (not shown) surface and subsurface runoff flows into a depression of a former lake. Runoff from the field will therefore hardly contribute to catchment runoff during a flood. No tracer pesticide from field 13 was found in runoff.

Leu (2003) found 24 times higher pesticide concentrations in a grab sample of surface runoff than in one of tile drain flow because more pesticide is held back in the soil, if preferential flow is the transport mechanism. Therefore, more pesticide should be removed from SOF fields than from tile drained fields. This was confirmed by the measurements. The amount measured in runoff of the tracer pesticide Alachlor from the SOF dominated field 7 was three times larger than from the tile drained field 1 and four times more of the tracer pesticide Terbutylazin from field 8 (SOF 2, and 3) was found than from field 2 (D 1). Although the timing of pesticide loss between SOF and tile drained fields is similar, the amount is smaller from the tile drained fields.

9.4 Conclusions

The results from the pesticide study confirm the results of the mapping and modelling of dominant runoff processes in the Ror catchment. From fields, where runoff was expected, the respective tracer pesticide could be found in runoff. From fields, where only little or no runoff was expected, little or no tracer pesticide could be found. Pesticide concentrations in runoff from the tile drained fields were lower than from the SOF fields, supporting the expected flow paths.

10 Applications of mapping and modelling approach

10.1 Introduction

The spatial distribution of runoff processes was mapped for the whole Ror and Isert catchment and the rainfall-runoff model developed. Now the runoff process maps and the model are used for extrapolations to a larger catchment area, to an extreme event and to a neighbouring catchment. The simulation results are evaluated.

10.2 Extrapolation to areas larger than calibration area

The model Qarea-pro was adapted using data from the Lindist and Rinderholz sub-catchments while the dominant runoff processes were mapped for the whole Ror catchment. In summer 2000, discharge was measured of the Ror catchment (2.1 km²) and the Summerau sub-catchment (0.6 km²). To simulate discharge for these two larger catchments the distribution of the dominant runoff processes was adapted to these catchments but the calibrated parameters were not changed.

A flood event with 80 mm of rainfall within 1 day, which occurred in September 2000 was simulated with the model (Figure 10.1).

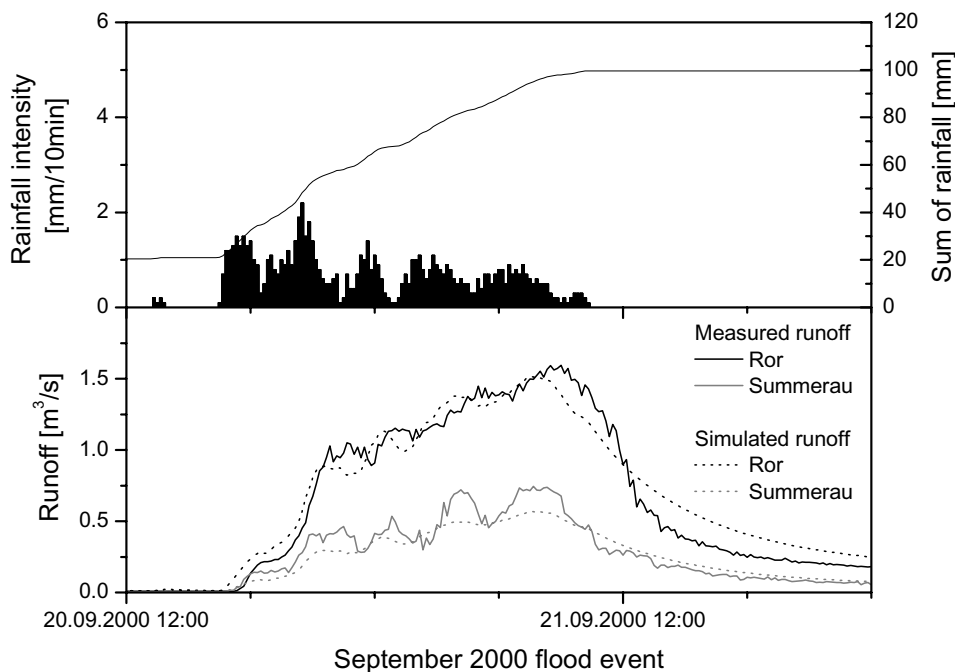


Fig. 10.1 Measured rainfall and observed and simulated runoff in the Ror catchment and Summerau sub-catchment for the September 2000 flood event.

For the Ror catchment, peak discharge and runoff volume are simulated adequately. Deviations again occur during the hydrograph recession. Simulated discharge for the Summerau sub-catchment reacts less pronounced than the observed and peak flow is slightly underestimated.

10.3 Extrapolation to events outside of calibration range

Heavy rainfall from 11th to 13th of May 1999 caused a considerable flood in the experimental catchments. 74 mm of rainfall in one day and 150 mm in three days were registered at Grüningen. This corresponds to the 8th highest daily and the third highest 3-daily rainfall in the 100 year measurement period (Table 10.1). The recurrence interval for this rainfall event is 10 to 30 years. In the Aabach in Mönchaldorf, the highest peak discharge in the last 23 years occurred ($46.5 \text{ m}^3/\text{s}$ or $1 \text{ m}^3/\text{s}\cdot\text{km}^2$). Locations of stations are shown in Figure 3.1.

Table 10.1 Sum of 1-, 2- and 3-day rainfall between the 11.05.99 and 13.05.99. For the permanent stations the rank of the rainfall sums in the measurement series is given as well.

Station	1 day rainfall 12.05.99 [mm]	Rank	2 day rainfall 11.+12.05.99 [mm]	Rank	3 day rainfall 11.-13.05.99 [mm]	Rank
Grüningen SMA ^{a)}	74.0	8	122.1	4	150.3	3
Ror	66.3		111.6		137.0	
Isert	72.2		127.0		153.8	
Hinwil SMA ^{b)}	75.8	8	128.4	3	153.4	3
Mönchaldorf AWEL ^{c)}	97.0	1	126.0 (12+13.5)		157.0 (12.-14.5)	
Uster SMA ^{b)}	91.2	2	154.6	1	172.6	1

Measurement period: ^{a)} 1900 - 2002, ^{b)} 1961 - 2002, ^{c)} 1980 - 2002

Figure 10.2 displays the cumulated rainfall of the rain gages in the region for the May 1999 event. Rainfall started on the 4th of May, the highest amounts occurred on the 12th of May. At Ror and Mönchaldorf 190 mm and 200 mm respectively were registered until the 24.5.99, less than at the nearby Grüningen station (230 mm). These regional and even local precipitation gradients make the estimation of the catchment precipitation for the Ror catchment difficult. Therefore, independent simulations for both precipitation records were made.

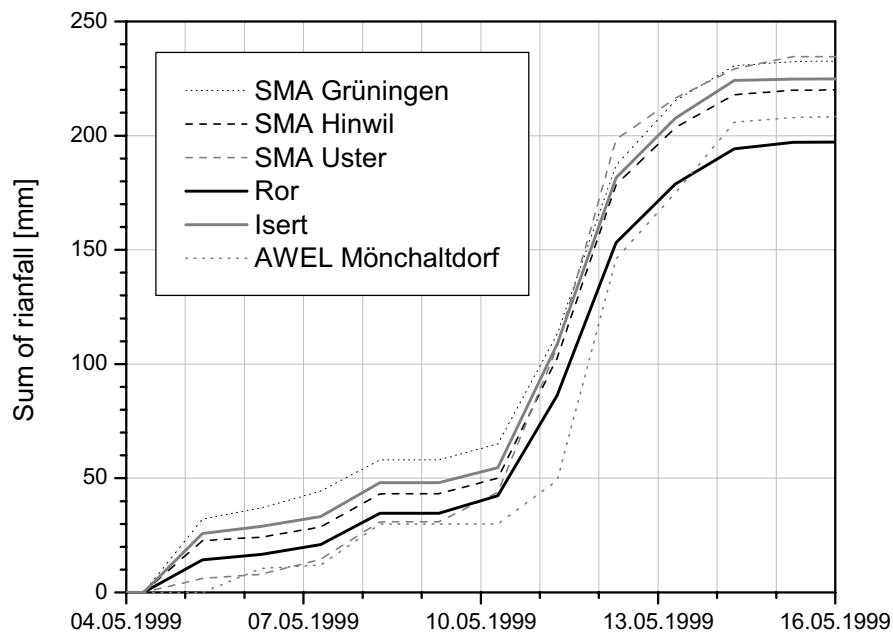


Fig. 10.2 Sum of rainfall between the 4.5.99 and 16.05.99 measured at raingauges in the region of the experimental catchment. Location of stations see Figure 3.1.

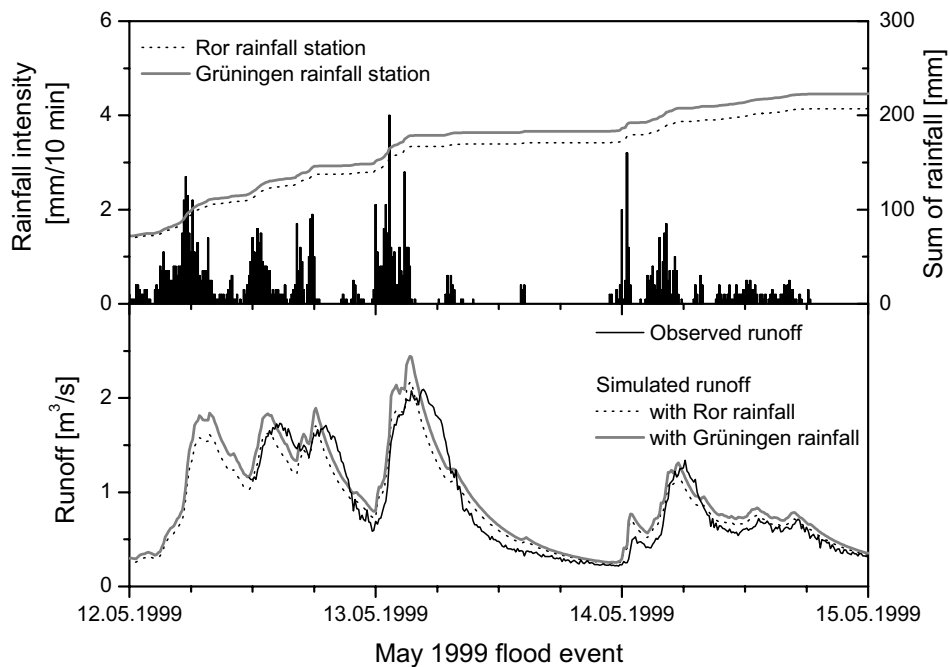


Fig. 10.3 Measured rainfall and observed and simulated runoff in the Ror catchment for the May 1999 flood event. Simulations using rainfall data from Ror and Grüningen are shown.

The model, developed with data from the September 2001 flood with return period 1 to 2 years, was used to simulate the much larger May 99 event. The simulated peak flows are accurate within the range of measurement errors. Peak discharge using the Grüningen rainfall is $0.3 \text{ m}^3/\text{s}$ higher than the one using the Ror data. These results suggest that the mapping and modelling approach is suitable to extrapolate to larger events.

10.4 Prediction of floods in ungauged catchments

The estimation of peak discharge and runoff volume in an ungauged catchment remains a problem. However, the uncertainty can be reduced if the distribution of the dominant runoff processes in a catchment is considered. In Figure 10.4 the different distributions of the dominant runoff processes in the neighbouring Ror and Isert catchments are displayed.

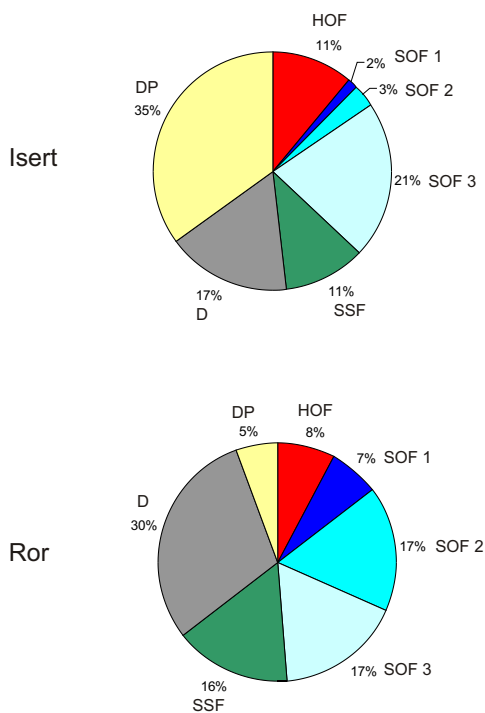


Fig. 10.4 Distribution of dominant runoff processes in the Isert and Ror catchment.

One third of the Isert catchment with runoff type DP does not contribute to flood discharge. Another 50 % are covered by the delayed reacting processes D, SSF and SOF 3, while only 5 % are fast reacting SOF 1 and SOF 2. In Ror the percentage of SOF 1 and SOF 2 is much higher (24 %) while little DP occurs (5 %). Therefore, lower peak discharges are expected in the Isert catchment.

Runoff and rainfall were measured in Isert and Ror during the May 1999 flood event (Figure 10.5), starting on the 12th of May. In Ror nearly 50 mm less rainfall was measured than in Isert. In contrast, peak discharge was higher in Ror than in Isert ($1.2 \text{ m}^3/\text{s}\cdot\text{km}^2$ in Ror, $0.4 \text{ m}^3/\text{s}\cdot\text{km}^2$ in Isert). The volumetric runoff coefficient in Ror was 0.5 while it reached only 0.25 in Isert.

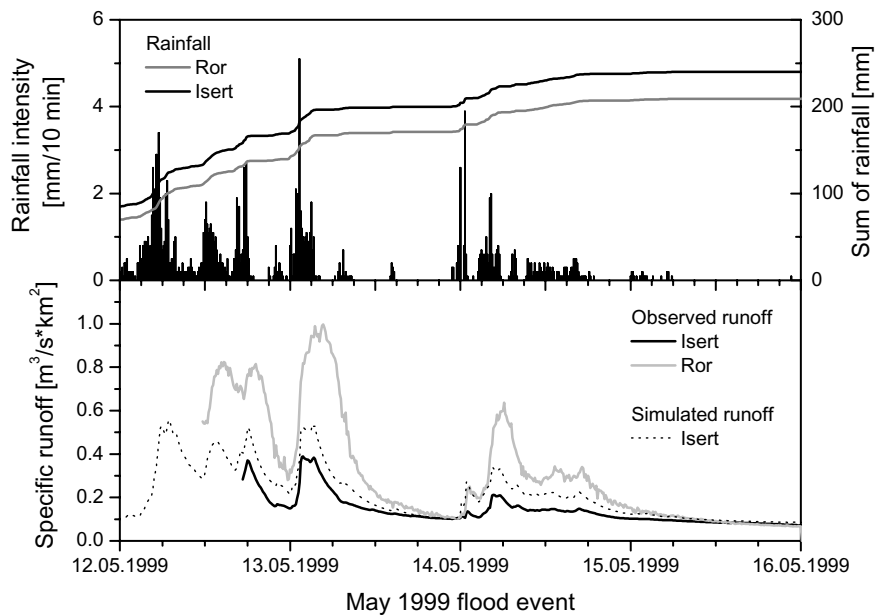


Fig. 10.5 Observed rainfall and runoff in Isert and Ror and simulated runoff in Isert during the May 1999 flood.

The model Qarea-pro was adapted to the process areas mapped in the Isert catchment without changing the calibrated parameters. With the mapping and modelling approach, the hydrologic reaction could be quantified and the attenuated reaction to precipitation understood.

10.5 Summary and conclusions

The model Qarea-pro, based on the dominant runoff process maps, was calibrated to a small flood event in two sub-catchments of the Ror catchment. It was able to simulate runoff of the whole Ror catchment, for a larger flood event and for the neighbouring Isert catchment without change of calibration parameters.

11 Conclusions

A vast number of different rainfall runoff models and ways to calibrate them have already been published. However, a real improvement in the quality of model simulation requires that the relevant processes of runoff formation are adequately represented in the model and that not all of the relevant model parameters have to be determined simultaneously by calibration only.

In the approach presented, runoff formation during flood events in catchments was studied. Based on intensive field work, the dominant runoff processes were determined on the plot scale and delineated in the catchments. The resulting maps integrate all hydrological knowledge about the catchments.

A set of rules was then developed, that allowed the automated determination of the dominant runoff processes from spatial data like soil or geological maps with good results. The current method can not differentiate between the SOF and SSF processes and does not consider the influence of topography on runoff formation. However, it can reduce greatly the amount of field work necessary for the process delineation, allowing the mapping of larger areas.

In the developed rainfall runoff model, the spatial distribution of the different runoff processes is considered and each process is conceptualized separately to reproduce the water storage capacity of the soil and the contributions of surface and subsurface flow. With this approach, important model parameters can be determined from field data and it allows a deeper insight into flood formation. Multi-criteria validation of the model is possible using data like soil water levels, results from sprinkling experiments or process observations during flood events. This increases the stability of the model simulation and allows a more reliable extrapolation to events or areas outside the calibration range. With the presented mapping and modelling approach, it is also possible to quantify the contributions of runoff from specific areas or fields within a catchment, allowing for example the interpretation of solute transport measurements.

Subsurface flow is governed by matrix flow, macropore flow, preferential lateral flow and the interaction between them. This complex interaction, which can lead to a surprisingly fast drainage of the soil, is not yet fully understood. However, a better process understanding of the drainage process on the catchment scale is required for long term model simulations.

The method of mapping dominant runoff processes and using this map for rainfall runoff simulations was successfully applied in several Swiss catchments for design flood estimations. Especially in small, alpine and often ungauged catchments, the method allows a better understanding of the flood forming processes and therefore a reduction of the uncertainty always inherent in such estimations.

References

- AG Boden, 1994. Bodenkundliche Kartieranleitung. Bundesanstalt für Geowissenschaften und Rohstoffe und den Geologischen Landesämtern in der Bundesrepublik Deutschland., Hannover, 392 pp.
- Ambrose, B., 2004. Variable 'active' versus 'contributing' areas or periods: a necessary distinction. *Hydrological Processes* 18: 1149 - 1155.
- Anderson, M.G. and Brooks, S.M. (Editors), 1996. *Advances in Hillslope Processes*, 1. John Wiley & Sons, Chichester, 683 pp.
- Anderson, M.G. and Burt, T.P., 1990. Process studies in hillslope hydrology: an overview. In: M.G. Anderson and T.P. Burt (Editors), *Process Studies in Hillslope Hydrology*. John Wiley & Sons, Chichester, pp. 1-8.
- Barling, R.D., Moore, I.D. and Grayson, R.B., 1994. A quasi-dynamic wetness index for characterising the spatial distribution of zones of surface saturation and soil water content. *Water Resources Research*, 30(4): 1029-1044.
- Betson, R.P., 1964. What is watershed runoff? *Journal of Geophysical Research*, 69: 1541-1552.
- Beven, K., 1989a. Interflow. In: H.J. Morel-Seytoux (Editor), *Unsaturated flow in hydrologic modelling, theory and practice.*, pp. 191-219.
- Beven, K., 1989b. Changing ideas in hydrology - The case of physically-based models. *Journal of Hydrology*, 105: 157-172.
- Beven, K. and Germann, P., 1982. Macropores and water flow in soils. *Water Resources Research*, 18(5): 1311-1325.
- Beven, K.J. and Kirkby, M.J., 1979. A physically-based, variable contributing area model of basin hydrology. *Hydrol. Sci. Bull.*, 24: 43-69.
- BGS, 1992. *Klassifikation der Böden der Schweiz*. Eidgenössische Forschungsanstalt für landwirtschaftlichen Pflanzenbau., Reckenholz, Zürich.
- Bisdom, E.B.A., Dekker, L.W. and Schoute, J.F.T., 1993. Water repellency of sieve fractions from sandy soils and relationships with organic material and soil structure. *Geoderma*, 56: 105-118.
- Bonell, M., 1998. Selected challenges in runoff generation research in forests from the hillslope to headwater drainage basin scale. *Journal of the American Water Resources Association*, 34(4): 765-785.
- Bonell, M., 1993. Progress in the understanding of runoff generation dynamics in forests. *Journal of Hydrology*, 150: 217-275.
- Boorman, D.B., Hollis, J.M. and Lilly, A., 1995. *Hydrology of soil types: a hydrologically-based classification of the soils of the United Kingdom*. 126, Institute of Hydrology, Wallingford.

- Bouma, J., Belmans, C.F.M. and Dekker, L.W., 1982. Water infiltration and redistribution in a silt loam with vertical worm channels. *Soil Sci. Soc. Am. J.*, 46: 917-921.
- Bronstert, A., 1994. Modellierung der Abflussbildung und der Bodenwasserdynamik von Hängen. Institut für Hydrologie und Wasserwirtschaft, IHW, Universität Karlsruhe (TH), Heft 46.
- Bronstert, A., 1999. Capabilities and limitations of detailed hillslope hydrological modelling. *Hydrological Processes*, 13: 21 - 48.
- Bunza, G., Jürging, P., Löhmannsröben, R., Schauer, T. and Ziegler, R., 1996. Abfluss- und Abtragsprozesse in Wildbacheinzugsgebieten, Grundlagen zum integralen Wildbachschutz. Schriftenreihe des Bayerischen Landesamtes für Wasserwirtschaft., Heft 27.
- Buttle, J.M., Dillon, P.J., Eerkes, G.R., 2004. Hydrologic coupling of slopes, riparian zones and streams: an example from the Canadian Shield. *Journal of Hydrology* 287: 161-177.
- Cappus, P., 1960. Bassin expérimental d'Alrance - étude des lois de l'écoulement - Application au calcul et à la prèvision des débits. *La Houille Blanche A*: 493-520.
- DeBano, L.F., 1991. The effect of fire on soil properties. INT-280, United States Department of Agriculture, Forest Service.
- Dieleman, P.J. and Trafford, B.D., 1976. Drainage testing., Food and Agriculture Organization of the United Nations., Rome.
- DIN 19682-10, 1998. Felduntersuchungen. Teil 10: Beschreibung und Beurteilung des Bodengefüges., Berlin.
- Doerr, S.H., Skakesby, R.A. and Walsh, R.P.D., 2000. Soil water repellency: its causes, characteristics and hydro-geomorphological significance. *Earth-Science Reviews*, 51: 33-65.
- Dunne, T. and Black, R.D., 1970a. An experimental investigation of runoff production in permeable soils. *Water Resources Research*, 6(2): 478-490.
- Dunne, T. and Black, R.D., 1970b. Partial area contributions to storm runoff in a small New England watershed. *Water Resources Research*, 14(5): 722-730.
- Dunne, T., Moore, T.R. and Taylor, C.H., 1975. Recognition and prediction of runoff-producing zones in humid regions. *Hydrol. Sci. Bull.*, 20: 305-327.
- Edwards, C.A., Shipitalo, M.J., Dick, W.A. and Owens, L.B., 1992. Rainfall intensity affects transport of water and chemicals through macropores in no-till soil. *Soil Sci. Soc. Am. J.*, 56(1): 52-58.
- Edwards, C.A., Shipitalo, M.J., Owens, L.B. and Norton, L.D., 1990. Effect of *Lumbricus Terrestris* L. burrows on hydrology of continuous no-till corn fields. *Geoderma*, 46: 73-84.
- Ehlers, W., 1975. Observation on earthworm channels and infiltration on tilled and untilled loess soil. *Soil Science*, 119(3): 242-249.

- Ellenberg, H., 1991. Zeigerwerte von Pflanzen in Mitteleuropa. *Scripta geobotanica*, Vol. 18. Verlag Erich Goltze, Göttingen.
- Elsenbeer, H., 2001. Pedotransfer functions in hydrology. *Journal of Hydrology*, 251: 121-122.
- EXTOXNET, 1996. The EXtension TOXicology NETwork, <http://extoxnet.orst.edu/>.
- Faeh, A.O., 1997. Understanding the Processes of Discharge Formation under Extreme Precipitation, a study based on the numerical simulation of hillslope experiments. 150, VAW - Versuchsanstalt für Wasserbau, Hydrologie und Glaziologie der ETH Zürich, Zürich.
- Faeh, A.O., Scherrer, S. and Naef, F., 1997. A combined field and numerical approach to investigate flow processes in natural macroporous soils under extreme precipitation. *Hydrology and Earth System Sciences*, 4: 787-800.
- FAL, 1997. Bodenkarte Kanton Zürich, Landwirtschaftsflächen 1:5000. Volkswirtschaftsdirektion des Kantons Zürich, Zürich.
- FAO/UNESCO, 1988. Soil map of the world. Revised Legend. 60, ISRIC, Rome.
- Feyen, H., 1998. Identification of runoff processes in catchments with a small scale topography., Diss. ETH No. 12868, Zürich, 147 pp.
- Flury, M., Flüeler, H., Jury, W.A. and Leuenberger, J., 1994. Susceptibility of soils to preferential flow of water: A field study. *Water Resources Research*, 30(7): 1945-1954.
- Freeze, R.A. and Cherry, J.A., 1979. *Groundwater*. Prentice-Hall, Inc., Englewood Cliffs, N.J., 604 pp.
- Frielinghaus, M., Petelkau, H., Seidel, C. and Roth, C.H., 1994. Möglichkeiten einer flächenhaften Beurteilung der Erosionsgefährdung durch Fahrspuren. *Mitteilungen Deutsche Bodenkundliche Gesellschaft*, 74: 181-184.
- Genereux, D., 1998: Quantifying uncertainty in tracer-based hydrograph separations. *Water Resources Research*, 34(4): 915-919.
- Germann, P.F., 1990. Macropores and hydrologic hillslope processes. In: M.G. Anderson and T.P. Burt (Editors), *Process studies in hillslope hydrology*. J.Wiley & Sons, Chichester, pp. 327-363.
- Grayson, R., Moore, I.D. and McMahon, T.A., 1992. Physically based hydrologic modeling. 2. Is the concept realistic? *Water Resources Research*, 26(10): 2659-2666.
- Haering Ch., Jäckli, H., Kobel, M., Kündig, R., Lienert, O., Philipp, R., Starck, P., Wyssling, L., 1993. Hydrogeologische Karte der Schweiz 1:100'000, Blatt Nr. 5 Toggenburg. Schweizerische Geotechnische Kommission, ETH-Zentrum, Zürich.
- Hantke, R. und Mitarbeiter, 1967. Geologische Karte des Kantons Zürich und seiner Nachbargebiete 1:50'000. Kommissionsverlag Leemann, Zürich.

- Harrach, T., 1984. Lockerungsbedürftige Böden einfach und sicher erkennen. *Arbeiten der DLG*, 179: 114-121.
- Hewlett, J., 1961. Watershed managements, Rep. for 1961, South Eastern Forest Experimental Station., US. Forest Service, Ashvill, North Carolina.
- Hewlett, J. and Hibbert, A.R., 1967. Factors affecting the response of small watersheds to precipitation in humid areas. In: W.E. Sopper and H.W. Lull (Editors), *Forest Hydrology*. Pergamon Press, Oxford, pp. 275-290.
- Hildebrand, E., 2002. Forstliche Bodenbewirtschaftung. In: Blume et al. (Editors), *Handbuch der Bodenkunde*, 14. Erg. Lfg. 12/02. ecomed, Landsberg/Lech, pp. Chapter 6.2.2.
- Horn, R., 1985. Die Bedeutung der Trittdichtung durch Tiere auf physikalische Eigenschaften alpiner Böden. *Zeitung für Kulturtechnik und Flurbereinigung*, 26: 42-51.
- Horn, R. and Rostek, J., 2000. Subsoil compaction proecesses - state of kownledge. *Advances in GeoExology*, 32: 44-54.
- Horton, R.E., 1933. The role of infiltration in the hydrologic cycle. *Trans. Am. Geophys. Union*, 14: 446-460.
- Hursh, C.R., 1944. Subsurface flow. *Transactions of the American Geophysical Union*, 14: 743-746.
- Hydrologisches Jahrbuch Kanton Zürich, 2000. AWEL, Amt für Abfall, Wasser, Energie und Luft.
- Jones, J.A.A., 1990. Piping effects in humid lands. In: C.G. Higgins and D.R.e. Coates (Editors), *Groundwater Geomorphology: the role of subsurface water in earth-surface processes and landforms*. *Geol. Soc. Am. Spec. Pap.*, pp. 111-138.
- Kahn, S. and K.R., R., 1996. Reappraisal of low to tile drains. I. Steady state response. *Journal of Hydrology*, 183: 351-366.
- Kanton Zürich, Oberforstamt und Amt für Raumplanung, 1988: *Kommentar zur Vegetationskundlichen Kartierung der Wälder im Kanton Zürich, Forstkreis 2*. Kanton Zürich, Zürich.
- Kemper, W.D. and Koch, E.J., 1966. Aggregate stability of soils from western portions of the United States and Canada.
- Kirkby, M.J. (Editor), 1978. *Hillslope Hydrology*. John Wiley & Sons, Chicester.
- Kirkby, M.J. and Chorley, R.J., 1967. Throughflow, overland flow and erosion. *Bull. Int. Assoc. Sci. Hydrol.*, 12: 5-21.
- Kölla, E., 1986. Zur Abschätzung von Hochwassern in Fliessgewässern an Stellen ohne Direktmessungen. *Mitteilung der Versuchsanstalt für Wasserbau, Hydrologie und Glaziologie, VAW der ETH Zürich*, 87.

- Kretzschmar, A., 1988. Structural parameters and functional patterns of simulated earthworm burrow systems. *Biol. Fertil. Soils*, 6: 252-261.
- Kuntze, H., Roeschmann, G. and Schwerdtfeger, G., 1994. *Bodenkunde*. Verlag Eugen Ulmer, Stuttgart, 424 pp.
- Letey, J., 1969. Measurement of contact angle, water drop penetration time, and critical surface tension., *Proceedings of the Symposium on Water-Repellent Soils*, 6-10 May 1968, University of California, Riverside, pp. 43-47.
- Leu, C.M., Singer, H., Stamm, Ch., Müller, S.R., Schwarzenbach, R.P., 2004a. Simultaneous assessment of sources, processes, and factors influencing herbicide losses to surface waters in a small agricultural catchment. *Environ. Sci. Technol.*, 38: 3827-3834.
- Leu, C.M., Singer, H., Stamm, Ch., Müller, S.R., Schwarzenbach, R.P., 2004b. Variability of herbicide losses from 13 fields to surface waters within a small catchment after a controlled herbicide application. *Environ. Sci. Technol.*, 38: 3835-3841.
- Leu, C.M., 2003. Sources, processes and factors determining the losses of Atrazine, Dimethenamid and Metolachlor to surface waters: A simultaneous assessment in six agricultural catchments. Unpub. PhD thesis ETH Zürich: 89 p.
- Lin, H.S., McInnes, K.J., Wilding, L.P. and Hallmark, C.T., 1999a. Effects of soil morphology on hydraulic properties: I. Quantification of soil morphology. *Soil Sci. Soc. Am. J.*, 63: 948-954.
- Lin, H.S., McInnes, K.J., Wilding, L.P. and Hallmark, C.T., 1999b. Effects of soil morphology on hydraulic properties: II. Hydraulic pedotransfer functions. *Soil Sci. Soc. Am. J.*, 63: 955-961.
- Löhmannsröben, R. and Schauer, T., 1996. Ableitung hydologischer Eigenschaften zur Beurteilung des Abfluss- und Abtragsgeschehens aus Boden- und vegetationskundlichen Kriterien. *Interpraevent 1996 - Garmisch-Partenkirchen*, 1: 99-112.
- Markart, G., Kohl, B., Zanetti, P., 1996. Einfluss der Bewirtschaftung, Vegetation und Boden auf das Abflussverhalten von Wildbacheinzugsgebieten., *Internationales Symposium Interpraevent 1996, Garmisch-Partenkirchen*, pp. 135-144.
- Markart, G., Kohl, B., Sotier, B., Schauer, T., Bunza, G., Stern, R., 2004. Provisorische Geländeanleitung zur Abschätzung des Oberflächenabflussbeiwertes auf alpinen Boden-/Vegetationseinheiten bei konvektiven Starkregen (Version1.0). *Schriftenreihe des Bundesamtes und Forschungszentrums für Wald, Wien*, Band 3, 83 p.
- McDonnell, J.J., 1990. A rational for old water discharge through macropores in a steep, humid catchment. *Water Resources Research*, 26(11): 2821-2832.
- McDonnell, J.J., Stewart, M.K. and Owens, I.F., 1991. Effect of catchment-scale subsurface mixing on stream isotopic response. *Water Resources Research*, 27(12): 3065-3073.

- McGlynn, B.L. and McDonnell, J.J., 2003a. Role of discrete landscape units in controlling catchment dissolved organic dynamics. *Water Resources Research*, 39(4): 1090-1117.
- McGlynn, B.L. and McDonnell, J.J., 2003b. Small catchment runoff sources. *Water Resources Research*, 39(11): 1310-1330.
- McGlynn, B.L., McDonnell, J.J., Shanley, J.B. and Kendall, C., 1999. Riparian zone flowpath dynamics during snowmelt in a small headwater catchment. *Journal of Hydrology*, 222: 75-92.
- Merz, J. and Mosley, M.P., 1998. Hydrological behaviour of pastoral hill country modified by extensive landsliding, northern Hawkes's Bay, New Zealand. *Journal of hydrology (NZ)*, 37(2): 113-139.
- Mikovari, A., Peter, C. and Leibundgut, C., 1995. Investigation of preferential flow using tracer techniques. *IAHS Publ.*, 229.
- Moore, T.R., 1974. Gley morphology and soil water regimes in some soils in south-central England. *Geoderma*, 11: 297-304.
- Moore, T.R., Dunne, T. and Tayler, C.H., 1976. Mapping runoff producing zones in humid regions. *Journal of water conservation*, 31(4): 160-164.
- Mosley, M.P., 1979. Streamflow generation in a forested watershed, New Zealand. *Water Resources Research*, 15: 795-806.
- Mosley, M.P., 1982. subsurface flow velocities through selected forest soils, South Island, New Zealand. *Journal of Hydrology*, 55: 65-92.
- Mückenhausen, E., 1975. Die Bodenkunde und ihre geologischen, geomorphologischen, mineralogischen und petrologischen Grundlagen. DLG-Verlag, Frankfurt am Main, 579 pp.
- Munsell, 1954. Munsell soil color charts. Munsell Color Company, Inc., Baltimore, Maryland, USA.
- Munyankusi, E., Gupta, S.C., Moncrief, J.F. and Berry, E.C., 1994. Earthworm macropores and preferential transport in a long-term manure applied Typic Hapludalf. *Journal of Environmental Quality*, 23(4): 773-784.
- Murer, E.J. et al., 1993. An improved sieving machine for estimation of soil aggregate stability (SAS). *Geoderma*, 56: 539-547.
- Naef, F., 1977. Ein Vergleich von mathematischen Niederschlag-Abfluss-Modellen. *Mitteilung der Versuchsanstalt für Wasserbau, Hydrologie und Glaziologie, VAW der ETH Zürich*(26): 114.
- Naef, F., 1981. Can we model the rainfall-runoff process today? *Hydrol. Sci. Bull.*, 26(3): 281-289.
- Naef, F. and Scherrer, S., 2003. Hochwasserabschätzung basierend auf Abflussmessungen. In: M. Spreafico, R. Weingartner, M. Barben and A. Ryser (Editors), *Hochwasserabschätzung in schweizerischen Einzugsgebieten*. Bundesamt für Wasser und Geologie, BWG, Bern, pp. 25-32.

- Naef, F., Scherrer, S., Thoma, C., Weiler, M. and Fackel, P., 2000. Die Beurteilung von Einzugsgebieten und ihren Teilflächen nach der Abflussbereitschaft unter Berücksichtigung der landwirtschaftlichen Nutzung - aufgezeigt an drei Einzugsgebieten in Rheinland-Pfalz. Untersuchung im Auftrag des Landesamts für Wasserwirtschaft, Rheinland Pfalz. Bericht B 003, IHW, Zürich.
- Nash, J.E., Sutcliffe, J.V., 1970. River flow forecasting through conceptual models, 1 - A discussion of principles. *Journal of Hydrology*, 10: 282-290.
- Pearce, A.J., Stewart, M.K. and Sklash, M.G., 1986. Storm runoff generation in humid headwater catchments. 1. Where does the water come from? *Water Resources Research*, 22(8): 1263-1272.
- Peschke, G., Etzenberg, C., Müller, G., Töpfer, J. and Zimmermann, S., 1998. Die Abflussbildung in ihrer Abhängigkeit von der wirksamen Kombination flächenvariabler Einflussfaktoren und vom Gebietszustand. Abschlussbericht zur Forschung innerhalb des Schwerpunktprogrammes Regionalisierung in der Hydrologie., Internationales Hochschulinstitut Zittau, Zittau.
- Peschke, G., Etzenberg, C., Töpfer, J., Zimmermann, S. and Müller, G., 1999. Runoff generation regionalization: analysis and a possible approach to a solution. *IAHS Publ.*, 254(Regionalization in Hydrology): 147-156.
- Peters, D.L., Buttle, J.M., Taylor, C.H. and LaZerte, B.D., 1995. Runoff production in a forested, shallow soil, Canadian shield basin. *Water Resources Research*, 31(5): 1291-1304.
- Pilgrim, D.H., Huff, D.D. and Steele, T.D., 1978. A field evaluation of surface and subsurface runoff, 2, Runoff processes. *Journal of Hydrology*, 65: 49-72.
- Roth, C.H., 2002. Physikalische Ursachen der Wassererosion. In: Blume et al. (Editors), *Handbuch der Bodenkunde*, 14. Erg. Lfg. 12/02. ecomed, Landsberg/Lech, pp. Chapter 6.3.1.1.
- Schachtschabel, P., Blume, H.-P., Brümmer, G., Hartge, K.H. and Schertmann, U., 1998. Scheffer / Schachtschabel, *Lehrbuch der Bodenkunde*. Ferdinand Enke Verlag, Stuttgart, 494 pp.
- Scherrer, S., 1997. Abflussbildung bei Starkniederschlägen. Identifikation von Abflussprozessen mittels künstlicher Niederschläge. 147, VAW - Versuchsanstalt für Wasserbau, Hydrologie und Glaziologie der ETH Zürich, Zürich.
- Scherrer, S. and Naef, F., 2003. A decision scheme to identify dominant flow processes at the plot-scale for the evaluation of contributing areas at the catchments-scale. *Hydrological Processes*, 17(2): 391-401.
- Seibert, J., Bishop, K., Rodhe, A., McDonnell, J.J., 2003. Groundwater dynamics along a hillslope: A test of the steady state hypothesis. *Water Resources Research*, 39(1): 1014-1023.
- Sidle, R.C. et al., 2000. Stormflow generation in steep forested headwaters: a linked hydrogeomorphic paradigm. *Hydrological Processes*, 14: 369-385.
- Sivapalan, M., Beven, K.J. and Wood, E.F., 1987. On hydrologic similarity, 2, A scaled model of storm runoff production. *Water Resources Research*, 23(2): 2266-2278.

- Smettem, K.R.J. and Collis-George, N., 1985. Statistical characterization of soil biopores using a soil peel method. *Geoderma*, 36(1): 27-36.
- Sobieraj, J.A., Elsenbeer, H., Vertessy, R.A., 2001. Pedotransfer functions for estimating saturated hydraulic conductivity: implications for modeling storm flow generation. *Journal of Hydrology*, 251: 202-220.
- Tani, M., 1997. Runoff generation processes estimated from hydrological observations on a steep forested hillslope with a thin soil layer. *Journal of Hydrology*, 200: 84-109.
- Tenholtern-R, Dumbeck-G and Harrach-T, 1993. Die Packungsdichte als Ausdruck makroskopischer Gefuegeeigenschaften von Auftragsboeden aus Loess. *Mitteilungen der Deutschen Bodenkundlichen Gesellschaft.*, 72(1): 261-264.
- Tomlin, C., 1997. The pestizide manual. British Crop Protection Council, Bear Farm, Binfield, Bracknell, 1606 pp.
- Troch, P., Verhoest, N., Gineste, P., Paniconi, C. and Mérot, P., 2000. Variable source areas, soil moisture and active microwave observations at Zwalmbeck and Coët-Dan. In: R. Grayson and G. Blöschl (Editors), *Spatial Patterns in Catchment hydrology - observations and modelling*. Cambridge University Press, pp. 187-208.
- Trojan, M.D. and Linden, D.R., 1992. Microrelief and rainfall effects on water and solute movements in earthworm burrows. *Soil Sci. Soc. Am. J.*, 56(3): 727-733.
- Uhlenbrook, S. and Leibundgut, C., 2002. Process-oriented catchment modelling and multiple-response validation. *Hydrological Processes*, 16(2): 423-440.
- USDA, 1975. *Soil Taxonomy*. Agric. Handbook, Nr. 436, Washington.
- Veneman, P.L.M., Spokas, L.A. and Lindbo, D.L., 1998. Soil moisture and redoximorphic features: A historical perspective. In: M.C. Rabenhorst, J.C. Bell and P.A. McDaniel (Editors), *Quantifying soil hydromorphology*. SSSA Special Publication, Madison, Wisconsin, USA, pp. 1-24.
- Verhoest, N.E.C., Troch, P.A., Paniconi, C. and De Troch, F.P., 1998. Mapping basin scale variable source areas from multitemporal remotely sensed observations of soil moisture behaviour. *Water Resources Research*, 34(12): 3235-3244.
- Warner, G.S. and Nieber, J.L., 1991. Macropore distribution in tilled vs. grass-surface cores as determined by computer tomography. *Preferential flow*, Proceedings of the national symposium.
- Wauchope, R., Buttler, T., Hornsby, A., Augustijn-Beckers, P. and Burt, J., 1992. The SCS/ARS/CES pesticide properties database for environmental decision-making. *Rev Environ Contam Toxicol.*, 123: 1-155.
- Weiler, M., 2001. Mechanisms controlling macropore flow during infiltration. Dye tracer experiments and simulations. *Schriftenreihe des Instituts für Hydromechanik und Wasserwirtschaft der ETH Zürich.*, Band 7: 150.

-
- Weiler, M. and McDonnell, J.J., 2004. Virtual experiments: a new approach for improving process conceptualization in hillslope hydrology. *Journal of Hydrology*.
- Weiler, M. and Naef, F., 2003. Simulating surface and subsurface initiation of macropore flow. *Journal of Hydrology*, 273: 139-154.
- Weiler, M., Naef, F. and Leibundgut, C., 1998. Study of runoff generation on hillslopes using tracer experiments and a physically-based numerical hillslope model. *IAHS Publ.*, 248: 353-360.
- Weyman, D.R., 1973. Measurements of the downslope flow of water in a soil. *Journal of Hydrology*, 20: 267-288.
- Whipkey, R.Z., 1965. Subsurface stormflow from forested watersheds. *Bull. Int. Assoc. Sci. Hydrol.*, 10: 74-85.
- Wigmosta, M.S. and Lettenmaier, D.P., 1999. A comparison of simplified methods for routing topographically driven subsurface flow. *Water Resources Research*, Vol. 35(No. 1): 255-264.
- Zehe, E. and Flühler, H., 2001. Preferential transport of isoproturon at a plot scale and a field scale tile-drained site. *Journal of Hydrology*, 247: 100-115.
- Zuidema, P.K., 1985. *Hydraulik der Abflussbildung während Starkniederschlägen. Eine Untersuchung mit Hilfe numerischer Modelle unter Verwendung plausibler Bodenkennwerte. Mitteilung der Versuchsanstalt für Wasserbau, Hydrologie und Glaziologie, VAW der ETH Zürich*, 79.

Acknowledgments

A special thankyou goes to my supervisor Dr. Felix Naef who was the “scientific backbone” of this project. Through him I came to ETH and got motivated to work in the field of runoff process research. Together we raised the money for this project and he provided great ideas in our many discussions.

I would also like to thank my supervisor Prof. Wolfgang Kinzelbach for letting me join his working group and giving valuably scientific, financial and political support.

Prof. Jeffrey J. McDonnell critically reviewed this document and made useful suggestions how to improve it. He also took the trouble to cross the Atlantic only to be my co-referee. Thank you Jeff.

A very big thankyou goes to Dr. Simon Scherrer. He introduced me to the mapping of dominant runoff processes and was always there to help and discuss.

Thanks to Peter Kienzler, Dr. Markus Weiler and Carla Thoma for the good working atmosphere while sharing the office and for the great scientific and non-scientific discussions we had.

For the good co-operation and especially for letting me use their pesticide data I want to thank Dr. Christian Leu, Dr. Stephan Müller and Dr. Christian Stamm from EAWAG. A special thankyou goes to Dr. Stephan Müller. Only his enthusiasm and ability to raise money allowed us to bridge a time of “no-money” right at the beginning of the project and therefore made its start possible at all.

The labour intensive field work was only possible because many people supported me. Special thanks to Thomy Keller, Veronika Trombini and Réne Weber from IHW, Cornelius Senn and Ernst Bleiker from D-BAUG, Werner Attinger, Anna Grünwald, Hans Wunderli and Jörg Leuenberger from ITÖ and Alfred Lueck from EAWAG. The students Andreas Gericke, Ivo Hilber, Michael Margreth, Felix Oberrauch, Marieke ten Voorde and Rudi van den Bos were doing a great job helping with field work, in the laboratory and with processing data.

Last but not least, the entire work would not have been possible without the kind private backup of Martin and my family.

The spatial data used was kindly made available by the Kanton Zürich, the Landestpographie and the Greifensee project. This project was funded by the ETH Zürich and the Bundesamt für Landwirtschaft.

Abbreviations

Latin symbols

a	runoff coefficient	
m a.s.l.	meter above sea level	[m]
AWEL	Amt für Wasser, Energie, Luft	
c_e	EC value for event water	[$\mu\text{S}/\text{cm}$]
C_{org}	Organic content	[%]
c_p	EC value for pre-event water	[$\mu\text{S}/\text{cm}$]
c_{SOF}	constant SOF module	[1/s]
c_t	EC value for measured discharge	[$\mu\text{S}/\text{cm}$]
D_e	equivalent depth / thickness of equivalent layer	[m]
dh	difference of water table height between the upslope and downslope cell	[m]
D_o	depth of the base of the aquifer	[m]
DP	deep percolation	
DRP	dominant runoff process	
EAWAG	Swiss Federal Institute of Environmental Science and Technology	
EC	electric conductivity	
ET	evapotranspiration rate	[mm/day]
f_{act}	degree of filling of the slow drainable porosity	
FLAB	Flächen gleicher Dominanz bestimmter Abflussmechanismen	
GIS	geographic information system	
h	depth of water table	[m]
h_{max}	soil depth	[m]
HOF	Hortonian overland flow	
HOF1	immediate Hortonian overland flow	
HOF2	delayed Hortonian overland flow	
HOST	Hydrology of Soil Types	
i	process intensity	
i	slope	[m/m]
IHW	Institute of Hydromechanics and Water Resources Management at ETH	
k_{DP}	storage coefficient DP module	[h]
k_{HOF}	storage coefficient for HOF surface runoff	[h]
K_{oc}	sorption coefficient	[ml/g]
k_{rest}	storage coefficient for surface runoff of all other processes	[h]
K_{sat}	saturated hydraulic conductivity	[cm/d]
l	length of hillslope	[m]
Mp/m^2	number of macropores per m^2	
n	effective porosity	
nc	number of cells	
n_f	fast drainable porosity	
n_s	slow drainable porosity	

OSM	Upper Freshwater Molasse	
$p(t)$	rainfall (at time t)	[mm/h] , [l/s]
$q(t)$	runoff (at time t)	[m ³ /s] , [l/s]
q_e	runoff event water (rainfall)	[m ³ /s] , [l/s]
q_p	runoff pre-event water	[m ³ /s] , [l/s]
$q_{\text{subsurface}}$	subsurface flow	[m ³ /s]
q_{surface}	surface flow	[m ³ /s]
q_t	runoff measured discharge	[m ³ /s]
S	tile drain spacing	[m]
S_{act}	actual soil storage capacity	[mm]
SMA	Swiss Meteo Institute	
S_{map}	mapped storage capacity	[mm]
SOF	saturated overland flow	
SOF1	immediate saturated overland flow	
SOF2	delayed saturated overland flow	
SOF3	strongly delayed saturated overland flow	
SSF	subsurface flow	
SSF1	fast subsurface flow	
SSF2	delayed subsurface flow	
SSF3	strongly delayed subsurface flow	
t	time	
T_{DR}	Time domain reflectometry	
THOF	temporary Hortonian overland flow	
$V(t)$	Volume of linear storage	[m ³]
WDPT	water drop penetration time	[s]

Greek symbols

β	water table slope	[m/m]
---------	-------------------	-------

Appendix A: Soil profile data

Table A.1 *Methods used to determine soil parameters.*

Parameter	Method	Reference
C _{org}	Obtained by oxidation with H ₂ O ₂ (% by weight.).	
Soil texture	Pipette method (sand 2 mm - 50 μ m, silt 2 - 50 μ m, clay < 2 μ m).	
Bulk density	Arithmetic average of dry weight of undisturbed soil samples in 100 cm ² cones.	
Shape and size of aggregates	Visual classification.	AG Boden, 1994
Bedding of aggregates	Visual classification.	DIN 19682-10
Stability of aggregates	Drop test.	DIN 19682-10
Content of coarse fragments	Visual comparison with coarse fragment chart.	BGS, 1992
Soil colour	Munsell soil colour chart.	Munsell, 1954
pH	in H ₂ O with pH indicator.	
Carbonate content	reaction after contact with HCl (10 %).	AG Boden, 1994
Percentage of vegetation cover	Visual comparison with plant coverage chart.	Rohr et al., 1990
Water content	Finger probe	AG Boden, 1994

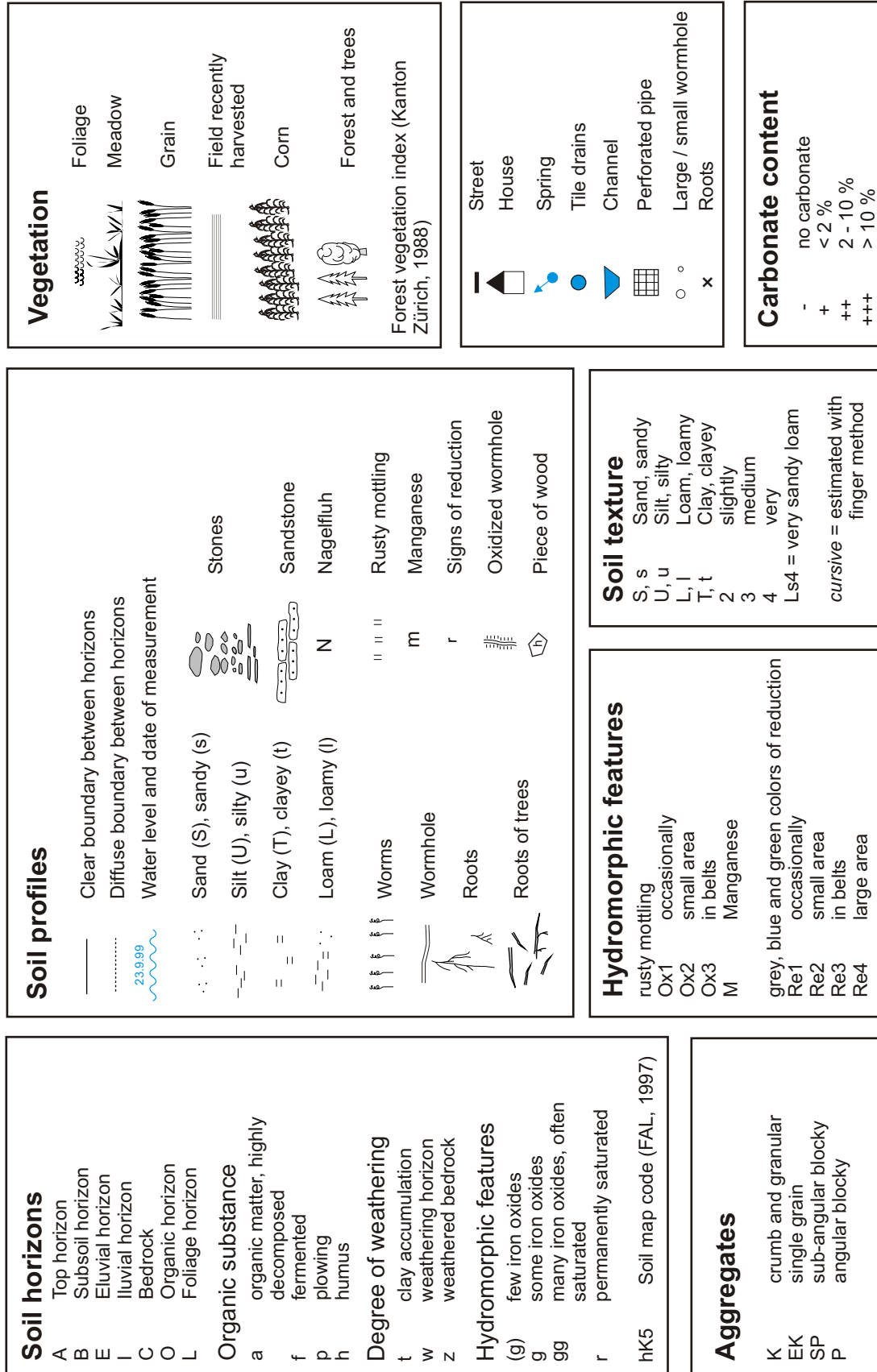


Fig. A.1 Soil profile legend.

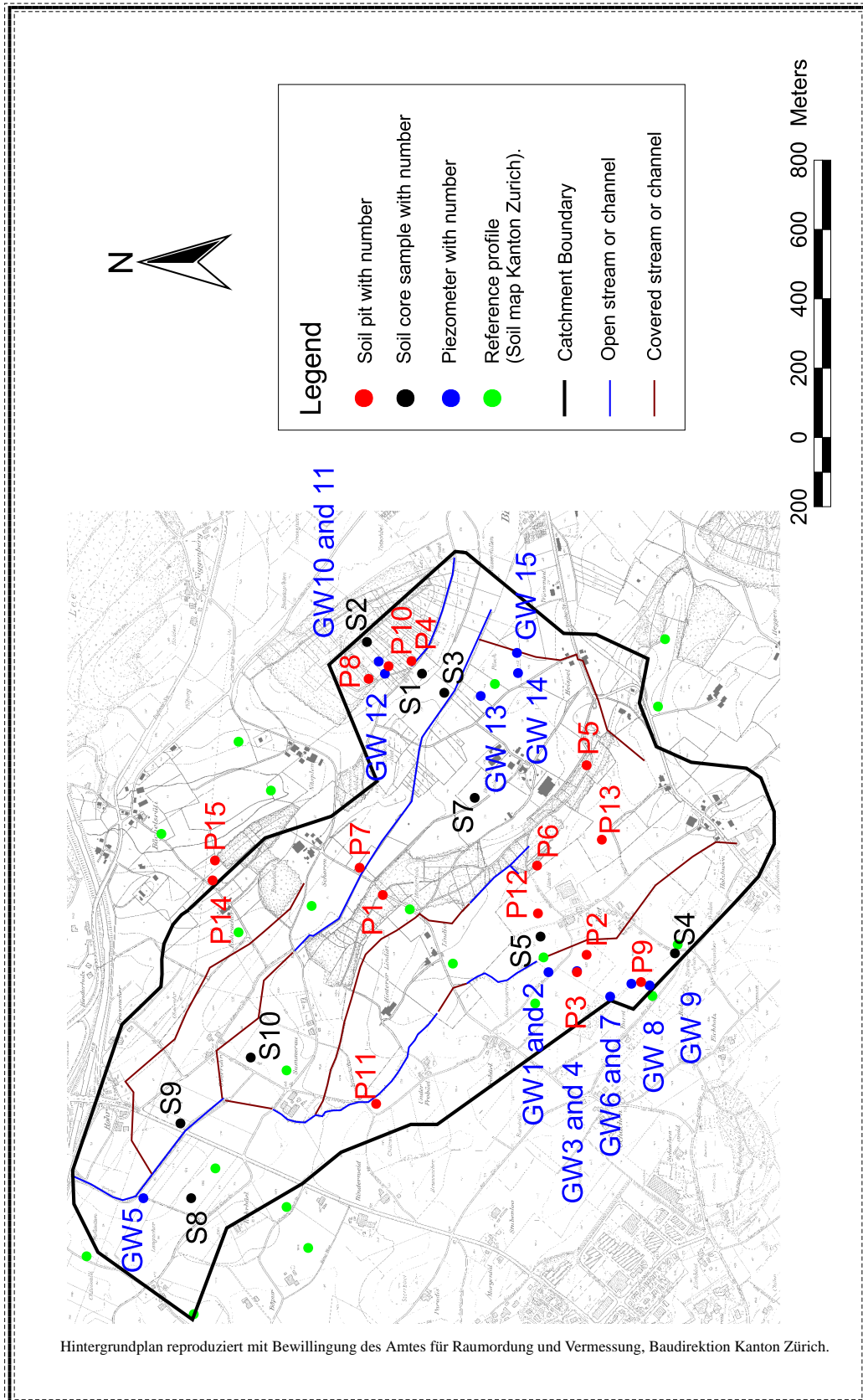



Fig. A.2 Location of soil profiles in Ror catchment.

Soil profile P 1: Braunerde

Site description



Catchment: Ror
 Location: Rinderholz
 Coordinates: 698'453 / 237'451
 Elevation: 512 m asl
 Land use: Typical woodruff beech forest (beech, fir, woodruff, ivy, forest vegetation index 7d)
 Geology: Sandstone of OSM
 Topography: Ridge
 Slope: < 1 %
 Exposition:

Soil surface

- 100 % vegetation cover,
- stable aggregates
- no top soil compaction
- L-Mull

Macroporosity

Many macropores (root channels and animal burrows).

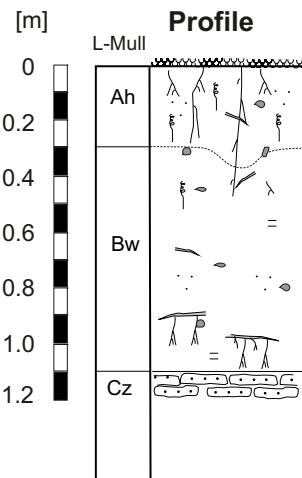
Lateral flowpaths

Root channels and animal burrows and weathered sandstone layer.

Geology

Sandstone of Molasse

Soil properties



Color	Soil texture		Bulk density	Hydromorphic features	Shape of peds	Packing density	pH	Content of				
	U	T						Coarse fragments	C _{org} [%]	Carbonate	Water	
brownish black	Ls3	30	22	very low	-	K	1	7	low	2.8	-	dry
brown	Lts	29	34	medium	-	SP		7	low	0.7	-	dry
grey					-			7			-	



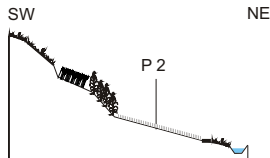
Experiments

Process evaluation

High intensity: SSF 3
 Low intensity: SSF 3

Soil profile P 2: Braunerde-Gley (tV8)

Site description



Catchment: Ror
 Location: Riet
 Coordinates: 698'278 / 236'854
 Elevation: 525 m asl
 Land use: Grain field, recently harvested
 Topography: Lower part of hillslope
 Slope: 5 %
 Exposition: NE

Soil surface

- 30 % vegetation cover (70% before harvest),
- stable aggregates
- low surface roughness,
- strong compaction of top soil under wheel tracks

Lateral flowpaths

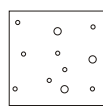
Geology

Molasse, groundwater surface near

Macroporosity

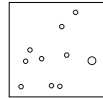
Horizontal cross sections 50 x 50 cm

depth 5 cm



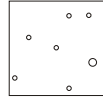
44 / 12 Mp/m² all / large d > 5 mm

15 cm



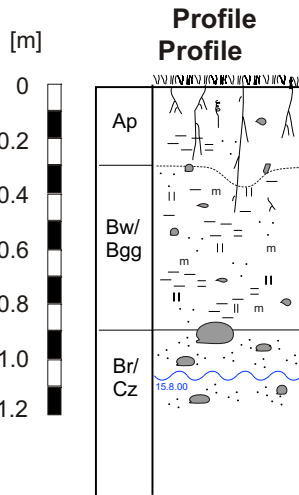
40 / 4 Mp/m² all / large

25 cm

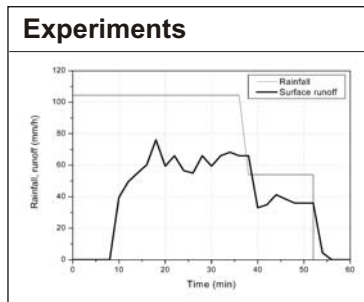
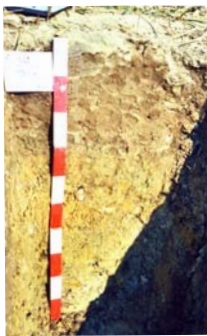


28 / 4 Mp/m² all / large

Soil properties



Color	Soil texture		Bulk density	Hydromorphic features	Shape of peds	Packing density	pH	Content of		
	U	T						Coarse fragments	C _{org} [%]	Carbonate
10 YR 4/2 dark greyish brown	Ls3	38 23	1.52 g/cm ³ medium		SP		5	1.1	-	
5Y 5/3 olive	Li2	42 29	plow pan poorly developed 1.59 g/cm ³ medium	Ox3 Re2 M	SP		5	0	-	
5Y 5/2 Olive grey	Slu	42 13		Re4				0	+++	Wet



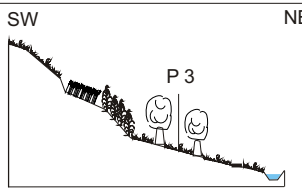
Process evaluation

High intensity: HOF 2 / SOF 2

Low intensity: SOF 2

Soil profile P 3: Braunerde - Gley (tV8)

Site description



Catchment: Ror
 Location: Riet
 Coordinates: 698'224 / 236'886
 Elevation: 527 m asl
 Land use: Permanent meadow with apple trees
 Topography: Lower part of hillslope
 Slope: 5 %
 Exposition: NE

Soil surface

- 100 % vegetation cover
- stable aggregates
- low surface roughness

Lateral flowpaths

Geology

Molasse, groundwater surface near

Macroporosity

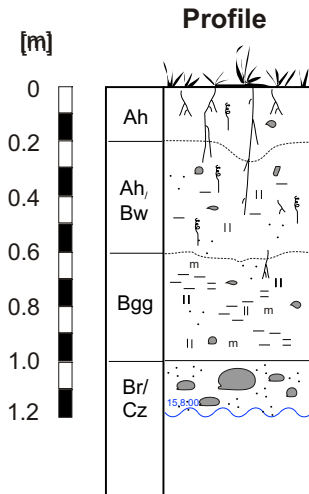
Horizontal cross sections 50 x 50 cm

depth 5 cm: 52 / 24 Mp/m² all / large d > 5 mm

15 cm: 72 / 20 Mp/m² all / large

30 cm: 80 / 20 Mp/m² all / large

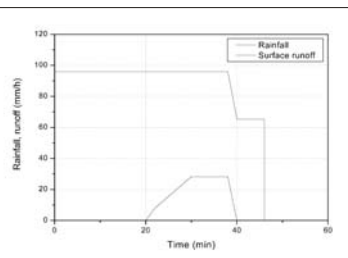
Soil properties



Color	Soil texture		Bulk density	Hydromorphic features	Shape of peds	Packing density	pH	Content of			
	U	T						Coarse fragments	C _{org} [%]	Carbonate	Water
10 YR 4/2 dark greyish brown	Ls3	36 24	1.15 g/cm ³ very low		K		5	Low	1.0	-	
10 YR 5/4 yellowish brown	Lt2	36 28	1.63 g/cm ³ medium	Ox1	SP		5	medium	0.4	-	
2.5Y 4/4 olive brown	Lt2	32 27	1.59 g/cm ³ medium	Ox2 Re2 M	P		6	high	0.2	-	
2.5Y 5/2 greyish brown	Ls3	37 22		Re 4			7		0.2	++	Wet



Experiments

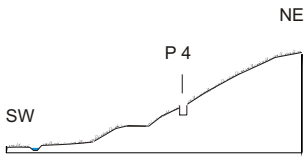


Process evaluation

High intensity: SOF 2
 Low intensity: SOF 2

Soil profile P 4: (Kalk-) Braunerde (cK31)

Site description



Catchment: Ror
 Location: Schüttsberg
 Coordinates: 699°140 / 237°367
 Elevation: 520 m asl
 Land use: Meadow
 Topography: Hillslope
 Slope: 11 %
 Exposition: SW

Soil surface

- 100 % vegetation cover
- stable aggregates
- low surface roughness

Lateral flowpaths

Animal burrows

Geology

Moraine (drumlin)

Macroporosity

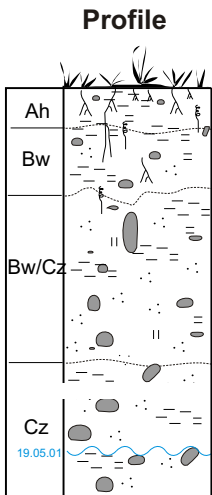
Horizontal cross sections 50 x 50 cm

depth 5 cm: 16 / 16 Mp/m² all / large d > 5 mm

15 cm: 0 / 0 Mp/m² all / large

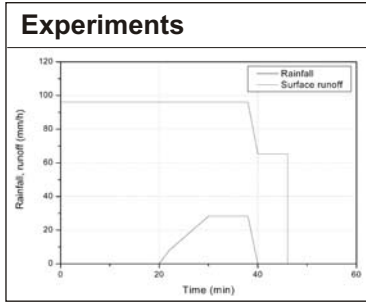
Mp/m² all / large

Soil properties



Color	Soil texture		Bulk density	Hydromorphic features	Shape of peds	Packing density	pH	Content of			
	U	T						Coarse fragments	C _{org} [%]	Carbonate	Water
10 YR 5/2 greyish brown	Lt2	35 27	1.2 g/cm ³ very low	-	K		6	low	7.1	+	dry
10 YR 6/3 pale brown	Ls3/Lt2	39 25	1.6 g/cm ³ medium	-	SP		6	low	2.6	++	slightly humid
10 YR 6/4 light yellowish brown	Slu	44 14	2.1 g/cm ³ very high	Ox1	SP		6-7	high	1.2	++	slightly humid
5 Y 7/3 pale yellow							8			+++	slightly humid ↓ wet

Water emerges in 2.1 m depth.



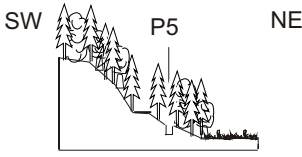
Process evaluation

High intensity: SSF 3

Low intensity: SSF 3

Soil profile P 5: Braunerde

Site description



Catchment: Ror
 Location: Rinderholz
 Coordinates: 698'833 / 236'854
 Elevation: 526 m asl
 Land use: Beech-fir forest with ivy, clover, stinging-nettle. Forest vegetation index 8a.
 Topography: Hillslope
 Slope: 28 %
 Exposition: NE

Soil surface

60 % vegetation cover
 Stable aggregates
 No top soil compaction
 L -Mull

Lateral flowpaths

Animal burrows, root channels and weathered sandstone layer

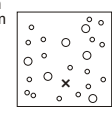
Geology

Molasse sandstone

Macroporosity

Horizontal cross sections 25 x 25 cm

depth 20 cm



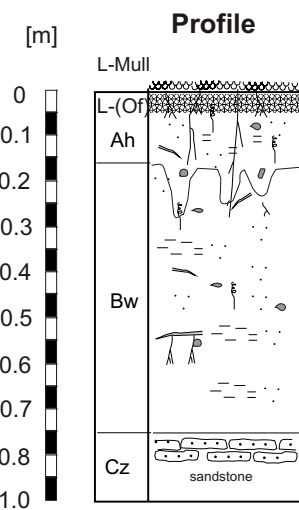
368 / 96 Mp/m²
 all / large
 d > 5 mm

Many very small macropores

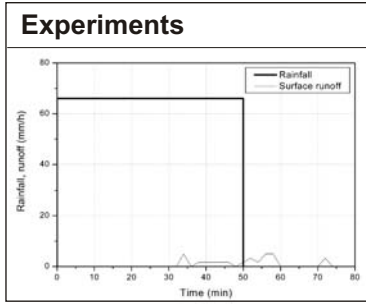
Mp/m²
 all / large

Mp/m²
 all / large

Soil properties



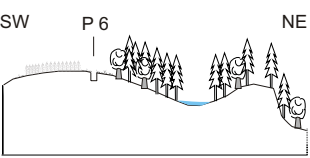
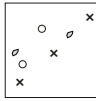
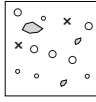
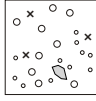
Color	Soil texture		Bulk density	Hydromorphic features	Shape of peds	Packing density	pH	Content of				
	U	T						Coarse fragments	C _{org} [%]	Carbonate	Water	
10 YR 3/3 dark brown	Ls4	25	20	1.3 g/cm ³ low	-	K	1	5	Low	2.5	-	humid
10 YR 4/4 dark yellowish brown	Ls4	24	21	1.4 g/cm ³ low	-	K		5	low	0.9	-	humid
									small pebbles			



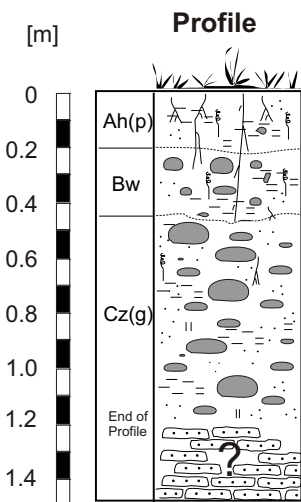
Process evaluation

High intensity: SSF 3
 Low intensity: SSF 3

Soil profile P 6: Braunerde (cB3)

<p>Site description</p>  <p>Catchment: Ror Location: Riet Coordinates: 698'539 / 236'699 Elevation: 531 m asl Land use: Meadow, 2 m next to corn field Topography: Hilltop Slope: 2 % Exposition: NE</p>	<p>Soil surface</p> <ul style="list-style-type: none"> - 90 % vegetation cover under grass, 20 % under corn - stable aggregates - soil compaction high under meadow, low under corn 	<p>Macroporosity</p> <p>Horizontal cross sections 30 x 30 cm</p> <p>depth 5 cm</p>  <p>33 / 33 Mp/m² all / large d > 5 mm</p> <p>15 cm</p>  <p>100 / 44 Mp/m² all / large</p> <p>25 cm</p>  <p>222 / 100 Mp/m² all / large</p>
<p>Lateral flowpaths</p>		<p>Geology</p> <p>Molasse sandstone</p>

Soil properties



Color	Soil texture		Bulk density	Hydromorphic features	Shape of peds	Packing density	pH	Content of		
	U	T						Coarse fragments	C _{org} [%]	Carbonate
10 YR 3/3 dark brown	Ls3 / Lt2	35 25	1.7 g/cm ³ high	-			6	medium	-	humid
10 YR 4/4 dark yellowish brown	Ls3 / Lt2	35	1.65 g/cm ³ medium	-			6	high	-	humid
10 YR 5/2 greyish brown	Si4	36 14	2.0 g/cm ³ very high	Ox1			8	very high	+++	very humid

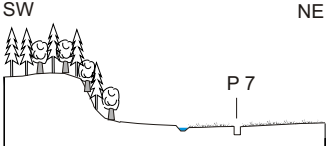
Depth of sandstone could not be determined. Possibly sandstone covered with coluvial or moraine layer.



<p>Experiments</p> <p>Two infiltration experiments were conducted close to the profile, one on land use meadow and one on land use corn. Both show high to very high infiltration rates at the beginning of the experiment (400 mm/h and 1100 mm/h respectively). The final infiltration rate on meadow is 60 mm/h. The final infiltration rate on the corn field was not reached.</p>	<p>Process evaluation</p> <p>High intensity: SOF 3</p> <p>Low intensity: SOF 3</p>
---	---

Soil profile P 7: Gley (vW14d)

Site description



Catchment: Ror
 Location: Schoren
 Coordinates: 698'533 / 237'519
 Elevation: 509 m asl
 Land use: Meadow
 Topography: Riparian zone
 Slope: < 1 %
 Exposition: SW

Soil surface

- 100 % vegetation cover
- stable aggregates
- medium top soil compaction

Lateral flowpaths

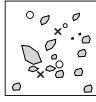

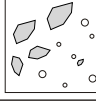
Possibly tile drains

Geology

former swamp over moraine

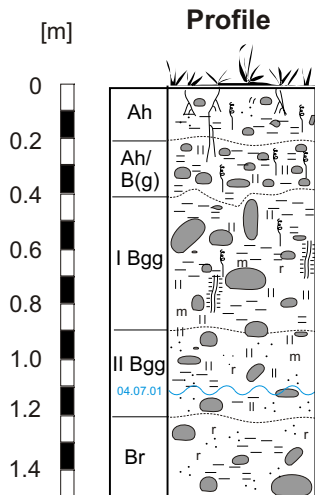
Macroporosity

Horizontal cross sections 30 x 30 cm

depth 5 cm		33 / 22	Mp/m ² all / large d > 5 mm
15 cm		22 / 22	Mp/m ² all / large
30 cm		77 / 33	Mp/m ² all / large

More than 10 worms were found during excavation of soil profile.

Soil properties



Color	Soil texture		Bulk density	Hydromorphic features	Shape of peds	Packing density	pH	Content of				
	U	T						Coarse fragments	C _{org} [%]	Carbonate	Water	
10 YR 4/2 dark greyish brown				-	SP	2		High		+++	Slightly humid	
5 Y 5/2 olive gray	Tu4	65	27	high	Ox1 Re1	P	2-3	7-8	Very high	1.5	+++	Humid
5 Y 5/3 olive	Ut4	70	25	2.1 g/cm ³ very high	Ox2 Re2	P	4	7	Very high	1.0	+++	humid
5 Y 5/3 olive	Sl4	34	14		Ox3 Re4	EK	2	8	Very high	0.3	+++	Very humid
5 Y 5/2 olive grey	Sl4	20	12		Re4	EK	2	8	Very high	0.6	+++	wet

Profile excavated down to 70 cm, drilling possible down to 170 cm.



Experiments

An infiltration experiment was conducted close to the profile. Very high infiltration rates could be observed at the beginning of the experiment (600 mm/h). The final infiltration rate is 100 mm/h.

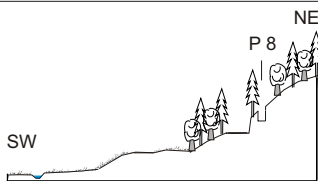
Process evaluation

High intensity: SOF 1

Low intensity: SOF 1 / D 1

Soil profile P 8: Braunerde

Site description



Catchment: Ror
 Location: Schlüssberg
 Coordinates: 699°048 / 237°517
 Elevation: 529 m asl
 Land use: Beech forest (beech, fir, spruce, forest vegetation index 8f).
 Topography: Hillslope
 Slope: 22 %
 Exposition: SW

Soil surface

- 25 % vegetation cover, rest covered with foliage
- stable aggregates
- no top soil compaction

Lateral flowpaths

Animal burrows and root channels, Ah/Bw horizon

Geology

Moraine (drumlin)

Macroporosity

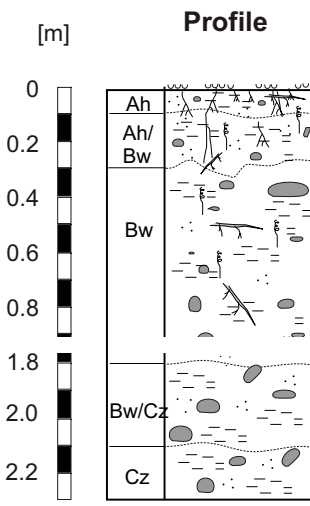
Horizontal cross sections 50 x 50 cm

depth 5 cm: 56 / 8 Mp/m² all / large d > 5 mm

15 cm: Many roots 76 / 36 Mp/m² all / large

25 cm: 28 / 28 Mp/m² all / large

Soil properties



Color	Soil texture	% weight		Bulk density	Hydromorphic features	Shape of peds	Packing density	pH	Content of			
		U	T						Coarse fragments	C _{org} [%]	Carbonate	Water
10 YR 2/2 very dark brown	Ls3	37	22	very low	-	K	1	5	low	7.3	-	dry
10 YR 3/3 dark brown	Ls3	33	22	1.6 g/cm ³ medium	-	SP	2	5		3.2	-	slightly humid
10 YR 4/3 dark brown to brown	Lt2	35	28	1.7 g/cm ³ medium	-	SP	2	5	medium	1.0	-	humid ↓ very humid
10 YR 5/3 brown	Slu	41	19	low	-			7		1.0	-	wet
5 Y 5/3 olive	Sl2	43	8		-			8		0.2	+++	very humid

Profile excavated down to 80 cm, drilling possible down to 270 cm.



Experiments

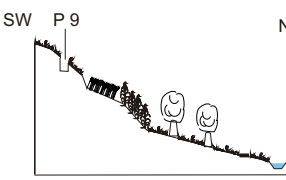
Process evaluation

High intensity: SOF 2 / SSF 3

Low intensity: SSF 3

Soil profile P 9: Braunerde (hK5)

Site description



Catchment: Ror
 Location: Riet
 Coordinates: 699'198 / 236'677
 Elevation: 544 m asl
 Land use: Meadow
 Topography: Hilltop
 Slope: 16 %
 Exposition: NE

Soil surface

- 70 % vegetation cover
- stable aggregates
- no top soil compaction

Lateral flowpaths

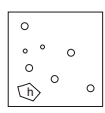
Geology

Marl over moraine (drumlin)

Macroporosity

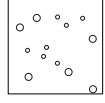
Horizontal cross sections 50 x 50 cm

depth 5 cm



> 28 / 20 Mp/m²
all / large
d > 5 mm

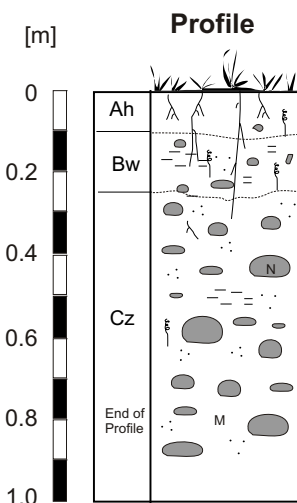
15 cm



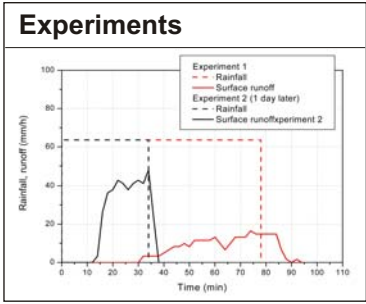
56 / 24 Mp/m²
all / large

Mp/m²
all / large

Soil properties



Color	Soil texture		Bulk density	Hydromorphic features	Shape of peds	Packing density	pH	Content of				
	U	T						Coarse fragments	C _{org} [%]	Carbonate	Water	
Dark brown	Lt2			-	K	1-2	5-6	low	> 5	-	dry	
2.5 Y 4/4 olive brown	Lt2	35	27	medium	-	SP - P	2-3	6-7	medium	5.9	++	dry
2.5 Y 5/4 light olive brown	Slu	42	15	1.65 g/cm ³ medium	Re 4 M	K - SP	2-3	7	very high	0.6	+++	slightly humid
				1.8 g/cm ³ high								



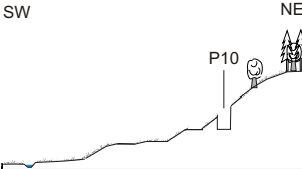
Process evaluation

High intensity: SOF 2

Low intensity: SOF 2

Soil profile P 10: Braunerde (bB3)

Site description



Catchment: Ror
 Location: Schlüssberg
 Coordinates: 699'099 / 237'464
 Elevation: 530 m asl
 Land use: Meadow
 Topography: Hillslope
 Slope: 20 %
 Exposition: SW

Soil surface

- 80 % vegetation cover
- stable aggregates
- no top soil compaction

Lateral flowpaths

Animal burrows

Geology

Moraine (drumlin)

Macroporosity

Horizontal cross sections 30 x 30 cm

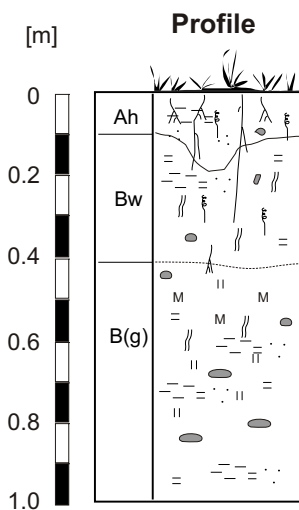
depth 14 cm: $> 111 / 67 \text{ Mp/m}^2$ all / large $d > 5 \text{ mm}$

18 cm: $> 44 / 33 \text{ Mp/m}^2$ all / large

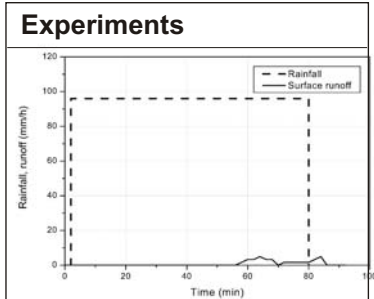
25 cm: $33 / 33 \text{ Mp/m}^2$ all / large

Many areas with high permeability

Soil properties



Color	Soil texture		Bulk density	Hydromorphic features	Shape of peds	Packing density	pH	Content of			
	U	T						Coarse fragments	C _{org} [%]	Carbonate	Water
brown			low	-	K	1-2	5	low	-	-	dry
10 YR 3/4 dark greyish brown	Lt2	36 28	1.6 g/cm ³ medium	-	SP	3-4	5	low	1.5	-	slightly humid
10 YR 4/6	Lt2	38 28	1.6 g/cm ³ medium	Ox1 M	SP	3-4	5	low	0.8	-	slightly humid
10 YR 4/2											



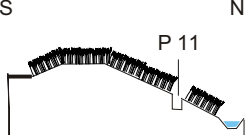
Process evaluation

High intensity: SOF 2

Low intensity: SSF 3

Soil profile P 11: Gley (tV3)

Site description



Catchment: Ror
 Location: Under Frohbüel
 Coordinates: 697'840 / 237'484
 Elevation: 505 m asl
 Land use: Wheat
 Topography: Hillslope and riparian zone
 Slope: 10 %
 Exposition: N

Soil surface

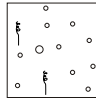
- 50 % vegetation cover
- stable aggregates
- no top soil compaction

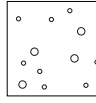
Lateral flowpaths

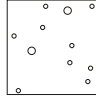
Geology
 Moraine

Macroporosity

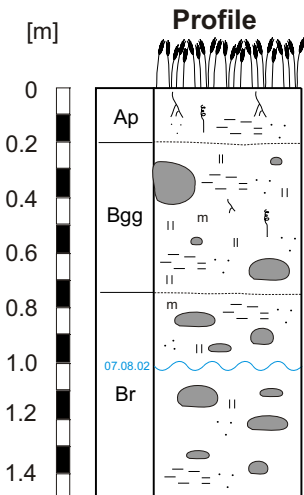
Horizontal cross sections 30 x 30 cm

depth 5 cm:  > 122 / 11 Mp/m² all / large d > 5 mm

15 cm:  133 / 44 Mp/m² all / large

30 cm:  122 / 22 Mp/m² all / large

Soil properties

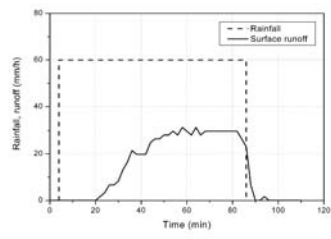


Color	Soil texture		Bulk density	Hydromorphic features	Shape of peds	Packing density	pH	Content of			
	% weight U	T						Coarse fragments	C _{org} [%]	Carbonate	Water
10 YR 3/3 dark brown	Ls3	35 20	1.4 g/cm ³ low	-	blocky	2-3	5	Medium	3.6	-	very humid
10 YR 5/4 yellowish brown	Ls3 / Lt2	34 26	1.6 g/cm ³ medium	Ox3 Re3 M	SP/- P	3	5	High	0.8	-	humid
2.5 Y 5/2 greyish brown	Ls3	38 23	1.5 g/cm ³ medium	Ox2 Re4 M		3	7	High	0.6	+	wet

Profile excavated down to 80 cm, drilling possible down to 166 cm.



Experiments

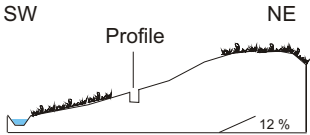


Process evaluation

High intensity: SOF 1
 Low intensity: SOF 1

Soil profile P 12: Braunerde (tB9)

Site description



Catchment: Ror
 Location: Rinderholz
 Coordinates: 698'405 / 236'995
 Elevation: 528 m asl
 Land use: Agricultural field, recently re-planted with grass after wheat.
 Geology: Sandstone of OSM
 Topography: Hillslope
 Slope: 12 %
 Exposition: SW

Soil surface

50 % vegetation cover,
 Aggregates decay after 2 min submerged in water,
 low surface roughness,
 WDPT time: 5 -10 s

Lateral flowpaths

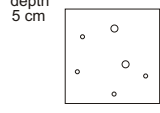
Some pipes and tile drains.

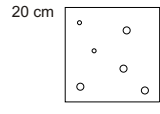
Geology

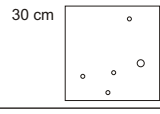
Sandstone of Molasse

Macroporosity

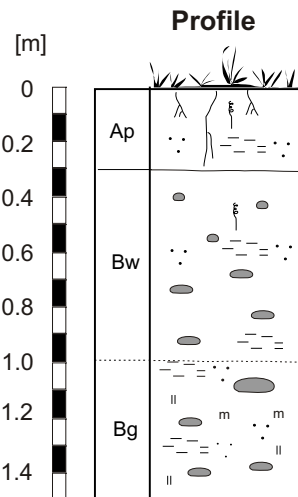
Horizontal cross sections 30 x 30 cm

depth 5 cm
 67 / 22 Mp/m² all / large d > 5 mm

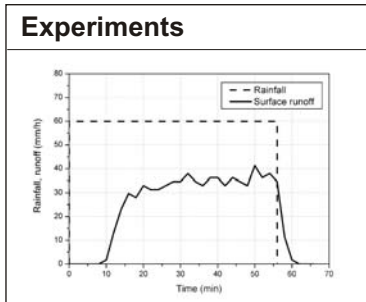
20 cm
 67 / 44 Mp/m² all / large

30 cm
 56 / 11 Mp/m² all / large

Soil properties



Color	Soil texture		Bulk density	Hydromorphic features	Shape of peds	Packing density	pH	Content of			
	U	T						Coarse fragments	C _{org} [%]	Carbonate	Water
10 YR 3/3 dark brown	35	22	1.3 g/cm ³ low		Blocky	2	5	low	3.3	-	humid
10 YR 4/3 brown	32	24	1.57 g/cm ³ medium		SP	2-3	5	low	1.2	-	humid
				Ox1 Re1 M				medium			very humid



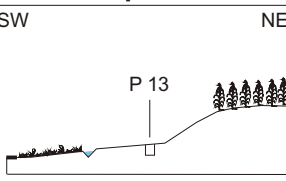
Process evaluation

High intensity: HOF 2 or SOF 1
 Low intensity: SOF 2

Soil profile P 13: Braunerde (bB3)

Site description

SW NE



Catchment: Ror
 Location: Riet
 Coordinates: 698°619 / 236°813
 Elevation: 535 m asl
 Land use: Field of beans (recently harvested)
 Topography: Plain
 Slope: 8 %
 Exposition: SW

Soil surface

- 35 % vegetation cover
- stable aggregates
- medium top soil compaction, some wheel tracks

Lateral flowpaths

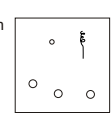
Geology

Sandstone of molasse

Macroporosity

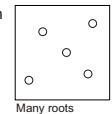
Horizontal cross sections 30 x 30 cm

depth 10 cm



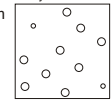
44 / 11 Mp/m²
all / large
d > 5 mm

20 cm



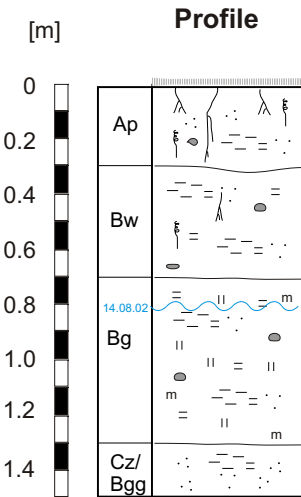
56 / 56 Mp/m²
all / large

30 cm



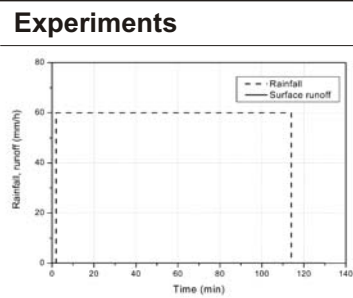
122 / 100 Mp/m²
all / large

Soil properties



Color	Soil texture		Bulk density	Hydromorphic features	Shape of peds	Packing density	pH	Content of				
	% weight							Coarse fragments	C _{org} [%]	Carbonate	Water	
	U	T										
10 YR 3/3 dark brown	Ls3	34	20	1.2 g/cm ³ very low	-	K	1	6	low	2.0	-	humid
10 YR 5/3 brown	Lt2	37	28	1.55 g/cm ³ medium	-	SP	2-3	6-7	low	0.5	-	humid
10 YR 5/4 yellowish brown	Lt2	33	30	high	Ox3 Re1 M	SP	3	6	low few weathered stones	0.5	-	wet
2.5Y 6/2 light brownish grey	Slu	48	11	very high	Re4			8			+++	wet

Depth of sandstone could not be determined. Profile excavated down to 80 cm, drilling possible down to 145 cm.

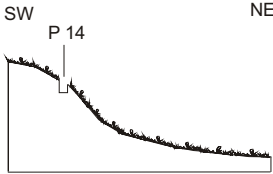


Process evaluation

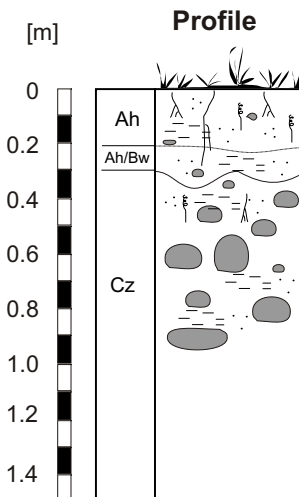
High intensity: SOF 3

Low intensity: SOF 3

Soil profile P 14: Braunerde (dB3/cB20)

<p>Site description</p>  <p>Catchment: Ror Location: Rohracher Coordinates: 698'496 / 237'950 Elevation: 518 m asl Land use: Meadow Topography: Hillslope Slope: 25 % Exposition: NE</p>	<p>Soil surface</p> <ul style="list-style-type: none"> - 100 % vegetation cover - stable aggregates - low bulk density of top soil 	<p>Macroporosity</p> <p>Horizontal cross sections 30 x 30 cm</p> <p>depth</p> <div style="display: flex; align-items: center; margin-bottom: 10px;"> <div style="width: 60px; height: 40px; border: 1px solid black; margin-right: 10px;"></div> <div style="text-align: right;">Mp/m² all / large d > 5 mm</div> </div> <div style="display: flex; align-items: center; margin-bottom: 10px;"> <div style="width: 60px; height: 40px; border: 1px solid black; margin-right: 10px;"></div> <div style="text-align: right;">Mp/m² all / large</div> </div> <div style="display: flex; align-items: center;"> <div style="width: 60px; height: 40px; border: 1px solid black; margin-right: 10px;"></div> <div style="text-align: right;">Mp/m² all / large</div> </div>
<p>Lateral flowpaths</p> <p>A horizon</p>		
<p>Geology</p> <p>Moraine (Drumlin)</p>		

Soil properties



Color	Soil texture		Bulk density	Hydromorphic features	Shape of peds	Packing density	pH	Content of			
	% weight							Coarse fragments	C _{org} [%]	Carbonate	Water
	U	T									
brown	Sl		very low	-	SP	1	6	medium	2-5	-	slightly humid
Light brown	Sl		medium	-	SP				<2		
yellowish brown			high	-			8	high	-	+++	slightly humid

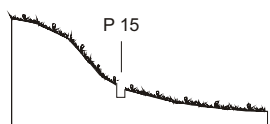


<p>Experiments</p>	<p>Process evaluation</p> <p>High intensity: SSF 1</p> <p>Low intensity: SSF 1</p>
---------------------------	---

Soil profile P 15: Braunerde (bB20)

Site description

SW NE



Catchment: Ror
 Location: Rohracher
 Coordinates: 698'554 / 237'943
 Elevation: 510 m asl
 Land use: Meadow
 Topography: foot of hillslope
 Slope: 20 %
 Exposition: NE

Soil surface

- 100 % vegetation cover
- stable aggregates

Lateral flowpaths

Animal burrows

Geology

Moraine (Drumlin)

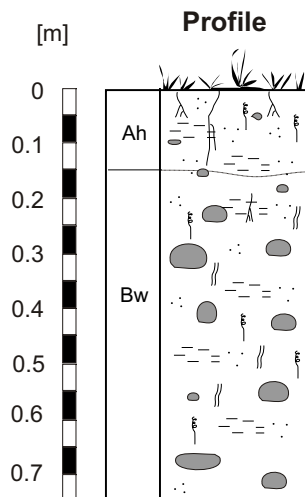
Macroporosity

Horizontal cross sections 30 x 30 cm

depth

very high macroporosity in top 1 m	Mp/m ² all / large d > 5 mm
	Mp/m ² all / large
	Mp/m ² all / large

Soil properties



Color	Soil texture		Bulk density	Hydromorphic features	Shape of peds	Packing density	pH	Content of			
	% weight							Coarse fragments	C _{org} [%]	Carbonate	Water
	U	T									
blackish brown	Ls		medium	-	SP		6-7	low	2-5	-	slightly humid
brown	Ls		high	-	P		6	high	-		slightly humid



Experiments

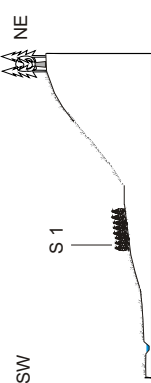
Process evaluation

High intensity: SOF 3 / DP

Low intensity: SOF 3 / DP

Soil Profile S 1: (Kalk-)Braunerde (bK11b)

Site description



Catchment: Ror
 Location: Schlüssberg
 Coordinates: 699°10'1" / 237°33'6"
 Elevation: 515 m asl
 Land use: Meadow
 Topography: hillslope
 Slope: 4 %
 Exposition: SW

Soil surface

- 100 % vegetation cover
- stable aggregates
- no top soil compaction

Lateral flowpaths

Geology

Moraine (drumlin)

Process evaluation

High intensity: SOF 3
 Low intensity: SOF 3




Soil properties

Horizon	Color	Soil texture % weight U T	Hydromorphic features	Shape of peds	pH	C _{org} [%]	Carbonate	Water	Remarks
Ap	dark brown	Us	-	K	5		2-5 %	slightly humid	low bulk density
Bw	brown	Us	-	SP	5		-	slightly humid	
lBwh	dark brown	U	Ox1		5		2-5 %	humid	
End of profile									

Soil Profile S 2: (Kalk-)Braunerde (dK9p)

Site description



Catchment: Ror
 Location: Schlusberg
 Coordinates: 699°194 / 237°498
 Elevation: 548 m asl
 Land use: Meadow
 Topography: Hillside
 Slope: 10 %
 Exposition: SW

Soil surface

- 60 % vegetation cover
- stable aggregates
- no top soil compaction

Lateral flowpaths

Animal burrows, A - horizon

Geology

Moraine (drumlin)

Process evaluation

High intensity: SSF 3
 Low intensity: SSF 3




Soil properties

Horizon	Color	Soil texture % weight U T	Hydromorphic features	Shape of peds	pH	Content of		Remarks
						C _{org} [%]	Carbonate	
Ah	dark brown	Sl	-	K	5-6		slightly humid	low bulk density
Bw	brown	Sl	-	SP	6-7		slightly humid	
BwCz	Greyish brown		Ox1		7		slightly humid	small pebbles
End of profile								

Soil Profile S 3: Gley (xG1a)

Site description



Catchment: Ror
 Location: Schlüssberg
 Coordinates: 699045 / 237271
 Elevation: 513 m asl
 Land use: Meadow
 Topography: Plain
 Slope: < 3 %
 Exposition: SW

Soil surface

- 100 % vegetation cover
- stable aggregates
- no top soil compaction

Lateral flowpaths

Tile drains

Geology

Former swamp over alluvium and moraine

Process evaluation

High intensity: D 1 / SOF 1
 Low intensity: D 1 / SOF 1


Soil properties

Horizon	Color	Soil texture % weight U T	Hydromorphic features	Shape of peds	pH	Content of		Remarks
						C _{org} [%]	Water	
Alt(a)	black	Sl		K	6		dry	very low bulk density
Bgg	Grey	Sl	Ox3 Re4		7		slightly humid	many small pebbles
Br	Grey	U	Re4		7		humid	
End of profile								



Soil Profile S 4: Braunerde (bB3d)

Site description



Catchment: Ror
 Location: Riet
 Coordinates: 698°282 / 236°595
 Elevation: 540 m asl
 Land use: Meadow
 Topography: Hillslope
 Slope: 14 %
 Exposition: NE

Soil surface

- 80 % vegetation cover
- stable aggregates
- no top soil compaction

Lateral flowpaths

Geology

Moraine (drumlin)

Process evaluation

High intensity: SOF 3
 Low intensity: SOF 3


Soil properties

Horizon	Color	Soil texture			Hydromorphic features	Shape of peds	pH	Content of		Remarks
		U	T	% weight				Carbonate	Water	
Ap	dark brown	LS			-	K	6-7	2-5	slightly humid	
Bw(g)	olive brown	LS			Ox1	SP	7	<1	slightly humid	many small pebbles
End of profile										



Soil Profile S 5: Gley (wW8d)

Site description



Catchment: Ror
 Location: Riet
 Coordinates: 698°344 / 236°991
 Elevation: 525 m asl
 Land use: Fellow land (poppy seed, wheat, cornflower, clover, milfoil, etc.)
 Topography: Plain
 Slope: 3.5 %
 Exposition: NW

Soil surface

- 80 % vegetation cover
- stable aggregates
- no top soil compaction

Lateral flowpaths

Possibly tile drains

Geology

Alluvium over molasse

Process evaluation

High intensity: SOF 1
 Low intensity: SOF 1

Soil properties

Horizon	Color	Soil texture % weight U T	Hydromorphic features	Shape of peds	pH	C _{org} [%]	Content of Carbonate	Water	Remarks
Ap	10 YR 3/2 Very dark greyish brown	L3 35 42		K	6	5.6	+	slightly humid	
Aa/ Bgg	10 YR 3/1 Very dark grey	Tu2 34 51	Ox3 Re3		6	8.2	-	humid	
Bgg	2.5 Y 5/2 greyish brown	Ls2 44 22	Ox3 Re4		6	0.5	+	humid	many remains of wood and roots, pieces of charcoal
									End of profile



Soil Profile S 6: Gley (tW8a)

Site description	
SW	NE
Catchment: Ror Location: Buechholz Coordinates: 698731 / 237177 Elevation: 512 m asl Land use: Grain field (recently harvested) Topography: Plain Slope: < 3 % Exposition: NE	

Soil surface
- 80 % vegetation cover
- stable aggregates
- no top soil compaction

Lateral flowpaths
Tile drains

Geology
Alluvium over molasse

Process evaluation
High intensity: D 3
Low intensity: D 3

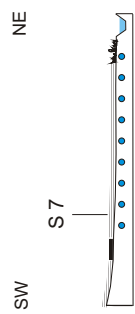
Soil properties

Horizon	Color	Soil texture % weight			Hydromorphic features	Shape of peds	pH	Content of		Remarks
		U	T	C _{org} [%]				Water		
Ap	10 YR 2/1 black	Lt3	39	40		K	7	12.2	slightly humid	
I Bgg	2.5 Y 6/2 light brownish grey	Lt								macropore filled with humus.
II Bgg	Patches of 10 YR 5/6 yellowish brown	Slt4	30	14	Ox3 Re4		7	0.1	slightly humid	many small pebbles, high content of coarse fragments.
End of profile										



Soil Profile S 7: Gley (vW17d)

Site description



SW NE

S 7

Catchment: Ror
 Location: Summerau
 Coordinates: 697745 / 237845
 Elevation: 494 m asl
 Land use: Grain field (recently harvested)
 Topography: Plain
 Slope: < 2 %
 Exposition: NE

Soil surface

- 80 % vegetation cover
- stable aggregates
- no top soil compaction

Lateral flowpaths

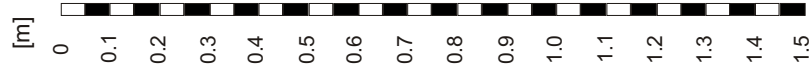
Tile drains

Geology

Molasse

Process evaluation

High intensity: D 1
 Low intensity: D 1

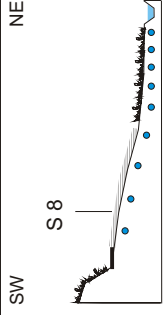


Soil properties

Horizon	Color	Soil texture			Hydromorphic features	Shape of peds	pH	Content of		Remarks
		U	T	% weight				Carbonate	Water	
Ap	10 YR 3/2 very dark greyish brown	L2	36	33		K	6-7	4.0	+	humid
I Bgg	10 YR 5/2 greyish brown Patches of 10 YR 5/6 yellowish brown	Ls4	28	22	Ox3 Re4		6	1.1	-	humid
II Bgg	10 YR 5/4 yellowish brown	Lts	29	30	Ox3 Re4		6	1.1	+	humid
										End of profile

Soil Profile S 8: Braunerde - Gley (bB26c)

Site description



Catchment: Ror
 Location: Langacher
 Coordinates: 697'530 / 238'014
 Elevation: 494 m asl
 Land use: Rape field (recently harvested)
 Topography: hillslope
 Slope: 10 %
 Exposition: NE

Soil surface

- 90 % vegetation cover
- stable aggregates
- no top soil compaction

Lateral flowpaths

Tile drains

Geology

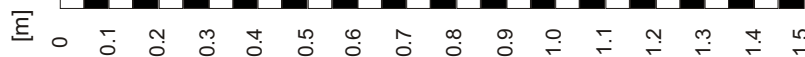
Molasse

Process evaluation

High intensity: D 3
 Low intensity: D 3

Soil properties

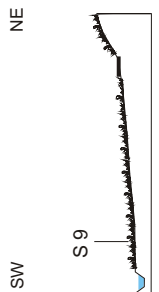
Horizon	Color	Soil texture			Hydromorphic features	Shape of peds	pH	Content of		Remarks
		U	T	% weight				Carbonate	Water	
Ap	10 YR 3/2 very dark greyish brown	37	22	22	-	K	5	2.9	-	humid
Bw(g)	10 YR 5/3 brown	45	21	21	Ox1		5	3.3	-	humid
I Bgg	10 YR 5/2 greyish brown	33	21	21	Ox3 Re2 M		6	1.3	-	very humid
II Bgg	2.5 Y 6/2 light brownish grey Patches of 10 YR 6/6 brownish yellow	38	29	29	Ox3 Re4		7	0.4	(+)	wet



Depth of profile 2 m

Soil Profile S 9: Gley (wG8d)

Site description



Catchment: Ror
 Location: Oberrohr
 Coordinates: 697 972 / 238 020
 Elevation: 491 m asl
 Land use: Meadow
 Topography: Plain
 Slope: < 3 %
 Exposition: SW

Soil surface

- 100 % vegetation cover
- stable aggregates
- no top soil compaction

Lateral flowpaths

Tile drains

Geology

Drained swamp

Process evaluation

High intensity: D 1
 Low intensity: D 1

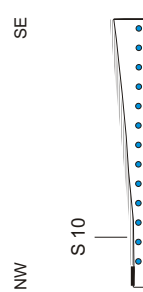


Soil properties

Horizon	Color	Soil texture			Hydromorphic features	Shape of peds	pH	Content of		Remarks	
		U	T	% weight				Carbonate	Water		
Ap	10 YR 4/2 dark greyish brown	Ls	24	32	Ox3 Re2	K	7	5.2	-	humid	
Bgg	10 YR 5/2 greyish brown Patches of 10 YR 5/6 yellowish brown	L3	38	39	Ox3 Re4 M		7	1.3	-	very humid	Many roots and wooden material
										End of profile	

Soil Profile S 10: Gley (vW17d)

Site description



Catchment: Ror
 Location: Oberrohr
 Coordinates: 687972 / 237843
 Elevation: 485 m asl
 Land use: Grain field (recently harvested)
 Topography: Plain
 Slope: 4 %
 Exposition: NW

Soil surface

80 % vegetation cover
 Stable aggregates
 No top soil compaction

Lateral flowpaths

tile drains

Geology

Alluvium over molasse

Process evaluation

High intensity: D 1
 Low intensity: D 1

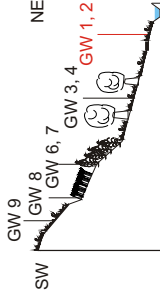
Soil properties

Horizon	Color	Soil texture % weight U T	Hydromorphic features	Shape of peds	pH	Content of		Remarks
						C _{org} [%]	Carbonate	
Ap	10 YR 4/2 dark greyish brown	L2 35	-	K	5	7.2	-	humid Old plant tissue, not decomposed
B _{gg}	10 YR 5/3 brown Patches of 10 YR 5/6 yellowish brown	L2 35	Ox3 R ₆ 3 M		5	0.3	-	very humid Geroll, weathered sandstone
	14.08.02							Water level at 0.8 m
								Wet
								End of profile



Groundwater well GW 1 and 2 : Braunerde Gley (tV8d) - Gley (wW8d)

Site description



Catchment: Ror
 Location: Riet
 Coordinates: 698227 / 236966
 Elevation: 524 m asl
 Land use: Meadow
 Topography: hillslope
 Slope: 4 %
 Exposition: NE

Soil surface

- 100 % vegetation cover
- stable aggregates
- no top soil compaction
- mull

Lateral flowpaths

Potentially tile drained

Geology

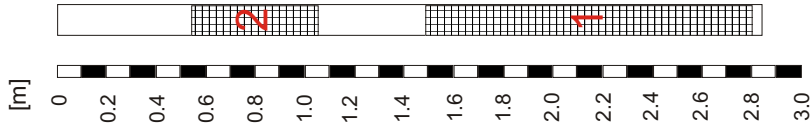
Former swamp over molasse

Process evaluation

High intensity: SOF 1
 Low intensity: SOF 1

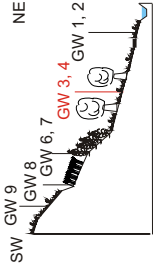
Soil properties

Horizon	Color	Soil texture			Shape of peds	Hydromorphic features	pH	Carbonate content %	C _{org} content %	Water content	Remarks
		U	T	% weight							
Ah	10 YR 4/2 dark greyish brown	L12	40	26	K		6-7	2.7	dry		
I Bgg	2.5 Y 6/2 light brownish grey	Lu	61	19	SP		7	0.4	dry	Big stones, many pebbles, possibly deposit	
II Bgg	10 YR 4/2 dark greyish brown	Ls2	41	24	SP	Ox3 Re3	7	1.1	very humid	- remains of wood - strong smell - bulk density very low, Possibly former swamp	
Br	2.5 Y 6/2 light brownish grey	Si4	40	15		Re4		0.2		Many small stones and pebbles	



Groundwater well GW 3 and 4 : Braunerde - Gley (tV8d)

Site description



Catchment: Ror
 Location: Riet
 Coordinates: 698'229 / 236'881
 Elevation: 527 m asl
 Land use: Meadow
 Topography: hillslope
 Slope: 5 %
 Exposition: NE

Soil surface

- 100 % vegetation cover
- stable aggregates
- no top soil compaction

Lateral flowpaths

Geology

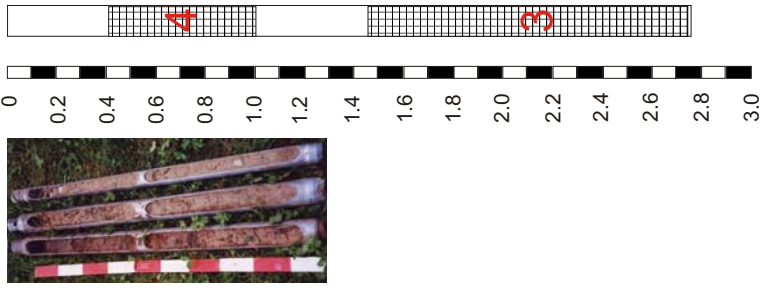
Kolluvium of moraine

Process evaluation

High intensity: SOF 2
 Low intensity: SOF 2

Soil properties

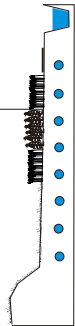
Horizon	Color	Soil texture % weight	Shape of peds	Hydromorphic features	pH	Carbonate content	C _{org} content %	Water content	Remarks
Ah	10 YR 4/2 dark greyish brown	Ls3 36	K		5	-	1.0	slightly humid	
Ah,Bw	10 YR 5/4 yellowish brown	L2 36	SP	Ox 1	5	-	0.4	slightly humid	possibly deposit
Bg	2.5Y 4/4 olive brown	L2 32	P	Ox 2 Re 1 M	6	-	0.2	slightly humid	
Br	2.5Y 5/2 greyish brown	Ls3 37		Re 4	7	++	0.2		Groundwater level at 1.25 m below surface



Groundwater well GW 5 : Buntgley (wW5a)

Site description

SE GW 5 NW



Catchment: Ror
 Location: Langacher
 Coordinates: 697'565 / 238'153
 Elevation: 490 m asl
 Land use: Grain field
 Topography: plain
 Slope: < 1%
 Exposition: -

Soil surface

- 100 % vegetation cover
- stable aggregates
- no top soil compaction

Lateral flowpaths

Tile drains

Geology

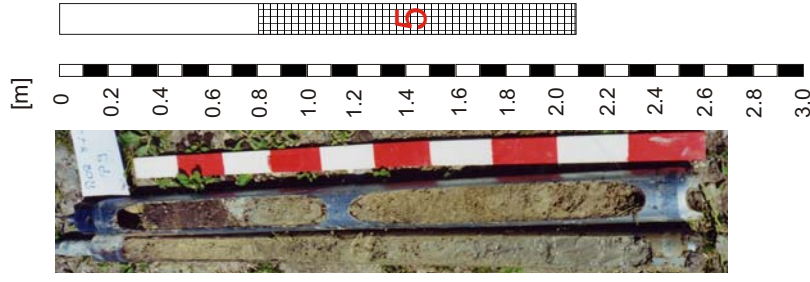
Former swamp over alluvium

Process evaluation

High intensity: D 1
 Low intensity: D 1


Soil properties

Horizon	Color	Soil texture	Shape of peds	Hydromorphic features	pH	Carbonate content	C _{org} % content	Water content	Remarks
Ap grey intermediate layer	10YR 2/1 black	Ls3 Us	K EK		7		4.2	slightly humid	Low bulk density
Bg	2.5 Y 5/2 greyish brown	S2	SP	Ox2 Re2	6.7		0.1	humid	Medium bulk density
I Br	2.5 Y 4/2 dark greyish brown	Ss	EK	Re4	8		2.7	wet	Low bulk density
II Br	2.5 Y 5/2 greyish brown	Us	EK	Re4	8		0	wet	Low bulk density



Groundwater well GW 6 and 7 : Braunerde (bB3)

Site description



Catchment: Ror
 Location: Riet
 Coordinates: 698°155 / 236°785
 Elevation: 536 m asl
 Land use: Grain field
 Topography: hillslope
 Slope: 6 %
 Exposition: NE

Soil surface

- 70 % vegetation cover
- stable aggregates
- no top soil compaction

Lateral flowpaths

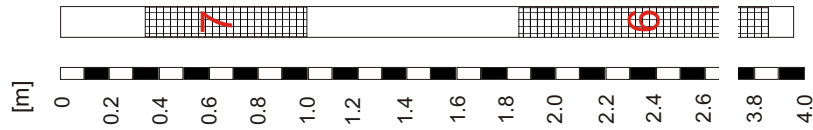
Animal burrows

Geology

Kolluvium of Moraine (drumlin)

Process evaluation

High intensity: SOF 3 / SSF 3
 Low intensity: SOF 3 / SSF 3




Soil properties

Horizon	Color	Soil texture % weight	Shape of peds	Hydromorphic features	pH	Carbonate content	C _{org} content %	Water content	Remarks
Ap(p)	2,5 Y 4/2 dark greyish brown	U Ls2 42	K	-	6		6.4	slightly humid	Earthworms
Bw	2,5 Y 4/3 olive brown	U Ls2 42	SP	-	8	+++	2.9	slightly humid	
Cz	5 Y 7/3 pale yellow	U Siu 49		-	8	+++	0.3	humid	High bulk density, many small stones and pebbles

Groundwater well GW 8: Gley (bB3)

Site description



Catchment: Ror
 Location: Riet
 Coordinates: 698°193 / 236723
 Elevation: 540 m asl
 Land use: Meadow
 Topography: hillslope
 Slope: 5 %
 Exposition: NE

Soil surface

- 100 % vegetation cover
- stable aggregates
- no top soil compaction

Lateral flowpaths

Geology

Moraine (drumlin)

Process evaluation

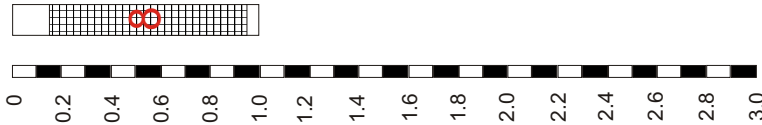
High intensity: SOF 1
 Low intensity: SOF 1

Soil properties

Horizon	Color	Soil texture % weight	Shape of peds	Hydromorphic features	pH	Carbonate content % C _{org}	Water content	Remarks
Ah	2.5 Y 3/2 very dark greyish brown	Ls2 U 45 T 22	K	-	6	8.2	wet	Waterlevel at soil surface
Br	5 Y 6/3 pale olive	Slu U 46 T 14	P	Re4	8	0.9	wet	High bulk density, many small rounded stones and pebbles




[m]



Groundwater well GW 9: (Kalk-) Braunerde (hK5)

Site description



SW **GW 9** GW 8 GW 6, 7 GW 3, 4 GW 1, 2 NE

Catchment: Ror
 Location: Riet
 Coordinates: 698°188 / 236°669
 Elevation: 545 m asl
 Land use: Meadow
 Topography: hillslope
 Slope: 16 %
 Exposition: NE

Soil surface

- 100 % vegetation cover
- stable aggregates
- no top soil compaction

Lateral flowpaths

Geology

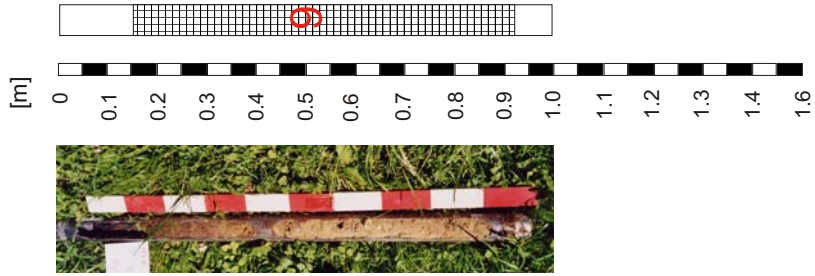
Moraine (drumlin)

Process evaluation

High intensity: SOF 2
 Low intensity: SOF 2

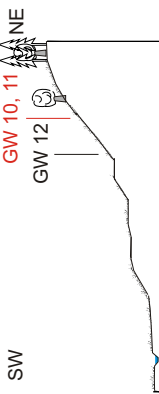
Soil properties

Horizon	Color	Soil texture % weight U T	Shape of peds	Hydromorphic features	pH	Carbonate content	C _{org} content %	Water content	Remarks
Ah	10 YR 4/2 dark greyish brown	Li2 36 32	K	-	6	++	10.9	slightly humid	
Bw	2.5 Y 6/4 light yellowish brown	Li2 40 29	SP	-	6	++	3.6	slightly humid	
Cz	2.5 Y 7/2 light grey (pale yellow)	Slu 47 15		Re4	8	+++	1.0	slightly humid	



Groundwater well GW 10 and 11: Braunerde (bB3)

Site description



Catchment: Ror
 Location: Schlüssberg
 Coordinates: 699°137 / 237°464
 Elevation: 537 m asl
 Land use: Meadow
 Topography: hillslope
 Slope: 18 %
 Exposition: SW

Soil surface

- 100 % vegetation cover
- stable aggregates
- no top soil compaction

Lateral flowpaths

Animal burrows

Geology

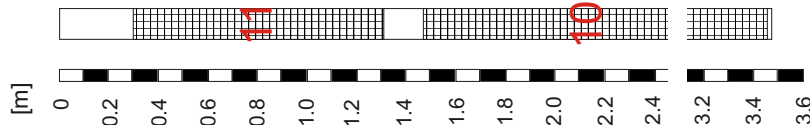
Moraine (drumlin)

Process evaluation

High intensity: SSF 3
 Low intensity: SSF 3

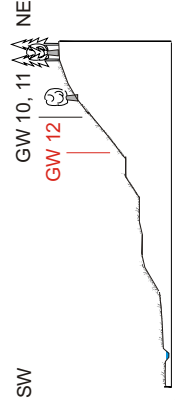
Soil properties

Horizon	Color	Soil texture			Shape of peds	Hydromorphic features	pH	Carbonate content	C _{org} % content	Water content	Remarks
		U	T	%weight							
Ah	10YR 4/3 dark brown	36	25	25	K	-	5	-	6.4	slightly humid	
Bw	10 YR 5/3 brown	Lis/L2 : 30	33	33	SP	-	5-6	-	2.9	slightly humid	
Cz	2.5 Y 6/2 light brownish grey	64	3	3		Ox1 Re2	7-8	+++	0.3	slightly humid	High bulk density, many small stones and pebbles



Groundwater well GW 12: Braunerde (bB3)

Site description



Catchment: Ror
 Location: Schlussberg
 Coordinates: 699°10'1"/237°44'5"
 Elevation: 528 m asl
 Land use: Meadow
 Topography: hillslope
 Slope: 20 %
 Exposition: SW

Soil surface

- 100 % vegetation cover
- stable aggregates
- no top soil compaction

Lateral flowpaths

Geology

Moraine (drumlin)

Process evaluation

High intensity: SSF 3
 Low intensity: SSF 3

Soil properties

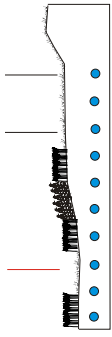
Horizon	Color	Soil texture % weight U T	Shape of peds	Hydromorphic features	pH	Carbonate content C _{org} %	Water content	Remarks
Ah	10YR 4/2 dark greyish brown	LL2 35 26	K	-	5	4.7	dry	Low bulk density
Ah/Bw	10 YR 5/3 brown	LL2 36 26	K		5	5.4	dry	
Bw	10 YR 5/4 yellowish brown	LL2 37 29	SP	M	7	1.4	slightly humid	Medium bulk density
Bw/Cz	10 YR 5/2 greyish brown	Ls3 37 20	SP		7	0.7	humid	
Cz	2.5 Y 6/2 light brownish grey					+++	humid	High bulk density, many small stones and pebbles



Groundwater well GW 13: Buntgley (tW8)

Site description

NW **GW 13** GW 14 GW 15 SE



Catchment: Ror
 Location: Poesch
 Coordinates: 6990362 / 237164
 Elevation: 5113 m asl
 Land use: Meadow
 Topography: plain
 Slope: < 1 %
 Exposition: -

Soil surface

- 100 % vegetation cover
- stable aggregates
- no top soil compaction

Lateral flowpaths

Tile drains

Geology

Alluvium over moraine

Process evaluation

High intensity: D 1
 Low intensity: D 1

Soil properties

Horizon	Color	Soil texture			Shape of peds	Hydromorphic features	pH	Carbonate content	C _{org} content %	Water content	Remarks
		U	T	% weight							
Ah	10YR 2/1 black	Ls2	42	22	K		6	(+)	6.2	very humid	Low bulk density
AhB(g)	10 YR 3/2 very dark greyish brown	Ls2	40	21	SP	Ox1	6	(+)	4.3	very humid	
I Bg	10 YR 5/2 greyish brown	Slu	46	13	SP	Ox2	7	++	0.4	very humid	
II Bgg	10 YR 4/1 dark grey	S4	35	15	EK	Ox3 Re3	8	+++	0.4	wet	Very low bulk density
III Bgg	2.5 Y 6/2 light brownish grey	Slu	46	14	P	Ox3 Re3	8	+++	0.5	humid	High bulk density, many small stones and pebbles
Br	2.5 Y 6/1 light brownish grey	Ls2	49	18	P	Re4	8	+++	0.3	humid	



Groundwater well GW 14 : Buntgley (tW8a)

Site description

NW GW 13 **GW 14** GW 15 SE

Catchment: Ror
 Location: Poesch
 Coordinates: 699°162 / 237°058
 Elevation: 513 m asl
 Land Use: Meadow
 Topography: hillslope
 Slope: < 1 %
 Exposition: -

Soil surface

- 100 % vegetation cover
- stable aggregates
- no top soil compaction

Lateral flowpaths

Tile drains

Geology

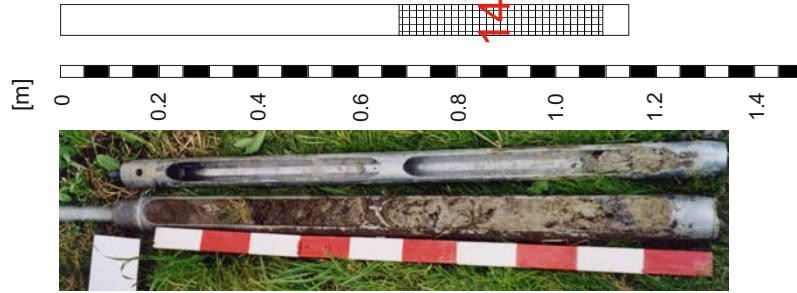
Alluvium over moraine

Process evaluation

High intensity: D 2
 Low intensity: D 2

Soil properties

Horizon	Color	Soil texture % weight U T	Shape of peds	Hydromorphic features	pH	Carbonate content C _{org} %	Water content	Remarks
Ah(p)	10YR 3/2 very dark greyish brown	L13 33 37	K	-	6	7.3	slightly humid	Low bulk density
I Bgg	5Y 5/2 olive grey	L13 40 36	P	Ox.3 Re.4	5	0.9	humid	Medium bulk density. Many round stones and pebbles
II Bgg	10 YR 4/1 dark grey	Sand and gravel				+++	humid	
III Bgg	2.5 Y 5/2 greyish brown	S14 33 16	SP	Ox.3 Re.4	8	0.6	humid	
Br	2.5 Y 6/1 light brownish grey					+++	wet	High bulk density
In depth of 1.10 m massive Sandstone (stratic block?)								



Groundwater well GW 15: Buntgley (tW8a)

Site description

NW GW 13 GW 14 **GW 15** SE

Catchment: Ror
 Location: Poesch
 Coordinates: 699 103 / 237 055
 Elevation: 5135 m asl
 Land use: Meadow
 Topography: hillslope
 Slope: <1 %
 Exposition: -

Soil surface

- 100 % vegetation cover
- stable aggregates
- no top soil compaction

Lateral flowpaths

Tile drains

Geology

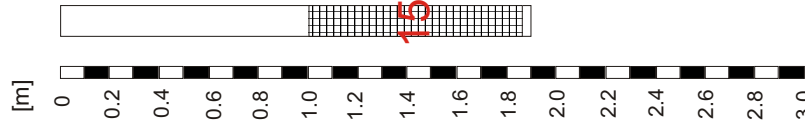
Alluvium over Moraine

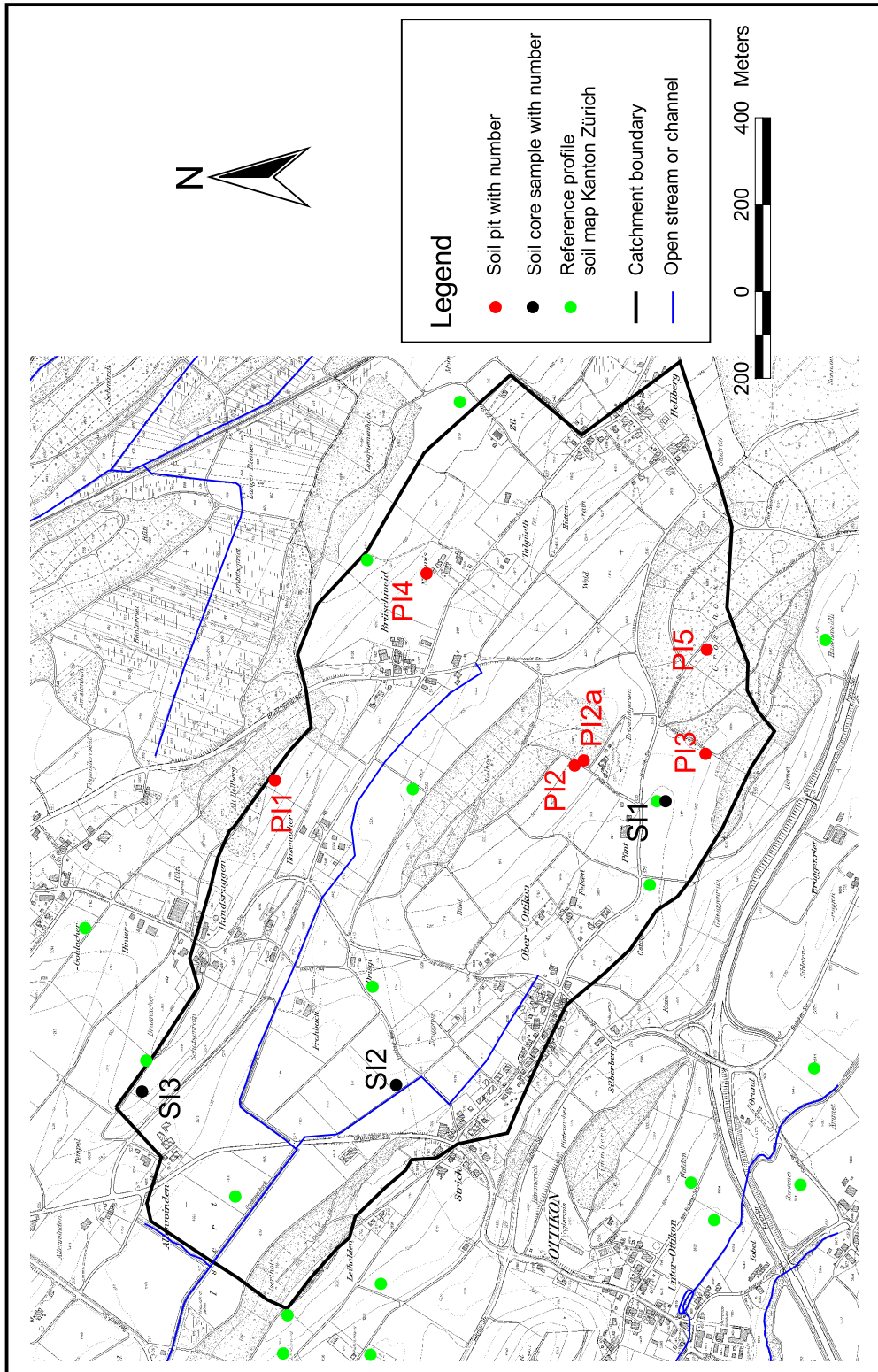
Process evaluation

High intensity: D 2
 Low intensity: D 2

Soil properties

Horizon	Color	Soil texture			Shape of peds	Hydromorphic features	pH	Carbonate content	C _{org} content %	Water content	Remarks
		U	T	% weight							
Ah	10YR 3/2 very dark greyish brown	Ls/L3	36	30	SP		5	-	5.5	slightly humid	Medium bulk density
I Bgg	2.5 Y 5/2 greyish brown	Ls	38	29	P	←	5	-	1.0	humid	
II Bgg	2.5 Y 5/2 greyish brown	Slu	12	42	EK	Ox 3 Re 4	8	+++	0	humid	
III Br	2.5 Y 6/2 light brownish grey	Tu3	30	55	SP	→	8	+++	0		→



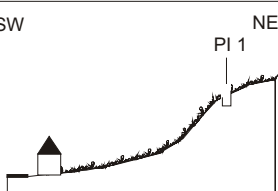


Hintergrundplan reproduziert mit Bewilligung des Amtes für Raumordnung und Vermessung, Baudirektion Kanton Zürich.

Fig. A.3 Location of soil profiles in Isert catchment.

Soil profile PI 1: Braunerde (dB20)

Site description



Catchment: Isert
 Location: Hasenacher
 Coordinates: 702'476 / 239'796
 Elevation: 566 m asl
 Land use: Meadow
 Topography: Hillslope
 Slope: 36 %
 Exposition: SW

Soil surface

- 100 % vegetation cover
- stable aggregates
- no top soil compaction

Lateral flowpaths

Animal burrows

Geology

Moraine (drumlin)

Macroporosity

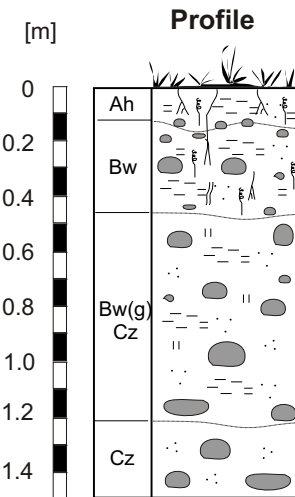
Horizontal cross sections 30 x 30 cm

depth 10 cm: 89 / 44 Mp/m² all / large d > 5 mm

20 cm: 22 / 0 Mp/m² all / large

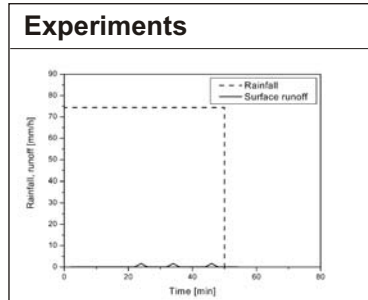
30 cm: 33 / 11 Mp/m² all / large

Soil properties



Color	Soil texture		Bulk density	Hydromorphic features	Shape of peds	Packing density	pH	Content of			
	U	T						Coarse fragments	C _{org} [%]	Carbonate	Water
10 YR 3/3 dark brown	Lt2	34 30	Low	-	K	1	5-6	medium	5.8	-	dry
10 YR 4/4 dark yellowish brown	Lt2	36 30	1.5 g/cm ³ medium	-	SP	2-3	6-7	high	1.7	+	slightly humid
10 YR 4/3 brown	Lt3	31 40	1.55 g/cm ³ medium	Ox1	SP	2-3	6-7	high	0.9	+	humid
10 YR 6/3 pale brown	Stu	44 11					8	high	-	+++	

Profile excavated down to 85 cm, drilling possible down to 200 cm.



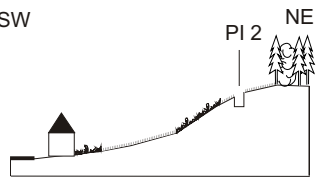
Process evaluation

High intensity: SOF 2

Low intensity: SSF 3

Soil profile PI 2: Parabraunerde (bT9)

Site description



Catchment: Isert
 Location: Pünt-Bielholz
 Coordinates: 702'510 / 239'106
 Elevation: 540 m asl
 Land use: Grain field
 Topography: Hillslope
 Slope: 16 %
 Exposition: SW

Soil surface

- < 5 % vegetation cover on grain field
- 80 % vegetation cover on meadow next to field
- unstable aggregates, soil surface sealing
- medium top soil compaction


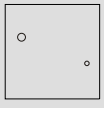
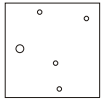
Lateral flowpaths

Geology

Moraine (drumlin), gravel rich

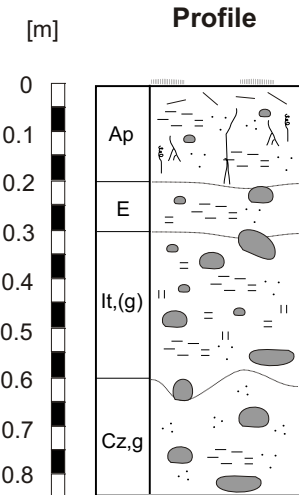
Macroporosity

Horizontal cross sections 30 x 30 cm

depth 10 cm		33 / 33	Mp/m ² all / large d > 5 mm
Meadow next to profile 20 cm		22 / 11	Mp/m ² all / large
Profile 25 cm		56 / 11	Mp/m ² all / large

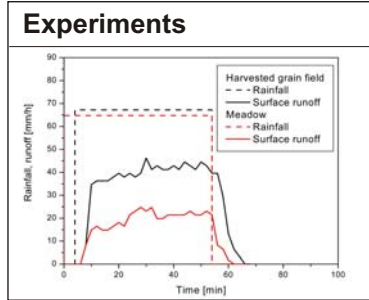
No macropores above in Ap (freshly plowed)

Soil properties



Color	Soil texture		Bulk density	Hydromorphic features	Shape of peds	Packing density	pH	Content of			
	U	T						Coarse fragments	C _{org} [%]	Carbonate	Water
10 YR 4/2 dark greyish brown	Ls3	39 20	1.45 g/cm ³ low	-	K	2	5	low	3.7	-	slightly humid
10 YR 4/3 brown	Lt2	36 27	1.7 g/cm ³ high Plow pan?	-	SP	3	5	medium	1.3	-	slightly humid
10 YR 4/3 brown	Lt3	33 31	1.55 g/cm ³ medium	Ox1	SP	3	6-7	high	1.0	+	slightly humid
10 YR 6/3 pale brown	Si3/Si4	41 12	2.0 g/cm ³ very high	Re1	P	3	7-8	high	0.7	+++	slightly humid

Profile excavated down to 95 cm, drilling possible down to 200 cm.

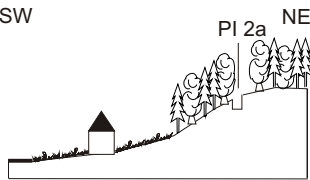


Process evaluation

High intensity: HOF 2
 Low intensity: SOF 3

Soil profile PI 2a: Braunerde

Site description



Catchment: Isert
 Location: Pünt-Bielholz
 Coordinates: 702'522 / 239'085
 Elevation: 540 m asl
 Land use: Forest (Beech, sporadic fir, ivy)
 Forest vegetation Index 6
 Topography: Hillslope
 Slope: 17 %
 Exposition: SW

Soil surface

- < 5 % vegetation cover, 100 % with foliage
- mullartiger Moder

Lateral flowpaths

Root channels and animal burrows

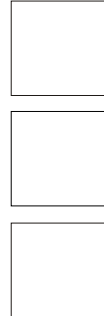
Geology

Moraine (drumlin), gravel rich

Macroporosity

Horizontal cross sections 30 x 30 cm

depth

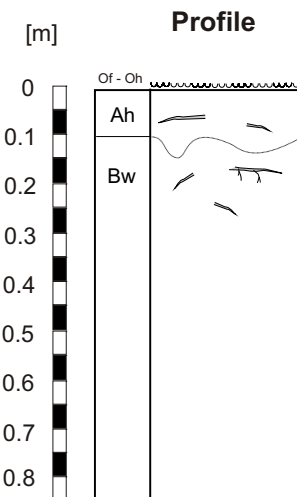


Mp/m²
all / large
d > 5 mm

Mp/m²
all / large

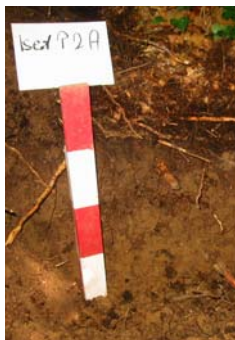
Mp/m²
all / large

Soil properties

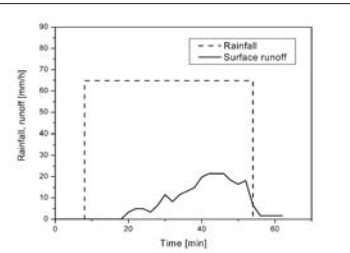


Color	Soil texture		Bulk density	Hydromorphic features	Shape of peds	Packing density	pH	Content of			
	U	T						Coarse fragments	C _{org} [%]	Carbonate	Water
10 YR 2/2 very dark brown			very low	-	K	1	4-5	low		-	slightly humid
10 YR 4/4 dark yellowish brown			very low	-	SP	1	5-6	low		-	slightly humid

Profile excavated down to 30 cm.



Experiments



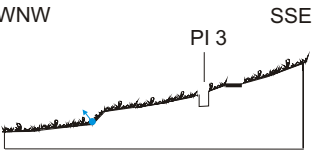
Process evaluation

High intensity: SOF 3

Low intensity: SSF 3

Soil profile PI 3: Braunerde (bB30)

Site description



Catchment: Isert
 Location: Hasenacher
 Coordinates: 702'537 / 238'805
 Elevation: 540 m asl
 Land use: Meadow
 Topography: Depression
 Slope: 12 %
 Exposition: WNW

Soil surface

- 100 % vegetation cover
- medium aggregate stability

Lateral flowpaths

Animal burrows

Geology

Interglacial gravel deposits, purely fluvial.
 0-5 m depth of gravel over highest possible groundwater level.

Macroporosity

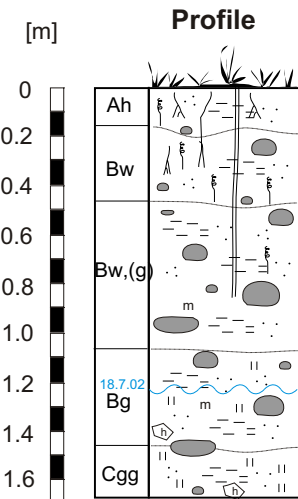
Horizontal cross sections 30 x 40 cm

depth 15 cm: 83 / 67 Mp/m² all / large d > 5 mm

25 cm: 75 / 50 Mp/m² all / large

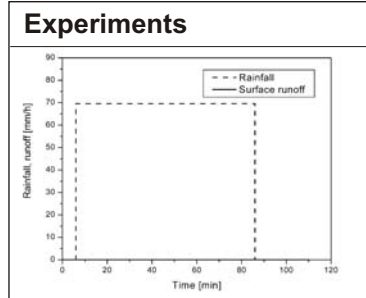
Mp/m² all / large

Soil properties



Color	Soil texture	% weight		Bulk density	Hydromorphic features	Shape of peds	Packing density	pH	Coarse fragments	Content of		
		U	T							C _{org} [%]	Carbonate	Water
10 YR 3/2 very dark grayish brown	Ls2/Ls3	40	22	1.1 g/cm ³ very low	-	K	1	6	low	8.3	-	slightly humid
10 YR 4/3 brown	Ls3	36	22	1.5 g/cm ³ medium	-	SP	2	5-6	high	1.6	-	humid
10 YR 4/2 dark grayish brown	Ls3	39	21	1.5 g/cm ³ medium	M	SP	2	6-7	high	1.6	-	humid
10 YR 3/3 dark brown	Ls3	37	22		Ox1 M			7	high	1.3	-	very humid
10 YR 5/4 yellowish brown	Ls3	34	19		Ox3			7-8	high	1.2	-	wet

Profile excavated down to 85 cm, drilling possible down to 195 cm.

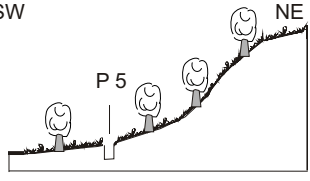
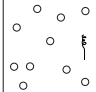
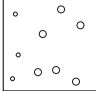
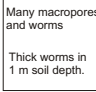


Process evaluation

High intensity: SOF 3

Low intensity: SOF 3

Soil profile PI 4: Parabraunerde (aT4)

<p>Site description</p>  <p>Catchment: Isert Location: Nasswis Coordinates: 702'952 / 239'447 Elevation: 535 m asl Land use: Meadow with fruit trees Topography: Base of hillslope Slope: 6 % Exposition: SW</p>	<p>Soil surface</p> <ul style="list-style-type: none"> - 100 % vegetation cover - stable aggregates 	<p>Macroporosity</p> <p>Horizontal cross sections 30 x 30 cm</p> <p>depth 10 cm  33 / 33 Mp/m² all / large d > 5 mm</p> <p>25 cm  99 / 66 Mp/m² all / large</p> <p>25 cm  Many macropores and worms Thick worms in 1 m soil depth. Mp/m² all / large</p>
<p>Lateral flowpaths</p>		<p>Geology</p> <p>Moraine (drumlin), gravel rich</p>

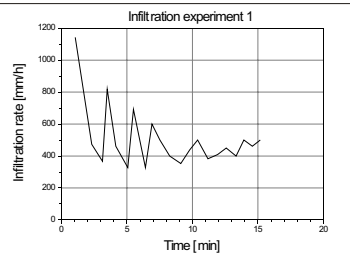
Soil properties

[m]	Profile	Color	Soil texture		Bulk density	Hydromorphic features	Shape of peds	Packing density	pH	Content of				
			U	T						Coarse fragments	C _{org} [%]	Carbonate	Water	
0	Ah		Ls3	38	20	1.3 g/cm ³ low	-	K	1	6	medium	5.1	-	slightly humid
0.2	E	10 YR 4/4 dark yellowish brown	Sl4	39	17	1.55 g/cm ³ medium	-	SP	1-2	7	high	1.4	-	slightly humid
0.4	It	10 YR 4/2 dark grayish brown	Lt2	38	22	1.5 g/cm ³ medium	Ox1 M	SP	2	7	high	1.9	-	slightly humid
0.6	Loam													
0.8	BCgg	2.5 Y 6/2 light brownish grey Patches in 2.5 Y 5/4 light olive brown	Ls3	34	20		Ox3 Re4 M			7	Many rounded pebbles. high	1.4	(+)	humid

Profile excavated down to 90 cm, drilling possible down to 200 cm.



Experiments



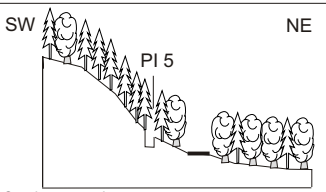
Process evaluation

High intensity: DP

Low intensity: DP

Soil profile PI 5: Parabraunerde

Site description



Catchment: Isert
 Location: Grossholz
 Coordinates: 702777 / 239'802
 Elevation: 540 m asl
 Land use: Spruce forest, sporadic fir and beech. Forest vegetation index 6: Typical woodruff beech forest
 Topography: Hillslope
 Slope: 23 %
 Exposition: NE

Soil surface

- 50 - 100 % vegetation cover
- stable aggregates in Ah, no surface sealing
- very unstable aggregates in E
- medium top soil compaction

Lateral flowpaths

Root channels and animal burrows

Geology

Gravel interglacial purely fluvial. 5-10m depth of gravel over highest possible groundwater level.

Macroporosity

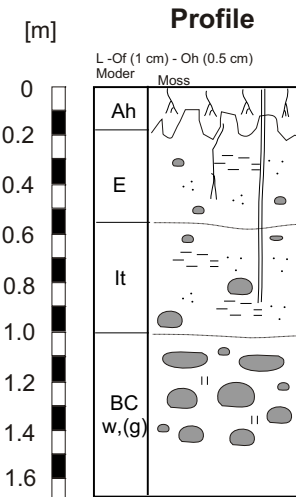
Horizontal cross sections 30 x 30 cm

depth 10 cm: Extremely loosely bedded, many roots. 11 / 11 Mp/m² all / large d > 5 mm

17 cm: 22 / 11 Mp/m² all / large

Mp/m² all / large

Soil properties



Color	Soil texture		Bulk density	Hydromorphic features	Shape of peds	Packing density	pH	Content of			
	U	T						Coarse fragments	C _{org} [%]	Carbonate	Water
			very low	-	K	1	6	low	> 5	-	slightly humid
10 YR 4/4 dark yellowish brown	Ls3/S14	39 19	0.9 g/cm ³ very low	-	K	1	7	low	2.9	-	humid
10 YR 4/4 dark yellowish brown	Ls2	41 22	1.2 g/cm ³ very low	-		1	7	medium	1.1	-	humid
				Ox1			7	high			humid wet

Profile excavated down to 80 cm, drilling possible down to 160 cm.




Experiments

Process evaluation

High intensity: DP
 Low intensity: DP

Soil Profile SI 1: Gley (kB6)

<p>Site description</p>  <p>Catchment: Isert Location: Pünt Coordinates: 702428 / 238897 Elevation: 530 m asl Land use: Meadow Topography: Plain Slope: < 3 % Exposition: NW</p>	<p>Soil surface</p> <ul style="list-style-type: none"> - > 90 % vegetation cover - stable aggregates - no top soil compaction 	<p>Lateral flowpaths</p> <p>Possibly tile drains</p>	<p>Geology</p> <p>Interglacial gravel deposits, purely fluvial. 0-5 m depth of gravel over highest possible groundwater level. Spring with 0.2 l/s. 20m next to and 1 m above profile.</p>
<p>Process evaluation</p> <p>High intensity: SOF 1 Low intensity: SOF 1</p>			

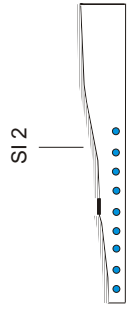


Soil properties

Horizon	Color	Soil texture			Hydromorphic features	Shape of peds	pH	Content of		Remarks
		U	T	W				Carbonate	Water	
Ah	10 YR 2/3 very dark brown				-	K	6		slightly humid	
Ah/Bg	10 YR 3/2 very dark greyish brown	40	24		Ox3 Re2 rusty mottling along root channels		6		humid	
Br	10 YR 5/2 greyish brown	34	19		Re4		7	5.66	++	Very high content of coarse fragments loss of soil core
										Water level in 75 cm depth. 18.7.02
										Depth of profile 1 m

Soil Profile SI 2: Gley (uG4)

Site description



SI 2

Catchment: Iserl
 Location: Strick
 Coordinates: 701775 / 239514
 Elevation: 515 m asl
 Land use: Grain field (recently harvested)
 Topography: Plain
 Slope: 7 %
 Exposition: SW

Soil surface

- 15 % vegetation cover
- stable aggregates
- no top soil compaction (harrowing 20 cm deep)

Lateral flowpaths

Tile drains (systematically drained), probably in sand layer in 1.2 - 1.4 m depth.

Geology

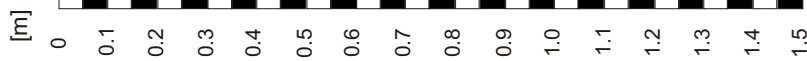
Interglacial gravel deposits with shallow cover of moraine. Gravel below groundwater level. Former swamp, today drained.

Process evaluation

High intensity: D 1
 Low intensity: D 1

Soil properties

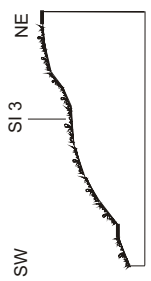
Horizont	Color	Soil texture % weight			Hydromorphic features	Shape of peds	pH	Content of		Remarks
		U	T	S				Carbonate	Water	
Ap	10 YR 3/1 very dark grey	10	7	10	K	7	-	slightly humid		
Aa	10 YR 2/1 black	Turf	6-7	>20			-	humid		
Bgg	2.5 Y 7/2 light grey Patches in 2.5 Y 6/6 olive yellow	Sl	8	+++	Ox3 Re4			wet	Very high content of rounded pebbles.	
		Ss			EK				Water level in 140 cm depth. 23.7.02	



Depth of profile 2 m

Soil Profile SI 3: Braunerde (dK21)

Site description



Catchment: Iserl
 Location: Allenwinden
 Coordinates: 701'760 / 240'102
 Elevation: 540 m asl
 Land use: Meadow
 Topography: Hillslope
 Slope: 19 %
 Exposition: SW

Soil surface

- 100 % vegetation cover
- stable aggregates
- no top soil compaction

Lateral flowpaths

Animal burrows

Geology

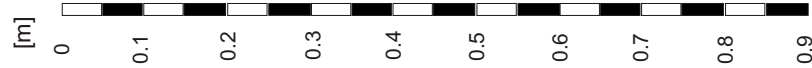
Moraine (drumlin)

Process evaluation

High intensity: SOF 2
 Low intensity: SSF 3

Soil properties

Horizon	Color	Soil texture % weight U T	Hydromorphic features	Shape of peds	pH	C _{org} [%]	Carbonate	Water	Remarks
Ah	10 YR 3/2 very dark greyish brown	Ls	-	K	6	2-5	++	slightly humid	
Bw	10 YR 4/3 dark brown	Ls	-		6-7		+++	slightly humid	
C(g)	10 YR 6/3 pale brown	Ls	Ox1		8			humid	High content of coarse fragments



Depth of profile 1 m

Appendix B: Hydrometric measurements

Table B.1 Groundwater wells in the Ror experimental catchment.

Ground water well	Swiss Coordinates [x / y]	Elevation [m a.s.l.]	Depth of measurements [m below surface]	Period of operation
GW 1	698227 / 236966	524.56	2.68	July 2000 - Jan 2003
GW 2	698227 / 236966	545.54	0.99	July 2000 - April 2002
GW 3	698229 / 236881	527.39	2.70	July 2000 - Jan 2003
GW 4	698230 / 236882	527.41	0.97	July 2000 - Jan 2003
GW 5	697565 / 238153	490.00	3.16	July 2000 - Okt 2001
GW 6	698155 / 236785	536.34	3.93	June 2001 - Jan 2003
GW 7	698154 / 236785	536.32	0.96	June 2001 - Jan 2003
GW 8	698193 / 236723	539.35	0.96	June 2001 - Jan 2003
GW 9	698188 / 236669	544.97	0.95	June 2001 - Jan 2003
GW 10	699137 / 237463	537.04	3.40	since June 2001
GW 11	699136 / 237464	537.01	1.26	since June 2001
GW 12	699101 / 237445	527.70	1.58	since June 2001
GW 13	699036 / 237164	510.98	2.00	since August 2001
GW 14	699162 / 237058	512.78	1.05	since August 2001
GW 15	699103 / 237055	512.91	1.86	since August 2001

Table B.2 Runoff gaging stations in the Ror experimental catchment.

Runoff gaging station	Periods of operation	Swiss coordinates [x / y]	Measurement device
Grueningen	May 1999 - July 1999 May 2000 - Dec 2000	697618 / 238359	ISCO + pressure transducer
Summerau	May 2000 - Dec 2000	697824 / 237763	Piezoresistive pressure transducer
Rinderholz	May 2000 - July 2000 May 2001 - Nov 2001 May 2002 - Dec 2002	698493 / 237529	ISCO Piezoresistive pressure transducer PCM 3
Poesch	Sep 2001 Feb 2002 - Dec 2002	698982 / 237294	PCM 3 flow and velocity measurements
Lindist	May 2001 - Okt 2002	698021 / 237365	Piezoresistive pressure transducer

Table B.3 *Raingauges in the vicinity of the Ror and Isert experimental catchments.*

Raingauge	Period of operation	Swiss coordinates [x / y]	Elevation [m asl]	Measure- ment inter- val	Operated by
Grüningen SMA	since 1900	700530/237300	490	day	SMA
Hinwil SMA	since 1961	703820/240750	540	day	SMA
Uster SMA	since 1961	694780/245160	440	day	SMA
Mönchaldorf AWEL	since 1980	696925/240800	440	day	AWEL
Tägernau 99	April - Aug 99			10 min	EAWAG
Isert 99	May - July 99			10 min	EAWAG
Ror 99	April - July 99	698261 / 237243	520	10 min	EAWAG
Ror 2000 1	May - July 00	697824 / 237763	495	10 min	EAWAG
Ror 2000 2	May - Dec 00	698822 / 237237	511	10 min	EAWAG + IHW
Ror N 1	May 01 - Dec 02	698822 / 237237	511	10 min	IHW
Ror N 2	Sep 01 - Dec 02	698352 / 236797	530	10 min	IHW
Ror N 3	Sep 01 - Dec 02	698261 / 237243	520	10 min	IHW

Appendix C: Kendall rank correlation coefficient

The Kendall rank correlation coefficient r_k is a nonparametric measure of the agreement between two rankings.

$$r_k = 1 - \frac{6 \cdot \sum D_i^2}{(n^3 - n) - (T_x + T_y)} \quad -1 \leq r_k \leq 1$$

$$T_x = \frac{1}{2} \cdot \sum (t_x^3 - t_x)$$

$$T_y = \frac{1}{2} \cdot \sum (t_y^3 - t_y)$$

D_i Differences in rank

n Sample size

t_x Number of tied rankings in x serie

t_y Number of tied rankings in y-serie

Appendix D: Objective function

The Nash - Sutcliff model efficiency (Nash and Sutcliff, 1970) is a measure of the degree of deviation between the value pairs Q_{obs} (observed runoff) and Q_{sim} (simulated runoff) from the bisecting line. A value of $E = 1$ indicates perfect agreement between observed and simulated runoff.

$$E = 1 - \frac{\sum_i (Q_{sim,i} - Q_{obs,i})^2}{\sum_i (Q_{obs,i} - \overline{Q_{obs}})^2} \quad E < 1$$

Curriculum Vitae PETRA SCHMOCKER - FACKEL**Personal:**

Born on July 14, 1971, Freudenstadt (Germany)

Marital status: married

Nationality: German

Education:

01/2000 - 2004 PhD- Thesis at " Institut für Hydromechanik und Wasserwirtschaft", ETH
Zürich, Switzerland

10/1994 - 07/1997 Studentship in Hydrology, Albert-Ludwigs-Universität, Freiburg,
Germany. Title of diploma thesis: "Regionalisierung von Parametern des
Wasserhaushaltsmodells LARSIM".

09/1993 - 06/1994 Bachelor of Science at Trent-University, Peterborough, Canada

10/1991 - 08/1993 Studentship in Geography (focus: Hydrology) at Albert-Ludwigs-
Universität, Freiburg, Germany

08/1983 - 06/1991 Kepler-Gymnasium, Freudenstadt, Germany

Professional experience:

11/1997 - 01/2000 Research assistant at " Institut für Hydromechanik und Wasserwirtschaft",
ETH Zürich, Switzerland

03/1996 - 05/1996 Practical training at "Ingenieurbüro Dr. Ing. Karl Ludwig", Karlsruhe,
Germany

07/1994 - 09/1994 Practical training at "Versuchsanstalt für Wasserbau" ETH-Zürich,
Switzerland

02/1993 - 03/1993 Practical training at " Wasserversorgung Kleine Kinzig", Reinerzau,
Germany

Publication:

Naef, F., Scherrer, S., Fackel, P., (1999) Abflussprozesse - wichtige Bausteine bei der
Abflussmodellierung. In: Koehler, G. (edit.), Bemessungsabflüsse für kleine Einzugsgebiete,
Berichte 9, Universität Kaiserslautern, S. 253 - 266.